RSC Advances

REVIEW

View Article Online
View Journal | View Issue

Cite this: *RSC Adv.*, 2024, **14**, 35769

Exploring heterocyclic scaffolds in carbonic anhydrase inhibition: a decade of structural and therapeutic insights

Nafeesa Naeem, [a] Amina Sadiq,[b] Gehan Ahmed Othman,[c] Habab M. Yassin[c] and Ehsan Ullah Mughal *[a]

Heterocyclic compounds represent a prominent class of molecules with diverse pharmacological activities. Among their therapeutic applications, they have gained significant attention as carbonic anhydrase (CA) inhibitors, owing to their potential in the treatment of various diseases such as epilepsy, cancer and glaucoma. CA is a widely distributed zinc metalloenzyme that facilitates the reversible interconversion of carbon dioxide and bicarbonate. This reaction is essential for numerous physiological and pathological processes. In humans, CA exists in sixteen different isoforms, labeled hCA-I to hCA-XV, each distributed across various tissues and organs and involved in crucial physiological functions. Clinically utilized CA inhibitors, such as brinzolamide, dorzolamide and acetazolamide, exhibit poor selectivity, leading to undesirable side effects. A significant challenge in designing effective CA inhibitors is achieving balanced isoform selectivity, prompting the exploration of new chemotypes. This review compiles recent strategies employed by various researchers in developing CAIs across different structural classes, including pyrazoline, quinoline, imidazole, oxadiazole, pyrimidine, coumarin, chalcone, rhodanine, phthalazine, triazole, isatin, and indole. Additionally, the review summarizes structure–activity relationship (SAR) analyses, isoform selectivity evaluations, along with mechanistic and *in silico* investigations. Insights derived from SAR studies provide crucial directions for the rational design of next-generation heterocyclic CA inhibitors, with improved therapeutic efficacy and reduced side effects. To the best of our knowledge, for the first time, we have comprehensively summarized all known isoforms of CA in relation to various heterocyclic motifs. This review examines the use of different heterocycles as CA inhibitors, drawing on research published over the past 11 years. It offers a valuable resource for early-career researchers, encouraging further exploration of synthetic heterocycles in the development of CA inhibitors.

Received 31st August 2024
Accepted 15th October 2024

DOI: 10.1039/d4ra06290f

rsc.li/rsc-advances

[a]*Department of Chemistry, University of Gujrat, Gujrat 50700, Pakistan. E-mail: ehsan.ullah@uog.edu.pk*
[b]*Department of Chemistry, Govt. College Women University, Sialkot 51300, Pakistan*
[c]*Biology Department, College of Science, King Khalid University, Abha, 61421, Saudi Arabia*

Ehsan Ullah Mughal

Ehsan Ullah Mughal obtained his PhD degree in Organic Chemistry from Bielefeld University, Germany in 2013. Currently, he is working as Tenured Associate Professor in the Department of Chemistry, University of Gujrat, Pakistan. He was a post-doc fellow at Max-Planck Institute for Polymer Research, Mainz, Germany from 2013 to 2014. His current research interests include the design and synthesis of bioactive heterocycles, synthetic flavonoids, transition metal-based terpyridine complexes and their uses in the fabrication of DSSCs and as efficient photocatalysts. His research in the field has resulted in more than 97 published articles (research papers and review papers) in reputable high impact journals. His publications have made a great impact in the field by receiving 2059 citations with h-index of 28.

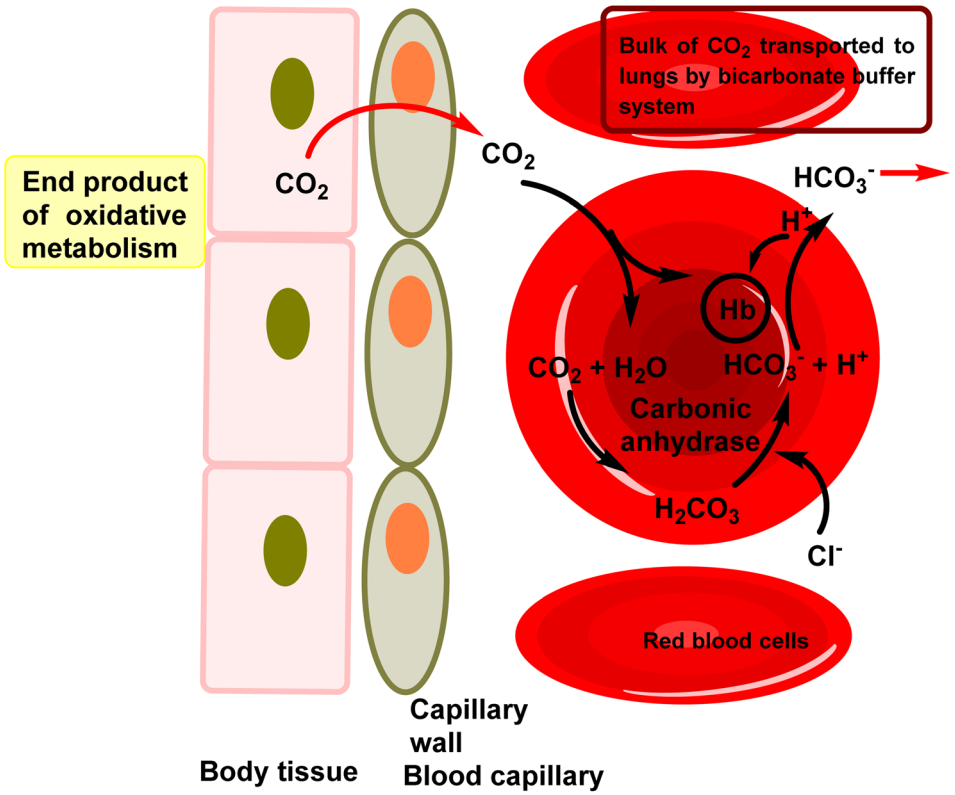

Fig. 1 The role of CA in erythrocytes involves facilitating the hydration of CO_2 in tissues and the dehydration of HCO_3^- in erythrocytes within the lungs.

1. Introduction

Heterocycles represent a class of molecules present in numerous biological compounds within the human body, characterized by the inclusion of heteroatoms such as sulfur, nitrogen and oxygen in a ring structure.[1] Their natural occurrence, intricate structure, and propensity for hydrogen bonding render heterocycles highly coveted for their potential application as pharmaceutical agents.[2] Medicinal chemists strategically design drug molecules that mimic the structure of endogenous heterocycles, aiming to either enhance or inhibit their physiological functions.[3,4] Recent advancements in synthetic methodologies have facilitated the creation of diverse heterocyclic scaffolds, thereby streamlining the process of drug discovery.[5,6] These compounds have attained considerable attention in recent years owing to their ability to interact with enzymes and modulate their activity.[7,8] Enzymes, vital biological molecules that catalyze various chemical reactions, play pivotal roles in cellular metabolism and signaling pathways, rendering them attractive targets for drug intervention.[9–11] Heterocyclic compounds can effectively engage with enzymes by binding to their active sites, consequently altering their activity and exerting inhibitory effects.[12] Particularly, the exploration of heterocyclic compounds as inhibitors of CA activity represents a promising avenue for therapeutic intervention.

Carbonic anhydrases (CAs, EC 4.2.1.1) represent a widely distributed superfamily of zinc-metalloenzymes.[13] Their primary function involves catalyzing the reversible hydration of carbon dioxide to bicarbonate and a proton ($CO_2 + H_2O \leftrightarrow HCO_3^- + H^+$).[14,15] This catalytic activity is integral to numerous biochemical and physiological processes across both prokaryotic and eukaryotic organisms.[16–18] They are involved in various physiological processes such as pH regulation, electrolyte transport, bone resorption, and biosynthetic reactions.[19,20] The varied functions of CA render them appealing therapeutic targets for numerous diseases, including cancer, epilepsy, obesity, glaucoma and several neurological disorders.[21–24] Furthermore, CA isoenzymes emerge as promising targets for Alzheimer's disease (AD) treatment.[25] These enzymes are extensively distributed throughout nature and are currently categorized into eight genetically unrelated families: the α-, β-, γ-, δ-, η-, ζ-, θ-, and ι-classes.[26,27] To date, nature has revealed eight genetically distinct CA families (a–i).[28] Among these, only the alpha class of CA (a-CAs) are exclusively found in higher vertebrates.[29] In *Homo sapiens*, only fifteen isoforms of have been identified, each differing in catalytic activity, tissue/subcellular localization, and physiological role.[30,31] In the lungs, CA in red blood cells catalyzes the conversion of HCO_3^- back into CO_2, which is then exhaled. In the human enzyme, zinc serves as an essential metal ion component.[32] The zinc ion is coordinated by three nitrogen atoms from three histidine residues within the protein[33] (Fig. 1).

The human alpha CAs comprise 15 distinct isoforms (I–XIV), with 12 demonstrating catalytic activity (Fig. 2).[34] These

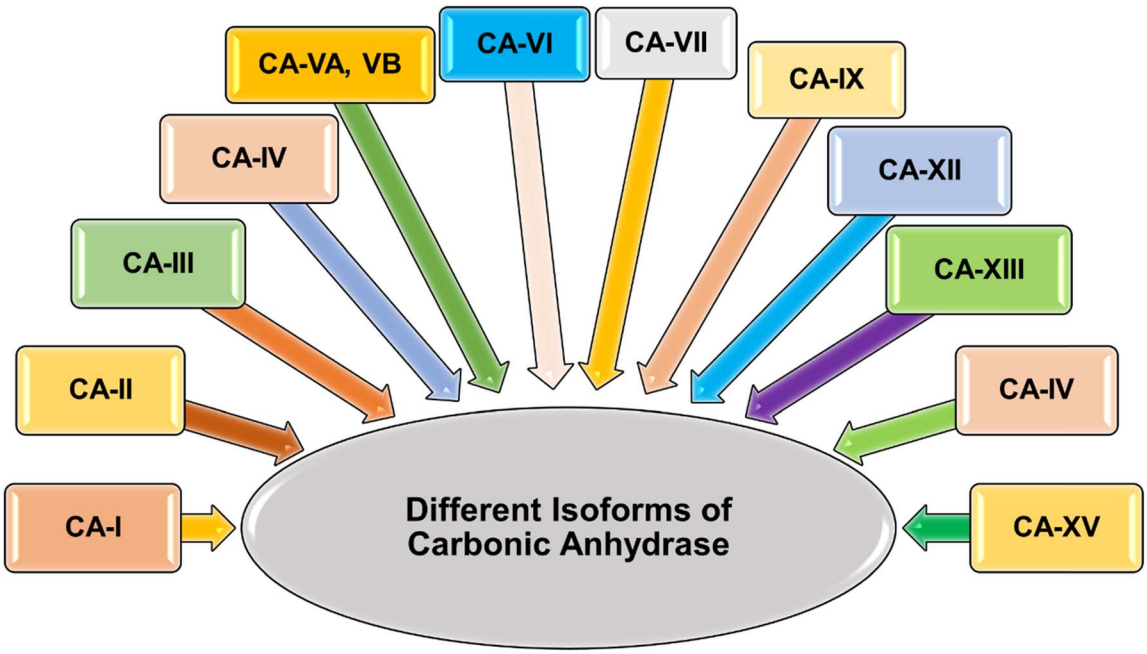

Fig. 2 Various isoforms of human carbonic anhydrase.

Table 1 Distribution of α-CAs across tissues/organs and associated diseases

CA type	Tissue/organ distribution	Associated diseases
CA-I	Erythrocytes, kidneys, liver, muscle, and brain	Glaucoma, epilepsy, osteoporosis
CA-II	Widespread distribution, especially in erythrocytes, kidneys, and eyes	Osteopetrosis, renal tubular acidosis, retinitis pigmentosa
CA-III	Skeletal muscle, liver, adipose tissue, and heart	Obesity, insulin resistance
CA-IV	Plasma membrane of various tissues including erythrocytes, kidney, and eye	Renal tubular acidosis, retinitis pigmentosa
CA-VA	Mitochondria of liver and adipose tissue	Obesity, metabolic disorders
CA-VB	Mitochondria of liver and adipose tissue	Obesity, metabolic disorders
CA-VI	Saliva, milk, and cerebrospinal fluid	Dental caries, Sjögren's syndrome
CA-VII	Brain, pancreas, and testes	Epilepsy, ataxia
CA-IX	Tumor cells, especially in hypoxic conditions	Cancer progression, metastasis
CA-XII	Plasma membrane of various tissues including kidney, colon, and pancreas	Cancer progression, metastasis
CA-XIII	Brain, gut, kidney, lung, reproductive tract	Sterility
CA-XIV	Heart, skeletal muscle, and brain	Epilepsy, retinopathies

isoforms differ in their catalytic activity, cellular localization, and distribution throughout various organs and tissues. Specifically, hCA-VIII, X, and XI are classified as non-catalytically active CA-related proteins.[35] CAs are categorized into four groups based on their localization: cytosolic isoforms (hCAs-I–III, VII, and XIII), transmembrane isoforms (hCAs-IV, IX, XII, and XIV), mitochondrial isoforms (hCAs-VA and VB), and the secreted isoenzyme hCA-VI, found in saliva and milk. Dysregulation of carbonic anhydrase isoforms is associated with various diseases, such as glaucoma (hCAs-I, II, IV, and XII), epilepsy (hCAs-VII and XIV), cerebral and retinal edema (hCAs-I and II), and different cancers (hCAs-IX and XII). Among the α-CA superfamily, CA-IX and CA-XII are notably significant due to their roles in the survival of hypoxic tumors.[36,37] These cancer-associated CAs are normally expressed at low levels in healthy tissues but are often overexpressed in a range of hypoxic solid tumors.[38–41] Such overexpression patterns are often attributed to the robust transcriptional activation of the hypoxia-inducible transcription factor 1 (HIF1), through which they exert influence over critical processes like cell proliferation, malignant cell invasion and adhesion.[42] The Table 1 outlines the distribution of various α-CAs across different organs/tissues and their involvement in various diseases.[43,44]

Over the years, extensive research has been conducted to develop small molecule inhibitors targeting CAs, with the aim of modulating their activity for therapeutic benefit. Among the various classes of CA inhibitors (CAIs), heterocyclic scaffolds have emerged as particularly promising candidates due to their structural diversity, synthetic accessibility, and ability to interact with the active site of CAs with high affinity and specificity.[33,45]

This systematic review aims to provide a comprehensive overview of the recent advancements in the design and development of heterocyclic scaffold-based CAIs for drug discovery. We will explore the diverse array of heterocyclic scaffolds employed, their structural features, synthetic strategies, and their inhibitory activities against different isoforms of CAs. Furthermore, we will discuss the structure–activity relationships (SAR) governing the interaction between heterocyclic scaffold-based CAIs and their target enzymes, highlighting key molecular determinants for potency, selectivity, and pharmacokinetic properties.

The significance of this review lies in its potential to offer insights into the design principles for developing novel CAIs with improved therapeutic efficacy and reduced off-target effects. By examining the latest advancements and trends in the field, we aim to provide researchers and medicinal chemists with valuable guidance for the rational design of heterocyclic scaffold-based CAIs, ultimately facilitating the discovery of next-generation therapeutics for various diseases associated with dysregulated CA activity.

Additionally, we will discuss the therapeutic potential of heterocyclic scaffold-based CAIs in the context of different disease indications, along with the challenges and future perspectives in this exciting area of drug discovery.

2. hCA structure and mechanism/ structural overview of carbonic anhydrases

X-ray crystallographic studies have offered valuable insights into the three-dimensional structures of catalytically active hCAs, aiding in the understanding of the active site architecture, amino acid residues, and ligand interactions crucial for drug development.[38,46,47] However, it's worth noting that the hCA-VA and VB are murine enzymes and hence are exceptions to these studies.[48]

The catalytic activity of hCAs relies on the presence of the essential zinc ion (Zn^{2+}), as corroborated by numerous investigations. The metal ion is located approximately 15 Å deep within the active site cleft and is coordinated by three conserved histidine residues: His94, His96, and His119, along with a water molecule or hydroxide ion. The Zn^{2+}-bound water molecule or hydroxide forms hydrogen bonds with nearby amino acids, including the conserved threonine residue Thr199 and the glutamic acid residue Glu106, within the binding pocket. This interaction enhances the nucleophilicity of the Zn^{2+}-bound water molecule (Fig. 3).[49,50] This results in the enzyme adopting a Zn^{2+}-bound water molecule or hydroxide state, representing the catalytically inactive or resting state, from which the enzyme can initiate another catalytic cycle by attacking a new CO_2 molecule.[51–53]

3. Importance of carbonic anhydrase inhibition

3.1. Therapeutic applications of CAIs

CAIs have demonstrated significant therapeutic potential in treating a wide range of diseases (Fig. 4), including:

(i) Glaucoma: CAIs reduce intraocular pressure by inhibiting CA in the ciliary processes of the eye, thereby decreasing the production of aqueous humor and alleviating symptoms associated with glaucoma.[54]

(ii) Cancer: CAIs have emerged as promising agents for cancer therapy due to their ability to disrupt tumor pH regulation, inhibit

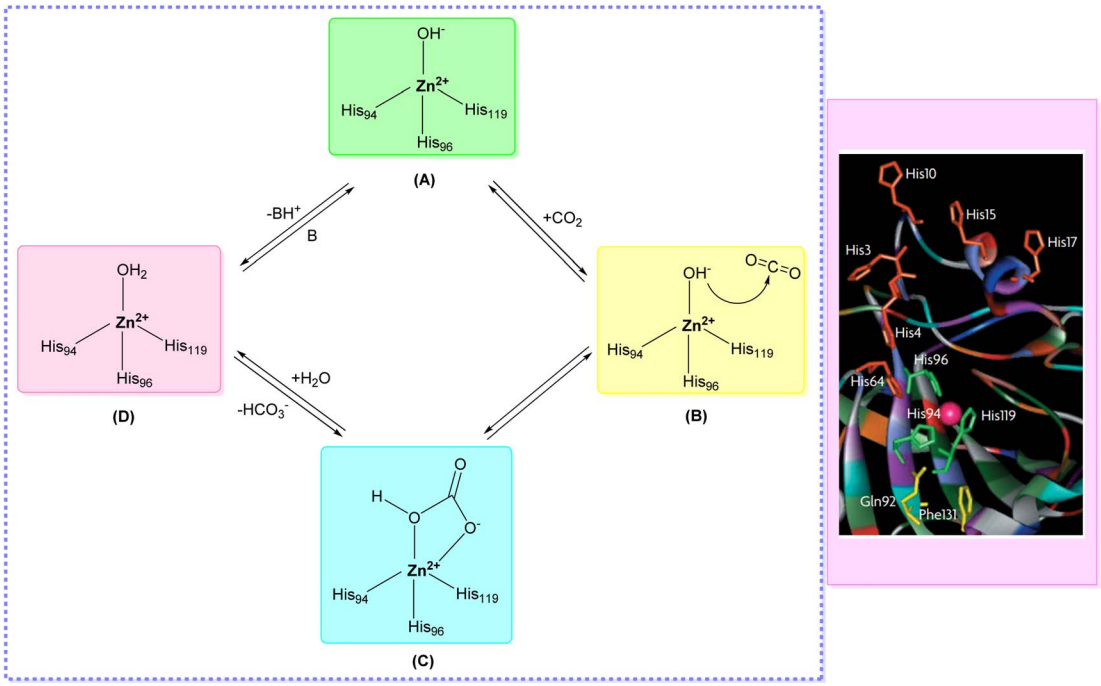

Fig. 3 Catalytic mechanism of hCAs entails the reversible hydration and dehydration reactions (A–D) between CO_2 with HCO_3^-.

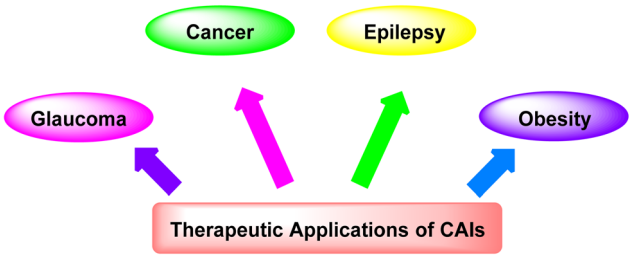

Fig. 4 Therapeutic applications of CAIs.

tumor cell proliferation, and enhance the effectiveness of chemotherapeutic agents.[55]

(iii) Epilepsy: CAIs have been explored as adjunctive therapy for epilepsy, as they modulate neuronal excitability by altering pH levels and bicarbonate concentrations in the brain, potentially reducing the frequency and severity of seizures.[56]

(iv) Obesity: CAIs have shown potential in managing obesity by targeting CA isoforms involved in lipid metabolism and appetite regulation, offering a novel approach for weight management.[57,58]

3.2. Challenges and limitations associated with current CAIs

Despite their therapeutic promise, current CAIs face several challenges and limitations, including:

(i) Side effects: some CAIs can cause adverse effects such as metabolic acidosis, electrolyte imbalances, renal dysfunction, and ocular irritation, limiting their clinical utility and patient compliance.[59]

(ii) Isoform selectivity: achieving selectivity for specific CA isoforms is challenging, as many CAIs exhibit broad-spectrum activity, leading to off-target effects and potential toxicity.[60]

(iii) Blood–brain barrier penetration: limited penetration of CAIs across the blood–brain barrier hinders their efficacy in neurological disorders such as epilepsy, where precise targeting within the central nervous system is essential.[61]

(iv) Resistance development: prolonged use of CAIs can lead to the development of drug resistance in certain disease contexts, necessitating the exploration of alternative treatment strategies and novel CAIs with improved efficacy profiles.[62]

Addressing these challenges through innovative drug design strategies, such as enhancing isoform selectivity, improving pharmacokinetic properties, and minimizing off-target effects, holds promise for advancing the clinical utility of CAIs in the treatment of various diseases.

4. Classification of carbonic anhydrase inhibitors based on various diseases

4.1. CAIs as diuretics

CAIs have been utilized as diuretics due to their ability to modulate renal physiology and fluid balance.

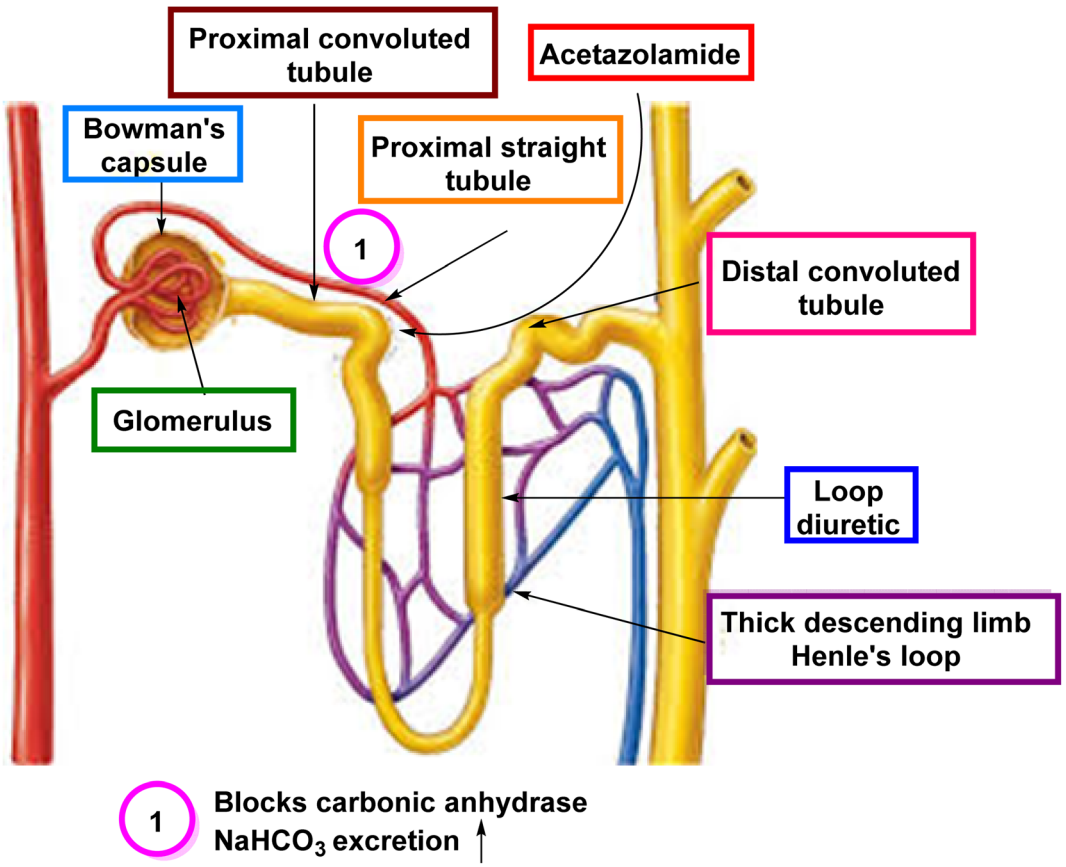

Fig. 5 Diuretic therapy with CAIs.

4.1.1 Mechanism of action. CAIs exert their diuretic effect by inhibiting CA enzymes in the proximal renal tubules. By blocking CA activity, these inhibitors reduce the reabsorption of bicarbonate ions (HCO_3^-) and impair sodium bicarbonate co-transport. This leads to an increase in the excretion of bicarbonate ions and sodium ions, along with accompanying water loss. AAZ and similar CAIs act in the proximal tubule by inhibiting CA activity, leading to an increase in $NaHCO_3$ excretion (Fig. 5).[63]

4.1.2 Clinical applications. CAIs have been employed as diuretics in conditions such as edema, heart failure, and hypertension. Their diuretic action helps to reduce fluid retention and alleviate symptoms associated with volume overload.[64]

4.1.3 Site of action. The proximal renal tubules are the primary site of action for CAIs as diuretics. By inhibiting CA enzymes in this region, CAIs disrupt bicarbonate reabsorption and promote diuresis by enhancing the excretion of sodium and water.[65]

4.1.4 Potential side effects. While CAIs can effectively promote diuresis, they may also lead to metabolic acidosis due to bicarbonate loss. Other potential side effects include electrolyte imbalances, renal dysfunction, and gastrointestinal disturbances. Careful monitoring of electrolyte levels and renal function is essential during CAI therapy.[66]

4.1.5 Clinical considerations. CAIs are typically used as adjunctive therapy or in cases where other diuretics are ineffective. They may be particularly beneficial in patients with metabolic alkalosis or those requiring a reduction in intraocular pressure, such as in cases of glaucoma.[67]

4.1.6 Selective CAIs. Selective inhibitors targeting specific CA isoforms have been developed to minimize side effects associated with non-selective inhibition. These selective CAIs offer the potential for targeted diuretic therapy with reduced risk of systemic adverse effects.[68]

4.2. CAIs as drugs for eye disorders

CAIs have found significant therapeutic applications in the treatment of various eye disorders.

4.2.1 Glaucoma management. CAIs, particularly topical ophthalmic formulations, are commonly prescribed as a first-line or adjunctive treatment for glaucoma. By inhibiting CA enzymes in the ciliary processes of the eye, CAIs reduce the production of aqueous humor, thereby lowering intraocular pressure (IOP). This helps to prevent optic nerve damage and slow the progression of glaucoma, ultimately preserving vision.[69]

4.2.2 Reduction of intraocular pressure. The primary mechanism of action of CAIs in treating glaucoma is the reduction of intraocular pressure. By decreasing the production of aqueous humor, CAIs alleviate the elevated pressure within the eye, which is a major risk factor for optic nerve damage and vision loss associated with glaucoma.[70,71]

4.2.3 Types of CAIs used. CAIs used for the treatment of glaucoma include both systemic oral medications and topical ophthalmic formulations. Oral CAIs such as methazolamide and AAZ are sometimes prescribed for patients with refractory or severe glaucoma. Topical CAIs, such as dorzolamide and

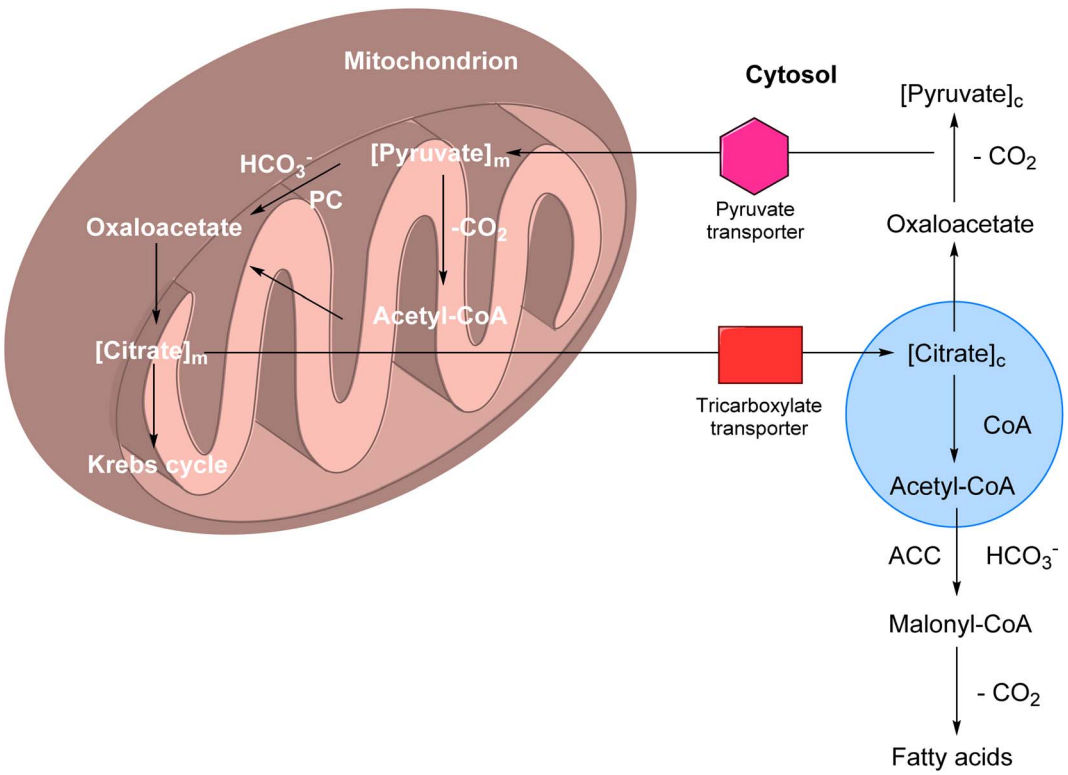

Fig. 6 Role of CA-VA, VB and CA-II in the *de novo* lipogenesis.

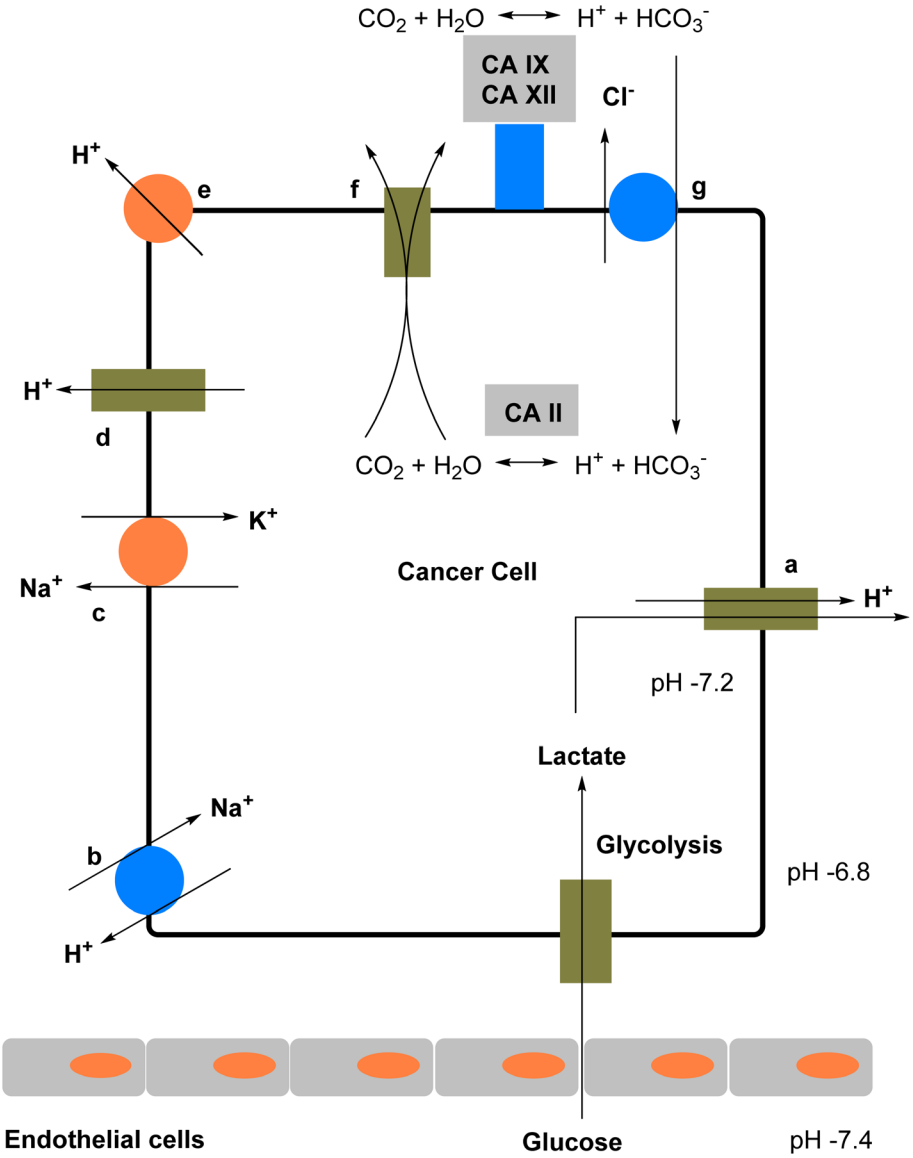

Fig. 7 Schematic representation illustrating the role of hCA-IX in regulating pH in hypoxic tumor cells.

brinzolamide, are more commonly used due to their localized action and reduced systemic side effects.[72]

4.2.4 Adjunctive therapy. In some cases, CAIs may be used as adjunctive therapy alongside other intraocular pressure-lowering medications, such as beta-blockers, prostaglandin analogs, or alpha agonists. Combining medications with different mechanisms of action can enhance their overall efficacy in managing glaucoma and achieving target IOP levels.[73]

4.2.5 Side effects and considerations. While CAIs are generally well-tolerated, they may cause ocular side effects such as stinging, burning, or blurred vision, particularly with topical formulations. Systemic side effects of oral CAIs may include electrolyte imbalances, metabolic acidosis, and renal dysfunction. Patient monitoring and proper dosing are essential to minimize the risk of adverse effects.[74]

4.3. CAIs as potential anti-obesity drugs

CAIs have emerged as potential candidates for the treatment of obesity due to their involvement in metabolic pathways and physiological processes related to energy balance.

4.3.1 Mechanism of action. CAIs exert their effects on body weight regulation through several mechanisms. One key mechanism is their inhibition of CA enzymes in tissues such as the liver, adipose tissue, and skeletal muscle. By modulating CA activity, CAIs may influence lipid metabolism, thermogenesis, and energy expenditure, thereby impacting body weight regulation. Mitochondrial CAs play a critical role in supporting the mitochondrial pyruvate carboxylase (PC) enzyme by supplying HCO_3^-, which are used to convert pyruvate into oxaloacetate. Oxaloacetate is then transformed into citrate through a reaction with acetyl coenzyme A (Ac-CoA). Unlike Ac-CoA and oxaloacetate, citrate can exit the mitochondria and enter the cytosol *via*

Table 2 Chemical structures of pyrazole-based sulfonamide analogues, K_i values against CAIs

Compound no.	Chemical structures & IUPAC names	K_i (nM) hCA-I	hCA-II	hCA-IX	hCA-XII	Ref.
1	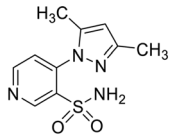 4-(3,5-Dimethyl-1*H*-pyrazol-1-yl) pyridine-3-sulfonamide	346	61.4	24.8	34.2	84
2	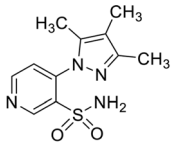 4-(3,4,5-Trimethyl-1*H*-pyrazol-1-yl) pyridine-3-sulfonamide	438	58.5	23.1	27.8	84
3	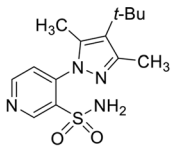 4-(*t*-Butyl-3,5-dimethyl-1*H*-pyrazol-1-yl) pyridine-3-sulfonamide	541	76.3	48.6	39.1	84
4	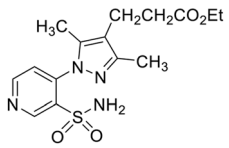 Ethyl 3-(3,5-dimethyl-1-(3-sulfamoyl pyridin-4-yl)-1*H*-pyrazol-4-yl)propanoate	397	134	19.5	22.6	84
5	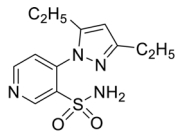 4-(3,5-Diethyl-1*H*-pyrazol-1-yl) pyridine-3-sulfonamide	278	87.1	31.7	16.8	84
Standards	AAZ	310	12	25	5.7	84
	MZA	780	14	27	3.4	
	EZA	25	8	34	22	
	IND	31	15	24	3.4	

the tricarboxylate transporter. In the cytosol, citrate is broken down into oxaloacetate and CoA by ATP citrate lyase. Oxaloacetate is then decarboxylated to produce pyruvate, which is transported back into the mitochondria by the pyruvate carboxylase transporter. Cytosolic HCO_3^-, supplied by CA-II, aids in the conversion of activated CoA into malonyl-CoA through the action of cytosolic acetyl-coenzyme A carboxylase (ACC). These malonyl-CoA units are then elongated in a similar process (Fig. 6).[58,75]

4.3.2 Appetite regulation. CAIs may also influence appetite regulation through their effects on central and peripheral signaling pathways involved in hunger and satiety. By modulating neuronal excitability and neurotransmitter release, CAIs could potentially decrease food intake and curb appetite, leading to reduced calorie consumption and weight loss.[75]

4.3.3 Metabolic effects. In addition to their effects on lipid metabolism and appetite regulation, CAIs may have broader metabolic effects that contribute to their anti-obesity properties. These effects may include improvements in insulin sensitivity, glucose metabolism, and inflammatory markers associated with obesity-related comorbidities such as insulin resistance and type 2 diabetes.[75]

4.3.4 Experimental and clinical studies. Preclinical studies in animal models of obesity have shown promising results with

Table 3 Chemical structures of sulfamide derivatives, K_i values against CAIs

Compound no.	Chemical structures & IUPAC names	K_i CA-I (μM)	CA-II (μM)	CA-V (μM)	CA-IX (μM)	CA-XII (μM)	CA-XIV (μM)	Ref.
6	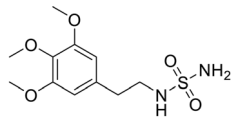 *N*-(3,4,5-Trimethoxyphenethyl) sulfamide	1.82	2.03	>50	0.221	1.52	0.22	85
7	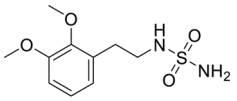 *N*-(2,3-Dimethoxyphenethyl) sulfamide	0.25	2.95	>50	>50	0.047	0.18	85
8	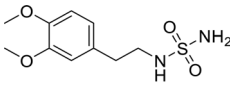 *N*-(3,4-Dimethoxyphenethyl) sulfamide	0.28	2.40	2.28	0.092	0.044	0.031	85
9	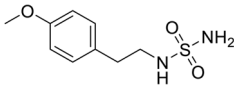 *N*-(4-methoxyphenethyl) sulfamide	0.061	1.47	3.25	0.376	0.021	0.007	85
10	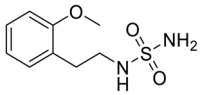 *N*-(2-Methoxyphenethyl) sulfamide	0.25	2.04	3.34	0.041	0.416	0.16	85
Standard	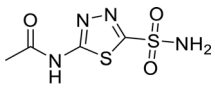 Acetazolamide (AAZ)	0.250	12	0.063	0.025	0.006	0.041	85

various CAIs, demonstrating reductions in body weight, adiposity, and metabolic parameters. Some clinical studies have also explored the use of CAIs for weight management in humans, although further research is needed to evaluate their long-term efficacy and safety in obesity treatment.[76]

4.3.5 Safety considerations. While CAIs offer potential benefits as anti-obesity drugs, safety considerations such as side effects and tolerability need to be carefully assessed. Common side effects of CAIs include gastrointestinal disturbances, metabolic acidosis, and electrolyte imbalances. Therefore, optimizing the therapeutic profile of CAIs and minimizing adverse effects are important considerations in their development as anti-obesity agents.[76]

4.4. Anticancer potential of CAIs

CAIs have gained significant attention in cancer research due to their potential as anticancer agents.

4.4.1 Tumor acidosis targeting. Cancer cells exhibit altered metabolism, leading to increased glycolysis and lactate production, which results in extracellular acidification known as tumor acidosis. CAIs target this acidic microenvironment by inhibiting CA enzymes, thereby disrupting pH regulation in cancer cells and impairing their survival and proliferation (Fig. 7).[77]

4.4.2 Angiogenesis inhibition. CAs play a crucial role in regulating pH and ion transport in tumor-associated blood vessels. By inhibiting CA activity, CAIs disrupt the angiogenesis essential for metastasis and tumor growth. This anti-angiogenic effect deprives cancer cells of oxygen and nutrients, leading to tumor regression.[78]

4.4.3 Metastasis suppression. CAIs have been shown to inhibit the invasive and metastatic properties of cancer cells by modulating cell adhesion, migration, and invasion. By targeting CAs involved in these processes, CAIs prevent cancer cells from spreading to distant organs and forming secondary tumors, thereby improving patient outcomes. Figure illustrates the proposed role of hCA-IX in tumor cell pH regulation. This shift aids in energy production in low-oxygen environments,

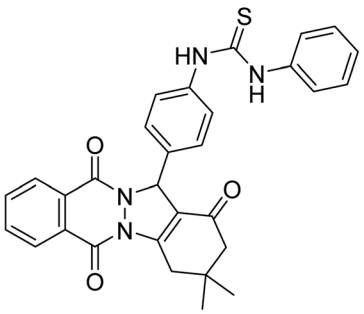

1-(4-(3,3-Dimethyl-1,6,11-trioxo-2,3,4,6,11,13-hexahydro-1H-indazolo[1,2-b]phthalazin-13-yl)phenyl)-3-phenylthiourea

IC_{50} = 6.40 μM for hCA-I
IC_{50} = 6.13 μM for hCA-II

11

Fig. 8 Chemical structure of compound **11** and its hCA-I and II inhibition.

contributing to the hypoxic phenotype associated with hCA-IX expression.[78]

4.4.4 Enhanced chemosensitivity. Combining CAIs with conventional chemotherapy agents has been explored as a strategy to enhance the efficacy of cancer treatment. CAIs sensitize cancer cells to chemotherapy-induced cell death by disrupting pH homeostasis and altering drug uptake, metabolism, and resistance mechanisms, leading to synergistic anticancer effects.[78]

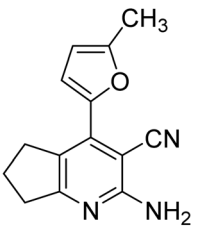

2-Amino-4-(5-methylfuran-2-yl)-6,7-dihydro-5*H*-cyclopenta[*b*]pyridine-3-carbonitrile

IC_{50} & K_i = 33 μM & 23.8 μM for hCA-I
IC_{50} & K_i = 56 μM & 41 μM for hCA-II

12

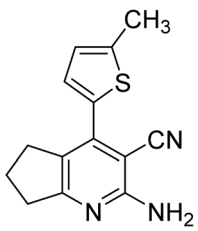

2-Amino-4-(5-methylthiophen-2-yl)-6,7-dihydro-5*H*-cyclopenta[*b*]pyridine-3-carbonitrile

IC_{50} & K_i = 34 μM & 31 μM for hCA-I
IC_{50} & K_i = 99 μM & 182 μM for hCA-II

13

Fig. 9 Chemical structures of compounds **12** and **13** and their IC_{50} and K_i values against hCA-I and II.

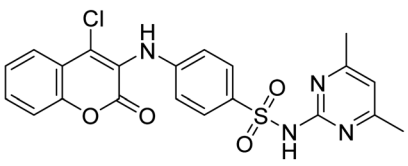

4-((4-Chloro-2-oxo-2H-chromen-3-yl)-methylene amino)-N-(4, 6-dimethyl-pyrimidin-2-yl) benzenesulfonamide

IC_{50} = 23 nM for hCA-II
IC_{50} = 124 nM for hCA-IX

14

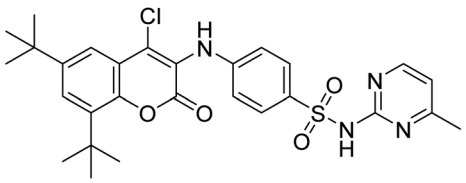

4-((6,8-Di-tert-butyl-4-chloro-2-oxo-2H-chromen-3-yl) methyleneamino)-N-(4-methylpyrimidin-2-yl) benzenesulfonamide

IC_{50} = 63 nM for hCA-II
IC_{50} = 24 nM for hCA-IX

15

Fig. 10 Chemical structures of compounds **14** and **15** and their IC_{50} values against hCA-II and IX.

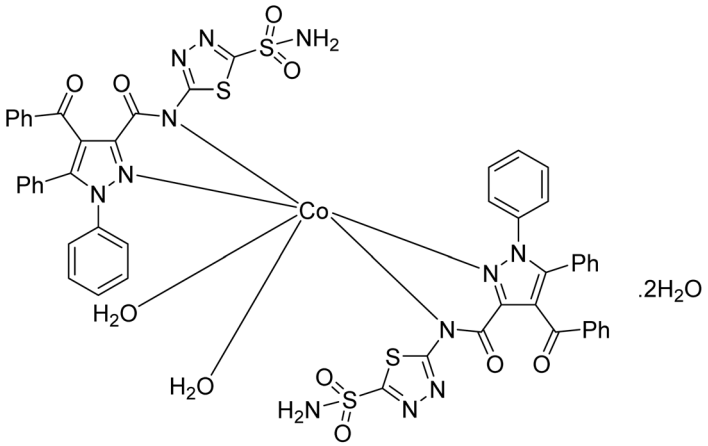

(Diaquabis (4-benzoyl-1,5-diphenyl-N-(5-sulfamoyl-1,3,4-thiadiazol-2-yl)-1H-pyrazole-3-carboxamide)cobalt(II) dihydrate

Hydratase IC_{50} & K_i
IC_{50} & K_i = 0.473 μM & 0.039 μM for hCA-I
IC_{50} & K_i = 0.213 μM & 0.078 μM for hCA-II
Esterase IC_{50}
IC_{50} = 0.058 μM for hCA-I
IC_{50} = 0.110 μM for hCA-II

16

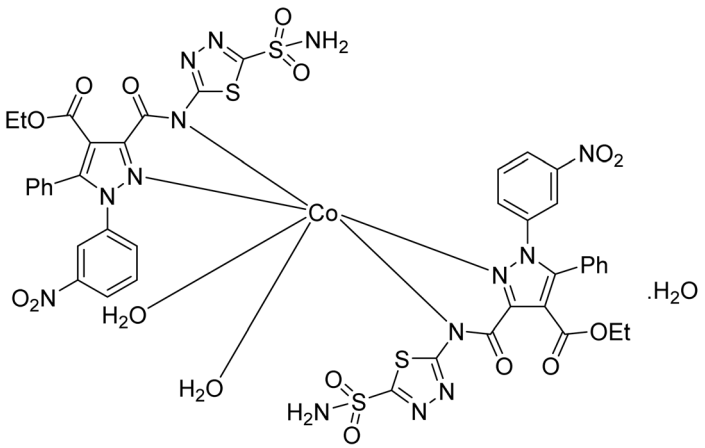

(Diaquabis(ethyl-1-(3-nitrophenyl)-5-phenyl-3-(5-sulfamoyl-1,3,4-thiadiazol-2-ylcarbamoyl)-1H-pyrazole-4-carboxylate)cobalt(II) monohydrate

Hydratase IC_{50} & K_i
IC_{50} & K_i = 0.065μM & 0.247 μM for hCA-I
IC_{50} & K_i = 0.833 μM & 0.363 μM for hCA-II
Esterase IC_{50}
IC_{50} = 0.297 μM for hCA-I
IC_{50} = 0.052 μM for hCA-II

17

Fig. 11 Chemical structures of compounds **16** and **17** and their IC_{50} and K_i values against hCA-I and II.

4.4.5 Selective isoform targeting. Selective inhibition of specific CA isoforms expressed in cancer cells has been investigated to minimize off-target effects and maximize therapeutic efficacy. Isoform-specific CAIs offer the potential for personalized cancer therapy tailored to the molecular characteristics of individual tumors, thereby improving treatment outcomes and reducing adverse effects.[77]

4.4.6 Translational research. Translational research efforts aim to validate the anticancer efficacy of CAIs in preclinical models and identify biomarkers predictive of treatment

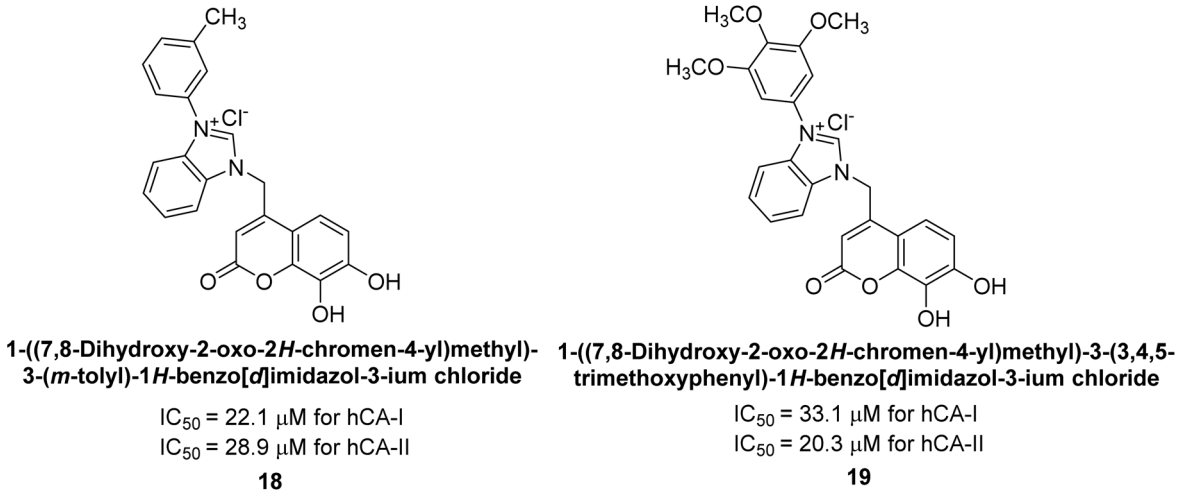

Fig. 12 Chemical structures of compounds **18** and **19** and their IC_{50} values against hCA-I and II.

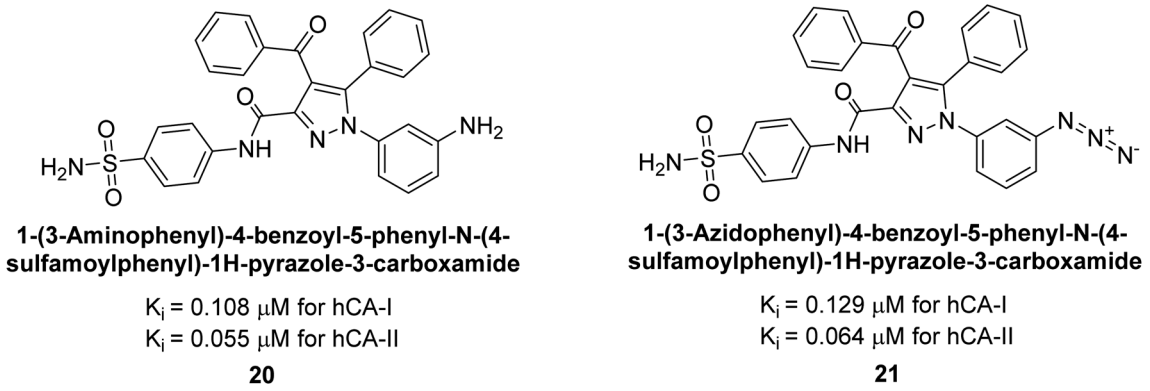

Fig. 13 Chemical structures of compounds **20** and **21** and their K_i values against hCA-I and II.

response to guide patient selection and optimize therapeutic strategies.[79]

4.4.7 Safety and tolerability. While CAIs hold promise as anticancer agents, safety considerations such as off-target effects and systemic toxicity need to be carefully evaluated. Strategies to enhance the selectivity and tolerability of CAIs while minimizing adverse effects are essential for their successful translation into clinical practice.[79]

4.5. CAIs as potential therapeutics for osteoporosis

Osteoporosis is a common skeletal condition marked by reduced bone strength and an elevated risk of fractures. Conventional therapies for osteoporosis primarily target bone resorption through antiresorptive agents or promote bone formation using anabolic agents. However, these treatments have limitations, underscoring the need for alternative therapeutic strategies. CAIs have emerged as potential candidates for osteoporosis therapy due to their involvement in bone metabolism and remodeling processes.[80]

4.5.1 Role of CAs in bone metabolism. CAs are zinc metalloenzymes involved in ion transport and pH regulation in various tissues, including bone. In bone, CA-II and XII are key isoforms expressed by osteoclasts, osteoblasts, and bone matrix cells, where they regulate osteoclast activity, osteoblast differentiation, and bone mineralization. Modulating CA activity represents a promising avenue for influencing bone metabolism and maintaining skeletal health.[81]

4.5.2 Potential benefits of CAIs in osteoporosis. Preclinical studies have demonstrated the potential benefits of CAIs in osteoporosis models. CAIs have been shown to inhibit bone resorption, promote bone formation, and improve bone architecture and strength. Additionally, CAIs may enhance fracture healing and reduce bone loss associated with aging or estrogen deficiency. These findings highlight the therapeutic potential of CAIs in osteoporosis management.[82]

4.5.3 Mechanisms of action of CAIs in bone. CAIs exert their effects on bone metabolism through various mechanisms, including modulation of pH regulation, ion transport, and signaling pathways involved in osteoclastogenesis and

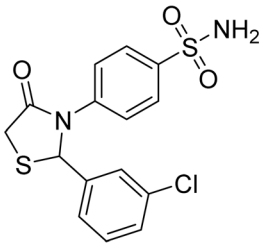

4-(2-(3-Chlorophenyl)-4-oxothiazolidin-3-yl) benzenesulfonamide

K_i = 2.2 nM for CA-IX

22

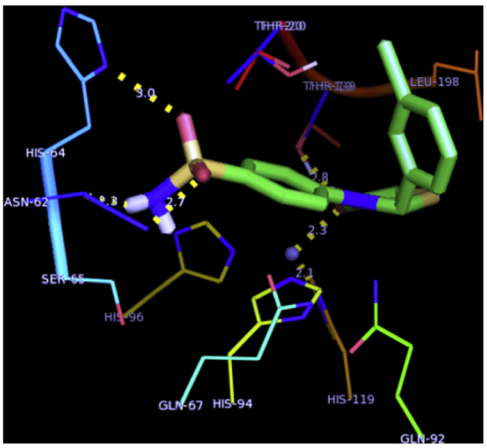

Fig. 14 Chemical structure and K_i value of compound **22** and its docking image inside the active pocket of CA-IX enzyme.

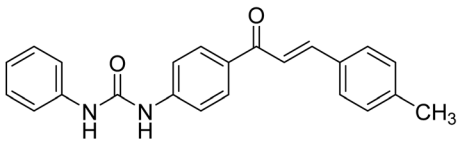

1-Phenyl-3-(4-(3-(*p*-tolyl)acryloyl)phenyl)urea

IC_{50} = 25.4 μM for hCA-I
IC_{50} = 27.2 μM for hCA-II

23

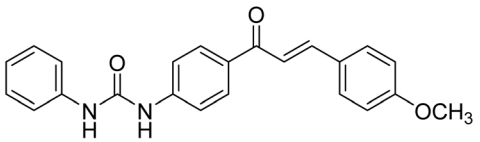

1-(4-(3-(4-Methoxyphenyl)acryloyl)phenyl)-3-phenylurea

IC_{50} = 23.1 μM for hCA-I
IC_{50} = 19.4 μM for hCA-II

24

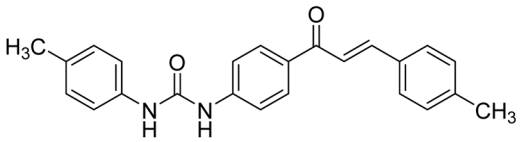

1-(*p*-Tolyl)-3-(4-(3-(*p*-tolyl)acryloyl)phenyl)urea

IC_{50} = 27.9 μM for hCA-I
IC_{50} = 14.4 μM for hCA-II

25

Fig. 15 Chemical structures of compounds **23**, **24** and **25** and their IC_{50} values against hCA-I and II.

osteoblast differentiation. By inhibiting CA activity, CAIs disrupt the delicate balance between bone resorption and formation, ultimately favoring bone preservation and remodeling.[83]

4.5.4 Selective targeting of CA isoforms. Selective inhibition of specific CA isoforms implicated in bone physiology offers the potential for tailored therapeutic interventions. Isoform-specific CAIs, such as CA-II and XII inhibitors, may provide enhanced efficacy and reduced off-target effects compared to non-selective inhibitors. Optimizing the selectivity and tissue specificity of CAIs is crucial for maximizing their therapeutic benefits in osteoporosis.[83]

4.5.5 Translational research and clinical perspectives. Clinical translation of CAIs for osteoporosis treatment is an area of active investigation. Early clinical trials have shown promising results regarding the efficacy and safety of CAIs in improving bone health parameters.[83]

5. Carbonic anhydrase inhibitors

Sławiński *et al.* (2013) synthesized a series of heterocyclic pyridine-3-sulfonamides and evaluated them against four isoforms of CA. The newly synthesized compounds displayed K_i values against hCA-I ranging from 169–5400 nM, against hCA-II ranging from 58.5–1238 nM, against hCA-IX ranging from 19.5–652 nM, and against hCA-XII ranging from 16.8–768 nM. Particularly, compounds **1–5**, which are pyrazole substituted pyridinesulfonamides, exhibited significant inhibitory efficacy against hCA-IX, with K_i values ranging from 19.5–48.6 nM, comparable to the clinically used sulfonamides such as acetazolamide (AAZ), methazolamide (MZA), ethoxazolamide (EZA)

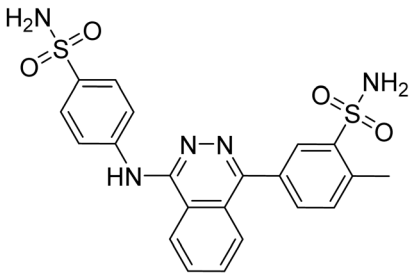

2-Methyl-5-(4-((4-sulfamoylphenyl)amino) phthalazin-1-yl)benzenesulfonamide

IC_{50} = 0.48 nM for CA-IX

26

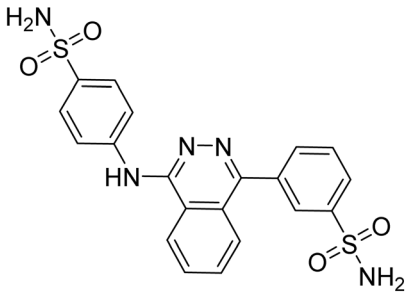

3-(4-((4-Sulfamoylphenyl)amino) phthalazin-1-yl)benzenesulfonamide

IC_{50} = 18.5 nM for CA-IX

27

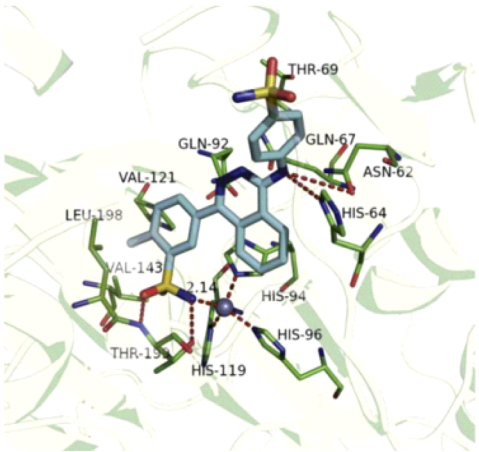

26

Fig. 16 Chemical structures of compounds **26** and **27** and their IC_{50} values against hCA-IX and docking image of compound **26** against CA-IX (PDB ID: 3IAI).

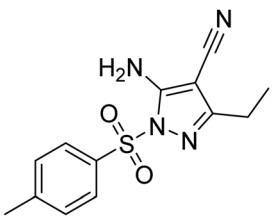

5-Amino-3-ethyl-1-(*p*-tosyl)-1*H*-pyrazole-4-carbonitrile

K_i = 0.47 μM for hCA-IX
K_i = 0.15 μM for hCA-XII

28

Fig. 17 Chemical structure of compound **28** and its K_i values against hCA-IX and XII.

and indisulam (IND) (with K_i values ranging from 24–50 nM)[84] (Table 2). Future studies exploring the SAR of these compounds, particularly focusing on the impact of substituents on their inhibitory potency and selectivity, would provide valuable insights for optimizing their pharmacological properties and therapeutic utility in treating diseases associated with CA dysregulation.

Supuran *et al.* (2013) synthesized a series of sulfamides containing the dopamine motif. These sulfamides were evaluated for their inhibitory effects on six α-CAs (CA-I, II, VA, IX, XII, and XIV). Compounds **6–10** showed excellent K_i values as compared to the standard AAZ (Table 3). These synthesized sulfamides exhibit potential for targeting medically relevant CA isoforms, suggesting promising applications in the treatment of epilepsy, obesity, tumors, or infections.[85]

Gencer *et al.* (2013) prepared a series of urea and thiourea derivatives, substituted with phthalazine and tested for their inhibitory effects on purified hCA-I and II. Compound **11** demonstrated the most potent inhibition (IC_{50} = 6.40 μM for hCA-I and 6.13 μM for hCA-II) (Fig. 8). This compound acts as a competitive inhibitor. The bulky nature of the synthesized compounds suggests a probable binding mode similar to coumarin derivatives rather than directly near the zinc ion.[86]

Altuntas *et al.* (2013) designed a series of 2-amino-3-cyanopyridine compounds and evaluated their inhibitory effects on hCA-I and II. Compounds **12** and **13** displayed the most promising K_i against hCA-I, with IC_{50} values of 33 and 34

Table 4 Chemical structures of substituted pyrazole derivatives, K_i values against CAIs

Compound no.	Chemical structures & IUPAC names	K_i (nM) CA-I	CA-II	CA-IX	CA-XII	Ref.
29	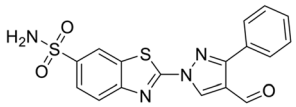 2-(4-Formyl-3-phenyl-1*H*-pyrazol-1-yl)-1,3-benzothiazole-6-sulfonamide	8806	10.9	1747	214	96
30	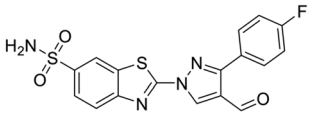 2-[3-(4-Fluorophenyl)-4-formyl-1*H*-pyrazol-1-yl]-1,3-benzothiazole-6-sulfonamide	15 690	10.4	1022	>10 000	96
31	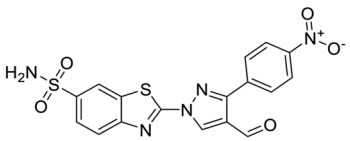 2-[4-Formyl-3-(4-nitrophenyl)-1*H*-pyrazol-1-yl]-1,3-benzothiazole-6-sulfonamide	2331	3.8	2109	74.5	96
32	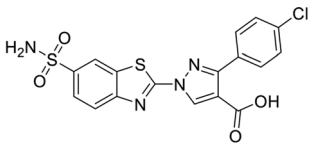 1-[6-(Aminosulfonyl)-1,3-benzothiazol-2-yl]-3-(4-chlorophenyl)-1*H*-pyrazole-4-carboxylic acid	407	7.3	2.8	5.5	96
33	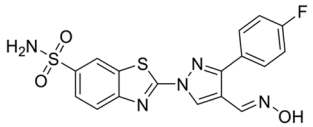 2-{3-(4-Fluorophenyl)-4-[(hydroxyimino)methyl]-1*H*-pyrazol-1-yl}-1,3-benzothiazole-6-sulfonamide	7161	8.5	224	83.8	96
34	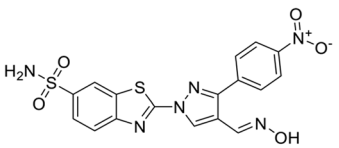 2-[4-[(Hydroxyimino)methyl]-3-(4-nitrophenyl)-1*H*-pyrazol-1-yl]-1,3-benzothiazole-6-sulfonamide	23 102	11.6	119	96.8	96
35	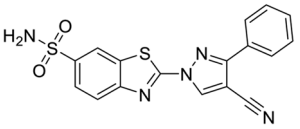 2-(4-Cyano-3-phenyl-1*H*-pyrazol-1-yl)-1,3-benzothiazole-6-sulfonamide	9819	139	81.6	6.6	96
36	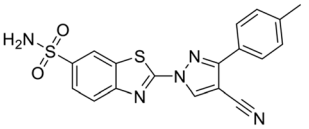 2-(4-Cyano-3-(4-methylphenyl)-1*H*-pyrazol-1-yl)-1,3-benzothiazole-6-sulfonamide	>50 000	48.1	186	7.2	96

Table 4 (*Contd.*)

Compound no.	Chemical structures & IUPAC names	K_i (nM) CA-I	CA-II	CA-IX	CA-XII	Ref.
37	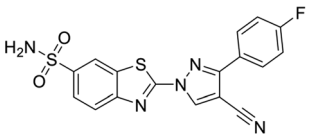 2-[4-Cyano-3-(4-fluorophenyl)-1*H*-pyrazol-1-yl]-1,3-benzothiazole-6-sulfonamide	12 108	27	739	7.4	96
Standard	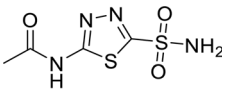 Acetazolamide (AAZ)	250	12	25	5.7	96

Table 5 Chemical structures of substituted benzenesulfonamide bearing different heterocyclic moieties, inhibition data against CAIs

Compound no.	Chemical structures & IUPAC names	K_i (nM) CA-I	CA-II	CA-IX	CA-XII	Ref.
38	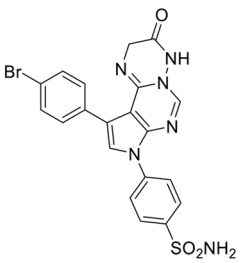 4-(10-(4-Bromophenyl)-3-oxo-3,4-dihydropyrrolo [2',3':4,5]pyrimido[1,6-*b*][1,2,4]triazin-8(2*H*)-yl) benzenesulfonamide	94.1	4.9	11.7	0.76	97
39	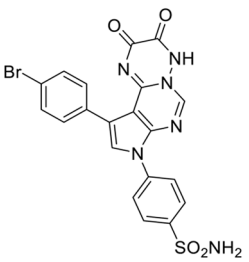 4-(10-(4-bromophenyl)-2,3-dioxo-3,4-dihydropyrrolo [2',3':4,5]pyrimido[1,6-*b*][1,2,4]triazin-8(2*H*)-yl) benzenesulfonamide	69.1	64.3	325	0.912	97
40	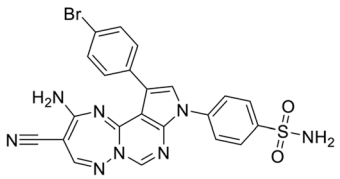 *p*-{13-Amino-3-(*p*-bromophenyl)-12-cyano-5,7,9,10,14-pentazatricyclo-[7.5.-0-.02,6]-tetradeca-1(14),2(6), 3,7,10,12-hexaen-5-yl}benzenesulfonamide	80.4	5.2	3.1	0.9	97

Table 5 (*Contd.*)

Compound no.	Chemical structures & IUPAC names	K_i (nM) CA-I	CA-II	CA-IX	CA-XII	Ref.
41	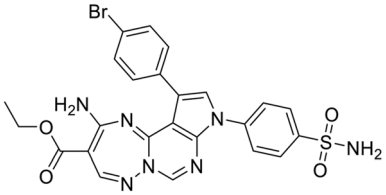 *p*-{13-Amino-3-(*p*-bromophenyl)-12-ethoxycarbonyl-5,7,9,10,14-pentazatricyclo [7.5.0.02,6]tetradeca-1(14),2(6),3,7, 10,12-hexaen-5-yl}benzenesulfonamide	126	7.3	3	0.83	97
42	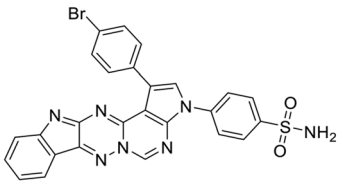 *p*-{5-(*p*-Bromophenyl)-2,7,9,11,12,20-hexazapenta cyclo-[11.7.0.03,11.04,8.014,19]-icosa-1(20), 2,4(8),5,9,12,14(19),15,17-nonaen-7-yl} benzenesulfonamide	498	8.5	2.7	0.72	97
43	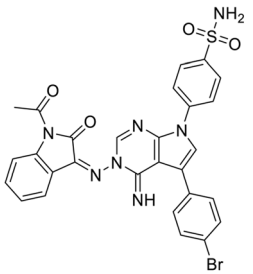 4-(3-(1-Acetyl-2-oxoindolin-3-ylideneamino)-5-(4-bromophenyl)-4-imino-3,4-dihydropyrrolo [2,3-*d*]pyrimidin-7-yl)benzenesulfonamide	25.1	5.6	3.1	0.81	97
44	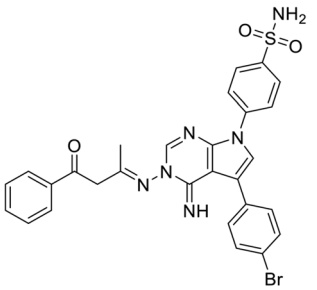 4-(5-(4-Bromophenyl)-4-imino-3-(4-oxo-4-phenylbutan-2-ylidene-amino)-3,4-dihydropyrrolo[2,3-*d*]pyrimidin-7-yl)benzenesulfonamide	16.3	3.9	2.8	0.94	97
Standard	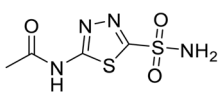 Acetazolamide (AAZ)	250	12.1	25	5.7	97

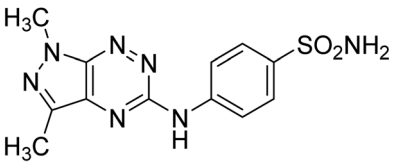

4-((1,3-Dimethyl-1*H*-pyrazolo[4,3-e][1,2,4] triazin-5-yl)amino)benzenesulfonamide

K_i = 270 μM for hCA-I
K_i = 8 μM for hCA-II
K_i = 43.8 μM for hCA-IX
K_i = 7.9 μM for hCA-XII

45

Fig. 18 Chemical structure of compound **45** and its K_i values against hCA-I, II, IX, XII.

μM and K_i values of 23.8 and 31 μM, respectively. Compound **12** exhibited the highest activity against hCA-II, showing an IC_{50} value of 56 μM and a K_i value of 41 μM, compared to the standard sulfanilamide, which has K_i values of 25.5 μM and 0.023 μM for hCA-I and II, respectively (Fig. 9). The target compounds act as a competitive inhibitors.[87]

Zhu *et al.* (2013) synthesized a series of sulfonamides incorporating coumarin moieties and determined their inhibitory effects on two CAs. These compounds were tested against the hCA-II and IX. Among them, compound **14** demonstrated the maximum potency against hCA-II with an IC_{50} = 23 nM, while compound **15** showed the strongest inhibition of hCA-IX with an IC_{50} = 24 nM as compared to standards AAZ and SA. These sulfonamides, bearing coumarin moieties, hold promise as lead candidates for targeting tumor-associated CA isozymes (Fig. 10).[88]

Table 6 Chemical structures of substituted aminobenzene sulfonamides along with dissociation constant data against hCA-II and IX

Compound no.	Chemical structures & IUPAC names	K_d (μM) CA-II	K_d (μM) CA-XII	Ref.
46	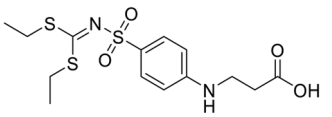 3-[(4-{[Bis(ethylthio)methylene]sulfamoyl }phenyl)amino]propanoic acid	40	>200	99
47	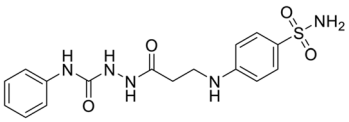 *N*-[(Phenylcarbamoyl)amino]-3-[(4-sulfamoyl phenyl)amino]propanamide	4.0	1.85	99
Standard	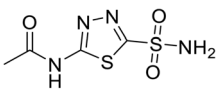 Acetazolamide (AAZ)	0.017	0.133	99

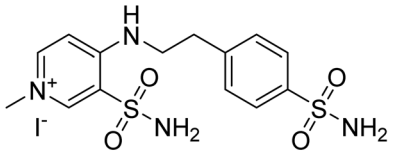

3-Sulfamoyl-4-[2-(4-sulfamoylphenyl) ethylamino]-1-methylpyridinium iodide

K_i = 923 nM for hCA-I
K_i = 61.3 nM for hCA-II
K_i = 5.9 nM for hCA-IX
K_i = 4.3 nM for hCA-XII

48

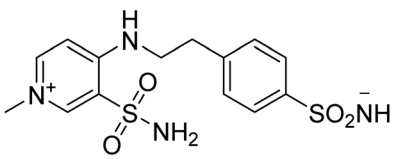

((4-(2-((1-Methyl-3-sulfamoylpyridin-1-ium-4-yl)amino)ethyl)phenyl)sulfonyl)amide

K_i = 887 nM for hCA-I
K_i = 60.1 nM for hCA-II
K_i = 6.2 nM for hCA-IX
K_i = 4.0 nM for hCA-XII

49

Fig. 19 Chemical structure of compounds **48** and **49** and their K_i values against hCA isoforms.

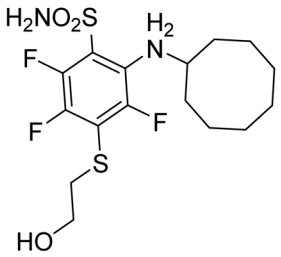

2-(Cyclooctyl-λ^4-azaneyl)-3,5,6-trifluoro-4-((2-hydroxyethyl)thio)benzenesulfonamide

K_d = 1.1 nM for hCA-IX

50

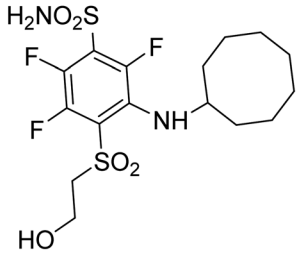

3-(Cyclooctylamino)-2,5,6-trifluoro-4-((2-hydroxyethyl)sulfonyl)benzenesulfonamide

K_d = 0.05 nM for hCA-IX

51

Fig. 20 Chemical structure of compounds **50** and **51** and their K_d values against hCA isoforms.

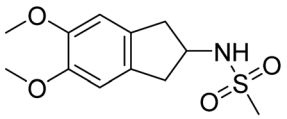

***N*-(5,6-Dimethoxy-2,3-dihydro-1H-inden-2-yl)methanesulfonamide**

K_I = 46 μM for hCA-I

K_I = 372 μM for hCA-II

58

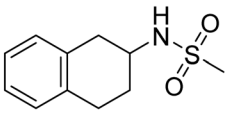

***N*-(1,2,3,4-Tetrahydronaphthalene-2-yl) methanesulfonamide**

K_I = 228 μM for hCA-I

K_I = 94 μM for hCA-II

59

Fig. 21 Chemical structure of compounds **58** and **59** and their K_d values against hCA-I and II.

Büyükkıdan *et al.* (2013) developed Co(II) complexes with pyrazole and evaluated their carbonic anhydrase inhibitory activity. For hCA-I, compounds **16** and **17** had IC_{50} values of 0.473 μM and 0.065 μM, respectively, while for hCA-II, the IC_{50} values were 0.213 μM and 0.833 μM. In esterase activity assays, IC_{50} values were 0.058 μM and 0.297 μM for hCA-I, and 0.110 μM and 0.052 μM for hCA-II. The K_i for esterase activity were 0.039 μM and 0.247 μM for hCA-I, and 0.078 μM and 0.363 μM for hCA-II (Fig. 11).[89]

Gençer *et al.* (2013) designed and synthesized a series of water-soluble benzimidazolium chloride salts, bearing chromone moiety and evaluated them against hCA-I and II. Results demonstrated inhibition of hCA isoenzyme activity by all synthesized compounds. Notably, compounds **18** and **19** demonstrated the highest activity against hCA-I and II, with IC_{50} values of 22.09 μM and 20.33 μM, respectively (Fig. 12).[90]

Ok *et al.* (2013) designed and synthesized a new series of pyrazole derivatives and evaluated against hCA enzymes. Remarkably, compounds **20** (K_i = 0.108 μM for hCA-I and 0.055 μM for hCA-II) and **21** (K_i = 0.129 μM for hCA-I and 0.064 μM for hCA-II) exhibited the maximum inhibition of both hCA-I and II isozymes (Fig. 13). Both derivatives act as a non-competitive inhibitor. Furthermore, the presence of resonance structures in the molecules reduces their inhibitory effect. The findings suggest that minor alterations in the –R moiety (substituents) significantly impact inhibitory activity. Additionally, the compounds' hydrogen bonding capability and hydrophilic/hydrophobic properties may influence their inhibition behavior. Overall, the study provides insights into the potential of pyrazole carboxamide derivatives as inhibitors of hCA enzymes.[91]

Suthar *et al.* (2013) designed sulfonamide derivatives as selective inhibitors of CA-IX for potential anti-cancer applications. Among the compounds tested, **22** emerged as the most potent CA-IX inhibitor with K_i value of 2.2 nM as compared to the standard AAZ (K_i = 25.2 nM). Moreover, studies revealed that **22** induced apoptosis in COLO-205 cells, characterized by cell shrinkage and nuclear fragmentation. In a solid tumor model, **22** reduced tumor volume by 64.83% with minimal increase in body weight, indicating its potential as an effective anticancer agent. Among the compounds screened virtually, compound **22** exhibited the lowest estimated free energy of binding at −7.15 kcal mol^{-1}. Molecular docking analysis indicated that compound **22**, the most potent inhibitor, could interact with the catalytic Zn(II) ion, which may account for its higher binding affinity for CA-IX (Fig. 14).[92]

Gençer *et al.* (2013) synthesized a series of phenylurea/phenylthiourea-substituted chalcones and investigated them against CA enzymes. Compounds **23** and **24** exhibited the highest activity against hCA-I with IC_{50} values of 25.4 μM and 23.1 μM, respectively. Compound **25** demonstrated the maximum activity against hCA-II with an IC_{50} value of 14.4 μM (Fig. 15).[93]

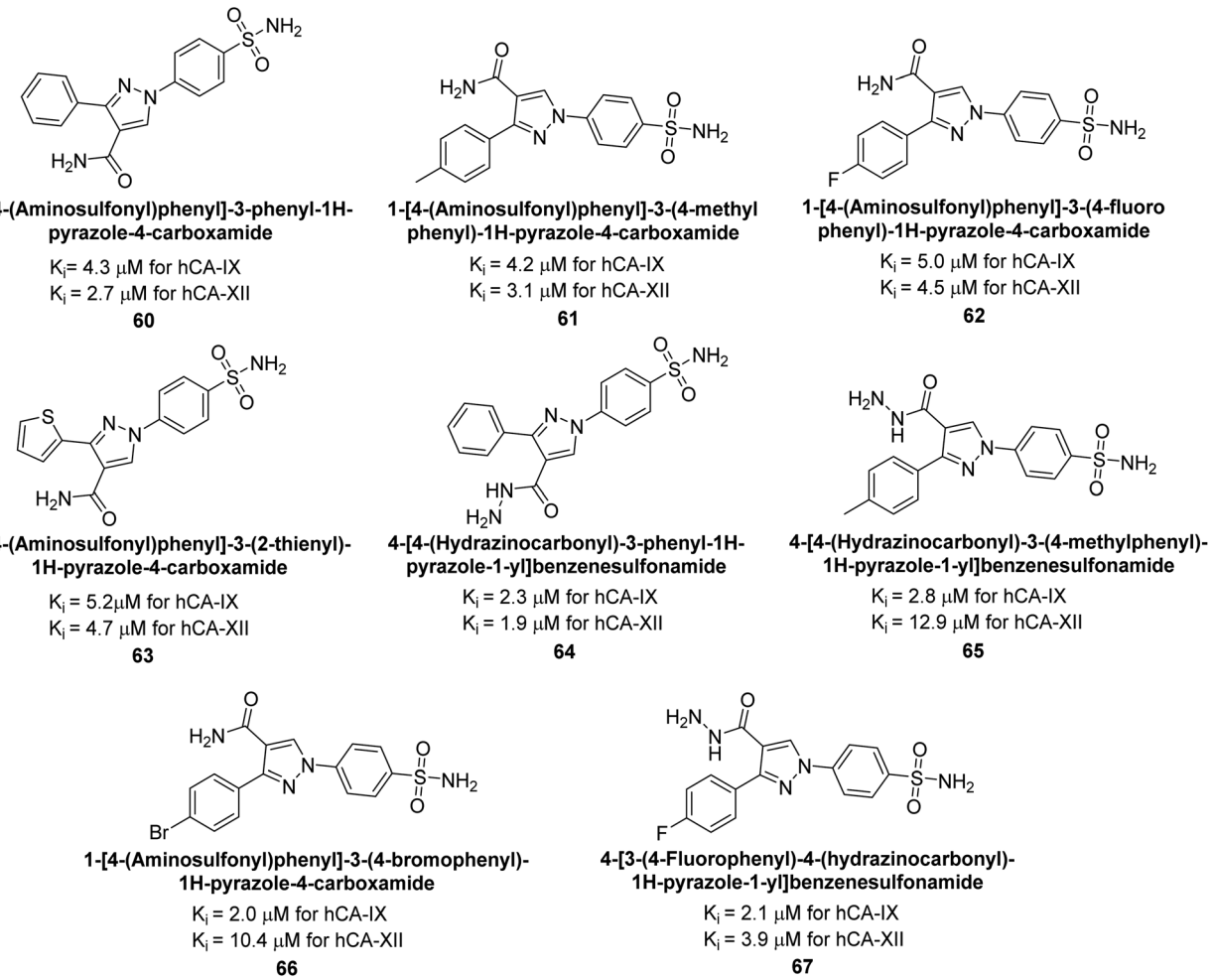

Fig. 22 Chemical structure of compounds 60–67 and their K_i values against hCA-IX and XII.

Xu *et al.* (2013) synthesized a series of new heterocyclic substituted benzene sulfonamides compound **26** emerged as the most potent and selective, inhibiting CA-IX at subnanomolar levels (IC_{50} of 0.48 nM), representing a 40-fold increase in potency compared to the lead compound **27** (IC_{50} = 18.5 nM). Furthermore, it exhibited over 103-fold selectivity over CA-I and CA-II (Fig. 16). Compound **26** exhibits a similar interaction profile: the sulfonamide nitrogen forms a hydrogen bond with the hydroxyl group of Thr199, and one of the sulfonamide oxygens interacts with the backbone amide of Thr199. The benzene rings engage with Val121, Val143, and Leu198 in the hydrophobic region, where methyl groups enhance the affinity. Introducing a methyl group at the *o*-position of the left benzenesulfonamide produced two highly effective CA-IX inhibitors. In the hydrophilic pocket, the linker NH forms hydrogen bonds with His64 and Asn62, which contribute to the high binding affinities for CA-IX (Fig. 16).[94]

Allouche *et al.* (2013) designed and synthesized a series of aminocyanopyrazole derivatives and evaluated their inhibitory effects on hCA-IX and XII. Compound **28** exhibited stronger inhibition against the tumor-associated transmembrane isoforms hCA-IX (K_i = 0.15 μM) and hCA-XII (K_i = 0.47 μM) compared to the cytosolic ones (Fig. 17).[95]

Supuran *et al.* (2014) synthesized and evaluated 1,3-diarylpyrazoles. Inhibition assays against hCA-II revealed that all synthesized compounds displayed varying degrees of inhibition, ranging from excellent to moderate. Specifically, compounds **29**, **30**, **31**, **32**, **33**, and **34** exhibited K_i values less than 12 nM, comparable to the K_i value of AAZ. Most compounds exhibited moderate inhibition of hCA-IX, except compound **32**, which displayed nearly 9 times greater potency compared to AAZ. In the case of hCA-XII, compounds **32**, **35**, **36**, and **37** displayed K_i values comparable to that of AAZ (Table 4).[96]

Ghorab *et al.* (2014) synthesized benzenesulfonamides incorporating various heterocyclic moieties exhibit promising inhibitory activity against hCA-I, II, IX and XII. Among the investigated compounds, derivatives **38**, **39**, and **40–44** demonstrated notable potency as inhibitors of hCA-IX and XII (Table 5). Their inhibitory activity was particularly significant, falling within the nanomolar and subnanomolar ranges, indicating high efficacy. Moreover, these compounds exhibited considerable selectivity towards the targeted isoforms. Overall, the findings of this study highlight the importance of rational

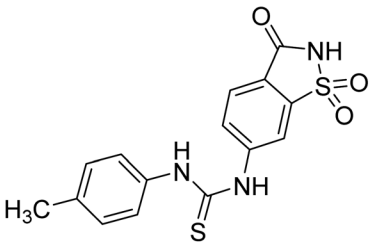

1-(1,1-Dioxido-3-oxo-2,3-dihydrobenzo[*d*] isothiazol-6-yl)-3-(*p*-tolyl)thiourea

IC_{50} = 13.67 μM for hCA-I
IC_{50} = 11.14 μM for hCA-II

68

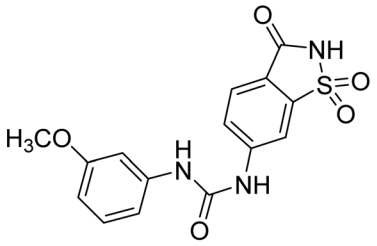

1-(1,1-Dioxido-3-oxo-2,3-dihydrobenzo[*d*] isothiazol-6-yl)-3-(3-methoxyphenyl)urea

IC_{50} = 41.65 μM for hCA-I
IC_{50} = 6.54 μM for hCA-II

69

Fig. 23 Chemical structure of compounds **68** and **69** and their IC_{50} values against hCA-I and II.

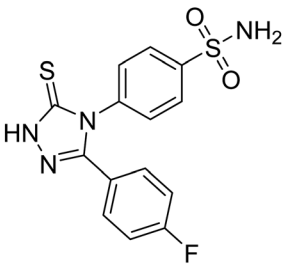

4-[3-(4-Fluorophenyl)-5-thioxo-1,5-dihydro-4H-1,2,4-triazol-4-yl]benzenesulfonamide

K_i = 2.8 μM for hCA-IX
K_i = 4.9 μM for hCA-XII

70

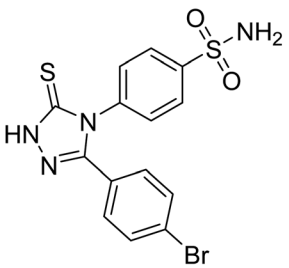

4-[3-(4-Bromophenyl)-5-thioxo-1,5-dihydro-4H-1,2,4-triazol-4-yl]benzenesulfonamide

K_i = 7.6 μM for hCA-IX
K_i = 1.3 μM for hCA-XII

71

Fig. 24 Chemical structure of compounds **70** and **71** and their K_i values against hCA-XI and XII.

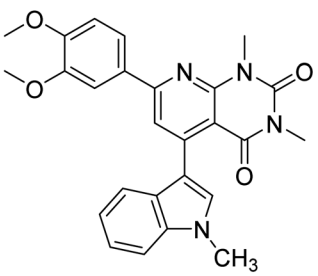

7-(3,4-Dimethoxyphenyl)-1,3-dimethyl-5-(1-methyl-1H-indol-3-yl)pyrido[2,3-d]pyrimidine-2,4(1H,3H)-dione

IC_{50} = 6.79 μM for hCA-I
IC_{50} = 8.06 μM for hCA-II

72

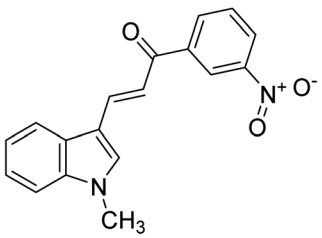

3-(1-Methyl-1H-indol-3-yl)-1-(3-nitrophenyl) prop-2-en-1-one

IC_{50} = 8.38 μM for hCA-I
IC_{50} = 7.22 μM for hCA-II

73

Fig. 25 Chemical structure of compounds **72** and **73** and their IC_{50} values against hCA-I and II.

design and synthesis in the development of novel CAIs with potential therapeutic applications.[97]

Mojzych *et al.* (2014) reported pyrazolo-triazine sulfonamides have emerged as a class of compounds with promising CA inhibitory activity. The pyrazolo-triazine scaffold offers structural diversity and flexibility, making it an attractive platform for the synthesis of novel hCAIs. Compound **45** showed good to moderate inhibitory activity against the isoforms of hCA. The hCA-I and hCA-II showed $K_i = 270$ μM and 8 μM, respectively (Fig. 18). The newly synthesized compounds showed negligible activity as inhibitors of hCA-I and displayed weak inhibition against hCA-II. Henceforth, compound **45**

Table 7 Chemical structures of substituted sulfonamides, inhibition data against CAIs

Compound no.	Chemical structures & IUPAC names	K_i (nM) CA-I	CA-II	CA-IX	CA-XII	Ref.
52	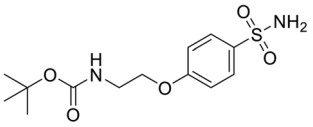 *tert*-Butyl 2-(4-sulfamoylphenoxy)-ethylcarbamate	5.3	5.0	8.3	7.2	102
53	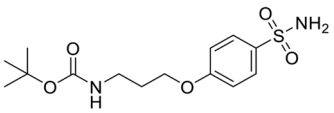 *tert*-Butyl 3-(4-sulfamoylphenoxy)-propylcarbamate	6.6	5.1	5.8	6.5	102
54	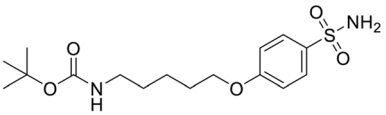 *tert*-Butyl 5-(4-sulfamoylphenoxy)-pentylcarbamate	7.9	5.5	7.1	5.7	102
55	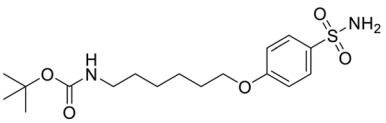 *tert*-Butyl 6-(4-sulfamoylphenoxy)-hexylcarbamate	6.1	5.2	6.9	6.4	102
56	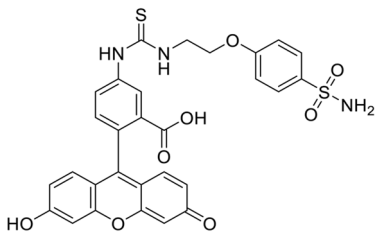 2-(6-Hydroxy-3-oxo-3*H*-xanthen-9-yl)-5-{3-[2-(4-sulfamoylphenoxy)-ethyl]-thioureido}-benzoic acid	18.0	5.0	8.5	8.6	102
57	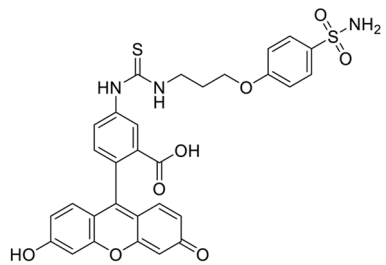 2-(6-Hydroxy-3-oxo-3*H*-xanthen-9-yl)-5-{3-[3-(4-sulfamoylphenoxy)-propyl]-thioureido}-benzoic acid	17.1	4.6	7.2	5.7	102
Standard	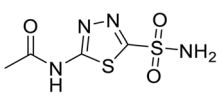 Acetazolamide (AAZ)	250	12.1	25	5.7	102

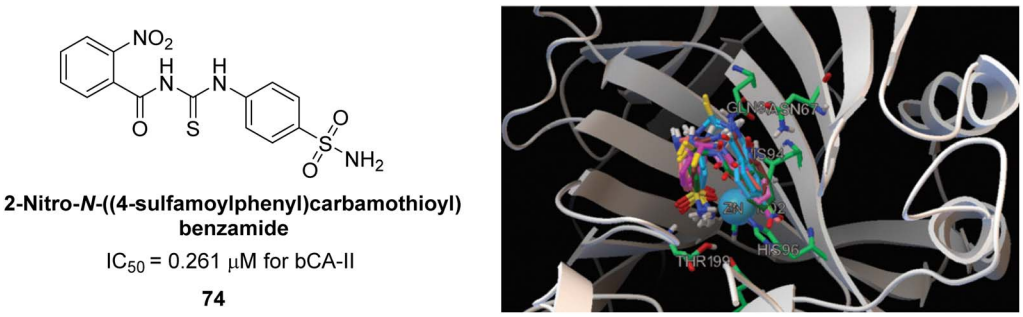

Fig. 26 Chemical structure of compound **74** and its IC_{50} value against bCA-II along with its docking image.

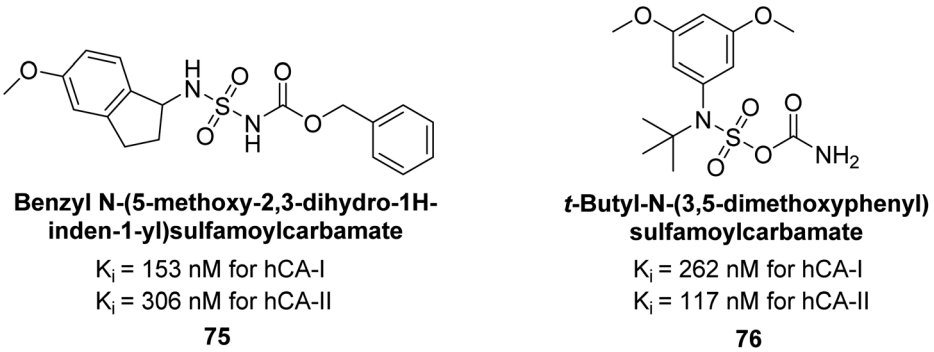

Fig. 27 Chemical structure of compounds **75** and **76** and their K_i values against hCA-I and II.

exhibited enhanced efficacy against the hCA-IX (K_i = 43.8 μM) and XII (K_i = 7.9 μM).[98]

Matulis *et al.* (2014) investigated the inhibitory potential of 4-amino-substituted benzenesulfonamides on hCAs. The majority of *N*-aryl-β-alanine derivatives exhibited enhanced binding affinity for hCA-II, whereas diazobenzenesulfonamides demonstrated nanomolar affinities specifically towards the hCA-I isozyme. Most *N*-aryl-β-alanine derivatives exhibited higher affinities for hCA-II compared to other tested CA isoforms. Notably, compound **46**, containing the tertiary sulfonamide group, exclusively bound to hCA-II (K_d = 40 μM). Compound **47** demonstrated increased binding potency towards hCA-XII (K_d = 1.85 μM) relative to other isoforms and standard AAZ (Table 6). Moreover, SAR analysis reveals key structural features that contribute to enhanced inhibition. Further investigations, including *in vivo* studies and optimization of pharmacokinetic properties, are warranted to advance these compounds toward clinical applications in diseases where hCA inhibition is therapeutically beneficial.[99]

Sławiński *et al.* (2014) synthesized and evaluated a series of novel N4-substituted 4-(2-aminoethyl)benzenesulfonamides as inhibitors against four isoforms of hCAs. Particularly, excellent inhibitory activity was observed against hCA-IX and XII. Among the target analogues, noteworthy K_i against hCA-IX (K_i = 5.9–10.7 nM) was observed, surpassing clinically utilized CAIs such as AAZ, DCP, EZA, MZA and IND (24–50 nM). Compounds **48** and **49** emerged as the excellent inhibitors against hCA-IX and hCA-XII (K_i = 5.9 and 6.2 nM for hCA-IX; 4.3 and 4.0 nM for hCA-XII, respectively), characterized by their cationic nature and significant affinity for hCA-IX and XII rather than the hCA-I and II (Fig. 19).[100]

Matulis *et al.* (2014) synthesized fluorinated benzenesulfonamides, featuring various substituents on the aryl ring. Several of these compounds exhibited strong and selective inhibition against CA-IX. The introduction of three fluorine atoms especially enhanced affinity by electron withdrawal, thereby lowering the pK_a of the benzenesulfonamide group. Compound **50** (K_d = 1.1 nM), which features bulky *o*-substituents, was observed to fit most effectively into the hydrophobic pocket of the hCA-IX active site but not in hCA-II, as demonstrated by co-crystal structure analysis with chimeric CA-IX. The most potent inhibitor compound **51** achieved an affinity of 0.050 nM for the catalytic domain of recombinant human CA-IX in human cells (Fig. 20). However, this heightened affinity compromised selectivity. The inhibitors identified in this study lay the groundwork for the development of novel anticancer therapeutics targeting hCA-IX.[101]

Supuran *et al.* (2014) synthesized a variety of fluorescent sulfonamides and demonstrated intriguing inhibitory properties against hCA-IX and XII. All derivatives **52–57** reported in this study exhibited potent inhibition against hCA-IX, with K_i values ranging from 5.8 to 32.6 nM. For instance, Boc-protected derivatives **52–55** displayed minimal variation in inhibition constants, ranging from 5.8 to 8.3 nM, while fluorescent sulfonamides **56** and **57** demonstrated consistent inhibitory activity (Table 7).[102]

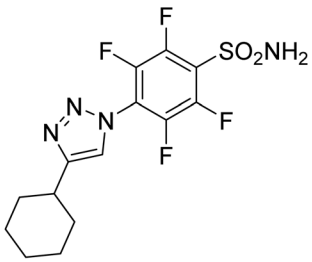

4-(4-Cyclohexyl-1*H*-1,2,3-triazol-1-yl)-2,3,5,6-tetrafluorobenzenesulfonamide

K_i = 1.5 nM for hCA-IX
K_i = 0.8 nM for hCA-XII

77

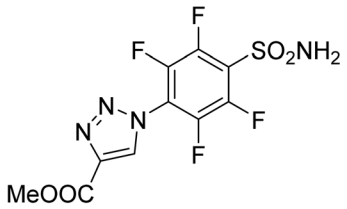

Methyl 1-(2,3,5,6-tetrafluoro-4-sulfamoyl phenyl)-1*H*-1,2,3-triazole-4-carboxylate

K_i = 115 nM for hCA-IX
K_i = 58.9 nM for hCA-XII

78

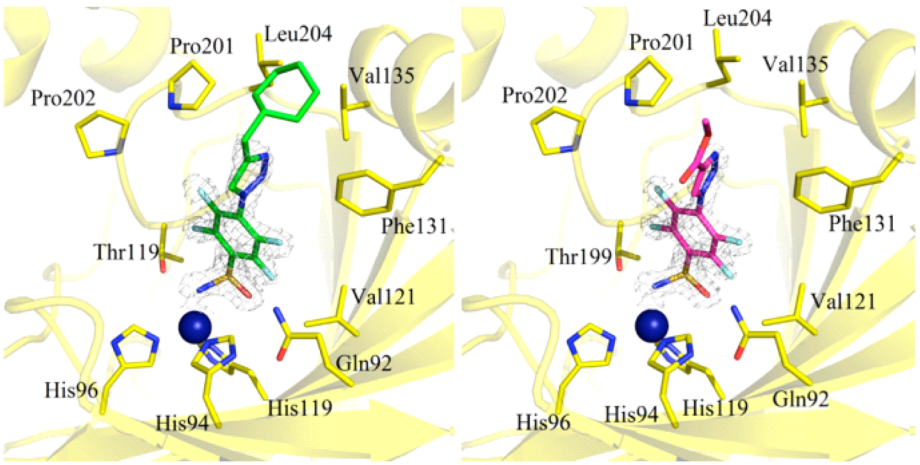

77 **78**

Fig. 28 Chemical structure of compounds **77** and **78** and their K_i values against hCA-IX and XII.

Göksu *et al.* (2014) synthesized sulfonamides and assessed their inhibitory effects on hCA-I and II. Among the synthesized analogs, compound **58** showed the most potent inhibition of hCA-I, with a K_i value of 46 μM and an r^2 of 0.978. In contrast, compound **59** demonstrated the highest inhibition of hCA-II, with a K_i value of 94 μM and an r^2 of 0.982 (Fig. 21). Further research and optimization of these compounds could lead to the development of new pharmaceutical agents with improved selectivity and efficacy for CA inhibition.[103]

Sharma *et al.* (2014) designed, synthesized and evaluated a library of 4-functionalized 1,3-diarylpyrazoles against hCA-I,

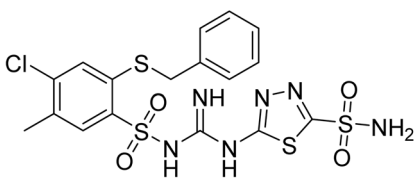

1-(2-Benzylthio-4-chloro-5-methylbenzenesulfonyl)-3-(2-sulfamoyl-1,3,4-thiadiazol-5-yl)guanidine

K_i = 4.7 nM for hCA-IX
K_i = 0.96 nM for hCA-XII

79

Fig. 29 Chemical structure of compound **79** its K_i values against hCA-IX and XII.

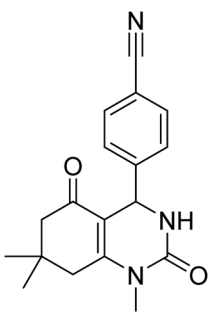

4-(1,7,7-trimethyl-2,5-dioxo-1,2,3,4,5,6,7,8-octahydroquinazoline-4-yl)benzonitrile

IC_{50} = 0.05 μM for hCA-I

80

Fig. 30 Chemical structure of compound **80** and its IC_{50} value against hCA-I.

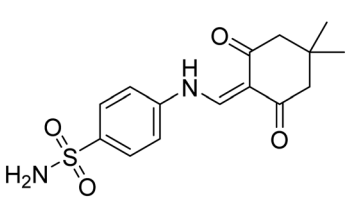

4-((4,4-Dimethyl-2,6-dioxocyclohexylidene) methylamino)benzene-sulfonamide

IC_{50} = 2.12 μM for hCA-I
IC_{50} = 6.41 μM for hCA-II

81

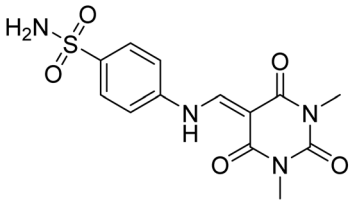

4-((1,3-Dimethyl-2,4,6-trioxo-tetrahydropyrimidin-5(6H)-ylidene)methylamino)benzene-sulfonamide

IC_{50} = 5.20 μM for hCA-I
IC_{50} = 2.52 μM for hCA-II

82

Fig. 31 Chemical structures of compounds **81** and **82** and their IC_{50} values against hCA-I and II.

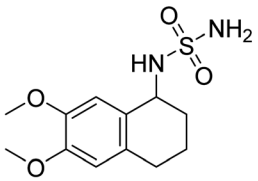

***N*-(6,7-Dimethoxy-1,2,3,4-tetrahydro naphthalen-1-yl)-sulphamide**

K_i = 0.71 μM for hCA-I
K_i = 0.69 μM for hCA-II

83

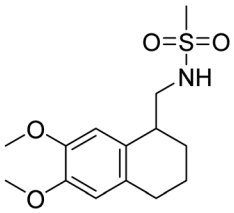

***N*-((6,7-Dimethoxy-1,2,3,4-tetrahydro naphthalen-1-yl)-methyl)methanesulphonamide**

K_i = 1.56 μM for hCA-I
K_i = 0.39 μM for hCA-II

84

Fig. 32 Chemical structure of compounds **83** and **84** and their K_i values against hCA-I and II.

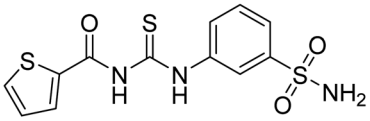

1-(2-Thienylcarbonyl)-3-(3-amino sulfonylphenyl)thiourea

IC_{50} = 0.052 μM for bCA-II

85

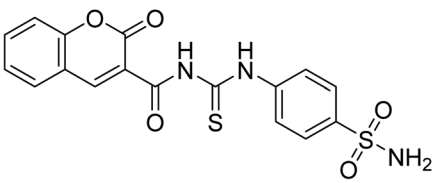

1-(-Oxo-2H-chromene-3-carbonyl)-3-(4-aminosulfonylphenyl)thiourea

IC_{50} = 0.011 μM for bCA-II

86

Fig. 33 Chemical structure of compounds **85** and **86** and their IC_{50} values against bCA-II.

II, IX and XII. Remarkably, compounds **60–65** exhibited low K_i < 5 nM for hCA-IX, while compounds **60**, **61**, **62**, **63**, **66** and **67** displayed K_i < 10 nM against hCA-XII (Fig. 22). Furthermore, these derivatives acted as selective hCAIs for isoforms IX and XII over the I and II and as compared to standard AAZ. Additionally, the compounds described in this study demonstrated noteworthy antitumor efficacy, indicating the need for further exploration to expand the understanding of the SAR within this intriguing class of sulfonamide CAIs.[104]

Gençer *et al.* (2014) investigated saccharin derivatives on purified hCA-I and II using CO_2 as a substrate. The findings revealed that all tested analogues exhibited inhibitory effects on both hCA-I and II enzyme activities. Particularly, compound **68** displayed the highest activity against hCA-I (IC_{50} = 13.67 μM), while compound **69** exhibited the greatest activity against hCA-II (IC_{50} = 6.54 μM) (Fig. 23). SAR analysis indicated that, generally, thiourea derivatives displayed greater inhibition of both hCA-I and II compared to urea derivatives. Based on the findings, it is suggested that saccharin derivatives hold a promising potential for the treatment of glaucoma.[105]

Sharma *et al.* (2014) designed triazole-based benzenesulfonamides and evaluated their inhibitory effects against hCA-IX and XII. All target derivatives showed moderate to good inhibitory potential, with K_i values ranging from 2.8 to 431 nM and 1.3 to 63 nM, against hCA-IX and XII, respectively. Compounds **70** and **71**, identified as the most potent inhibitors of hCA-IX

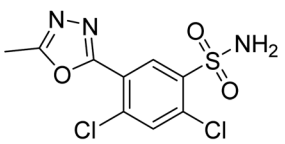

2,4-Dichloro-5-(5-methyl-1,3,4-oxadiazol-2-yl) benzenesulfonamide

K_i = 718 nM for hCA-I
K_i = 8.7 nM for hCA-II
K_i = 2.8 nM for hCA-IX
K_i = 6.3 nM for hCA-XII

87

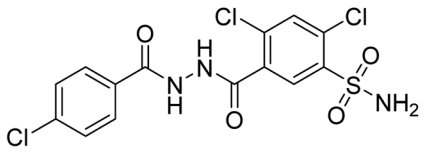

2,4-Dichloro-5-[2-(4-chlorobenzoyl)hydrazine carbonyl]benzenesulfonamide

K_i = 3025 nM for hCA-I
K_i = 10.1 nM for hCA-II
K_i = 4.8 nM for hCA-IX
K_i = 2.7 nM for hCA-XII

88

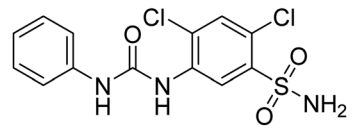

2,4-Dichloro-5-(3-phenylureido) benzenesulfonamide

K_i = 2340 nM for hCA-I
K_i = 44 nM for hCA-II
K_i = 7.0 nM for hCA-IX
K_i = 2.8 nM for hCA-XII

89

Fig. 34 Chemical structure of compounds **87**, **88** and **89** and their K_i values against hCA-I, II, IX and XII.

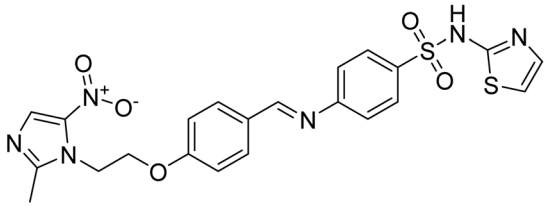

4-(4-(2-(2-Methyl-5-nitro-1H-imidazole-1-yl)ethoxy)benzylideneamino)-N-(thiazol-2-yl)benzenesulfonamide

K_i = 16 nM for hCA-II
K_i = 93 nM for hCA-IX

90

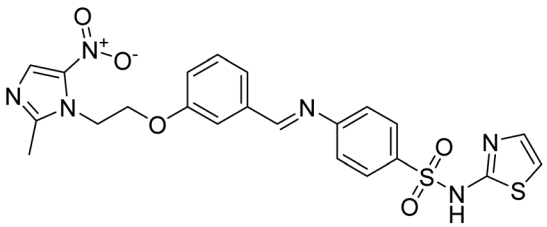

4-(3-(2-(2-Methyl-5-nitro-1H-imidazole-1-yl)ethoxy)benzylideneamino)-N-(thiazol-2-yl)benzenesulfonamide

K_i = 89 nM for hCA-II
K_i = 38 nM for hCA-IX

91

Fig. 35 Chemical structure of compounds **90** and **91** and their K_i values against hCA-I, II, IX and XII.

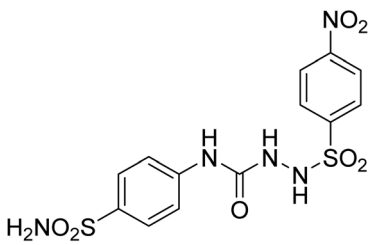

2-((4-Nitrophenyl)sulfonyl)-*N*-(4-sulfamoyl phenyl)hydrazine-1-carboxamide

K_i = 6.0 nM for hCA-II
K_i = 0.79 nM for hCA-IX

92

Fig. 36 Chemical structure of compound **92** and their K_i values against hCA-II and IX.

and XII, exhibited significantly higher IC_{50} as compared to the standard AAZ (Fig. 24). Additionally, the activity profile revealed that both the nuclear triazole scaffold and triazole fused with thiadiazines serve as highly effective inhibitors of hCA-IX and XII.[106]

Gençer *et al.* (2014) investigated the inhibitory effects of indolylchalcones and pyrimidines on hCA-I and II. Among the synthesized derivatives, **72** and **73** exhibited the highest inhibitory activities against hCA-I (IC_{50} = 6.79 μM) and hCA-II (IC_{50} = 7.22 μM), respectively (Fig. 25). SAR analysis indicated that chalcones exhibited greater IC_{50} values than pyrimidine derivatives against both hCA-I and II. Furthermore, the presence of a methyl group bonded to the uracil ring increased inhibitory activities against both hCA-I and II. Hence, the compounds

Table 8 Chemical structures of substituted pyrazoline along with dissociation constant data against hCA-II and IX

Compound no.	Chemical structures & IUPAC names	K_i (nM) hCA-II	K_i (nM) hCA-XII	Ref.
93	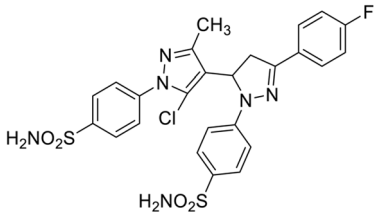 4,4'-(5'-Chloro-5-(4-fluorophenyl)-3'-methyl-3,4-dihydro-1'*H*,2*H*-[3,4'-bipyrazole]-1',2-diyl) dibenzenesulfonamide	1.4	3.0	119
94	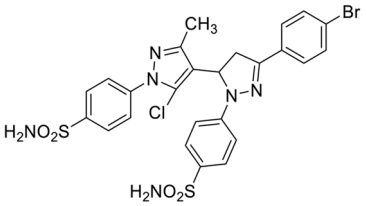 4,4'-(5-(4-Bromophenyl)-5'-chloro-3'-methyl -3,4-dihydro-1'*H*,2*H*-[3,4'-bipyrazole]-1',2-diyl) dibenzenesulfonamide	5.5	0.47	119
95	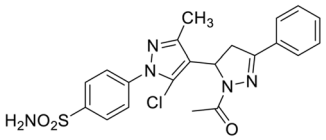 4-(2-Acetyl-5'-chloro-3'-methyl-5-phenyl-3,4-dihydro-1'*H*,2*H*-[3,4'-bipyrazol]-1'-yl) benzenesulfonamide	0.17	0.58	119
96	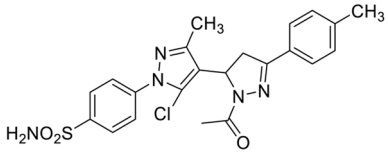 4-(2-Acetyl-5'-chloro-3'-methyl-5-(*p*-tolyl)-3,4-dihydro-1'*H*,2*H*-[3,4'-bipyrazol]-1'-yl) benzenesulfonamide	0.54	4.0	119
97	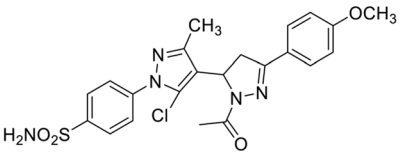 4-(2-Acetyl-5'-chloro-5-(4-methoxyphenyl)-3'-methyl-3,4-dihydro-1'*H*,2*H*-[3,4'-bipyrazol] -1'-yl)benzenesulfonamide	1.1	0.54	119
98	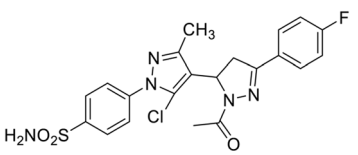 4-(2-Acetyl-5'-chloro-5-(4-fluorophenyl)-3'-methyl -3,4-dihydro-1'*H*,2*H*-[3,4'-bipyrazol]-1'-yl) benzenesulfonamide	1.7	0.57	119

Table 8 (*Contd.*)

Compound no.	Chemical structures & IUPAC names	K_i (nM) hCA-II	K_i (nM) hCA-XII	Ref.
99	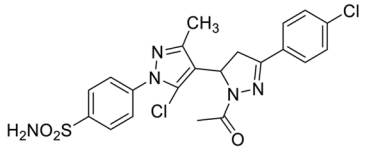 4-(2-Acetyl-5'-chloro-5-(4-chlorophenyl)-3'-methyl -3,4-dihydro-1'*H*,2*H*-[3,4'-bipyrazol]-1'-yl) benzenesulfonamide	0.26	3.9	119
100	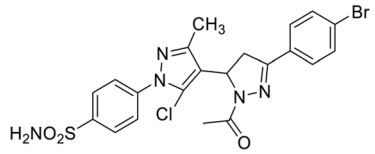 4-(2-Acetyl-5-(4-bromophenyl)-5'-chloro-3'-methyl -3,4-dihydro-1'*H*,2*H*-[3,4'-bipyrazol]-1'-yl) benzenesulfonamide	0.30	5.1	119
101	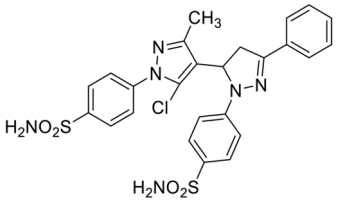 4,4'-(5'-Chloro-3'-methyl-5-phenyl-3,4-dihydro -1'*H*,2*H*-[3,4'-bipyrazole]-1',2-diyl) dibenzenesulfonamide	10.9	9.4	119
102	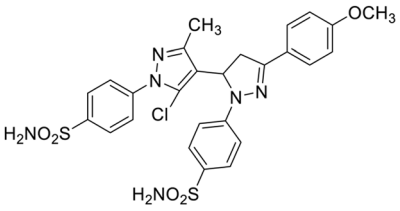 4,4'-(5'-Chloro-5-(4-methoxyphenyl)-3'-methyl- 3,4-dihydro-1'*H*,2*H*-[3,4'-bipyrazole]-1',2-diyl) dibenzenesulfonamide	1.5	5.9	119
Standard	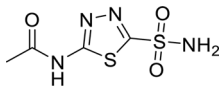 Acetazolamide (AAZ)	12.1	5.7	119

examined in this study are promising candidates for drug development and further assessment in *in vivo* studies.[107]

Iqbal *et al.* (2014) synthesized a series of thioureas-based sulfonamides, and assessed for their IC_{50} on bovine CA (bCA-II). These compounds demonstrated considerable activity, with the most potent inhibitor in the series **74** exhibiting an IC_{50} = 0.261 μM. Both molecular docking and SAR analyses indicate that *ortho* substitution with bulky electronegative groups (*e.g.*, $-NO_2$) enhances the inhibitory activity against CA. The increased inhibition observed for compound **74** is attributed to the enhanced stability of the enzyme–inhibitor complex, which is facilitated by Thr200 forming two hydrogen bonds: one with the nitrogen atom of the amide group and the other with the oxygen atom of the nitro group (Fig. 26).[108]

Maraş *et al.* (2014) synthesized and evaluated sulfamides and demonstrated competitive inhibition of hCA-I and II at nanomolar concentrations. Among the synthesized compounds, derivative **75** was the most effective inhibitor of hCA-I (K_i = 153.88 nM), while derivative **76** was the most potent against hCA-II (K_i = 117.80 nM) (Fig. 27). These findings

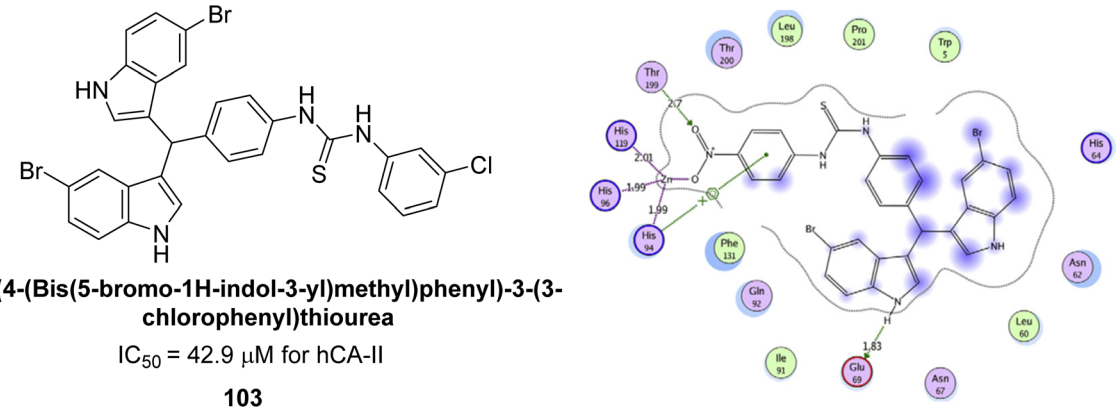

Fig. 37 Chemical structure of compound **103** and its IC_{50} value against hCA-II along with its docking image.

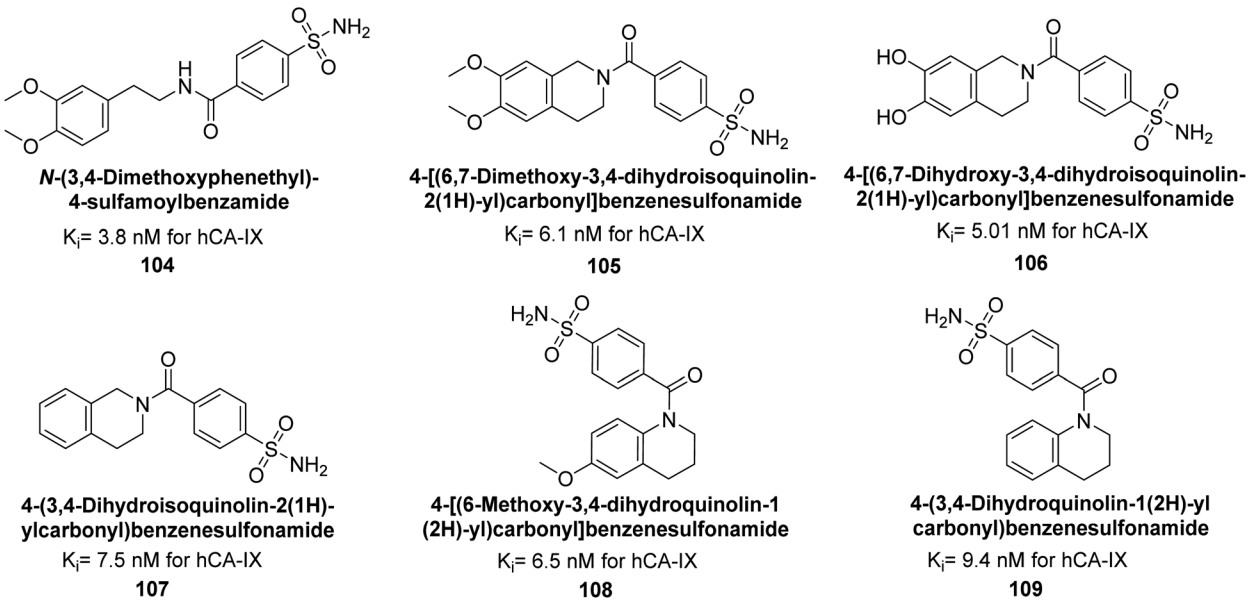

Fig. 38 Chemical structure of compounds **104–109** and their K_i values against hCA-IX.

indicate that the synthesized sulfamide carbamates and sulfamides have the potential to serve as potent inhibitors of hCA isoenzymes, making them promising candidates for the treatment of conditions such as obesity, glaucoma and epilepsy.[109]

Sechi *et al.* (2014) synthesized benzene- and tetrafluorobenzene-sulfonamides using click chemistry and evaluated against hCA-IX and XII isoforms. Remarkably, only two compounds 77 and **78**, featuring an electron-withdrawing carboxymethyl group, exhibited reduced activity against hCA-IX and XII as compared to the standard AAZ (Fig. 28). Compound 77, featuring a nonpolar, puckered cyclohexyl ring, was located in the hydrophobic pocket formed by residues L204, P202, V135 and F131. In contrast, the tail of compound **78** was oriented toward the bulk solvent and did not engage in polar or hydrophobic interactions with the protein surface (Fig. 28).[110]

Sławiński *et al.* (2014) synthesized a series of substituted guanidines and evaluated them against two isoforms CA-IX and XII. Interestingly, certain compounds exhibited potent inhibitory activity against hCA-IX, with K_i values ranging from 4.7 to 21 nM, surpassing the reference sulfonamides AAZ, MZA, EZA, DCP, and IND, which had K_i values of 24 to 50 nM. Among these, compound **79** emerged as the most potent inhibitor of hCA-IX (K_i = 4.7 nM), and hCA-XII (K_i = 0.96 nM) (Fig. 29). Future perspectives could involve further optimization of these compounds to enhance their selectivity and efficacy as potential anticancer agents, as well as exploring their therapeutic potential in preclinical and clinical studies. Additionally, structural modifications could be explored to improve pharmacokinetic properties and reduce off-target effects, ultimately advancing their utility in cancer therapy.[111]

Gençer *et al.* (2014) designed, synthesized and assessed hCA-I properties of 1,4-dihydropyrimidinone compounds. The compounds were synthesized using a multicomponent Biginelli reaction. Among the synthesized compounds, compound **80** (IC_{50} = 0.0547 μM) showed excellent inhibitory activity (Fig. 30). These findings underscore the potential of substituted 1,4-dihydropyrimidinone compounds as promising candidates for

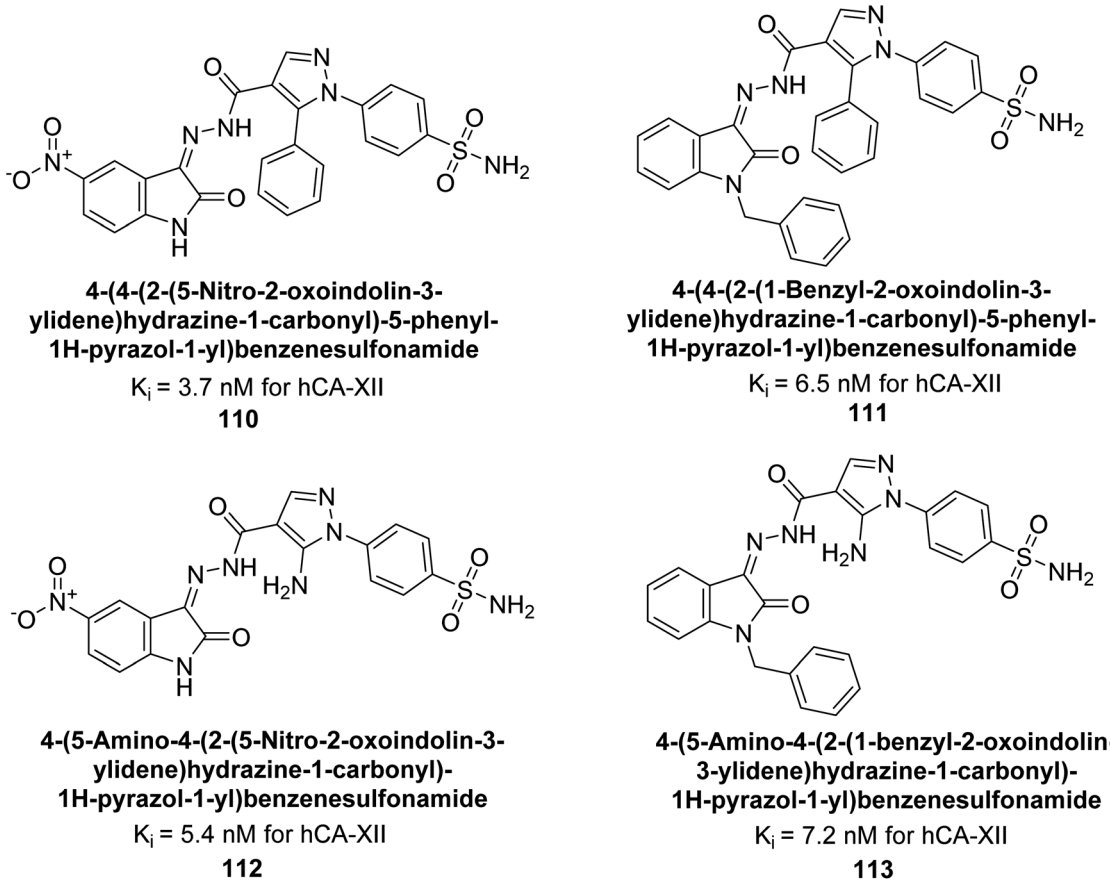

Fig. 39 Chemical structure of compounds **110–113** and their K_i values against hCA-XII.

further development as CA inhibitors with potential implications in cancer therapy.[112]

Gençer *et al.* (2014) synthesized 1,3-dicarbonyl derivatives of substituted sulfonamides and assessed their inhibitory effects on hCA-I and II. The compounds showed effective inhibition of both isoforms, with compounds **81** and **82** demonstrating the highest activity due to methyl substitutions, achieving IC_{50} values of 2.12 μM for hCA-I and 2.52 μM for hCA-II (Fig. 31). These sulfonamide derivatives are promising for glaucoma treatment and allow further *in vivo* evaluation.[113]

Gülçin *et al.* (2014) designed and synthesized sulphamides and sulfonamides and assessed heir inhibitory activity against hCA-I and II. Among the tested derivatives, compounds **83** and **84** displayed a particularly potent inhibitory effect on hCA, with $K_i = 0.71$ μM and 1.56 μM (hCA-I) and $K_i = 0.69$ μM and 0.39 μM (hCA-II), respectively (Fig. 32), against the reference standard AAZ. These findings suggest that the target compounds hold as potent inhibitors of CA, highlighting their potential for further exploration as therapeutic agents.[114]

Saeed *et al.* (2014) synthesized sulfonamide-thiourea and evaluated their inhibitory activity against bCA-II with inhibition constants falling within the range of 0.011 to 17.1 μM. Remarkably, among the compounds evaluated, compound **85** and **86** exhibited the highest potency as inhibitors, demonstrating IC_{50} values of 0.052 μM and 0.011 μM, respectively (Fig. 33). These analyses aimed to elucidate the structural interactions and dynamics governing the inhibitory properties observed, providing valuable insights for further development of potential therapeutic agents targeting CA enzymes.[115]

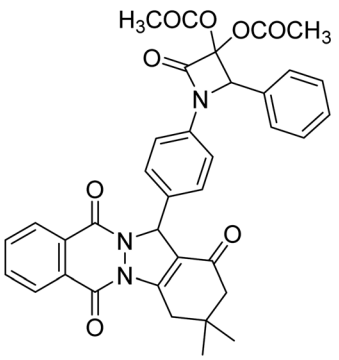

Fig. 40 Chemical structure of compound **114** and its IC_{50} values against hCA-I and II.

Table 9 Chemical structures of Schiff base derivatives, inhibition data against CAIs

Compound no.	Chemical structures & IUPAC names	K_i (nM) CA-I	CA-II	CA-IX	CA-XII	Ref.
115	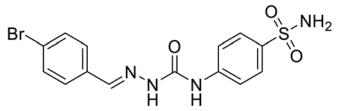 2-(4-Bromobenzylidene)-*N*-(4-sulfamoyl phenyl)hydrazinecarboxamide	95.2	6.2	90.4	92.3	124
116	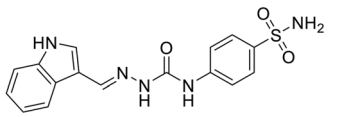 2-((1*H*-Indol-3-yl)methylene)-*N*-(4-sulfamoyl phenyl)hydrazinecarboxamide	71.2	4.0	103	63.1	124
117	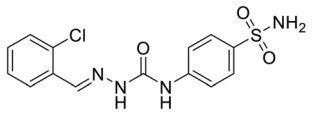 2-(2-Chlorobenzylidene)-*N*-(4-sulfamoyl phenyl)hydrazinecarboxamide	77.6	4.2	213	42.3	124
118	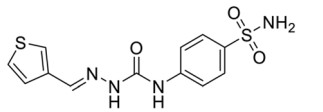 *N*-(4-Sulfamoylphenyl)-2-(thiophen-3-ylmethylene) hydrazine-1-carboxamide	79.3	4.6	395	23.8	124
119	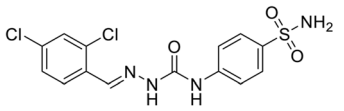 2-(2,4-Dichlorobenzylidene)-*N*-(4-sulfamoyl phenyl)hydrazinecarboxamide	6530	75.0	98.1	90.7	124
120	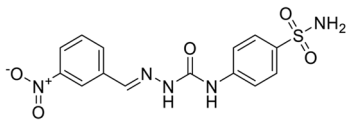 2-(3-Nitrobenzylidene)-*N*-(4-sulfamoyl phenyl)hydrazinecarboxamide	4930	51.6	415	83.9	124
121	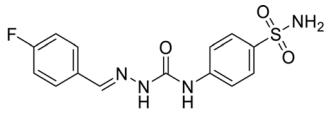 2-(4-Fluorobenzylidene)-*N*-(4-sulfamoylphenyl) hydrazinecarboxamide	675	5.6	27.3	95.8	124
122	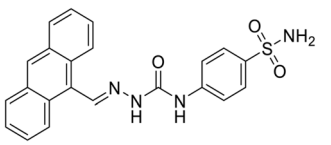 2-(Anthracen-9-ylmethylene)-*N*-(4-sulfamoyl phenyl)hydrazinecarboxamide	1640	19.5	381	21.5	124
Standard	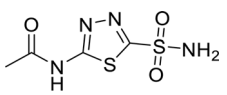 Acetazolamide (AAZ)	250	12	25	5.8	124

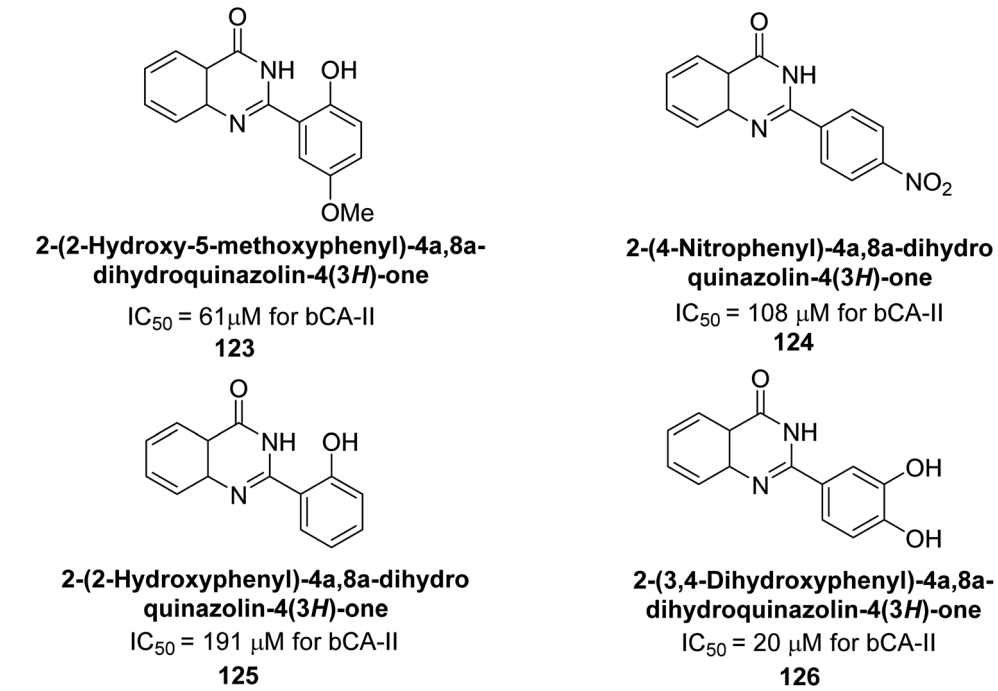

Fig. 41 Chemical structure of compounds **123–126** and their IC_{50} values against bCA-II.

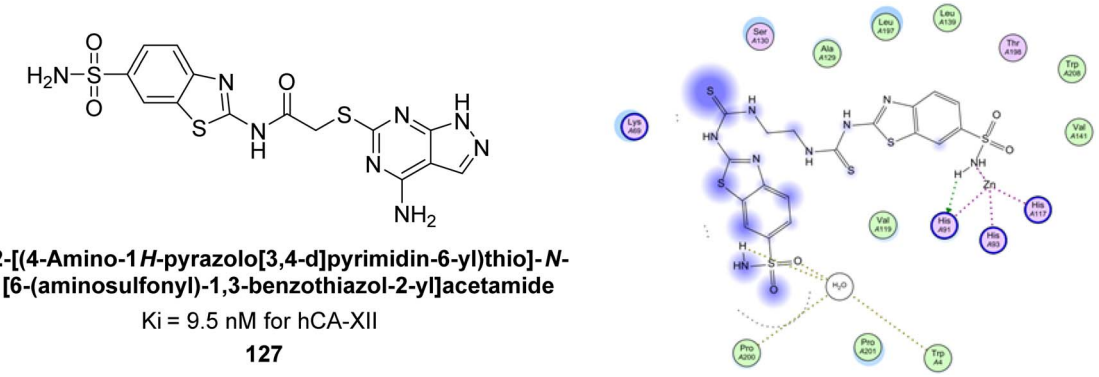

Fig. 42 Chemical structure of compound **127** and its K_i value against hCA-XII along with its docking image.

Sławiński *et al.* (2014) synthesized substituted sulfonamides and assessed for their inhibitory activity against hCA-I, II, IX and XII. The investigated compounds exhibited varying inhibitory potencies against these isoforms. Remarkably, the compounds demonstrated excellent inhibitory activity against hCA-IX, with synthesized compounds showing potent K_i values ranging from 2.8 to 21.7 nM compared to clinically used CA inhibitors with K_i values between 24 and 50 nM. Particularly, compound **87** emerged as the most potent hCA-IX inhibitor with a $K_i = 2.8$ nM, which was 8.5-fold stronger than IND ($K_i =$ 24 nM). Furthermore, compounds **88** and **89** demonstrated superior inhibitory potency against hCA-XII with K_i values of 2.7 and 2.8 nM, respectively, surpassing the reference sulfonamides MZA and IND ($K_i = 3.4$ nM) (Fig. 34).[116]

Zhu *et al.* (2014) designed and synthesized metronidazole-sulfonamides and evaluated for their inhibitory effects on hCA-II and IX. Many of these compounds demonstrated significant inhibition against hCA-II and IX, with IC_{50} values falling within the ranges of 16–137 nM and 38–169 nM, respectively. Of all the compounds tested, compounds **90** (IC_{50} = 16 nM) and **91** (IC_{50} = 38 nM) emerged as the most potent inhibitors against hCA-II and IX, respectively (Fig. 35).[117]

Supuran *et al.* (2014) synthesized sulfonyl semicarbazides and measured for their inhibitory effects on hCA. These compounds were evaluated against a panel of hCA isoforms including I, II, IX, and XII, with AAZ serving as the standard reference. The 4-nitro substituted derivative **92** was identified as the most potent inhibitor, with K_i values of 6.0 nM for hCA-II and 0.79 nM for hCA-IX (Fig. 36). The study highlighted the

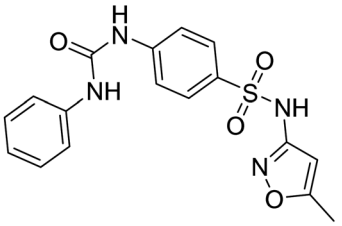

***N*-(5-Methyl-isoxazol-3-yl)-4–(3-phenyl-ureido)-benzenesulfonamide**

K_i = 73 μM for hCA-I
K_i = 85 μM for hCA-VII
128

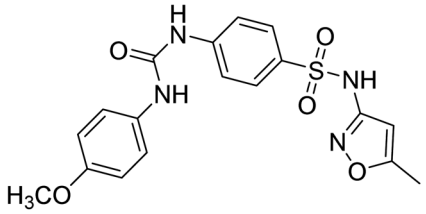

4-[3–(4-Methoxy-phenyl)-ureido]-*N*-(5-methyl-isoxazol-3-yl)-benzenesulfonamide

K_i = 96 μM for hCA-II

129

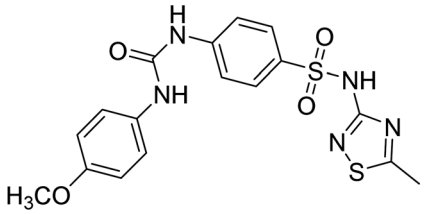

4-[3-(4-Methoxy-phenyl)-ureido]-*N*-(5-methyl-[1,3,4]thiadiazol-2-yl)-benzenesulfonamide

K_i = 87 μM for hCA-II

130

Fig. 43 Chemical structures of compounds **128–130** and their K_i values against hCA-I, II and VII.

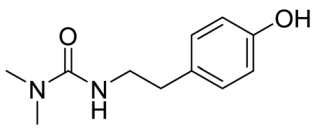

3-(4-Hydroxyphenethyl)-1,1-dimethylurea

K_i = 0.307 nM for hCA-II

131

Fig. 44 Chemical structure of compound **131** and its K_i value against hCA-II.

importance of *p*-substitution on the sulfonyl-substituted aromatic ring in influencing both potency and selectivity for specific hCA isoforms. Overall, the research developed highly potent and selective hCA inhibitors with promising therapeutic potential.[118]

Supuran *et al.* (2015) synthesized pyrazolines and assessed for their inhibitory activity against CA enzymes. Particularly, compounds **93**, **94**, and **95–100** exhibited superior inhibition against hCA-XII (K_i = 0.47–5.1 nM) compared to AAZ (K_i = 5.7 nM), with compounds **95**, **97**, **98** and **101** showing nearly a 10-fold improvement over the reference drug. Against hCA-II, all tested compounds surpassed the standard drug, particularly

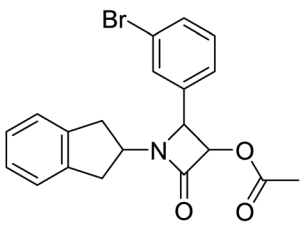

2-(3-Bromophenyl)-1-(2,3-dihydro-1H-inden-2-yl)-4-oxoazetidin-3-yl acetate

K_i = 0.35 nM for hCA-I
K_i = 3.39 nM for hCA-II
132

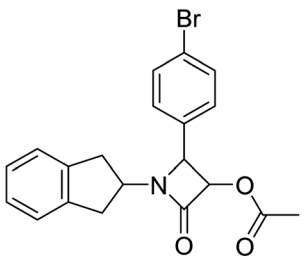

2-(4-Bromophenyl)-1-(2,3-dihydro-1H-inden-2-yl)-4-oxoazetidin-3-yl acetate

K_i = 0.97 nM for hCA-I
K_i = 0.93 nM for hCA-II
133

Fig. 45 Chemical structures of compounds **132** and **133**, and their K_i value against hCA-I and II.

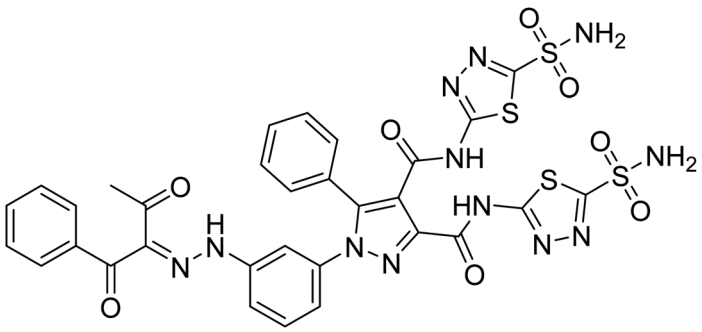

1-(3-(2-(1,3-Dioxo-1-phenylbutan-2-ylidene)hydrazinyl)phenyl)-5-phenyl-N3,N4-bis(5-sulfamoyl-1,3,4-thiadiazol-2-yl)-1H-pyrazole-3,4-dicarboxamide

K_i = 0.119 μM for hCA-I

134

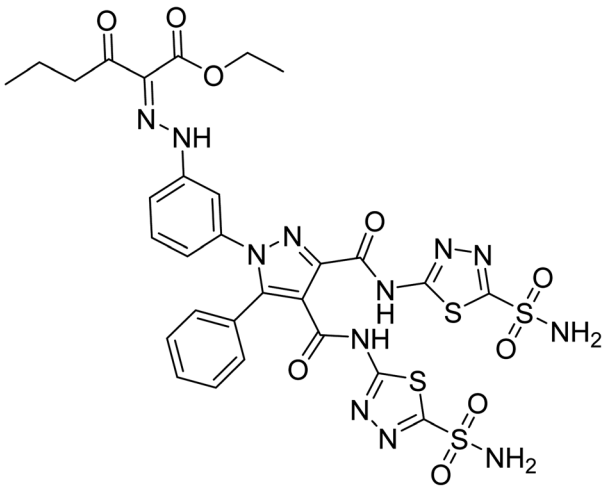

Ethyl 3-oxo-2-(2-(3-(5-phenyl-3,4-bis((5-sulfamoyl-1,3,4-thiadiazol-2-yl)carbamoyl)-1H-pyrazol-1-yl)phenyl)hydrazono) hexanoate

K_i = 0.084 μM for hCA-II

135

Fig. 46 Chemical structures of compounds **134** and **135**, and their K_i value against hCA-I and II.

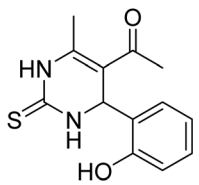

1-(4-(2-Hydroxyphenyl)-6-methyl-2-thioxo-1,2,3,4-tetrahydropyrimidin-5-yl)ethanone

K_i = 47.40 nM for hCA-I
K_i = 76.06 nM for hCA-II

136

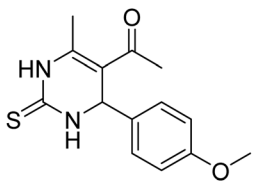

1-(4-(4-Methoxyphenyl)-6-methyl-2-thioxo-1,2,3,4-tetrahydropyrimidin-5-yl)ethanone

K_i = 77.68 nM for hCA-I
K_i = 30.63 nM for hCA-II

137

Fig. 47 Chemical structures of compounds **136** and **137**, and their K_i value against hCA-I and II.

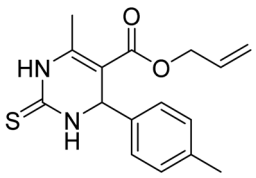

Allyl 6-methyl-2-thioxo-4-(p-tolyl)-1,2,3,4-tetrahydropyrimidine-5-carboxylate

K_i = 218.5 pM for hCA-I

K_i = 155.4 pM for hCA-II

138

Fig. 48 Chemical structure of compound **138** and its K_i value against hCA-I and II.

compounds **93**, **97**, **98** and **102** (K_i = 1.1–1.7 nM), which were significantly more potent inhibitors than AAZ (K_i = 12.1 nM) (Table 8).[119]

Ismail *et al.* (2015) designed and synthesized bisindolylmethanes and assessed for their potential inhibitory activity against hCA-II. Particularly, bisindoles with halogen substituents at the fifth position demonstrated enhanced inhibitory activity compared to their unsubstituted counterparts. Moreover, docking investigations of the active compound **103** (IC_{50} = 42.9 μM) indicated that the *p*-positioned nitro (NO_2) substituent is adept at fitting into the core of the active site and interacting with the Zn ion. Compounds containing a NO_2 substituent exhibited close interaction with Zn ion, His94, His119, Thr199 and His96 disrupting the Zn–OH– Glu106–Thr199 hydrogen bond network (Fig. 37). Despite the bulky nature of the indole ring, it was unable to directly interact with the active site. However, the NH group of the indole ring was observed to form a hydrogen bond with Glu69, contributing to the stabilization of the ligand–receptor complex. These newly discovered compounds demonstrate inhibitory activity worthy of consideration for future development.[120]

Gitto *et al.* (2015) synthesized a series of substituted benzenesulfonamides and assessed as inhibitors of hCAs. These novel sulfonamide derivatives underwent screening against hCA-IX, with AAZ and topiramate (TPM). Notably, compounds **104–109** exhibited low nanomolar inhibition of the hCA-IX isoform (K_i values < 10 nM) (Fig. 38). These findings contribute to the development of targeted therapies for conditions associated with dysregulated CA activity, particularly in cancer.[121]

Supuran *et al.* (2015) synthesized a series of benzenesulfonamide derivatives containing pyrazole and isatin functionalities based on celecoxib as the lead compound. The biological activity of these derivatives was evaluated against hCA-IX and XII. The majority of the tested compounds demonstrated significant inhibition of hCA-IX with K_i as low as 2.5×10^2 nM, surpassing the potency of the standard drug AAZ. Specifically, compounds **110–113** displayed notable inhibitory activity against hCA-XII, with K_i values ranging from 3.7–7.2 nM (Fig. 39). Compounds **110** and **112**, featuring a 5-nitro substitution on the isatin moiety, exhibited selectivity towards inhibiting hCA-XII. Molecular docking studies revealed that the NO_2 group in these compounds interacted with Asp132 in the active site of hCA-IX and with Asp130 and Lys67 in hCA-XII (Fig. 39).[122]

Gençer *et al.* (2015) synthesized a series of substituted β-lactam derivatives and assessed their inhibitory effects on the activity of hCA-I and II. Remarkably, the compound **114** exhibited the most potent inhibitory effect, with IC_{50} values of 6.97 μM for hCA-I and 8.48 μM for hCA-II (Fig. 40). The bulky phthalazine group influences the inhibitory effects of these compounds. They likely bind similarly to coumarin derivatives. Additionally, the interaction involves the enzyme's active site and the β-lactam ring.[123]

Toraskar *et al.* (2015) synthesized and evaluated Schiff bases from sulfanilamide semicarbazone and various heterocyclic aldehydes and evaluated against different CA isoforms.

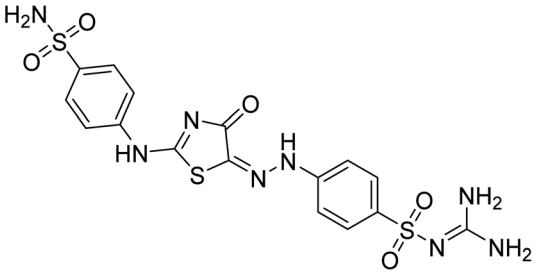

***N*-(Diaminomethylene)-4-(2-(4-oxo-2-((4-sulfamoylphenyl)amino)thiazol-5(4H)-ylidene)hydrazinyl)benzenesulfonamide**

K_i = 0.85 nM for hCA-I

139

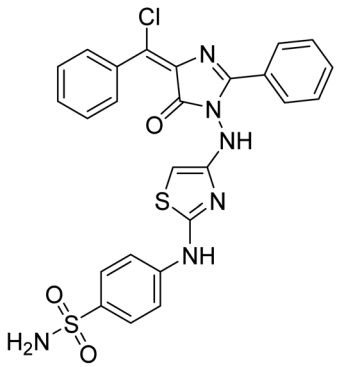

4-((4-((4-(Chlorobenzylidene)-5-oxo-2-phenyl-4,5-dihydro-1H-imidazol-1-yl)amino)thiazol-2-yl)amino)benzenesulfonamide

K_i = 29.2 nM for hCA-IX

140

Fig. 49 Chemical structures of compounds **139** and **140** and their K_i value against hCA-I and IX.

Table 10 Chemical structures of substituted pyrazoline benzene sulfonamides along with K_i values against hCA-I and II

Compound no.	Chemical structures & IUPAC names	K_i (nM) hCA-I	K_i (nM) hCA-II	Ref.
141	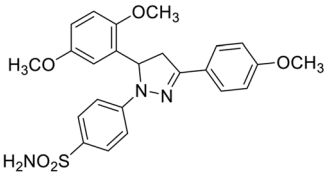 4-(5-(2,5-Dimethoxyphenyl)-3-(4-methoxyphenyl)-4,5-dihydro-1*H*-pyrazol-1-yl)benzenesulfonamide	26.5	18.9	134
142	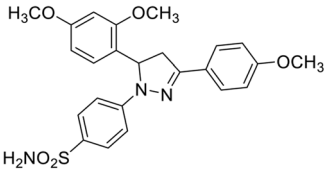 4-(5-(2,4-Dimethoxyphenyl)-3-(4-methoxyphenyl)-4,5-dihydro-1*H*-pyrazol-1-yl)benzenesulfonamide	39.7	20.5	134
143	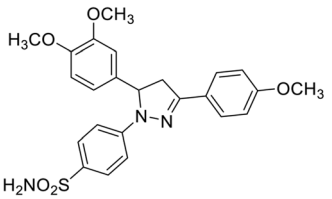 4-(5-(3,4-Dimethoxyphenyl)-3-(4-methoxyphenyl)-4,5-dihydro-1*H*-pyrazol-1-yl)benzenesulfonamide	55.5	28.8	134
144	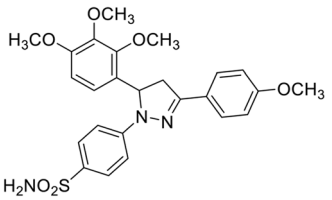 4-(3-(4-Methoxyphenyl)-5-(2,3,4-trimethoxyphenyl)-4,5-dihydro-1*H*-pyrazol-1-yl)benzenesulfonamide	31.4	19.9	134
145	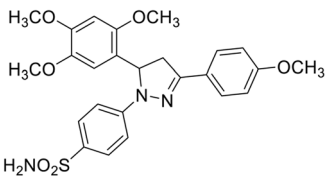 4-(3-(4-Methoxyphenyl)-5-(2,4,5-trimethoxyphenyl)-4,5-dihydro-1*H*-pyrazol-1-yl)benzenesulfonamide	29.9	25.9	134
146	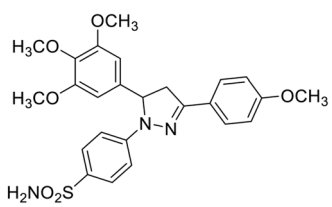 4-(3-(4-Methoxyphenyl)-5-(3,4,5-trimethoxyphenyl)-4,5-dihydro-1*H*-pyrazol-1-yl)benzenesulfonamide	34.1	20.2	134

Table 10 (*Contd.*)

Compound no.	Chemical structures & IUPAC names	K_i (nM) hCA-I	K_i (nM) hCA-II	Ref.
Standard	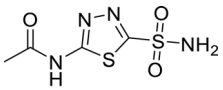 Acetazolamide (AAZ)	276.3	117.8	134

Compounds **115**, **116**, **117** and **118** demonstrated hCA-I inhibition (IC_{50} = 71.2–95.2 nM), surpassing the standard AAZ. Only **119** (2,4-dichlorophenyl) and **120** (3-nitrophenyl) were moderately effective hCA-II inhibitors, with K_i of 51.6–75.0 nM. For CA-IX, only compound **121** (4-fluorophenyl) showed comparable activity to AAZ (K_i = 27.3 nM). Compounds **118** and **122** (with 2-thienyl and 9-anthranyl moieties, respectively) were effective hCA-XII inhibitors (K_i = 21.5–23.8 nM) (Table 9).[124]

Khan *et al.* (2015) synthesized quinazoline derivatives and tested for their inhibitory activity against bCA-II. Compounds **123** (IC_{50} = 61.33 μM), **124** (IC_{50} = 108.30 μM), **125** (IC_{50} = 191.93 μM) and **126** (IC_{50} = 20.94 μM) exhibited selective inhibition of bCA-II, compared to the standard AAZ (IC_{50} = 0.12 μM) for bCA-II. The inhibitory activity of these derivatives is attributed to the different substituents (–NO_2, –OH, –OMe) the motif (Fig. 41).[125] Further refinement of these lead molecules, through

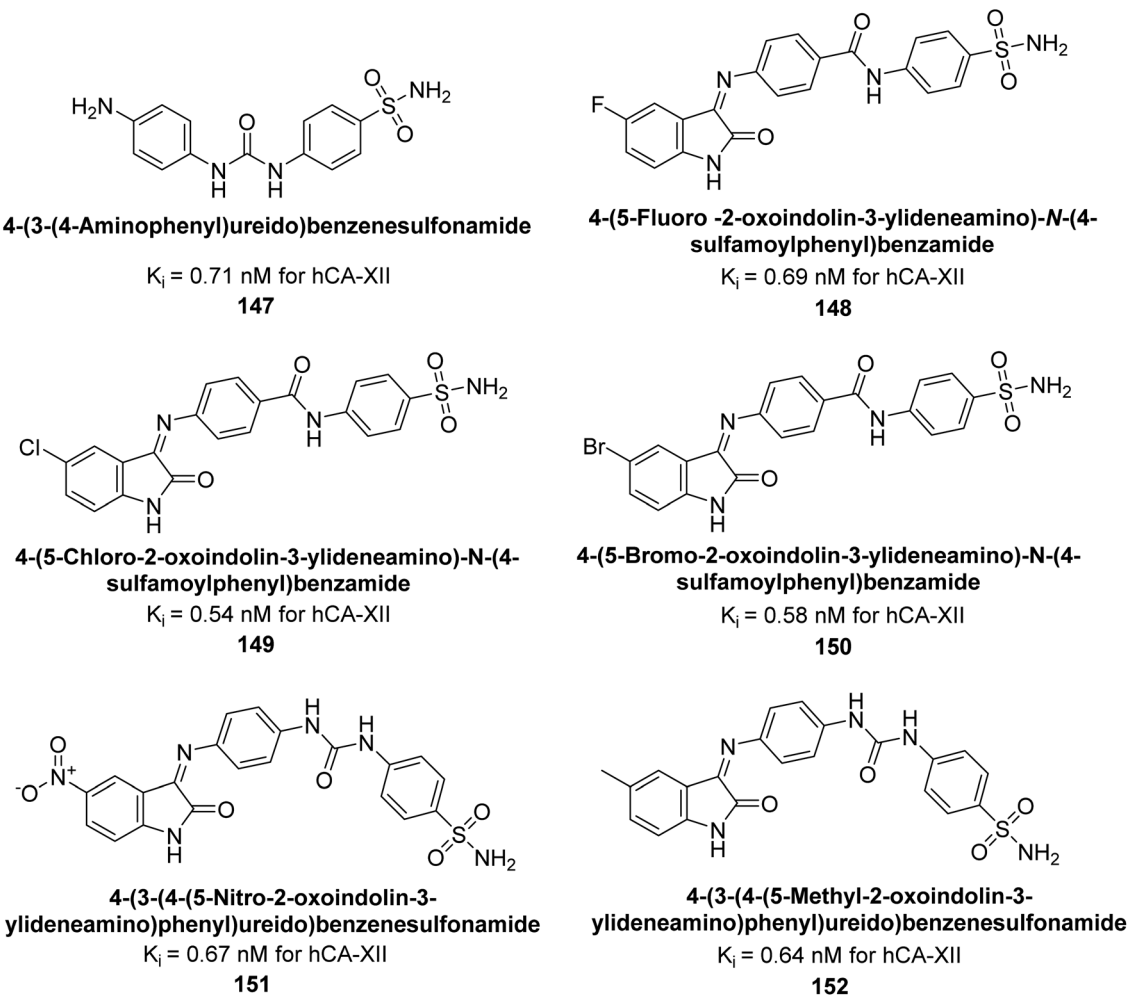

Fig. 50 Chemical structures of compounds **147–152** and their K_i value against hCA-XII.

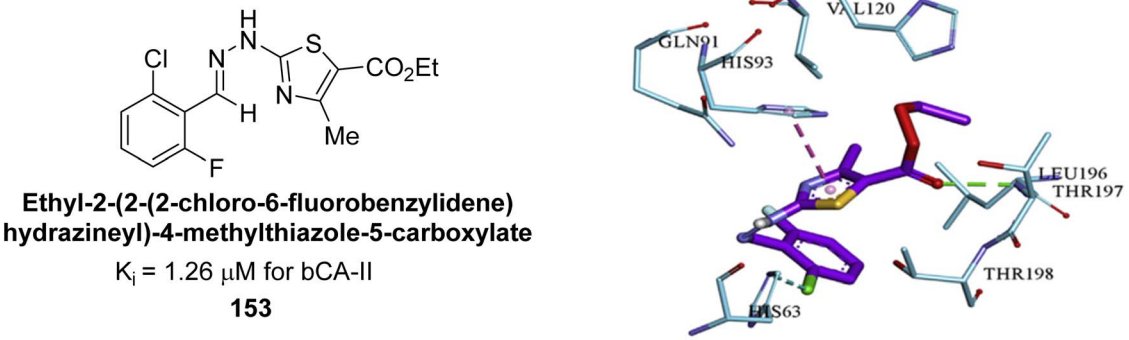

Ethyl-2-(2-(2-chloro-6-fluorobenzylidene) hydrazineyl)-4-methylthiazole-5-carboxylate

K_i = 1.26 μM for bCA-II

153

Fig. 51 Chemical structure of compound **153** and its K_i value against bCA-II along with its docking image.

kinetic and *in vivo* studies, may yield potent inhibitors for both enzymes.

Supuran *et al.* (2015) synthesized 2-aminobenzothiazole derivatives and evaluated as inhibitors of hCA-XII. Compound **127** (K_i = 9.5 nM) demonstrated selective inhibition of hCA-XII, indicating that certain heterocyclic moieties can be utilized to design effective and selective inhibitors for hCA-XII as compared to AAZ (K_i = 22 nM). Compound **127** primarily binds through coordination of the deprotonated primary sulfonamide group with the active site zinc ion. Secondary interactions involve the benzothiazole ring occupying regions more than 5 Å from the zinc, enhancing binding. The amide linker between

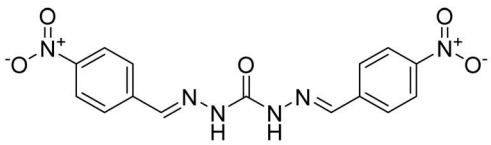

Bis[(4-nitrophenyl)methylidene]carbonic dihydrazide

IC_{50} = 1.33 μM for bCA-II

154

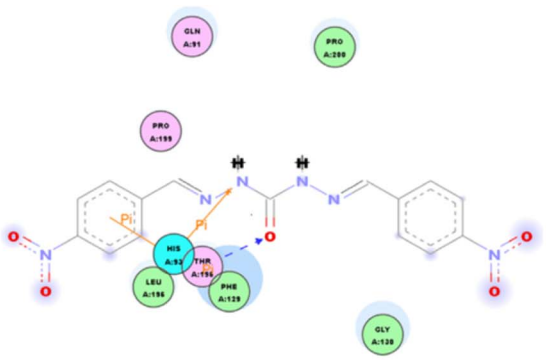

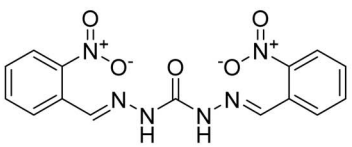

Bis[(2-nitrophenyl)methylidene]carbonic dihydrazide

IC_{50} = 1.85 μM for bCA-II

155

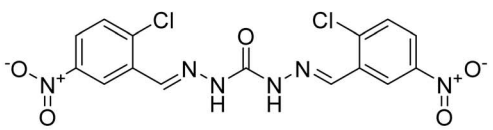

Bis[(2-chloro-5-nitrophenyl)methylidene]carbonic dihydrazide

IC_{50} = 1.37 μM for bCA-II

156

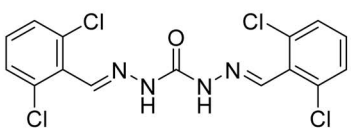

Bis[(E)-(2,6-dichlorophenyl)methylidene]carbonic dihydrazide

IC_{50} = 1.46 μM for bCA-II

157

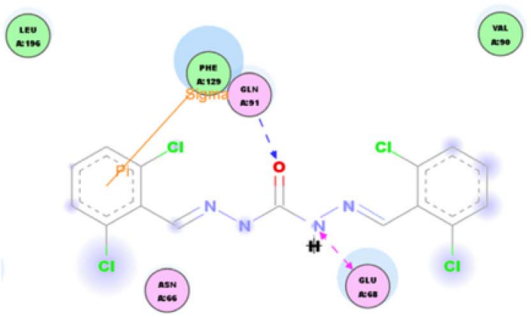

Fig. 52 Chemical structures of compounds **154–157** and their IC_{50} value against bCA-II along with docking images of **154** and **157**.

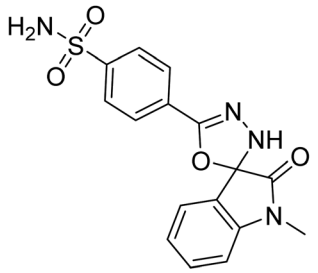

4-(1-Methyl-2-oxo-3'H-spiro[indoline-3,2'-[1,3,4]oxadiazole]-5'-yl)benzenesulphonamide

K_i = 0.042 μM for hCA-I

158

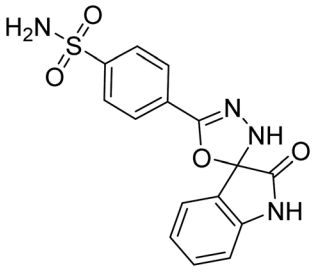

4-(2-Oxo-3'H-spiro[indoline-3,2'-[1,3,4] oxadiazole]-5'-yl) benzenesulphonamide

K_i = 0.151 μM for hCA-II

159

Fig. 53 Chemical structures of compounds **158** and **159** and their K_i values against hCA-I and II.

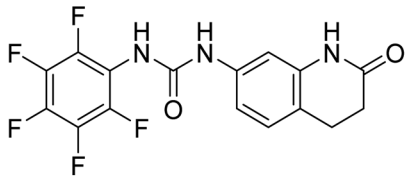

1-(2-Oxo-1,2,3,4-tetrahydroquinolin-7-yl)-3-(perfluorophenyl)urea

K_i = 243.6 nM for hCA-IX

160

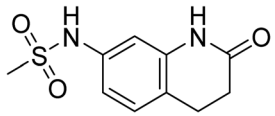

***N*-(2-oxo-1,2,3,4-tetrahydroquinolin-7-yl)methanesulfonamide**

K_i = 292.8 nM for hCA-IX

161

Fig. 54 Chemical structures of compounds **160** and **161** and their K_i values against hCA-IX.

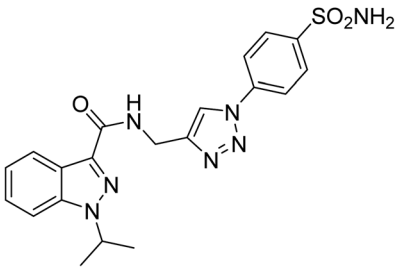

1-Isopropyl-*N*-((1-(4-sulfamoylphenyl)-1*H*-1,2,3-triazol-4-yl)methyl)-1*H*-indazole-3-carboxamide

K_i = 1.8 nM for hCA-IX

162

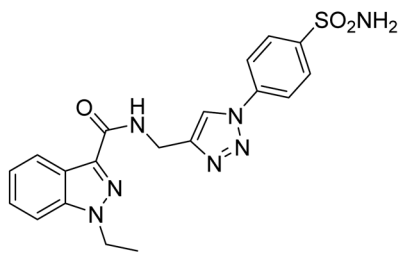

1-Ethyl-*N*-((1-(4-sulfamoylphenyl)-1*H*-1,2,3-triazol-4-yl)methyl)-1*H*-indazole-3-carboxamide

K_i = 2.3 nM for hCA-IX

163

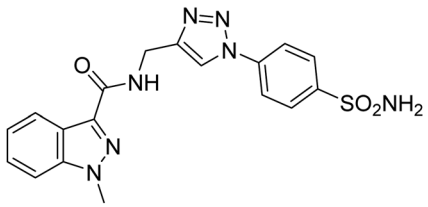

1-Methyl-*N*-((1-(4-sulfamoylphenyl)-1*H*-1,2,3-triazol-4-yl)methyl)-1*H*-indazole-3-carboxamide

K_i = 2.0 nM for hCA-IX

164

Fig. 55 Chemical structures of compounds **162**, **163** and **164** and their K_i values against hCA-IX.

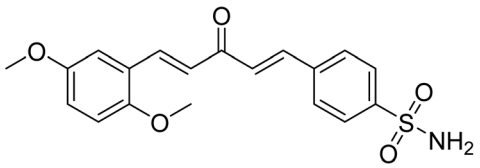

4-((1E,4E)-5-(2,5-dimethoxyphenyl)-3-oxopenta-1,4-dien-1-yl)benzenesulfonamide

K_i = 0.89 nM for hCA-II

165

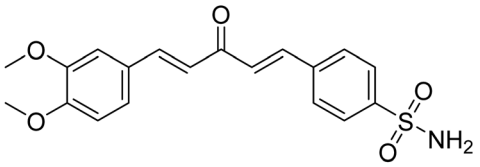

4-((1E,4E)-5-(3,4-dimethoxyphenyl)-3-oxopenta-1,4-dien-1-yl)benzenesulfonamide

K_i = 0.75 nM for hCA-II

166

Fig. 56 Chemical structures of compounds **165** and **166** and their K_i values against hCA-II.

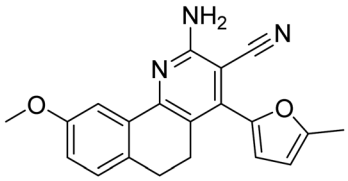

2-Amino-5,6-dihydro-9-methoxy-4-(5-methylfuran-2-yl)benzo[h]quinolin-3-carbonitrile

K_i = 2.84 μM for hCA-I

K_i = 4.56 μM for hCA-II

167

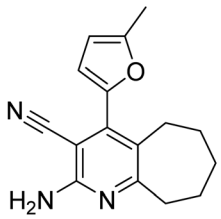

2-Amino-6,7,8,9-tetrahydro-4-(5-methylfuran-2-yl)-5H-cyclohepta[b]pyridine-3-carbonitrile

K_i = 53.9 μM for hCA-I

K_i = 2.56 μM for hCA-II

168

Fig. 57 Chemical structures of compounds **167** and **168** and their K_i values against hCA-I & II.

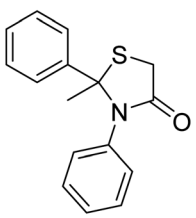

2-Phenyl-2-methyl-3-phenyl-thiazolidine -4-one

K_i = 23.76 nM for hCA-I

169

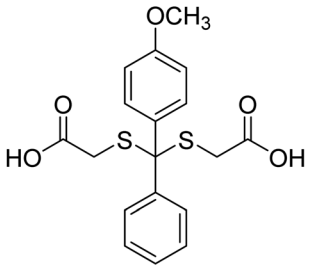

4-Methoxyanilide-1,1-bis-(hydroxycarbonyl methylthio)-1-phenylethane

K_i = 58.92 nM for hCA-II

170

Fig. 58 Chemical structures of compounds **169** and **170** and their K_i values against hCA-I & II.

the heterocycles facilitates favorable conformations and interactions with a solvent-exposed region defined by Ser130, Arg60, Gln89 and Asn62 (Fig. 42).[126]

Supuran *et al.* (2016) synthesized substituted benzenesulfonamides and evaluated their inhibitory effects on various hCA isoforms. Remarkably, compound **128** showed moderate inhibition with K_i values of 73.7 μM for hCA-I and 85.8 μM for hCA-VII. Compounds **129** and **130** inhibited hCA-II with K_i values of 96.0 μM and 87.8 μM, respectively (Fig. 43). The SAR study indicated that modifications to the phenyl ring generally did not significantly affect inhibition, except for the 4-methoxy substitution.[127]

Gülçin *et al.* (2016) synthesized a series of urea and phenolic derivatives and evaluated their K_i values against hCA-I and II. The compounds effectively inhibited hCA-I and II, with K_i values ranging from 0.307 to 0.432 nM for hCA-I and 0.149 to 0.278 nM for hCA-II. In comparison, AAZ, a clinically established CA inhibitor, had a K_i value of 49.60 nM for hCA-II. Compound **131**, with a phenolic hydroxyl group, showed the highest potency against hCA-II, with a K_i value of 0.307 nM (Fig. 44). The inhibition of hCA-II is attributed to the compound's ability to bind

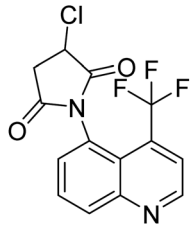

3-Chloro-1-(4-(trifluoromethyl)quinolin-5-yl) pyrrolidine-2,5-dione

K_i = 23.27 nmol/L for hCA-I

171

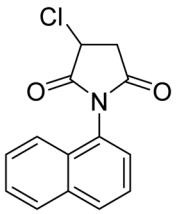

3-Chloro-1-(naphthalen-1-yl)pyrrolidine-2,5-dione

K_i = 10.64 nmol/L for hCA-II

172

Fig. 59 Chemical structures of compounds **171** and **172** and their K_i values against hCA-I & II.

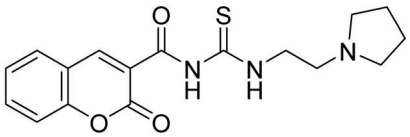

2-Oxo-N-((2-(pyrrolidin-1-yl)ethyl)carbamothioyl) -2H-chromene-3-carboxamide

K_i = 107.9 nM for hCA-IX

173

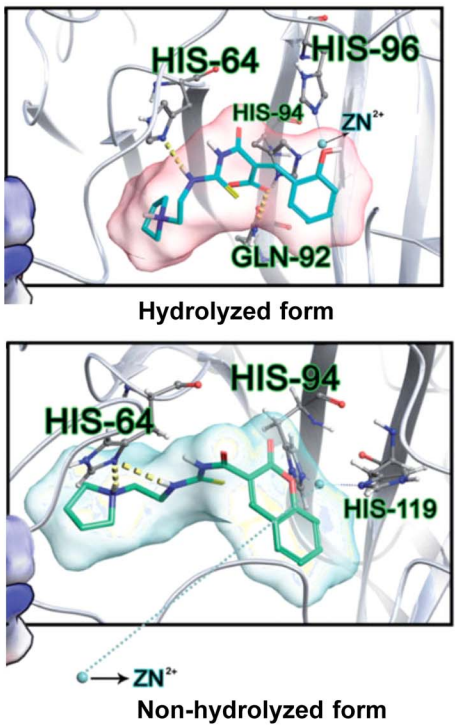

Fig. 60 Chemical structure of compound **173** and its K_i value against hCA-IX along with its docking images in hydrolyzed and non-hydrolyzed forms.

to the catalytic Zn^{2+} ion in the enzyme's active site, mimicking the tetrahedral transition state.[128]

Gülçin *et al.* (2016) synthesized β-lactams and assessed their K_i values against hCA-I and II. The β-lactams demonstrated inhibitory activity, with K_i values ranging from 0.44 to 6.29 nM for hCA-I and 0.93 to 8.34 nM for hCA-II. Notably, β-lactam derivative **132** showed the highest potency against hCA-I with a K_i value of 0.35 nM, while derivative **133** exhibited the strongest inhibition of hCA-II with a K_i value of 0.93 nM (Fig. 45). These findings indicate that β-lactams, with various functional groups, inhibit hCA-I and II in the nanomolar range and could serve as novel CAIs, complementing existing sulfonamides.[129]

Beydemir *et al.* (2016) synthesized a series of pyrazole-3,4-dicarboxamides and assessed their inhibitory effects on hCA-I and II. The K_i values ranged from 0.119 to 3.999 μM for hCA-I and from 0.084 to 0.878 μM for hCA-II. Among the tested compounds, compound **134** (–Me and –Ph substituents) exhibited the strongest inhibitory effect (K_i = 0.119 μM) on hCA-I, while compound **135** (–Pr and –OEt substituents) showed the highest inhibition (K_i = 0.084 μM) on hCA-II (Fig. 46).[130]

Gülçin *et al.* (2016) synthesized tetrahydropyrimidinethiones and evaluated their inhibitory effects on hCA-I and II. The compounds showed strong inhibition, with K_i values ranging from 47.40 to 76.06 nM for hCA-I and from 30.63 to 76.06 nM for hCA-II. Compound **136** was the most potent inhibitor of hCA-I with a K_i of 47.40 nM, surpassing AAZ, a clinically used CA inhibitor. Compound **137** exhibited the highest inhibition of hCA-II, with a K_i value of 30.63 nM (Fig. 47). These cyclic

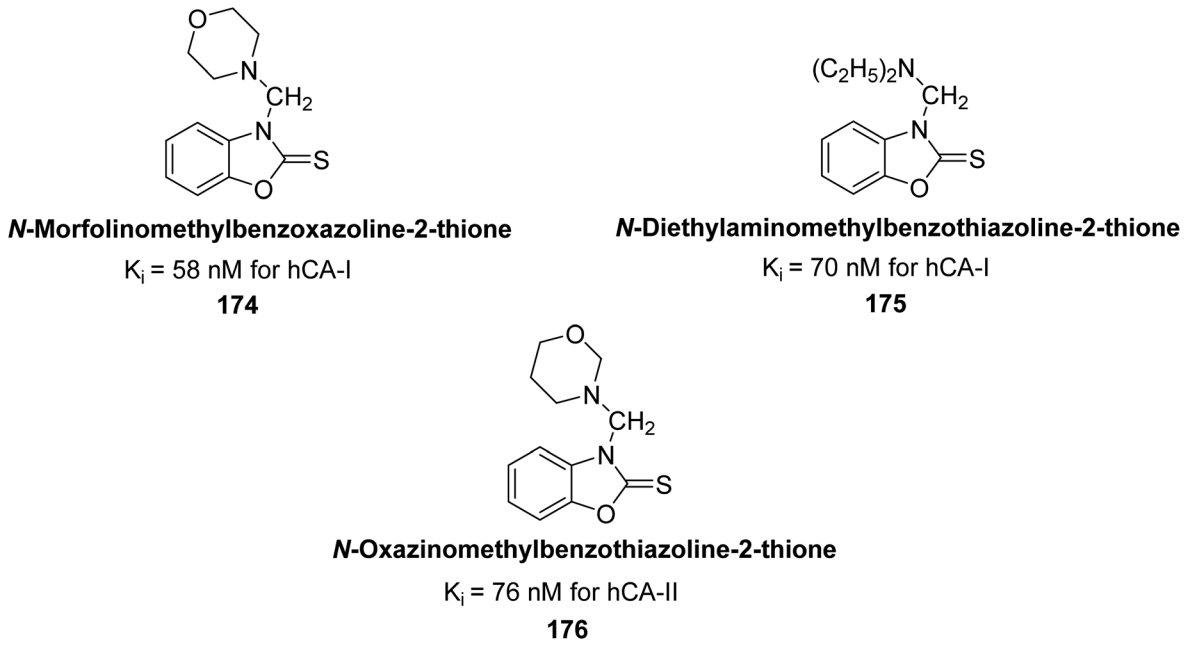

Fig. 61 Chemical structures of compounds **174**, **175** and **176** and their K_i values against hCA-I & II.

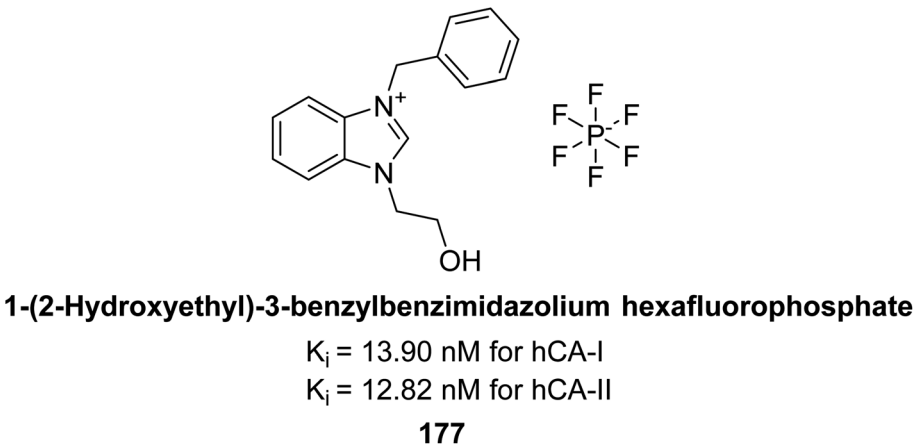

Fig. 62 Chemical structure of compound **177** and its K_i values against hCA-I & II.

thioureas effectively interacted with both hydrophilic and hydrophobic regions of the hCA-II active site.[131]

In another study, Gülçin *et al.* (2016) synthesized tetrahydropyrimidine thiones and assessed for their inhibition of hCA-I and II. These new thiones effectively inhibited both isoforms, with K_i values ranging from 218.5–261.0 pM for hCA-I and from 181.8 to 273.6 pM for hCA-II. In contrast, AAZ, a moderate hCA-I inhibitor, exhibited a K_i of 369.4 pM. The most potent hCA-I inhibition was achieved with compound **138**, showing a K_i value of 218.5 pM. Additionally, the strongest hCA-II inhibition was also observed with compound **138**, which had a K_i value of 155.4 pM (Fig. 48). This relatively unexplored class of derivatives could offer valuable insights into the field of non-sulfonamide CA inhibitors.[132]

Amin *et al.* (2016) synthesized substituted benzenesulfonamides and evaluated for their K_i on hCA-I and IX. These new sulfonamides demonstrated excellent inhibition across all three isoforms, with K_i values ranging from 0.84 to 702 nM for hCA-I and 5.6 to 29.2 nM for hCA-IX. The most effective inhibitor for hCA-I is compound **139**, which features a sulfaguanidine moiety and has a K_i of 0.85 nM. For hCA-IX, compound **140** displayed excellent inhibition with a K_i of 29.2 nM, demonstrating potency comparable to that of AAZ (Fig. 49).[133]

Kucukoglu *et al.* (2016) synthesized a series of pyrazoline benzenesulfonamides and assessed for their inhibitory activity on hCA-I and II. All synthesized compounds exhibited superior CA inhibitory activity compared to the reference compound AAZ, with K_i ranging from 26.5 to 55.5 nM for hCA-I and from 18.9 to 28.8 nM for hCA-II. The compounds **141–146** [**141** (30.1

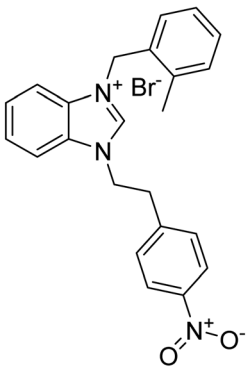

1-[2-(4-Nitrophenyl)ethyl]-3-(2-methylbenzyl) benzimidazolium bromide

K_i = 17.33 nM for hCA-I

K_i = 45.31 nM for hCA-II

178

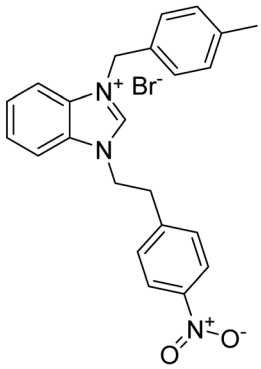

1-[2-(4-Nitrophenyl)ethyl]-3-(4-methylbenzyl) benzimidazolium bromide

K_i = 54.48 nM for hCA-I

K_i = 33.98 nM for hCA-II

179

Fig. 63 Chemical structures of compounds **178** and **179** and their K_i values against hCA-I & II.

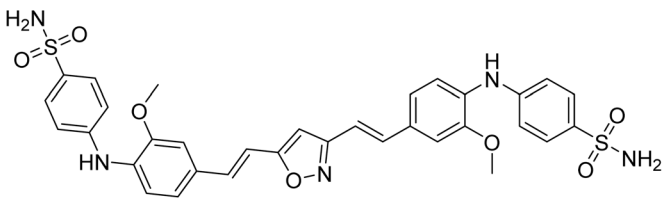

4,4'-{Isoxazole-3,5-diylbis[(E)ethene-2,1-diyl(2-methoxy-4,1-phenylene)imino]}dibenzenesulfonamide

K_i = 0.99 μM for hCA-I

K_i = 0.71 μM for bCA-II

180

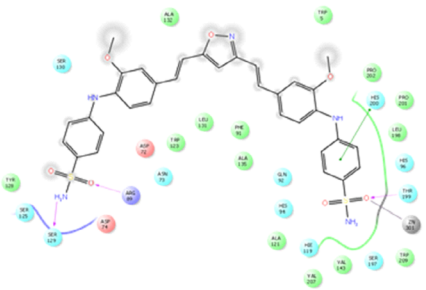

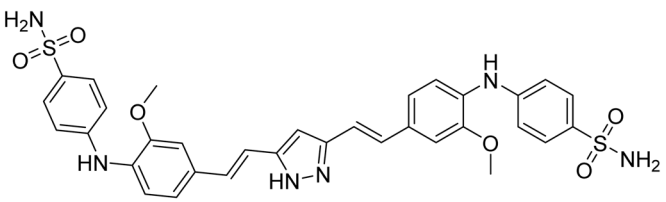

4,4'-{1H-pyrazole-3,5-diylbis[(E)ethene-2,1-diyl(2-methoxy-4,1-phenylene)imino]}dibenzenesulfonamide

K_i = 0.67 μM for bCA-II

181

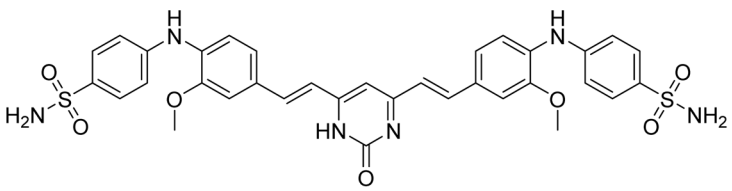

4,4'-{(2-Oxo-1,2-dihydropyrimidine-4,6-diyl)bis[(E)ethene-2,1-diyl(2-methoxy-4,1-phenylene)imino]}dibenzenesulfonamide

K_i = 0.71 μM for bCA-II

182

Fig. 64 Chemical structures of compounds **180**, **181** and **182** and their K_i values against hCA-I & bCA-II along with docking image of compound **180**.

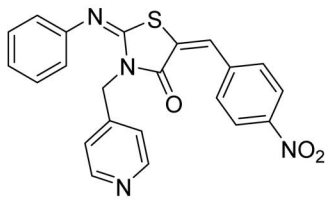

(*E*)-5-((*E*)-4-Nitrobenzylidene)-2-(phenylimino)-3-(pyridin-4-ylmethyl)thiazolidin-4-one

K_i = 1.61 μM for CA-IX

183

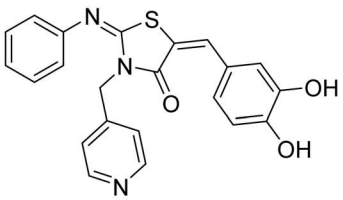

(*E*)-5-((*E*)-3,4-Dihydroxybenzylidene)-2-(phenylimino)-3-(pyridin-4-ylmethyl)thiazolidin-4-one

K_i = 1.84 μM for CA-IX

184

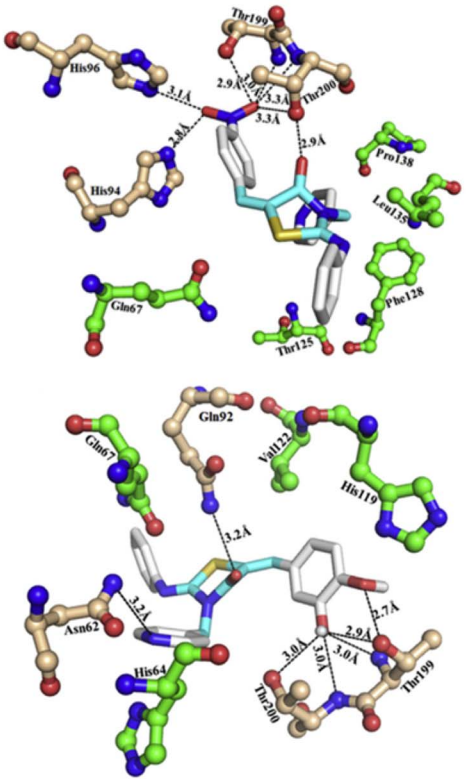

Fig. 65 Chemical structures of compounds **183** and **184** and their K_i values against hCA-IX along with their docking images.

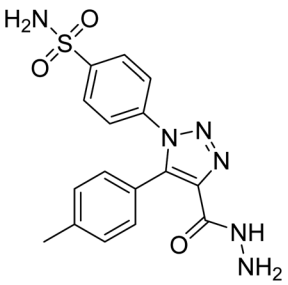

4-[4-(Hydrazinocarbonyl)-5-(p-tolyl)-1H-1,2,3-triazol-1-yl]benzenesulfonamide

K_i = 27.2 nM for hCA-I

185

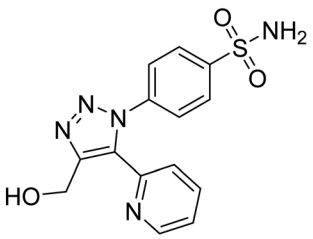

4-(4-(Hydroxymethyl)-5-(pyridin-2-yl)-1H-1,2,3-triazol-1-yl)benzenesulfonamide

K_i = 14.3 nM for hCA-IX

186

Fig. 66 Chemical structures of compounds **185** and **186** and their K_i values against hCA-I and IX.

nM), **142** (40.8 nM), **143** (46.2 nM), **144** (38.5 nM), **145** (49.2 nM), **146** (36.5 nM)] were found to be 5.9–9.7 times more potent inhibitors of hCA-I compared to AAZ. For hCA-II, the IC_{50} values of the compounds ranged from 23.8 to 30.1 nM, whereas AAZ had an IC_{50} value of 146.5 nM. This indicates that compounds **141–146** [**141** (24.7 nM), **142** (30.1 nM), **143** (26.7 nM), **144** (23.8 nM), **145** (25.7 nM), **146** (23.9 nM)] were 4.8–6.3 times more potent inhibitors of hCA-II than AAZ (Table 10).[134]

Eldehna *et al.* (2016) synthesized substituted isatin-based benzenesulfonamides and evaluated for their inhibitory activity against hCA-I, II, IX and XII. The K_i for hCA-I ranged from 7.9–894 nM, for hCA-II from 7.5–1645 nM, for hCA-IX from

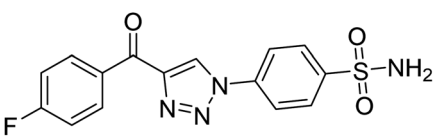

4-(4-(4-Fluorobenzoyl)-1H-1,2,3-triazol-1-yl) benzenesulfonamide

K_i = 52.4 nM for hCA-IV

187

Fig. 67 Chemical structure of compound **187** and its K_i value against hCA-IV.

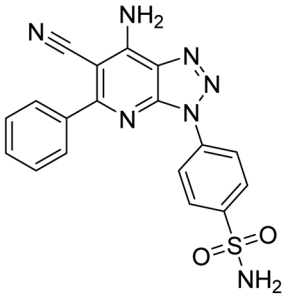

4-(7-Amino-6-cyano-5-phenyl-3H-[1,2,3] triazolo[4,5-b]pyridin-3-yl)benzenesulfonamide

K_i = 46.4 nM for hCA-IX

188

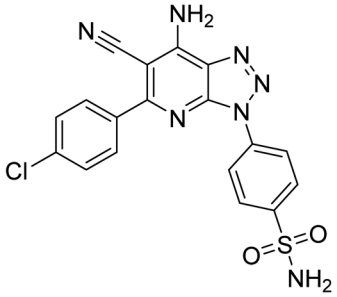

4-(7-Amino-5-(4-chlorophenyl)-6-cyano-3H-[1,2,3] triazolo[4,5-b]pyridin-3-yl)benzenesulfonamide

K_i = 42.6 nM for hCA-IX

189

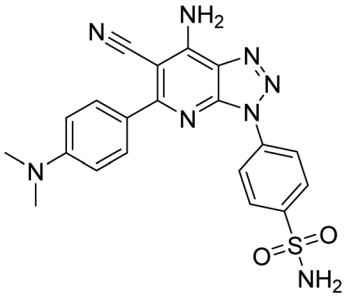

4-(7-Amino-6-cyano-5-(4-(dimethylamino)phenyl)-3H-[1,2,3] triazolo[4,5-b]pyridin-3-yl)benzenesulfonamide

K_i = 35.1 nM for hCA-IX

190

Fig. 68 Chemical structures of compounds **188**, **189** and **190** and their K_i values against hCA-IX.

5.0–240 nM, and for hCA-XII from 0.47–2.83 nM. Sulfonamides **147**, **148**, **149**, **150**, **151** and **152** exhibited exceptional potency against hCA-XII, with K_i between 0.47 and 0.71 nM (Fig. 50). Given the involvement of these isoforms in various pathologies where their inhibition could have therapeutic potential, the synthesized derivatives may represent valuable additions to the repertoire of sulfonamide-based CAI.[135]

Saeed *et al.* (2017) synthesized a series of benzyledinyl–hydrazinyl substituted thiazole derivatives and assessed for their inhibitory potential against bCA-II. The majority of these compounds exhibited excellent inhibitory activity against inhibitory potency against bCA-II, with compound **153** showing the highest activity (IC_{50} = 1.26 μM) (Fig. 51). The high potency of compound **153** is attributed to the presence of *ortho*-positioned halogen atoms (–F and –Cl), which activate the thiourea nitrogen through a negative inductive effect. Molecular docking studies of these potent dual inhibitors provided insights into their binding site interactions.[136]

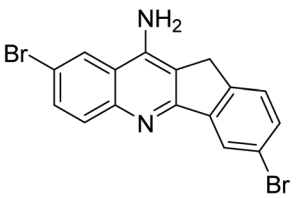

3,8-Dibromo-11*H*-indeno[1,2-*b*]quinolin-10-amine

K_i = 120.9 nM for hCA-I

K_i = 267.5 nM for hCA-II

191

Fig. 69 Chemical structure of compound **191** and its K_i values against hCA-I and II.

Khan *et al.* (2017) synthesized a series of carbohydrazones and assessed their *in vitro* inhibitory activity against bCA. Among these, compounds **154** (IC_{50} = 1.33 μM), **155** (IC_{50} = 1.85 μM), **156** (IC_{50} = 1.37 μM), and **157** (IC_{50} = 1.46 μM) demonstrated superior inhibition compared to the standard reference drug zonisamide (IC_{50} = 1.86 μM) (Fig. 52). Compound **154**, featuring a nitro group at the *p*-position of the phenyl ring, exhibited the strongest enzyme inhibition with an IC_{50} = 1.33 μM. Compound **155**, with a nitro group at the *o*-position, showed slightly lower activity (IC_{50} = 1.85 μM). Compound **157**, with 2,6-dichloro substituents, had significant inhibitory potential (IC_{50} = 1.46 μM), suggesting increased potency with chloro groups at both *ortho* positions, but decreased effectiveness with *ortho* and *para* substitution (2,4-dichloro). Cheminformatic analysis indicated that compounds **154** and **155** possess properties consistent with lead-like candidates. The figure presents a 2D interaction map of compounds **154** and

Table 11 Chemical structures of substituted sulfonamides, inhibition data against CAIs

Compound no.	Chemical structures & IUPAC names	K_i (nM) CA-I	CA-II	CA-VII	CA-IX	Ref.
192	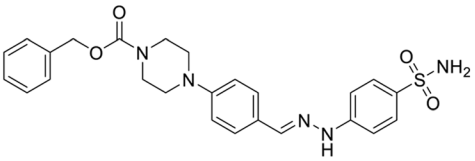 Benzyl 4-(4-((2-(4-sulfamoylphenyl)hydrazono)methyl) phenyl)piperazine-1-carboxylate	919.6	93.9	11.4	1631.4	155
193	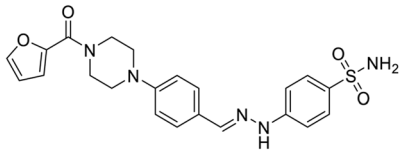 4-(2-(4-(4-(Furan-2-carbonyl)piperazin-1-yl) benzylidene)hydrazinyl)benzenesulfonamide	321.8	30.8	6.2	1788.6	155
194	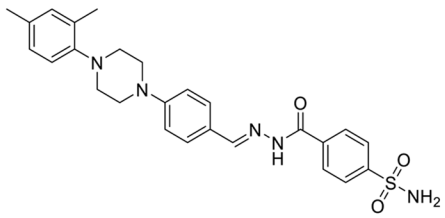 4-(2-(4-(4-(2,4-Dimethylphenyl)piperazin-1-yl)benzylidene) hydrazinecarbonyl)benzenesulfonamide	>10 000	9385.9	17.8	1660.9	155
Standard	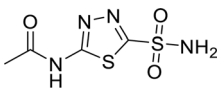 Acetazolamide (AAZ)	250	12.1	2.5	25.8	155

157, illustrating their binding modes with the active site residues of the enzyme (Fig. 52).[137]

Gencer *et al.* (2017) synthesized spiroindoline-substituted sulphonamide compounds and assessed their inhibitory effects on hCA-I and II. Remarkably, compound **158** demonstrated the highest inhibition of hCA-I with a K_i value of 0.042 μM, while compound **159** showed the greatest inhibition of hCA-II with a K_i value of 0.151 μM (Fig. 53).[138] The findings suggest that these compounds could have potential medical

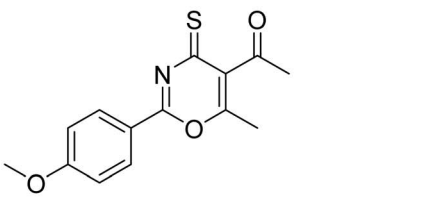

1-(2-[4-Methoxyphenyl]-6-methyl-4-thioxo-4H-1,3-oxazin-5-yl)ethanone

K_i = 0.144 μM for bCA-II

195

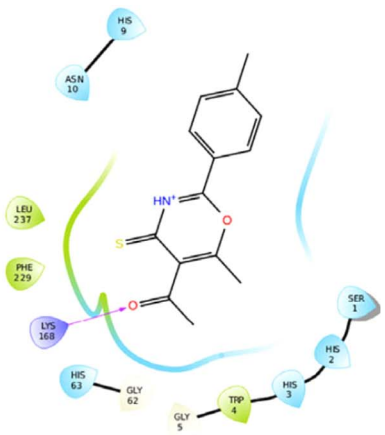

Fig. 70 Chemical structure of compound **195** and its K_i value against bCA-II along with docking image of compound **195**.

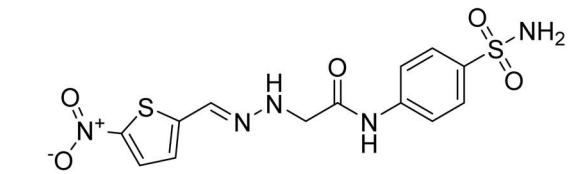

2-(2-((5-Nitrothiophen-2-yl)methylene)hydrazinyl) -N-(4-sulfamoylphenyl)acetamide

K_i = 0.1676 μM for hCA-I

196

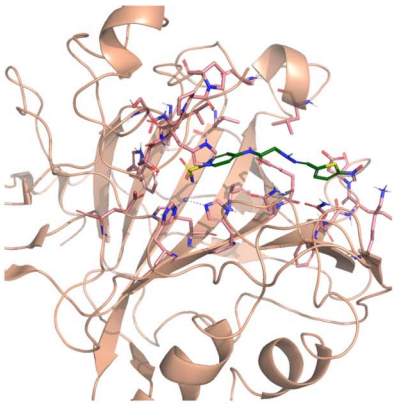

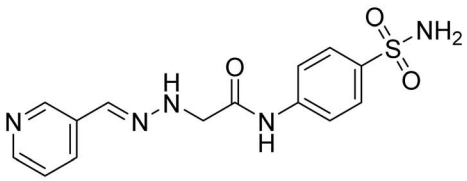

2-(2-(Pyridin-3-ylmethylene)hydrazinyl)-N-(4-sulfamoylphenyl)acetamide

K_i = 0.2880 μM for hCA-II

197

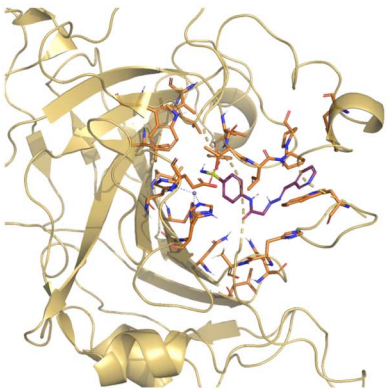

Fig. 71 Chemical structures of compounds **196** and **197**; their K_i values against hCA-I and II along with docking images of compounds **196** and **197**.

applications. Consequently, they warrant further evaluation through *in vivo* studies.

Supuran *et al.* (2017) synthesized substituted 3,4-dihydroquinolin-2(1*H*)-one, and evaluated for their inhibitory effects on four CA isoforms: hCA-I, II, IV and IX. The most effective hCA-IX inhibitors were compounds **160** and **161**, with K_i ranging from 243.6 to 292.8 nM. These compounds are notably different: compound **160** is a urea derivative containing a pentafluorophenyl group, whereas compound **161** features a secondary sulfonamide functionality (Fig. 54).[139]

Arifuddin *et al.* (2017) synthesized substituted indazole-3-carboxamide hybrids and evaluated as inhibitors of hCA-IX. Specifically, compounds **162**, **163**, and **164** demonstrated potent inhibition of the tumor-associated, hypoxia-induced hCA-IX, with K_i values of 1.8, 2.3, and 2.0 nM, respectively (Fig. 55). Compounds **162**, **163**, and **164** exhibited 11- to 14-fold greater potency due to the alkyl substituents (isopropyl, ethyl and methyl, respectively) compared to the sulfonamide standard AAZ (K_i = 25 nM).[140]

Kamal *et al.* (2017) synthesized sulfonamide derivatives inspired by curcumin and evaluated them against four isoforms: hCA-I, II, IX, and XII. The new compounds showed moderate inhibition of hCA-I (K_i = 191.8–904.2 nM), high inhibition of hCA-II (K_i = 0.75–8.8 nM), potent inhibition of hCA-IX (K_i = 2.3–87.3 nM), and inhibition of hCA-XII (K_i = 6.1–71.8 nM). Markedly, compound **165** displayed nearly 9-fold selectivity for hCA-II (K_i = 0.89 nM) over hCA-IX and XII, while compound **166** showed 3-fold and 70-fold selectivity for hCA-II (K_i = 0.75 nM) over hCA-IX and XII, respectively (Fig. 56). This selectivity difference is attributed to the varying placement of methoxy groups on the second aryl ring derived from chalcone.[141]

Gülçin *et al.* (2017) synthesized novel 2-amino-3-cyanopyridines and assessed their inhibitory effects on hCA-I and II. Compound **167** demonstrated the highest inhibition of hCA-I with a K_i = 2.84 μM, while compound **168** was the most potent inhibitor of hCA-II with a K_i = 2.56 μM (Fig. 57). These compounds are promising candidates for future drug development.[142]

Gülçin *et al.* (2017) synthesized amides and thiazolidine-4-ones and accessed their hCA activity. These compounds demonstrated effective inhibition profiles with K_i values ranging from 23.76 to 102.75 nM against hCA-I and 58.92 to 136.64 nM against hCA-II. In comparison, AAZ (standard) exhibited K_i values of 482.63 nM against hCA-I and 1019.60 nM against hCA-II. Among the inhibitor compounds, compound **169** exhibited the highest inhibition of hCA-I with a K_i value of 23.76 nM. Additionally, the compound **170** demonstrated the most potent inhibition of hCA-II with a K_i of 58.92 nM (Fig. 58).[143]

Gülçin *et al.* (2017) synthesized pyrrolidine-2,5-diones derivatives in good yields. Compound **171**, featuring two carbonyl groups and one chlorine group, demonstrated potent inhibition of hCA-I with a K_i of 23.27 nmol L^{-1}. Furthermore, compound **172**, which also includes two carbonyl groups and

Table 12 Chemical structures of substituted sulfonamides, inhibition data against CAIs

Compound no.	Chemical structures & IUPAC names	K_i (nM) CA-I	CA-IX	CA-XII	Ref.
198	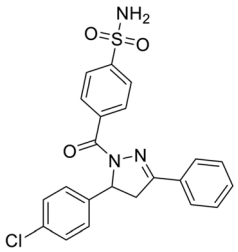 4-(5-(4-Chlorophenyl)-3-phenyl-4,5-dihydro-1*H*-pyrazole-1-carbonyl)benzenesulfonamide	195.0	7.9	34.0	158
199	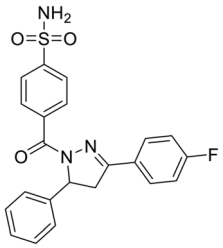 4-(3-(4-Fluorophenyl)-5-phenyl-4,5-dihydro-1*H*-pyrazole-1-carbonyl)benzenesulfonamide	102.9	23.1	10.1	158
200	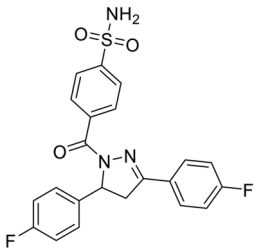 4-(3,5-Bis(4-fluorophenyl)-4,5-dihydro-1*H*-pyrazole-1-carbonyl)benzenesulfonamide	140.7	5.5	7.1	158
201	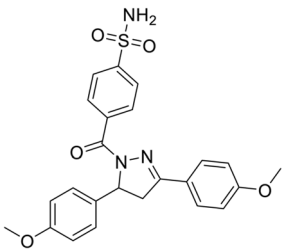 4-(3,5-Bis(4-methoxyphenyl)-4,5-dihydro-1*H*-pyrazole-1-carbonyl)benzenesulfonamide	875.9	37.0	18.8	158
202	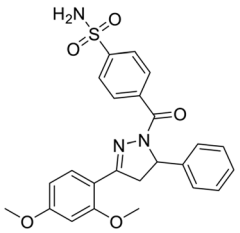 4-(3-(2,4-Dimethoxyphenyl)-5-phenyl-4,5-dihydro-1*H*-pyrazole-1-carbonyl)benzenesulfonamide	807.8	32.9	9.7	158

Table 12 (*Contd.*)

Compound no.	Chemical structures & IUPAC names	K_i (nM) CA-I	CA-IX	CA-XII	Ref.
203	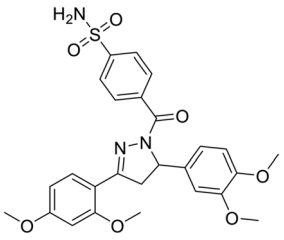 4-(3-(2,4-Dimethoxyphenyl)-5-(3,4-dimethoxy phenyl)-4,5-dihydro-1*H*-pyrazole-1-carbonyl)benzenesulfonamide	2961.3	36.3	28.9	158
204	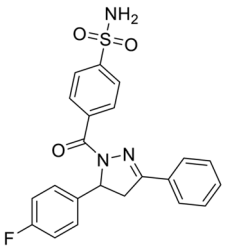 4-(5-(4-Fluorophenyl)-3-phenyl-4,5-dihydro-1*H*-pyrazole-1-carbonyl)benzenesulfonamide	87.8	44.5	9.4	158
Standard	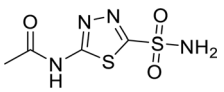 Acetazolamide (AAZ)	250	25	5.7	158

a chlorine group, proved to be the most effective inhibitor of hCA-II with a K_i of 10.64 nmol L^{-1} (Fig. 59). It is widely recognized that compounds containing carbonyl (–CO) and chlorine (–Cl) groups exhibit effective CAI properties.[144]

Durdagi *et al.* (2017) synthesized coumaryl-carboxamide derivatives and evaluated for their inhibitory activity against hCA-I, II, VII, and IX. Specifically, compound **173** selectively inhibited hCA-IX with a K_i of 107.9 nM (Fig. 60). Compound **173** displayed the highest activity against hCA-IX, with superior docking scores for both hydrolyzed (−9.006 kcal mol^{-1}) and non-hydrolyzed (−8.429 kcal mol^{-1}) forms compared to hCA-I, II, and VII. Docking studies showed that the hydrolyzed form of **173** interacted with His96, His64, His94, and Gln92 at the hCA-IX active site, while the non-hydrolyzed form interacted with His64, His94, and His119 (Fig. 60).[145]

Supuran *et al.* (2017) synthesized different alkoxymethyl derivatives of mercaptobenzoxazole and 2-aminothiazole. This study investigated the inhibitory effects of these molecules on hCA-I and II. The newly synthesized molecules significantly inhibited both hCA isoenzymes, with K_i values ranging from 58 to 157 nM for hCA-I and 76 to 215 nM for hCA-II. In particular, compound **174** (K_i = 58 nM) and compound **175** (K_i = 70 nM) exhibited stronger inhibition of the hCA-I isoform compared to the standard compound AAZ (K_i = 333 nM). For hCA-II, the most significant inhibition was observed with compound **176** (K_i = 76 nM) (Fig. 61).[146]

Gülçin *et al.* (2018) synthesized a series of *N*-heterocyclic carbene precursors with 2-hydroxyethyl substitutions. These novel NHC precursor derivatives exhibited significant inhibitory activity against hCA-I and II. The K_i were found to range from 13.90 to 41.46 nM for hCA-I and 12.82 to 49.95 nM for hCA-II, respectively. Compound **177** exhibited the most potent inhibition of the hCA-I isoform, with a K_i value of 13.90 nM and **177** exhibited a K_i value of 12.82 nM against hCA-II (Fig. 62).[147]

Gülçin *et al.* (2018) synthesized a series of benzimidazolium salts evaluated their hCA-I and II activities. Compound **178** showed the highest inhibition of hCA-I with a K_i value of 17.33 nM, while compound **179** demonstrated excellent inhibition of hCA-II with a K_i value of 33.98 nM (Fig. 63). Compared to the standard drug AAZ, which has K_i values of 132.55 nM and 176.15 nM for hCA-I and II, respectively, these compounds exhibited superior inhibitory profiles.[148]

Ahmed *et al.* (2018) synthesized a series of sulfonamides based on a curcumin scaffold and assessed their inhibitory activity against hCA-I and bCA-II isoforms. Compound **180** showed the highest inhibition of hCA-I with a K_i value of 0.99 μM. For bCA-II, compounds **180**, **181**, and **182** had K_i values of 0.71, 0.67, and 0.71 μM, respectively (Fig. 64). These compounds

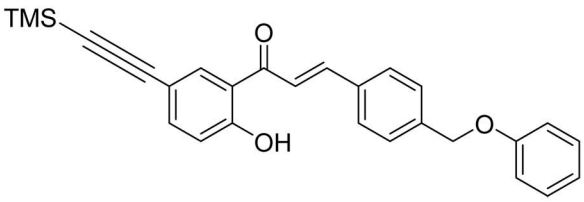

(1-(2-Hydroxy-5-(trimethylsilyl)phenyl)-3-(4-(phenoxymethyl)phenyl)prop-2-en-1-one

IC_{50} = 0.054 μM for bCA-II

205

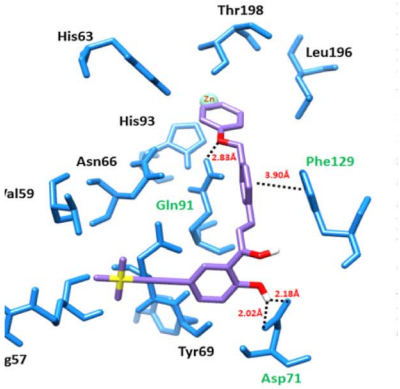

Fig. 72 Chemical structure of compound **205**; its IC_{50} value against bCA-II along with docking image of compound **205**.

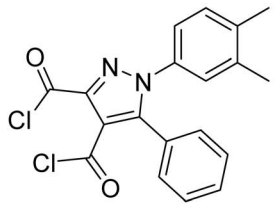

1-(3,4-Dimethylphenyl)-5-phenyl-1H-pyrazole-3,4-dicarbonyldichloride

K_i = 1.03 nM for hCA-I

K_i = 1.82 nM for hCA-II

206

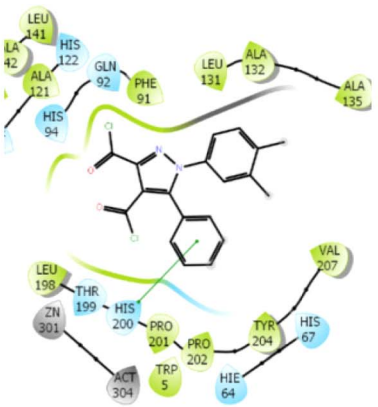

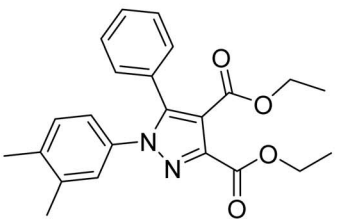

Diethyl 1-(3,4-dimethylphenyl)-5-phenyl-1H-pyrazole-3,4-dicarboxylate

K_i = 6.58 nM for hCA-I

K_i = 8.93 nM for hCA-II

207

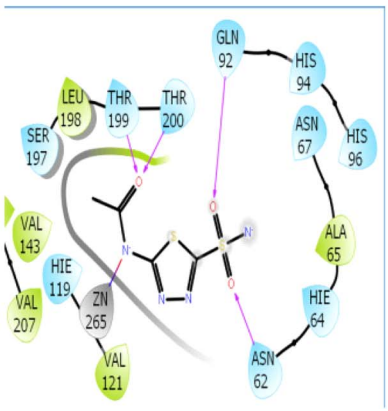

Fig. 73 Chemical structures of compounds **206** and **207**; their K_i values against hCA-I and II along with docking images of compound **206** and **207**.

exhibited inhibitory activities comparable to the standard drug AAZ, and molecular docking studies suggested they bind to hCA-I in a similar manner (Fig. 64).[149]

Azam *et al.* (2018) synthesized pyridinethiazolidinone derivatives and tested them as inhibitors of CA-IX. Compounds **183** and **184** demonstrated strong inhibition with IC_{50} values of 1.61 μM and 1.84 μM, respectively (Fig. 65). Their binding affinities for CA-IX were high, with KD values of 11.21 μM for **183** and 2.32 μM for **184**. Docking studies showed that both compounds effectively bind to the CA-IX active site, forming multiple hydrogen bonds and van der Waals interactions with key residues.[150]

Sharma *et al.* (2018) synthesized a library of substituted 1,2,3-triazole carboxylates and assessed for their inhibitory activity against hCA-I, II, IV, and IX which are established drug targets. Carboxylic acid hydrazide **185** showed the highest inhibition potency against hCA-II with a K_i of 27.2 nM, while derivative **186** demonstrated superior inhibition of hCA-IX with a K_i of 14.3 nM, outperforming the reference drug AAZ (K_i = 25.8 nM) (Fig. 66).[151]

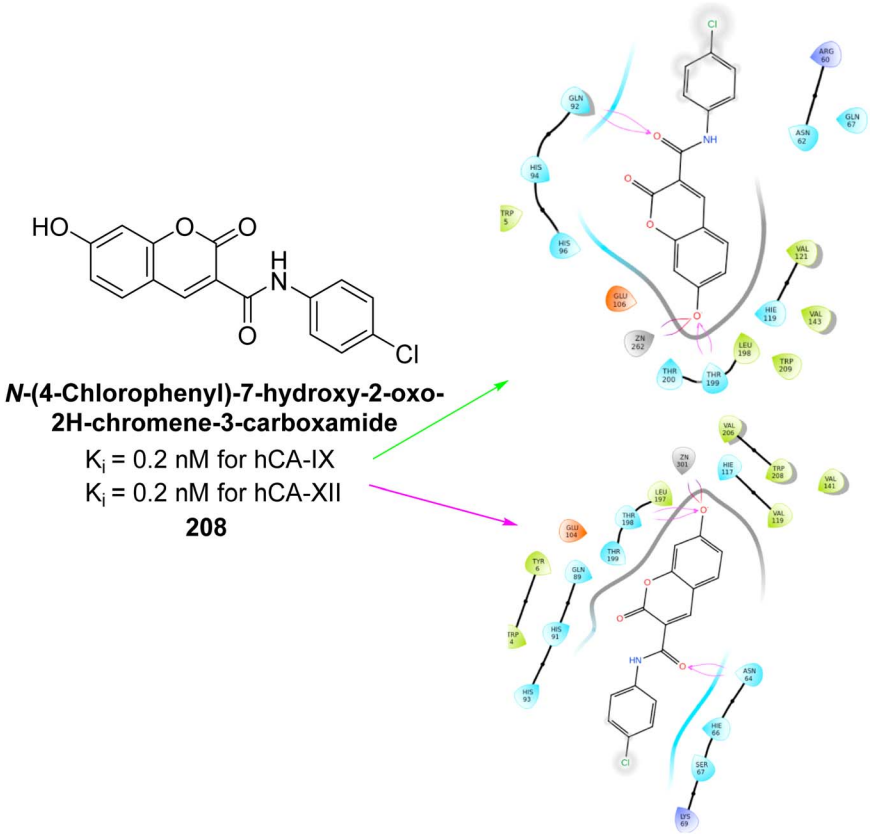

Fig. 74 Chemical structure of compound **208**; its K_i value against hCA-IX and XII along with docking images of compound **208**.

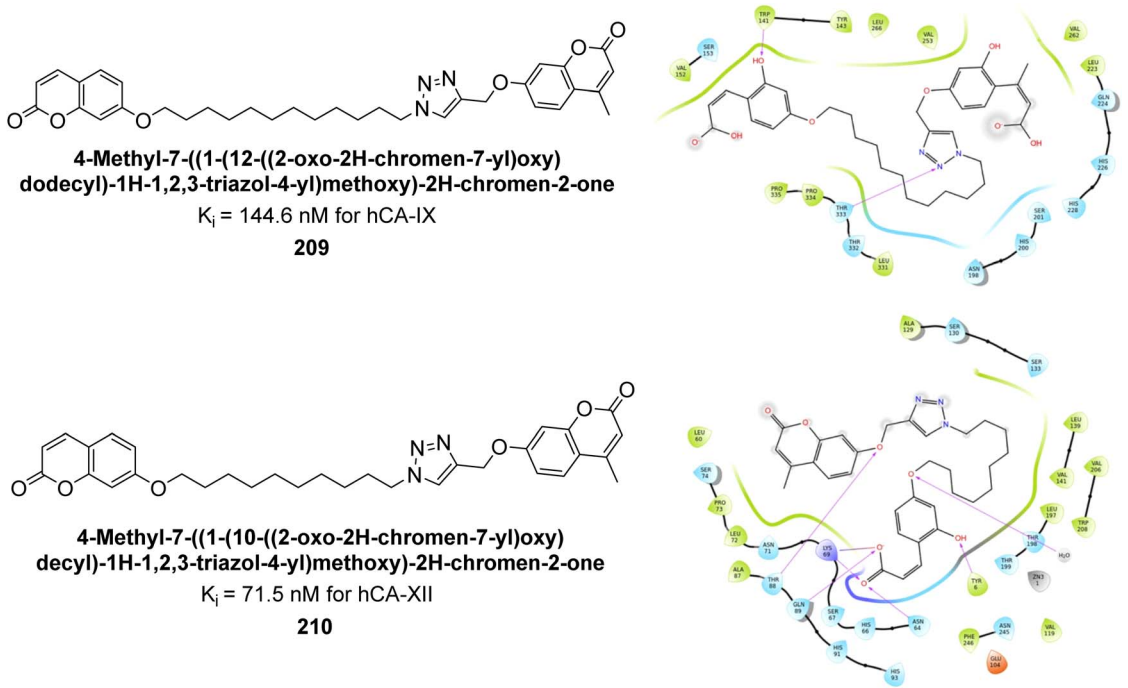

Fig. 75 Chemical structures of compounds **209** and **210**; their K_i values against hCA-IX and XII along with their docking images.

Supuran *et al.* (2018) synthesized a series of benzenesulfonamide bearing 1,2,3-triazole ring, and evaluated against hCA-I, II, IV, and IX. All newly synthesized compounds demonstrated excellent inhibition of the hCA-I, with K_i ranging from 30.1 to 86.8 nM, significantly lower than the standard drug AAZ, which has a K_i of 250 nM. For the hCA-IV, compound **187** showed

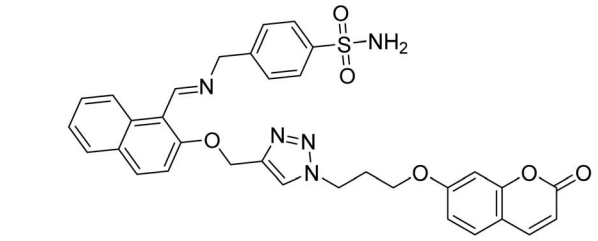

4-((((2-((1-(3-((2-oxo-2H-chromen-7-yl)oxy)propyl)-1H-1,2,3-triazol-4-yl)methoxy)naphthalen-1-yl)methylene)amino)methyl) benzenesulfonamide

K_i = 45.5 nM for hCA-IX

211

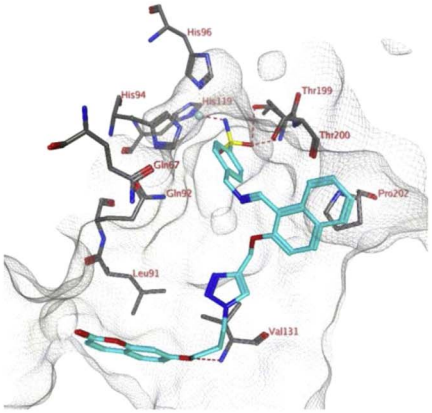

Fig. 76 Chemical structure of compound **211**; its K_i value against hCA-IX along with docking image of compound **211**.

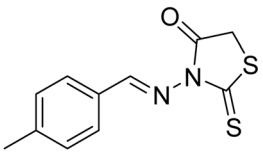

3-((4-Methylbenzylidene)amino)-2-thioxothiazolidin-4-one

K_i = 47.7 nM for hCA-I

K_i = 52.8 nM for hCA-II

212

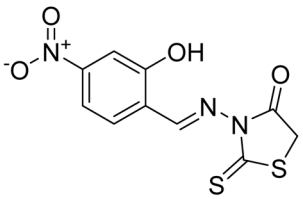

3-((2-Hydroxy-4-nitrobenzylidene)amino)-2-thioxothiazolidin-4-one

K_i = 44.7 nM for hCA-I

K_i = 55.5 nM for hCA-II

213

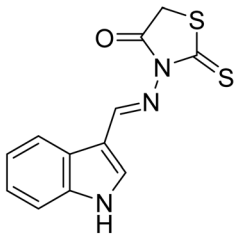

3-(((1H-Indol-3-yl)methylene)amino)-2-thioxothiazolidin-4-one

K_i = 43.5 nM for hCA-I

K_i = 46.6 nM for hCA-II

214

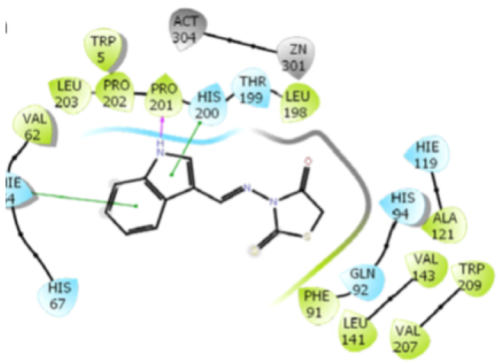

Fig. 77 Chemical structures of compounds **212**, **213** and **214**; their K_i values against hCA-I and II along with docking image of compound **214**.

superior inhibition (K_i = 52.4 nM) compared to AAZ (K_i = 74 nM) (Fig. 67), while for the hCA-IX, all compounds exhibited moderate inhibition potential. This study contributes to the ongoing exploration of the 1,2,3-triazole moiety in medicinal chemistry.[152]

Supuran *et al.* (2018) synthesized and characterized triazole benzenesulfonamides and assessed against four isozymes: hCA-I, II, IV and IX. The results indicated that the hCA-IX was the most susceptible to inhibition by these derivatives. Especially, compound **188** (K_i = 46.4 nM), **189** (K_i = 42.6 nM) and **190** (K_i = 35.1 nM) emerged as the most potent CA inhibitors (Fig. 68). *p*-Substitution on benzenesulfonamide with a triazolopyridine moiety was found to be highly effective for CA inhibition. Adding an aryl group at the 5-position of triazolopyridine increased affinity for hCA-IX. Particularly, the *N*-dimethyl derivative **190** demonstrated the highest potency in this study.[153]

Ökten *et al.* (2018) designed and synthesized bromoindenoquinolines and evaluated them against hCA-I and II. Indenoquinolines with Br substituents at the C-3 and C-8 positions showed notable inhibition of hCA-I and II, outperforming other derivatives and AAZ. Among all the synthesized derivatives, only compound **191** exhibited significant inhibitory activity, with IC_{50} values of 120.9 nM and 267.5 nM, compared to AAZ

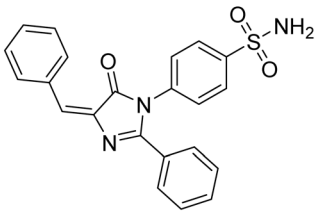

4-(4-Benzylidene-5-oxo-2-phenyl-4,5-dihydro-1H-imidazol-1-yl)benzenesulfonamide
K_i = 58.7 nM for hCA-IX
K_i = 76.5 nM for hCA-XII
215

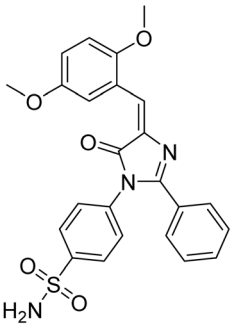

4-(4-(2,5-Dimethoxybenzylidene)-5-oxo-2-phenyl-4,5-dihydro-1H-imidazol-1-yl)benzenesulfonamide
K_i = 23.0 nM for hCA-IX
K_i = 54.8 nM for hCA-XII
216

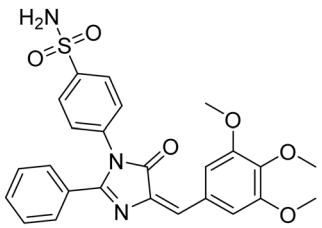

4-(5-Oxo-2-phenyl-4-(3,4,5-trimethoxybenzylidene)-4,5-dihydro-1H-imidazol-1-yl)benzenesulfonamide
K_i = 68.2 nM for hCA-IX
K_i = 179.6 nM for hCA-XII
217

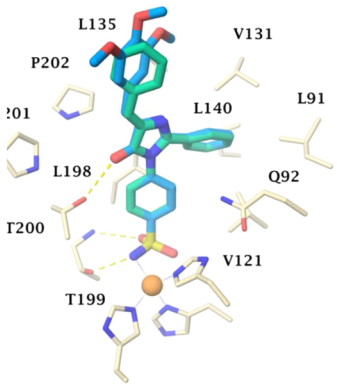

Fig. 78 Chemical structures of compounds **215**, **216** and **217**; their K_i values against hCA-IX and XII along with docking image of compound **217**.

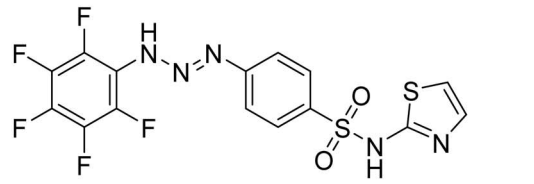

4-[3-(Perfluorophenyl)triaz-1-en-1-yl]-N-(thiazol-2-yl)-benzenesulfonamide
K_i = 450.37 nM for hCA-I
K_i = 504.37 nM for hCA-II
218

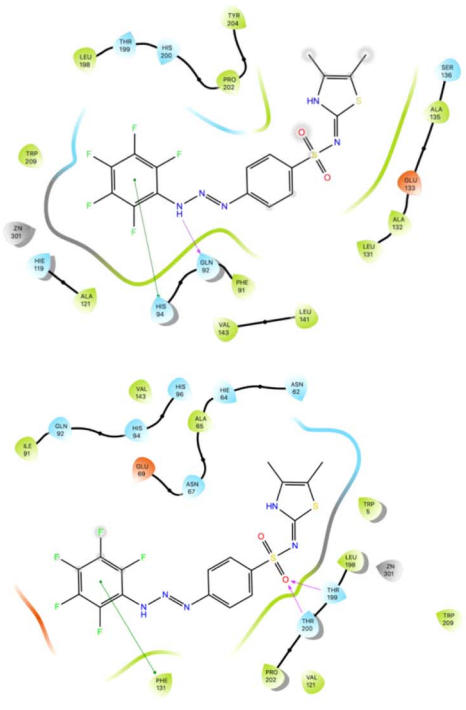

Fig. 79 Chemical structure of compound **218**; its K_i values against hCA-I and II along with docking images of compound **218**.

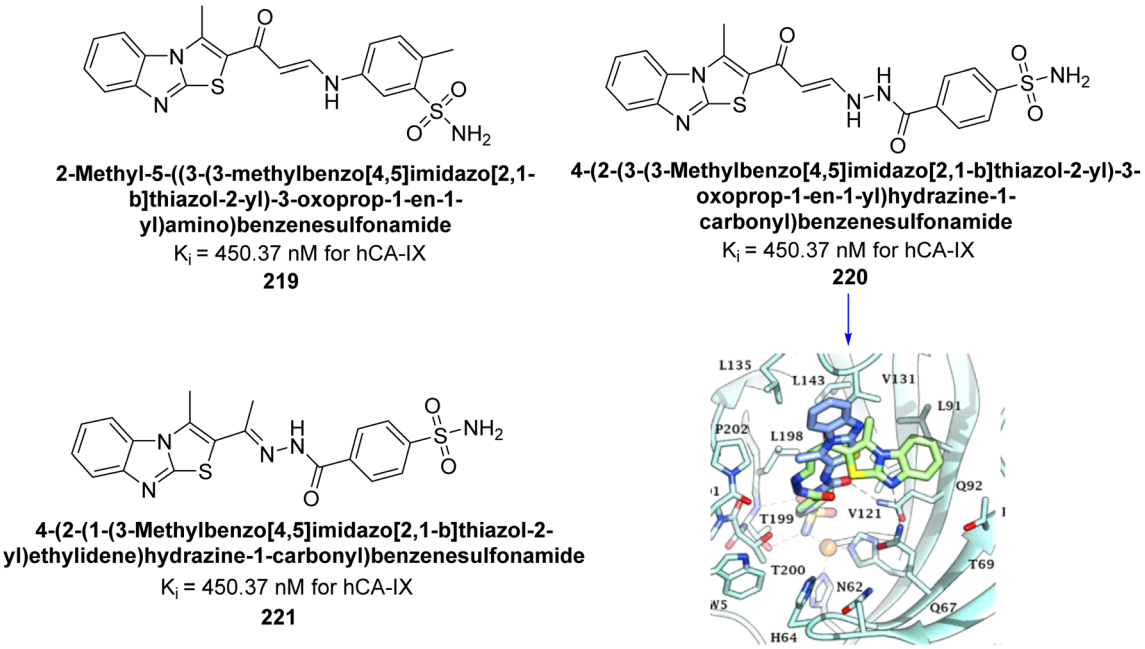

Fig. 80 Chemical structures of compounds **219**, **220** and **221**; their K_i values against hCA-IX along with docking image of compound **220**.

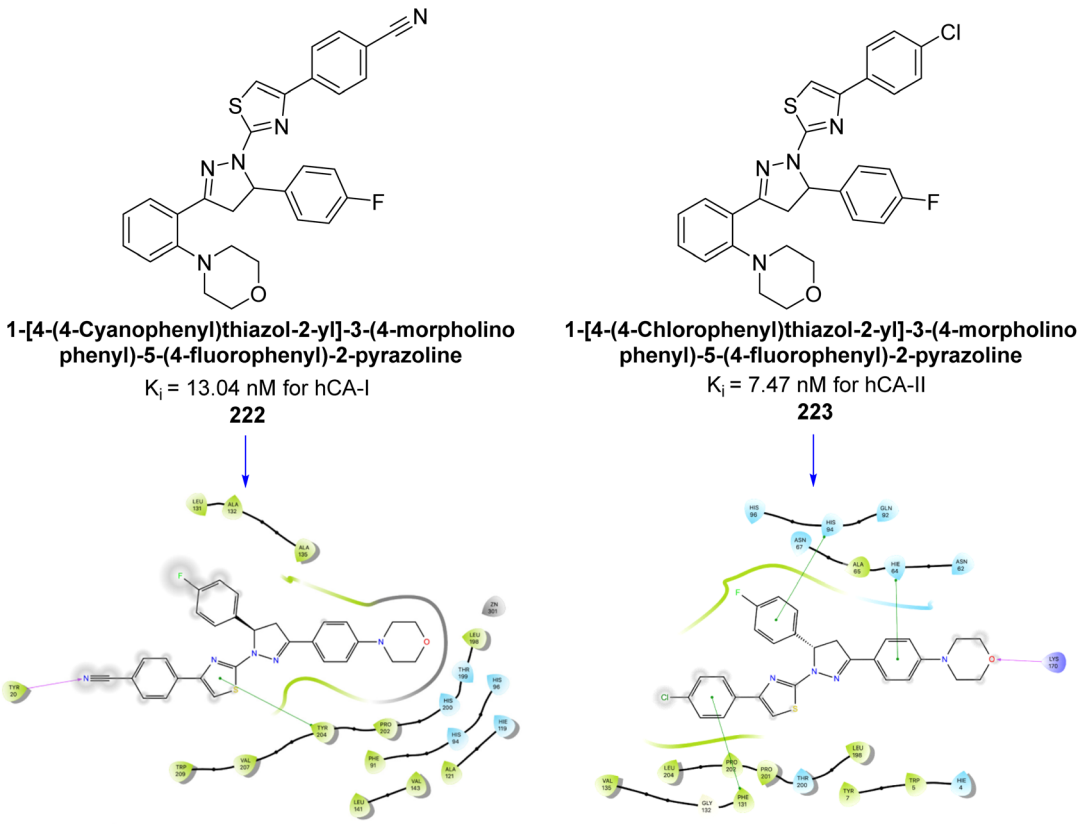

Fig. 81 Chemical structures of compounds **222** and **223**; their K_i values against hCA-I and II along with their docking images.

(Fig. 69). This study suggests that indenoquinoline amine derivatives substituted with bromine and phenyl groups have potential as promising inhibitors of hCA-I and II.[154]

Supuran *et al.* (2018) synthesized novel benzenesulfonamide derivatives and evaluated against hCA-I, II, VII, and IX. The target compounds exhibited strong inhibition of hCA-VII, with less effectiveness against other hCA isoforms. The benzyl

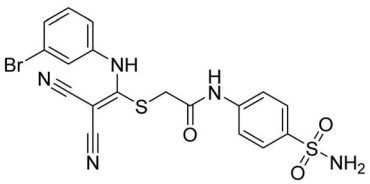

2-[1-(3-Bromophenylamino)-2,2-dicyanovinyl thio]-N-(4-sulfamoylphenyl)acetamide
K_i = 9.01 nM for hCA-I
224

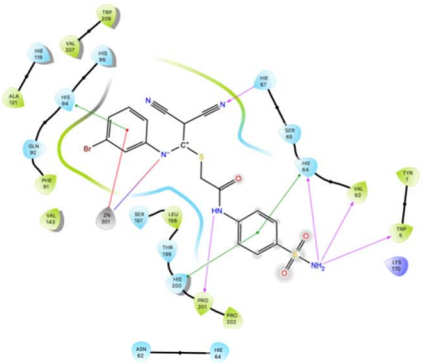

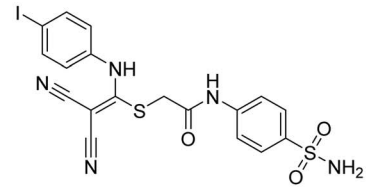

2-[2,2-Dicyano-1-(4-iodophenylamino)vinyl thio]-N-(4-sulfamoylphenyl)acetamide
K_i = 7.41 nM for hCA-II
225

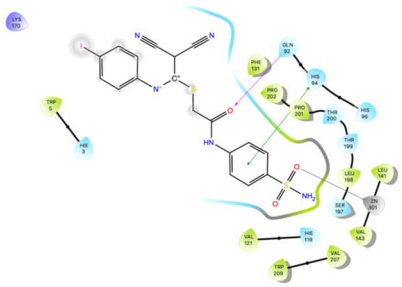

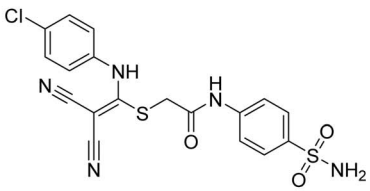

2-[1-(4-Chlorophenylamino)-2,2-dicyanovinyl thio]-N-(4-sulfamoylphenyl)acetamide
K_i = 7.37 nM for hCA-I
226

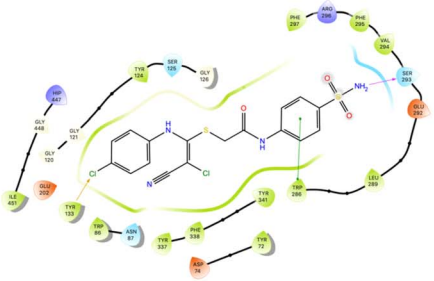

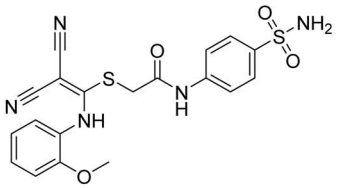

2-[2,2-Dicyano-1-(2-methoxyphenylamino)vinyl thio]-N-(4-sulfamoylphenyl)acetamide
K_i = 48.28 nM for hCA-I
227

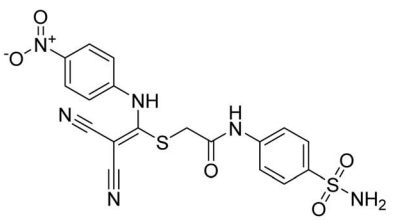

2-[2,2-Dicyano-1-(4-nitrophenylamino)vinyl thio]-N-(4-sulfamoylphenyl)acetamide
K_i = 105.94 nM for hCA-I
228

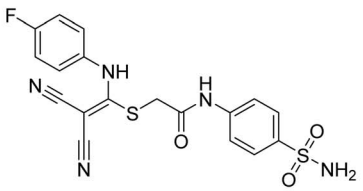

2-[2,2-Dicyano-1-(4-fluorophenylamino)vinyl thio]-N-(4-sulfamoylphenyl)acetamide
K_i = 56.75 nM for hCA-II
229

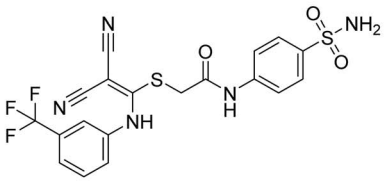

2-[2,2-Dicyano-1-(3-(trifluoromethyl)phenylamino)vinyl thio]-N-(4-sulfamoylphenyl)acetamide
K_i = 49.92 nM for hCA-II
230

Fig. 82 Chemical structures of compounds **224**–**230**; their K_i values against hCA-I and II along with docking images of compounds **224**, **225** and **226**.

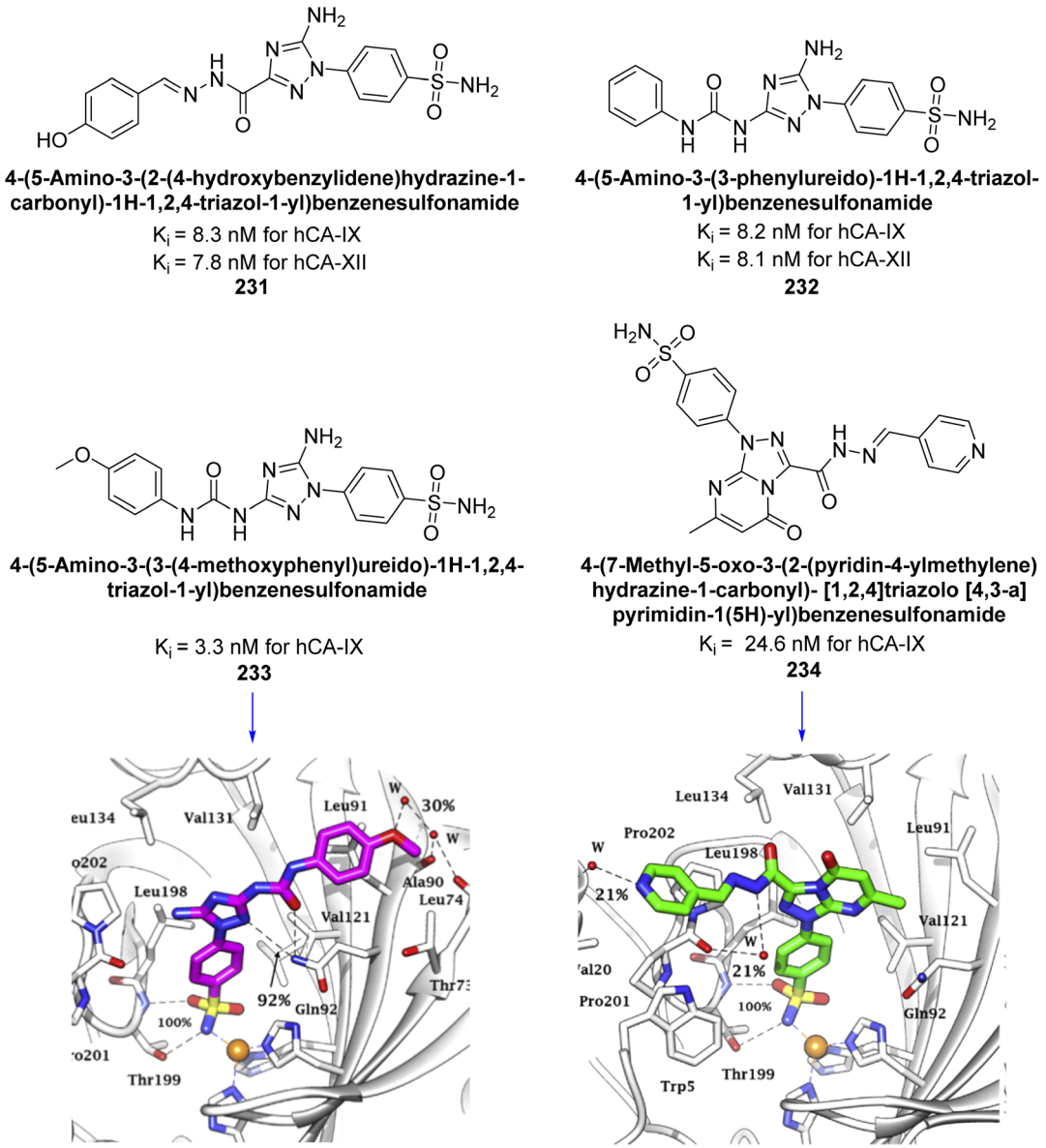

Fig. 83 Chemical structures of compounds **231–234**; their K_i values against hCA-IX and XII along with docking images of compounds **233** and **234**.

carbamate piperazine derivative **192** had a $K_i = 11.4$ nM, while the furoyl piperazine derivative **193** showed an even lower $K_i = 6.2$ nM. Among the benzylidenehydrazine carbonyl series, the *o*,*p*-dimethyl piperazine derivative **194** was the most selective hCA-VII inhibitor, with a K_i of 17.8 nM. The findings indicate that compounds **192** and **193** are potent inhibitors of hCA-II and VII, while compound **194** is a highly selective inhibitor of hCA-VII with low nanomolar inhibition (Table 11). These three compounds were therefore chosen for further investigation of their anticonvulsant effects in preclinical animal models of epilepsy.[155]

Ashraf *et al.* (2018) synthesized 1,3-oxazine derivatives and evaluated their inhibitory activity against bCA-II. Compound **195**, featuring a 4-methoxy phenyl group, was the most potent, with an $IC_{50} = 0.144$ μM, outperforming the standard AAZ ($IC_{50} = 0.997$ μM). Molecular docking studies showed that compound **195** binds effectively to the enzyme's active site, interacting with key residues including His2, Lys168, His3, Ser1, Trp4, Asn10, Gly5, Gly63, His9, Leu 237, Phe229 and His63. This compound is suggested as a promising lead for developing more effective CAIs (Fig. 70).[156]

Sağlık *et al.* (2019) synthesized new sulfonamide-hydrazone derivatives and evaluated their inhibitory effects on hCA-I and II. Compound **196** demonstrated the highest inhibition of hCA-I, with a $K_i = 0.1676$ μM, while compound **197** was most effective against hCA-II, with a $K_i = 0.2880$ μM. Docking studies showed that compound **196** interacts with hCA-I through a hydrogen bond with Gln92, a π–π interaction with His200, and a salt bridge with Lys57. Compound **197** binds to hCA-II *via* three hydrogen bonds: the amide carbonyl group with Asn62 and Asn67, and the pyridine nitrogen with Trp5 (Fig. 71).[157]

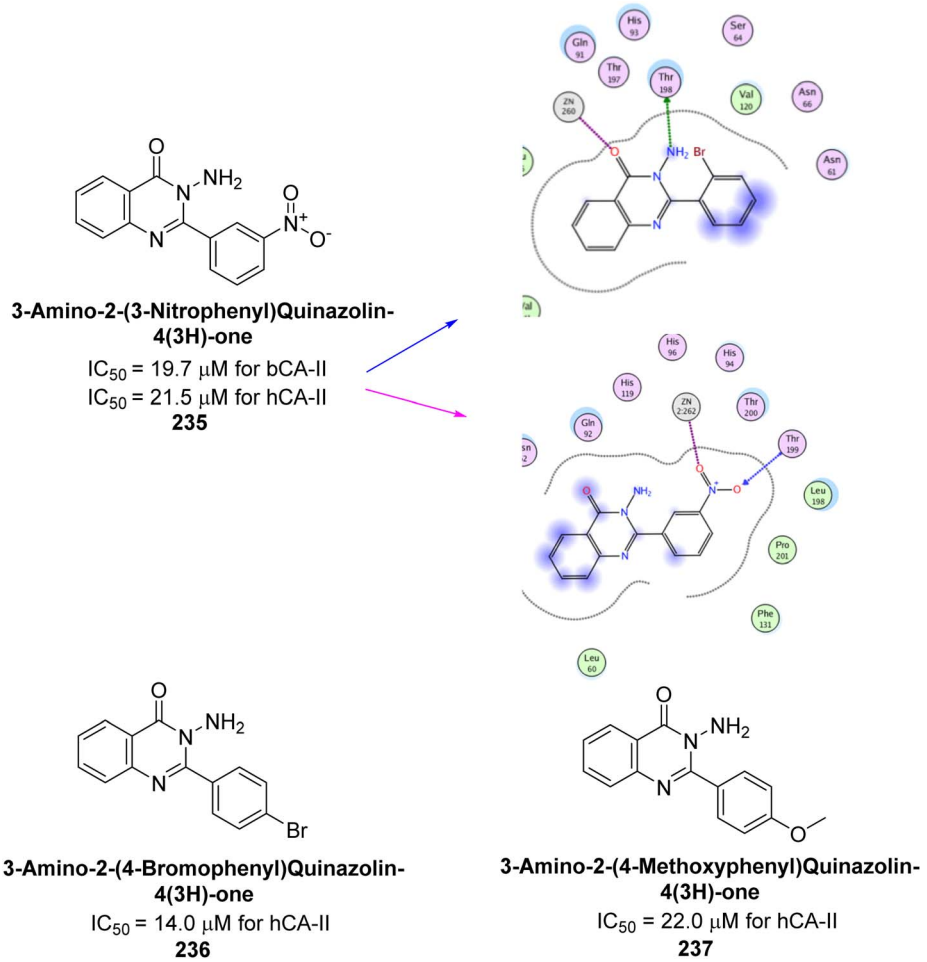

Fig. 84 Chemical structures of compounds **235–237**; their IC_{50} values against bCA-II and hCA-II along with docking image of compound **235**.

Supuran *et al.* (2019) synthesized pyrazoline-linked benzenesulfonamides and evaluated against hCA-I, IX, and XII. All the compounds demonstrated potent inhibition of hCA-I, with K_i ranging from 87.8 to 244.1 nM, beating AAZ (K_i = 250.0 nM). Compounds **198**, **199**, **200**, **201**, **202**, and **203** showed effective inhibition of hCA-IX, with K_i values between 5.5 and 37.0 nM, either surpassing or matching the efficacy of AAZ. Additionally, compounds **199**, **200**, **202** and **204** exhibited strong inhibitory activity against hCA-XII, with K_i values ranging from 7.1–10.1 nM, compared to AAZ (K_i = 5.7 nM) (Table 12).[158]

Larik *et al.* (2019) synthesized a novel silyl-yne chalcone derivatives and the derivatives were tested for inhibition of bCA-II. All compounds showed better inhibition than the standard AAZ. Among them, compound **205** emerged as the most potent, with an IC_{50} value of 0.054 μM. Binding analysis indicated that compound **205** binds to the active site of bCA-II, with a single π–π stacking interaction observed between the ligand's ring structure and Phe129, with a bond length of 4.90 Å (Fig. 72).[159]

Taslimi *et al.* (2019) synthesized substituted pyrazole compounds and assessed their inhibition of hCA-I and II. The K_i values ranged from 1.03–22.65 μM for hCA-I and from 1.82–27.94 μM for hCA-II. Remarkably, compounds **206** (K_i = 1.03 nM for hCA-I and 1.82 nM for hCA-II) and **207** (K_i = 6.58 nM for hCA-I and 8.93 nM for hCA-II) were the most active. Compound **207** interacts with Phe297 and Trp286 *via* π–π interactions and forms hydrogen bonds with Phe295 and Tyr72, with additional π–π interactions involving the aromatic ring (Fig. 73). These findings highlight the potential of these compounds in drug development for anticholinergic and antiepileptic therapies.[160]

Arifuddin *et al.* (2019) synthesized novel 7-hydroxycoumarin-3-carboxamides and evaluated their inhibition of hCA-IX and XII. Compound **208** exhibited the highest efficacy, with a K_i = 0.2 μM against both isoforms. Docking studies revealed that compound **208** binds effectively in the catalytic clefts of hCA-IX and XII, interacting with key residues such as Thr199, Zn262 and Gln92 in hCA-IX, and Zn301, Asn64 and Thr198 in hCA-XII (Fig. 74). These interactions contribute to its potent sub-micromolar inhibition and suggest its potential as a lead for anticancer therapy, particularly for metastatic hypoxic tumors.[161]

Durdagi *et al.* (2019) synthesized novel bis-coumarin derivatives linked by a triazole moiety and assessed their inhibition of hCA-I, II, IX, and XII. Compound **209** demonstrated the strongest inhibition of hCA-IX with a K_i = 144.6 nM, while compound **210** had the highest inhibition of hCA-XII with a K_i = 71.5 nM. Although no direct correlation between alkyl chain length and inhibition was observed, compounds with longer alkyl chains (10 and 12 carbons) were more effective. This suggests that longer chains provide

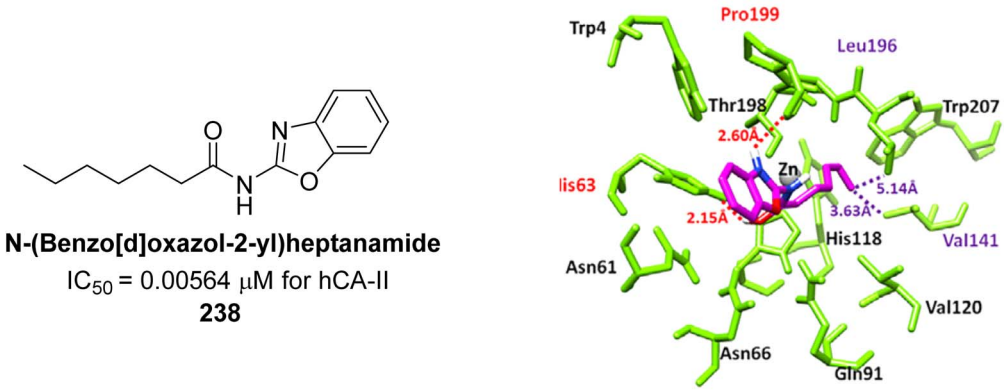

N-(Benzo[d]oxazol-2-yl)heptanamide

IC_{50} = 0.00564 μM for hCA-II

238

N-(Benzo[d]oxazol-2-yl)stearamide

IC_{50} = 0.00596 μM for hCA-II

239

Fig. 85 Chemical structures of compounds **238** and **239**; their IC_{50} values against hCA-II along with docking image of compound **238**.

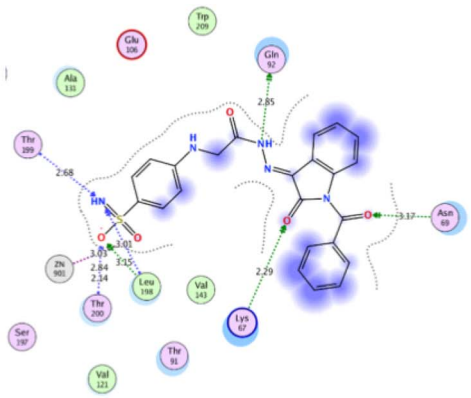

4-((2-(2-(1-Benzoyl-2-oxoindolin-3-ylidene)hydrazinyl)-2-oxoethyl)amino) benzenesulfonamide

K_i = 21.5 nM for hCA-XII

240

4-((2-(2-(1-(4-Methoxybenzoyl)-2-oxoindolin-3-ylidene) hydrazinyl)-2-oxoethyl) amino)benzenesulfonamide

K_i = 22.3 nM for hCA-XII

241

Fig. 86 Chemical structures of compounds **240** and **241**; their K_i values against hCA-XII along with docking image of compound **240**.

greater molecular flexibility, allowing the coumarin moieties to better interact with the enzyme's active sites (Fig. 75).[162]

Kurt *et al.* (2019) synthesized coumarin-sulfonamide derivatives and evaluated their inhibition of hCA-IX and XII. Compound **211** was the most effective inhibitor of hCA-IX, with a K_i = 45.5 nM. It also demonstrated selective anti-proliferative activity, with IC_{50} = 17.01 μM in HT-29 cells and 118.73 μM in HEK293T cells. Compound **211** inhibited hCA-IX and XII expression in HT-29 cells, indicating its potential as a selective

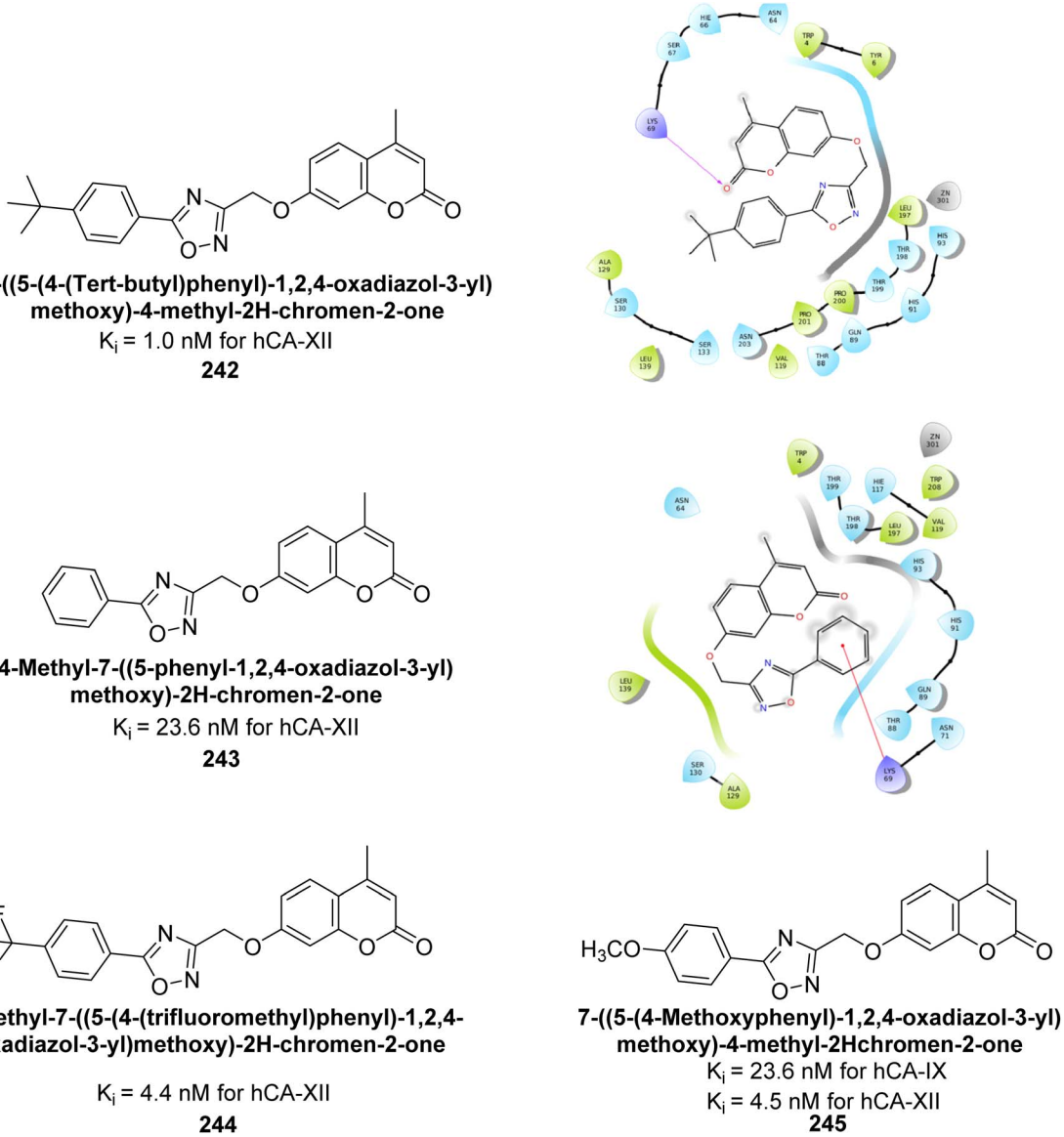

Fig. 87 Chemical structures of compounds **242–245**; their K_i values against hCA-IX and XII along with docking images of compounds **242** and **243**.

therapeutic agent for colon cancer by targeting these isoforms (Fig. 76).[163]

Bayindir *et al.* (2019) synthesized novel *N*-substituted rhodanine derivatives using a green, one-pot method and tested their inhibitory effects on hCA-I and II. The K_i values ranged from 43.55–89.44 nM for hCA-I and from 16.97–64.57 nM for hCA-II. Compound **214** showed the strongest inhibition of hCA-I with a $K_i = 43.55$ nM, outperforming the standard drug AAZ ($K_i = 110.11$ nM). Compounds **212** and **213** also demonstrated significant inhibition of hCA-II, with K_i values better than AAZ ($K_i = 116.97$ nM) (Fig. 77).[164]

Supuran *et al.* (2019) synthesized imidazolone-based benzenesulfonamides. These compounds were evaluated as inhibitors of hCA-I, II, IX and XII. Compounds **215**, **216**, and **217** showed notable selectivity for hCA-IX and XII over hCA-I and II, with selectivity indices ranging from 6.2–19.4 for hCA-IX and 3.3–8 for hCA-XII. Among these, compound **216** was the most potent inhibitor of hCA-IX, with a $K_i = 23$ nM, outperforming the standard drug AAZ, which has a $K_i = 25$ nM (Fig. 78). Moreover, a molecular docking study was conducted to understand the binding interactions of the synthesized imidazolones within the active sites of CA-IX, using PDB structure 5FL4. This analysis helped rationalize the observed inhibitory activities of the compounds.[165]

Akocak *et al.* (2020) synthesized 1,3-diaryltriazene-substituted sulfathiazole derivatives and evaluated for their inhibitory effects on hCA isoforms I and II. The K_i ranged from 450.37 to 1094.34 nM for hCA-I and 504.37 to 1205.36 nM for hCA-II. Among these, compound **218** demonstrated particularly potent inhibition against hCA-I and hCA-II with K_i values of 450.37 and 504.37, respectively (Fig. 79). Additionally, the binding interactions of the compound **218** were characterized

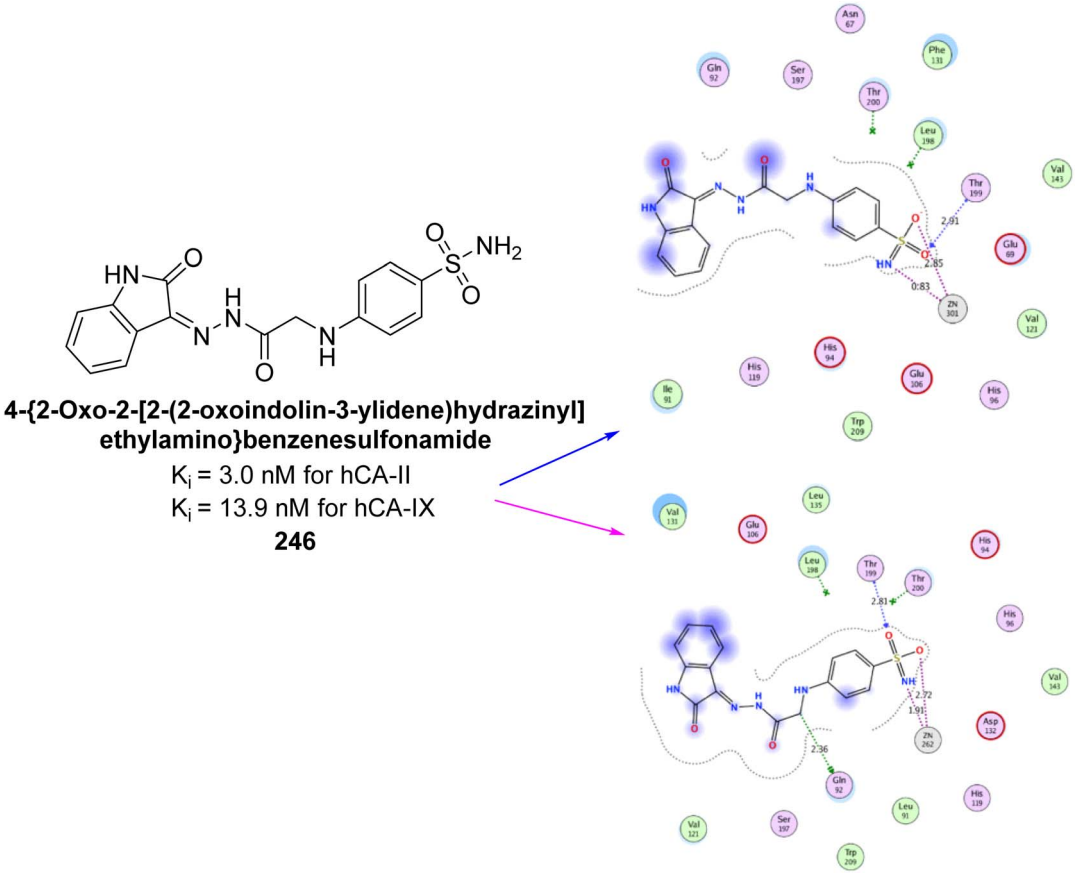

Fig. 88 Chemical structure of compound **246**; its K_i values against hCA-II and IX along with docking images of compound **246**.

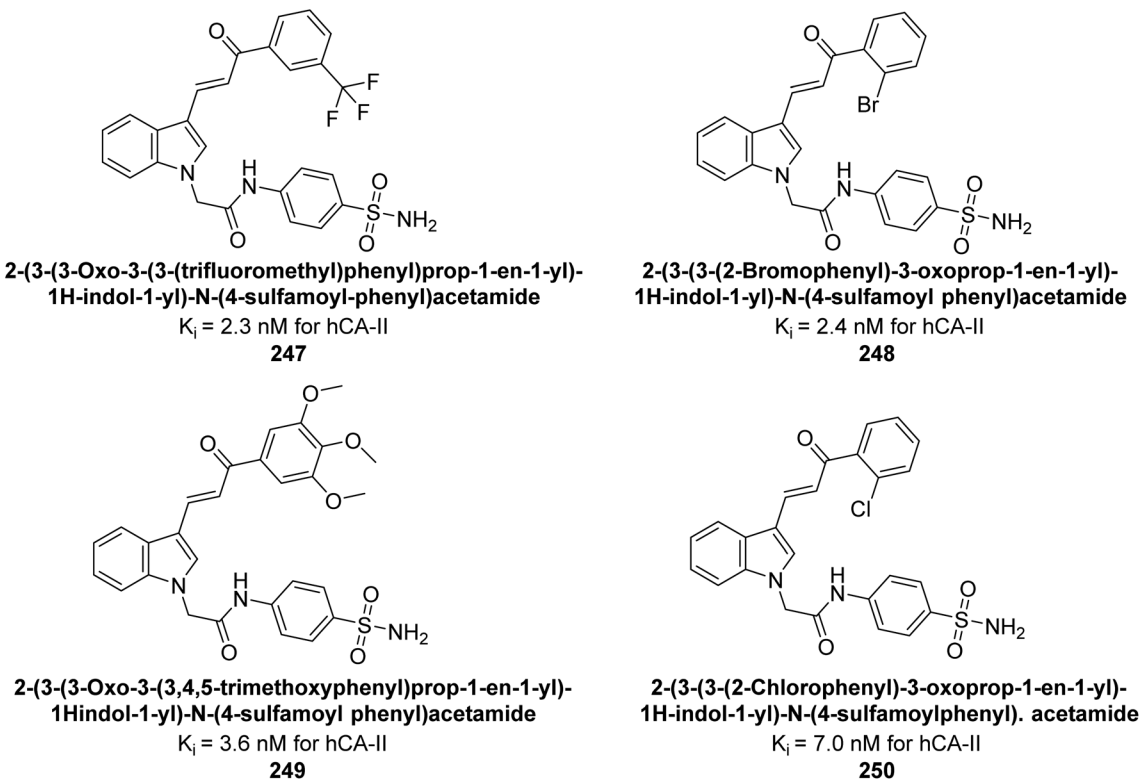

Fig. 89 Chemical structures of compounds **247–250**; their K_i values against hCA-II.

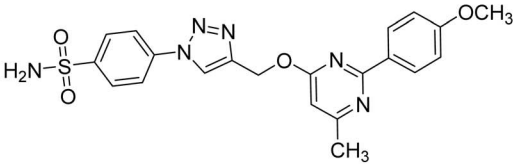

4-(4-(((2-(4-Methoxyphenyl)-6-methylpyrimidin-4-yl)oxy)methyl)-1*H*-1,2,3-triazol-1-yl)benzenesulfonamide

K_i = 9.4 nM for hCA-XII

251

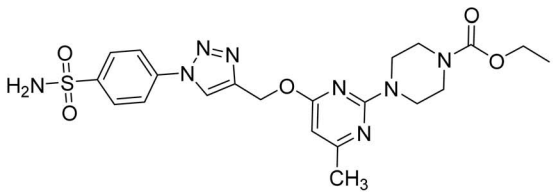

Ethyl 4-(4-methyl-6-((1-(4-sulfamoylphenyl)-1*H*-1,2,3-triazol-4-yl)methoxy)pyrimidin-2-yl)piperazine-1-carboxylate

K_i = 1.8 nM for hCA-XII

252

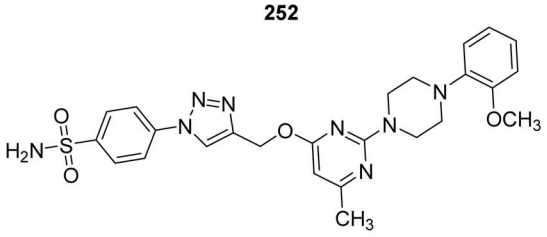

4-(4-(((2-(4-(2-Methoxyphenyl)piperazin-1-yl)-6-methylpyrimidin-4-yl)oxy)methyl)-1*H*-1,2,3-triazol-1-yl)benzenesulfonamide

K_i = 0.82 nM for hCA-XII

253

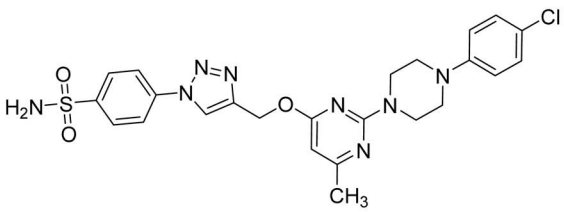

4-(4-(((2-(4-(4-Chlorophenyl)piperazin-1-yl)-6-methylpyrimidin-4-yl)oxy)methyl)-1*H*-1,2,3-triazol-1-yl)benzenesulfonamide

K_i = 2.9 nM for hCA-IX

K_i = 0.82 nM for hCA-XII

254

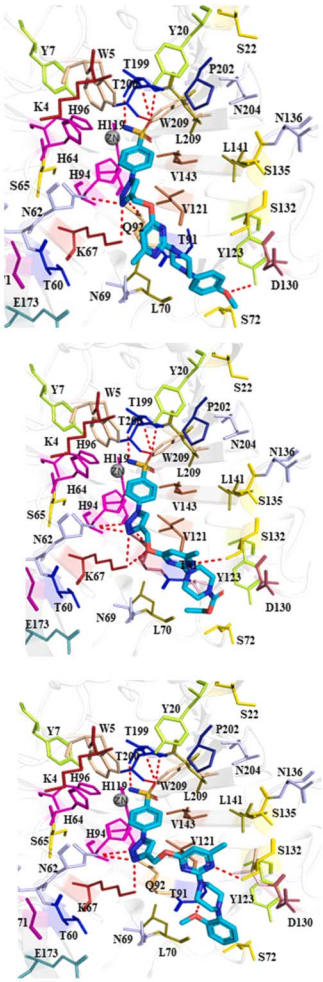

Fig. 90 Chemical structures of compounds **251–254**; their K_i values against hCA-IX and XII along with docking images of compounds **251–254**.

by several key stabilizations. The benzenesulfonamide compound formed a strong hydrogen bond with Gln92 (2.15 Å) and engaged in π–π interactions with His94 and Phe131. The sulfonyl group created hydrogen bonds with Thr199 (1.90 Å) and Thr200 (2.74 Å), while the $-SO_2$ group also bonded with Trp279 (2.24 Å). Hydrophobic interactions were observed between the thiazole, benzene, and fluorobenzene moieties and residues Tyr70, Trp84, Trp279, Phe330, Tyr121. These interactions suggest that these compounds have potential as lead candidates for developing selective inhibitors of metabolic enzymes.[166]

Eldehna *et al.* (2020) synthesized thiazolo-benzimidazole and tested against hCA-I, II, and IX. Remarkably, compounds **219**, **220**, and **221** exhibited strong inhibition of hCA-IX with K_i values of 6.2, 9.7, and 5.5 nM, respectively, and showed good selectivity for hCA-IX over hCA-I and II. Docking studies revealed that the thiazolo-benzimidazole scaffold effectively mimics the phenyl moiety, establishing hydrophobic

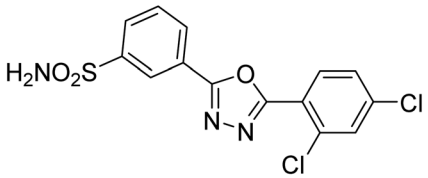

3-(5-(2,4-Dichlorophenyl)-1,3,4-oxadiazol-2-yl)benzenesulfonamide
K_i = 75.8 nM for hCA-I
K_i = 15.4 nM for hCA-XIII
255

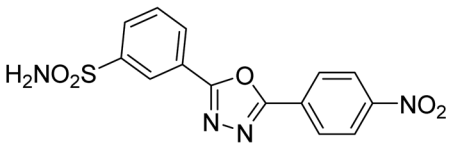

3-(5-(4-Nitrophenyl)-1,3,4-oxadiazol-2-yl)benzenesulfonamide
K_i = 16.2 nM for hCA-XIII
256

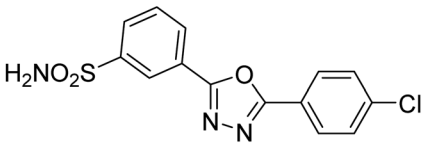

3-(5-(4-Chlorophenyl)-1,3,4-oxadiazol-2-yl)benzenesulfonamide
K_i = 16.4 nM for hCA-XIII
257

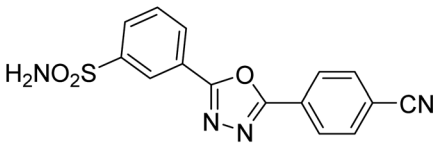

3-(5-(4-Cyanophenyl)-1,3,4-oxadiazol-2-yl)benzenesulfonamide
K_i = 17.0 nM for hCA-XIII
258

Fig. 91 Chemical structures of compounds **255–258**; their K_i values against hCA-I & XIII.

interactions and hydrogen bonds within the hCA-IX active site (Fig. 80).[167]

Sever *et al.* (2020) synthesized a series of new thiazolyl-pyrazolines and evaluated for their efficacy using *in vitro* for hCA-I and II. Compound **222**, featuring a cyanophenyl moiety at the 4th position of the thiazole scaffold, was the most potent, with a K_i = 13.04 nM. The synthesized compounds exhibited greater potency against hCA-II than AAZ (K_i = 98.28 nM). Particularly, compound **223**, with a chlorophenyl group at the 4th position of the thiazole scaffold, was the most potent inhibitor of hCA-II, with a K_i = 7.47 nM. Compound **222**, featuring a cyano group, interacted with Tyr204 through a π–π interaction and formed a hydrogen bond with Tyr20 (2.16 Å). Compound **223** showed an oxygen in the morpholine ring forming a hydrogen bond with Lys170 (2.12 Å). Additionally, face-to-face stacking interactions were observed between His64, His94, and Phe13 with benzene rings, while hydrophobic interactions involved residues Trp5, Val135, Tyr7, Ala65, Pro201, Leu198, Pro202, and Leu204 (Fig. 81).[168]

Arslan *et al.* (2020) synthesized a series of novel sulfonamide-based ketenes and evaluated for their inhibitory effects on hCA-I and II. The compounds **224**, **225** and **226** which contain halogen substitutions, showed the most potent inhibition, with K_i values in the low nanomolar range (9.01, 7.41 and 7.37 nM, respectively). Additionally, compounds **227** and **228** selectively inhibited hCA-I, while **229** and **230** selectively inhibited hCA-II (Fig. 82). Molecular docking studies were conducted to further investigate the interactions between the ligands and their respective receptors (Fig. 82).[169]

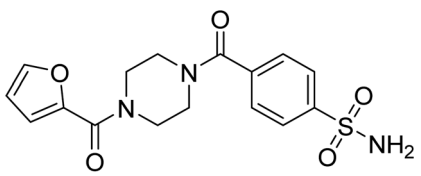

4-(4-(Furan-2-carbonyl)piperazine-1-carbonyl) benzenesulfonamide
K_i = 4.3 nM for hCA-VII
259

Fig. 92 Chemical structure of compound **259**; its K_i values against hCA-VII.

Supuran *et al.* (2020) synthesized various triazolopyrimidine-based and triazole-based benzenesulfonamides. Especially, sulfonamides **231**, **232** and **233** exhibited strong inhibition of hCA-IX and XII. Among them, pyrimidine-based sulfonamide **234** and triazole-based sulfonamide **233** demonstrated high selectivity for hCA-IX (Fig. 83). The strong inhibitory activity of compound **234** against hCA-IX is due to its effective interactions with a hydrophobic pocket formed by Val20, Trp5, Pro201, and Pro202. In compound **233**, the phenylureido tail binds to a different pocket in hCA-II than in hCA-IX and XII. This variation is attributed to the Phe131 residue in hCA-II, which sterically blocks ligand binding in the region where it interacts with Gln92 and Leu91 in hCA-IX, and Thr91 and Lys67 in hCA-XII (Fig. 83).[170]

Shafiq *et al.* (2020) synthesized quinazolinone derivatives and assessed their inhibitory effects on bCA-II and hCA-II. The compounds exhibited moderate to significant inhibition, with IC_{50} values ranging from 8.9 to 67.3 μM for bCA-II and 14.0 to 59.6 μM for hCA-II. SAR analysis suggested that a nitro group at the R position enhances activity. The most active compound, **235**, acted as a competitive inhibitor of both bCA-II and hCA-II, with K_i values of 13.0 μM and 14.25 μM, respectively. Compounds **236** and **237** showed higher selectivity for hCA-II, confirmed by molecular docking studies (Fig. 84).[171]

Saeed *et al.* (2020) synthesized a series of 2-substituted benzoxazoles and evaluated for their hCA-II inhibitory activity.

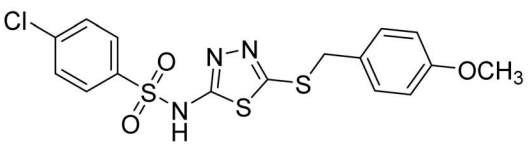

4-Chloro-*N*-(5-((4-methoxybenzyl)thio)-1,3,4-thiadiazol-2-yl)benzenesulfonamide

IC_{50} = 0.60 μM for bCA-II

260

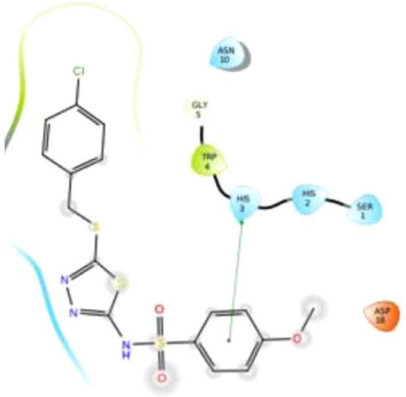

Fig. 93 Chemical structure of compound **260**; its K_i values against bCA-II and its docking image.

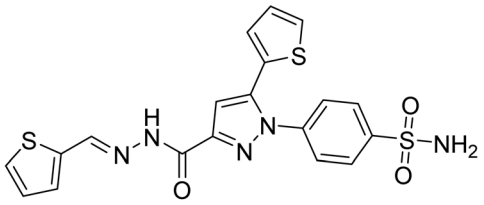

4-(3-(2-(Thiophene-2-yl-methylen)hydrazine-1-carbonyl)-5-(thiophene-2-yl)-1H-pyrazole-1-yl)benzenesulfonamide

K_i = 7.0 nM for hCA-IX

261

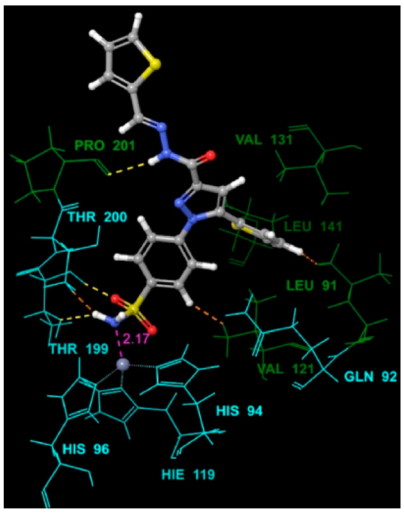

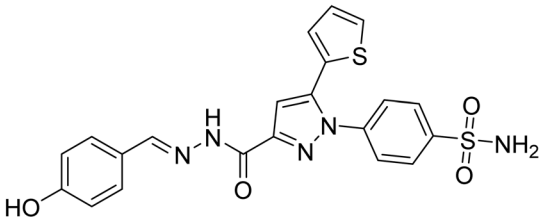

4-(3-(2-(4-Hydroxybenzylidene)hydrazine-1-carbonyl)-5-(thiophene-2-yl)-1H-pyrazole-1-yl)benzenesulfonamide

K_i = 10.6 nM for hCA-IX

262

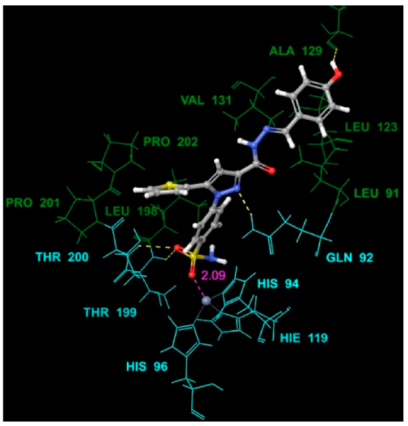

Fig. 94 Chemical structures of compounds **261** and **262**; their K_i values against hCA-IX along with docking images.

Among them, compounds **238** and **239** demonstrated the highest inhibitory potential, with IC_{50} values of 0.00564 μM and 0.00596 μM, respectively. These values indicate a significantly stronger inhibitory effect compared to the standard AAZ, which has an IC_{50} value of 0.997 μM. Compound **238** confirmed an optimal binding conformation within the hCA-II binding pocket, primarily through hydrogen bonds with residues His63 and Pro199, which were more significant than hydrophobic interactions in the docking complex analysis (Fig. 85). Preliminary findings indicate that compound **238** exhibits favorable drug-like properties and may hold potential for further biomedical applications.[172]

George *et al.* (2020) synthesized benzenesulfonamide derivatives and assessed against hCA-XII. The derivatives, specifically compounds **240** and **241**, demonstrated the highest activity against hCA-XII, with K_i values of 21.5 nM and 22.3 nM,

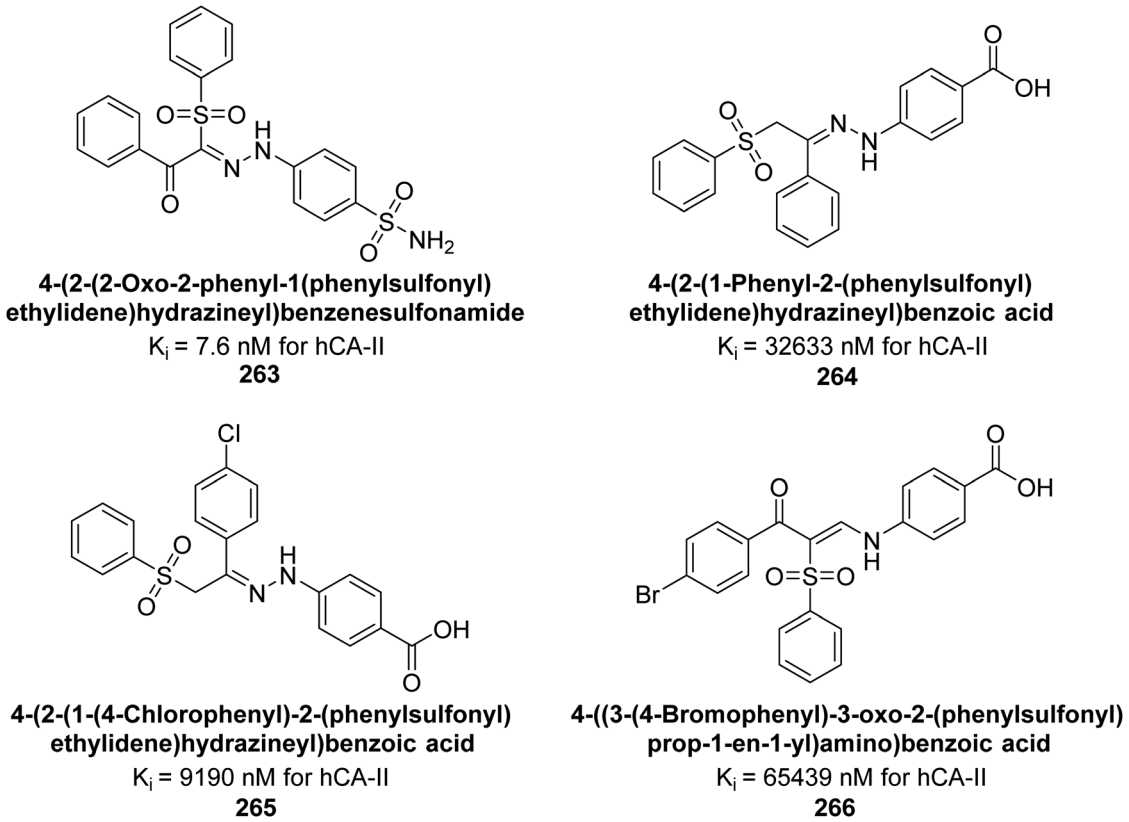

Fig. 95 Chemical structures of compounds **263–266**; their K_i values against hCA-II.

respectively. These compounds featured unsubstituted benzoyl and methoxybenzoyl groups, which contributed to their potent inhibitory effects. Moreover, compound **240** exhibited a binding mode similar to that of AAZ, interacting with key sites including Zn^{2+}, Thr199, Thr200, and Leu198 through metal coordination and hydrogen bonding (Fig. 86).[173]

Supuran *et al.* (2020) synthesized coumarin-linked 1,2,4-oxadiazoles and evaluated their inhibitory activity against hCA-IX and XII. Compounds **242**, **243**, **244**, and **245** displayed potent inhibition of hCA-XII, with compound **242** showing the strongest inhibition (K_i = 1 nM). Compound **245** was the most effective against hCA-IX (K_i = 23.6 nM). These results highlight compound **242** as a promising lead for hCA-XII inhibitors and compound **245** for dual hCA-IX/XII inhibition. Molecular docking studies were conducted to explore the binding interactions of the potent compounds **242** and **243** within the hCA-XII active site (Fig. 87).[174]

George *et al.* (2020) synthesized 2-oxindole benzenesulfonamide conjugates with various linkers and tested their inhibitory activity against hCA-I, II, IX, and XII. Several compounds demonstrated distinguished activity, particularly towards hCA-I, II, and IX, surpassing the standard AAZ. Particularly, compound **246** showed the strongest inhibition against hCA-II and IX, with K_i values of 3.0 and 13.9 nM, respectively. Molecular docking studies of compound **246** revealed binding modes similar to AAZ, aligning with its potent inhibition (Fig. 88).[175]

Supuran *et al.* (2021) designed indolyl chalcone-linked sulfonamides and evaluated their inhibition of hCA-I, II, IX, and XIII isoforms. Compounds **247** (2.3 nM), **248** (2.4 nM), **249** (3.6 nM), and **250** (7.0 nM) showed superior potency against hCA-II compared to the standard AAZ (12.1 nM) (Fig. 89). Additionally, several compounds exhibited inhibition of hCA-XIII and hCA-IX within the 50–100 nM range. Compounds **247–250** are considered promising leads for further development as potent hCA-II inhibitors, targeting ocular disorders and cancer through structural optimization.[176]

Supuran *et al.* (2021) synthesized triazole-sulfonamide pyrimidine derivatives *via* click chemistry. These compounds demonstrated strong inhibitory activity against hCA-II and moderate to excellent activity against hCA-IX and XII. Remarkably, compounds **251** (K_i = 9.4 nM), **252** (K_i = 1.8 nM), and **253** (K_i = 0.82 nM) exhibited high selectivity for hCA-XII. Compound **254** showed potent inhibition of both hCA-IX (K_i = 2.9 nM) and hCA-XII (K_i = 0.82 nM). Molecular docking confirmed favorable interactions of these compounds with active site residues of hCA-XII and IX. The docking study indicates that the benzenesulfonamide moiety fits precisely into the active catalytic pocket near the zinc ion of CA (Fig. 90). These derivatives show promising results as selective anticancer agents targeting CA.[177]

Arifuddin *et al.* (2021) synthesized benzenesulfonamide-linked 1,3,4-oxadiazole hybrids and evaluated their inhibitory effects on hCA-I and XIII. Many compounds exhibited strong inhibition, surpassing the standard drug AAZ against hCA-XIII. Compound **255** (75.8 nM) was three times more potent than AAZ (250.0 nM) against hCA-I. Additionally, compounds **255** (15.4 nM), **256** (16.2 nM), **257** (16.4 nM), and **258** (17.0 nM)

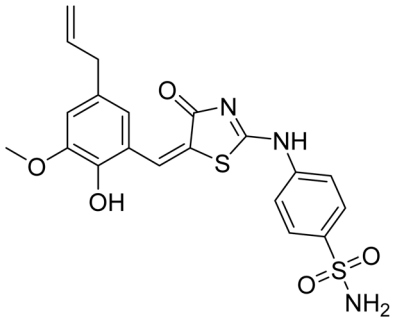

4-(5-(5-Allyl-2-hydroxy-3-methoxybenzylidene)-4-oxo-4,5-dihydrothiazol-2-ylamino)benzenesulfonamide
IC_{50} = 0.011 μM for hCA-IX
267

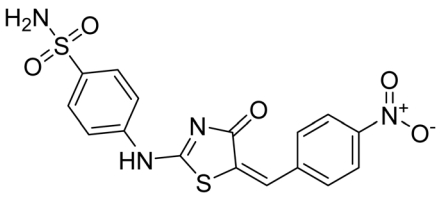

4-(5-(4-Nitrobenzylidene)-4-oxo-4,5-dihydrothiazol-2-ylamino)benzenesulfonamide
IC_{50} = 0.017 μM for hCA-IX
268

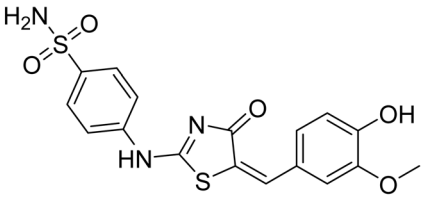

4-(5-(4-Hydroxy-3-methoxybenzylidene)-4-oxo-4,5-dihydrothiazol-2-ylamino)benzenesulfonamide
IC_{50} = 0.026 μM for hCA-IX
269

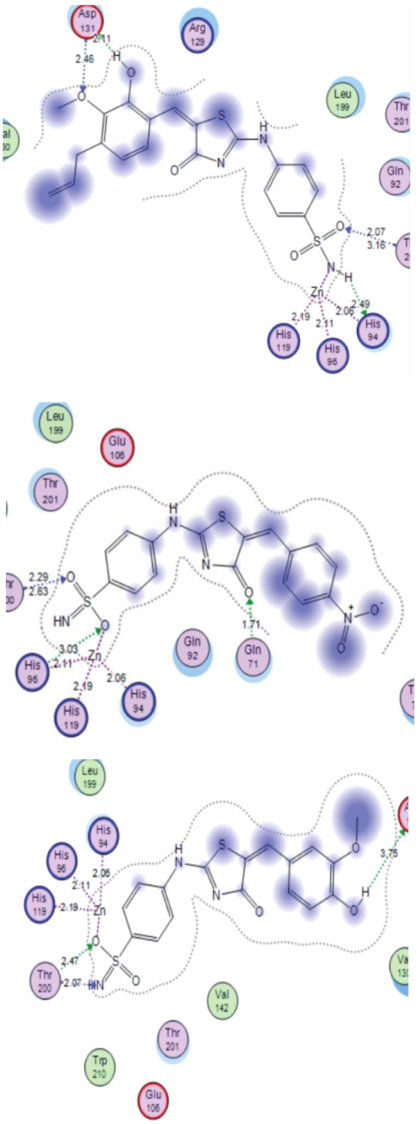

Fig. 96 Chemical structures of compounds **267–269**; their IC_{50} values against hCA-IX along with docking images.

outperformed AAZ (17.0 nM) against hCA-XIII. The presence of EWGs (–Cl, $–NO_2$, –CN) contributed to enhanced activity, making these compounds promising leads for selective hCA-XIII inhibitors (Fig. 91).[178]

Gitto *et al.* (2021) designed and synthesized a series of benzenesulfonamides and assessed against selected druggable hCA isoforms. Remarkably, compound **259** demonstrated remarkable affinity for hCA-VII (K_i: 4.3 nM) and exhibited good selectivity over the widely distributed hCA-I, outperforming TPM (Fig. 92).[179]

Ashraf *et al.* (2021) synthesized sulfonamide derivatives with thiadiazole and evaluated their bCA-II inhibitory activity. Derivative **260** was the most potent, with an IC_{50} of 0.60 μM, outperforming AAZ (IC_{50} = 0.984 μM). Kinetic analysis revealed mixed-type inhibition for **260**, with K_i and K_i' values of 2.91 μM and 3.88 μM, respectively, indicating a preference for competitive binding. Docking studies showed hydrogen bonding between **260** and His3 and Trp4, along with π–π stacking with Trp4. Compound **260** also exhibited anticancer activity, inhibiting 40% of MCF-7 cell growth at 125 μM (Fig. 93). These findings suggest that derivative **260** could serve as a lead compound for designing more potent CA inhibitors.[180]

Gul *et al.* (2021) synthesized pyrazole-based benzenesulfonamides and evaluated their inhibitory activity against hCA isoforms. Compound **261** exhibited high selectivity for hCA-IX (K_i = 7.0 nM), with 127 times greater selectivity over hCA-I, while compound **262** (K_i = 10.6 nM) showed 47 times higher selectivity for hCA-IX over hCA-II compared to AAZ. Compound **261** formed two hydrogen bonds in the hCA-IX complex *versus* one in hCA-I, with a shorter zinc coordination bond in hCA-IX. Compound **262**'s sulfonamide moiety coordinated with the Zn ion, forming hydrogen bonds with Thr199, Thr200, Gln92, and

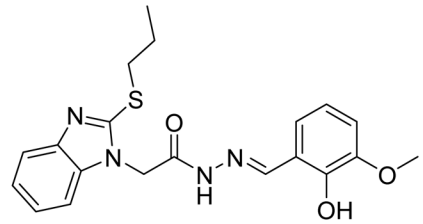

N'-(2-Hydroxy-3-methoxybenzylidene)-2-(2-(propylthio)-1H-benzo[d]imidazol-1-yl)acetohydrazide

IC_{50} = 13.3 μM for bCA-II

270

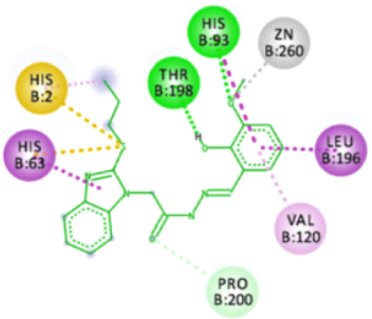

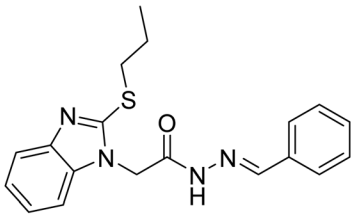

N'-Benzylidene-2-(2-(propylthio)-1H-benzo[d]imidazol-1-yl)acetohydrazide

IC_{50} = 17.2 μM for bCA-II

271

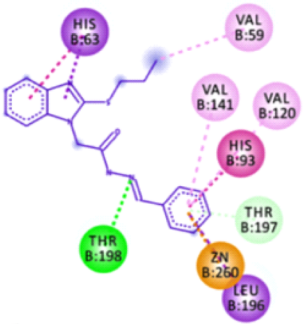

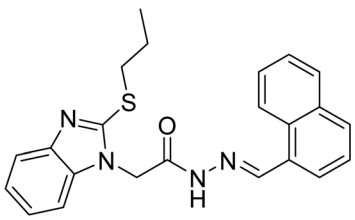

N'-(Naphthalen-1-ylmethylene)-2-(2-(propylthio)-1Hbenzo[d]imidazol-1-yl)acetohydrazide

IC_{50} = 14.6 μM for bCA-II

272

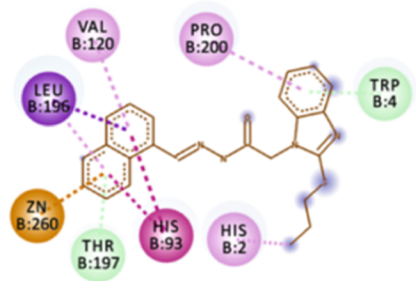

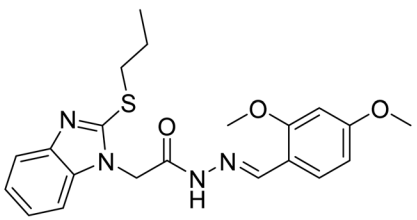

N'-(2,4-Dimethoxybenzylidene)-2-(2-(propylthio)-1Hbenzo[d]imidazol-1-yl)acetohydrazide

IC_{50} = 14.5 μM for bCA-II

273

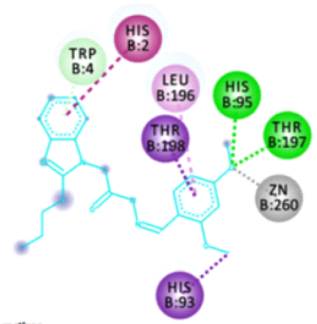

Fig. 97 Chemical structures of compounds **270**–**273**; their IC_{50} values against bCA-II along with docking images.

Ala129, contributing to its strong binding affinity for hCA-IX (Fig. 94).[181]

Supuran *et al.* (2021) designed and prepared benzenesulfonamide and benzoic acid derivatives using a tail/dual tail approach to enhance potency and selectivity as CAIs. Benzenesulfonamide derivatives demonstrated moderate to potent inhibitory activity, particularly towards hCA-II, with compound **263** showing a K_i of 7.6 nM. In contrast, the benzoic acid analogues exhibited no significant activity, except for compounds **264**, **265** and **266** which showed weak activity (Fig. 95).[182]

Hassan *et al.* (2021) synthesized aryl thiazolone-benzenesulfonamides and evaluated their inhibitory effects on hCA-IX. Particularly, three sulfonamide derivatives, **267**, **268**

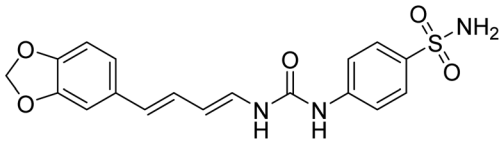

4-(3-((1E,3E)-4-(Benzo[d][1,3]dioxol-5-yl)buta-1,3-dien-1-yl)ureido)benzenesulfonamide

K_i = 93.4 nM for hCA-II
K_i = 38.7 nM for hCA-IX
K_i = 57.5 nM for hCA-XII

274

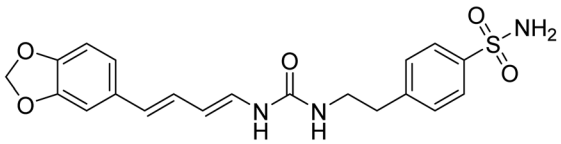

4-(2-(3-((1E,3E)-4-(Benzo[d][1,3]dioxol-5-yl)buta-1,3-dien-1-yl) ureido) ethyl) benzenesulfonamide

K_i = 88.6 nM for hCA-II
K_i = 68.2 nM for hCA-IX
K_i = 45.6 nM for hCA-XII

275

Fig. 98 Chemical structures of compounds **274** and **275**; their K_i values against hCA-II, XI and XII.

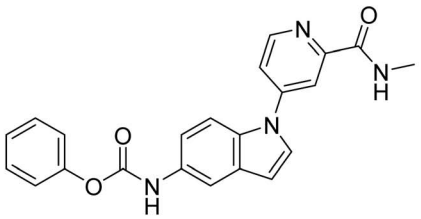

Phenyl 1-(2-(methylcarbamoyl)pyridin-4-yl)-1H-indol-5-ylcarbamate

IC_{50} = 0.0440 μM for bCA-II

276

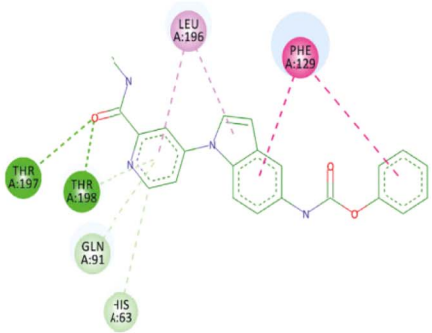

Fig. 99 Chemical structure of compound **276**; its IC_{50} value against bCA-II and its docking image.

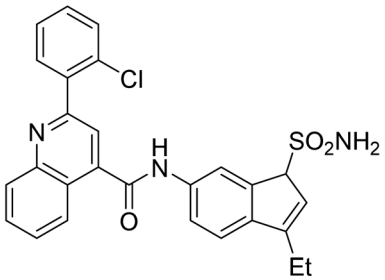

2-(2-Chlorophenyl)-*N*-(3-ethyl-1-sulfamoyl-1*H*-inden-6-yl)quinoline-4-carboxamide

K_i = 1.57 μM for hCA-IX

277

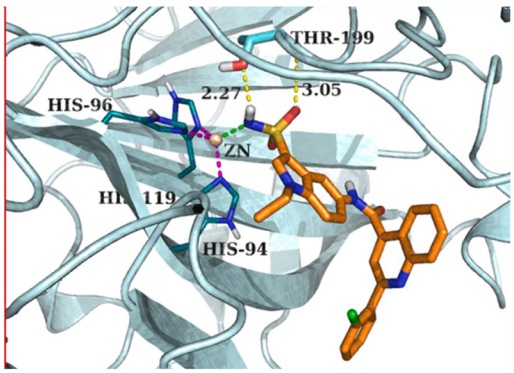

Fig. 100 Chemical structure of compound **277**; its K_i value against hCA-IX along with docking image.

and **269** demonstrated excellent inhibition of hCA-IX with IC_{50} values ranging from 10.93 to 25.06 nM, and significantly less inhibition of hCA-II with IC_{50} values from 1.55 to 3.92 μM, indicating remarkable selectivity for hCA-IX over hCA-II. Docking results of active analogues **267**–**269** indicated precise fit within the active site, forming coordination and hydrogen bonds. The remarkable potency of these compounds against hCA-IX is likely due to their similar predicted binding patterns (Fig. 96).[183]

Saadiq *et al.* (2021) reported the synthesis of benzimidazole-derived *N*-acylhydrazones and their *in vitro* evaluation as potent bCA-II inhibitors. Among the target compounds, several exhibited higher inhibition than the standard AAZ (IC_{50}: 18.6 μM), including compound **270** (IC_{50}: 13.3 μM), compound **271** (IC_{50}: 17.2 μM), compound **272** (IC_{50}: 14.6 μM), and compound **273** (IC_{50}: 14.5 μM). Molecular docking of the most active compounds confirmed their binding interactions with the enzyme's active site, corroborating the experimental results (Fig. 97).[184]

Eldehna *et al.* (2021) developed new CA inhibitors using natural piperine as a tail moiety. Among the synthesized piperine-sulfonamides, the *p*-regioisomers **274** and **275** exhibited the strongest inhibitory activity, with nanomolar potency against hCA-II (K_i = 93.4 and 88.6 nM), hCA-IX (K_i = 38.7 and 68.2 nM), and hCA-XII (K_i = 57.5 and 45.6 nM) (Fig. 98).[185]

Zaib *et al.* (2022) synthesized indole-picolinamide hybrids and found that compound **276** is a highly potent inhibitor of bCA-II, with an IC_{50} of 0.0440 μM, which is 22 times more

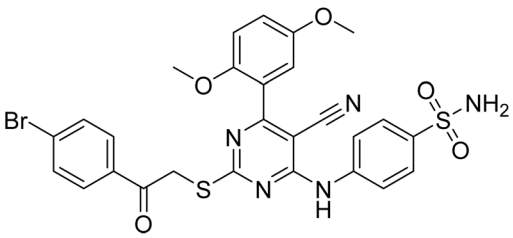

4-((2-((2-(4-Bromophenyl)-2-oxoethyl)thio)-5-cyano-6-(2,5-dimethoxyphenyl)pyrimidin-4-yl)amino)benzenesulfonamide

K_i = 1.72 nM for hCA-II

278

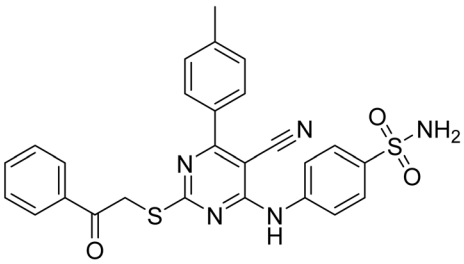

4-((5-Cyano-2-((2-oxo-2-phenylethyl)thio)-6-(p-tolyl)pyrimidin-4-yl)amino)benzene sulfonamide

K_i = 7.4 nM for hCA-IX

279

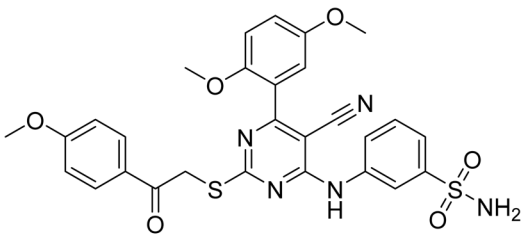

3-((5-Cyano-6-(2,5-dimethoxyphenyl)-2-((2-(4methoxy phenyl)-2-oxoethyl)thio)pyrimidin-4-yl) amino)benzenesulfonamide

K_i = 7.0 nM for hCA-IX

K_i = 4.67 nM for hCA-XII

280

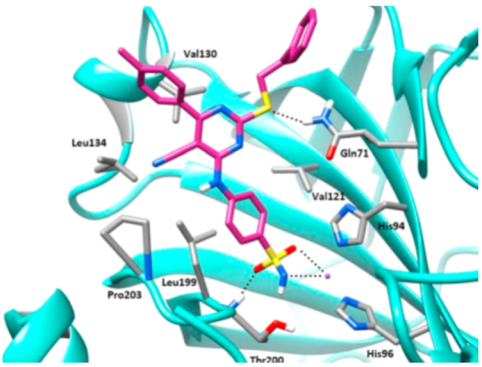

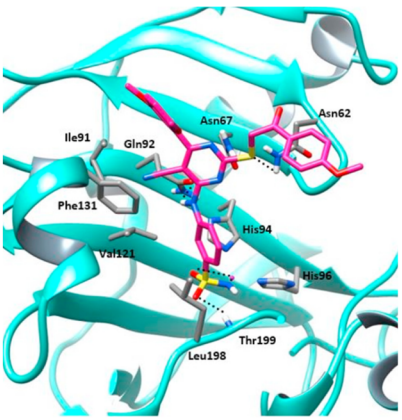

Fig. 101 Chemical structures of compounds 278–280; their K_i values against hCA-IX and XII along with docking images.

effective than AAZ (IC_{50} = 0.9618 μM). The enhanced activity of 276 is attributed to its phenyl carbamate moiety. Substituting the carbamate linker with other linkers while keeping the phenyl ring unchanged resulted in reduced activity. Molecular docking studies confirmed that compound **276** interacts with His118, Thr197, His93, and His95 in the active site, exhibiting π-donor hydrogen, π–π T-shaped interactions, and π-alkyl interactions, as well as conventional hydrogen bonds (Fig. 99). These findings suggest that compound **276** could be a promising lead for developing new CA-II inhibitors.[186]

Supuran *et al.* (2022) developed and evaluated a series of quinoline/pyridine-linked indole-3-sulfonamide derivatives for their inhibitory effects on hCA-IX and XII. Among these, compound **277** showed prominent inhibition of hCA-IX with a K_i of 1.57 μM. Similar to the standard AAZ, compound **277** formed hydrogen bonds with Thr199 and engaged in hydrophobic interactions with several active site residues, including Asn62, Ser65, and Leu135. These interactions stabilize compound **277** within the hCA-IX active site, making these derivatives promising candidates for selective hCA-IX inhibitors in cancer therapy (Fig. 100).[187]

Mohsen *et al.* (2022) developed a series of 2-thiopyrimidine benzenesulfonamides utilizing a dual-tail design. This approach combines a benzenesulfonamide moiety for Zn^{2+} binding with a 2,4-disubstituted thiopyrimidine tail. Among the compounds, **278** was the most potent with a K_i of 1.72 nM and demonstrated high selectivity for hCA-II over hCA-IX and XII, with selectivity indices of 50 and 5.26, respectively. Compounds **279** and **280** also showed strong inhibition of hCA-IX (K_i = 7.4 and 7.0 nM, respectively) and better potency against hCA-XII

Table 13 Chemical structures of substituted 1,2,3-triazoles, inhibition data against CAIs

Compound no.	Chemical structures & IUPAC names	K_i (nM) hCA-II	hCA-IV	hCA-IX	Ref.
281	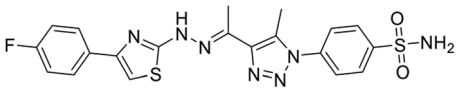 4-(4-(1-(2-(4-(4-Fluorophenyl)thiazol-2-yl)hydrazono)ethyl)-5-methyl-1*H*-1,2,3-triazol-1-yl)benzenesulfonamide	18.1	5416	279.8	189
282	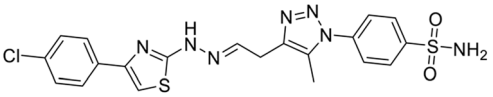 4-(4-(1-(2-(4-(4-Chlorophenyl)thiazol-2-yl)hydrazono) ethyl)-5-methyl-1*H*-1,2,3-triazol-1-yl)benzenesulfonamide	14.1	8871	7893	189
283	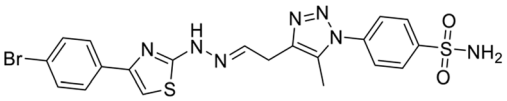 4-(4-(1-(2-(4-(4-Bromophenyl)thiazol-2-yl)hydrazono) ethyl)-5-methyl-1*H*-1,2,3-triazol-1-yl)benzenesulfonamide	14.9	8717	270.2	189
284	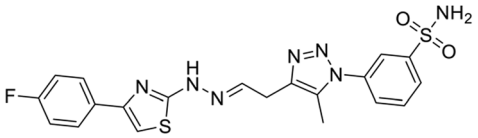 3-(4-(1-(2-(4-(4-Fluorophenyl)thiazol-2-yl)hydrazono) ethyl)-5-methyl-1*H*-1,2,3-triazol-1-yl)benzenesulfonamide	17.8	88	113	189
285	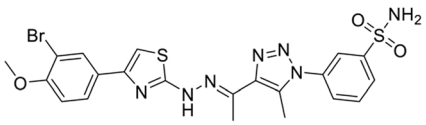 3-(4-(1-(2-(4-(3-Bromo-4-methoxyphenyl)thiazol-2-yl)hydrazono) ethyl)-5-methyl-1*H*-1,2,3-triazol-1-yl)benzenesulfonamide	810.4	5667	856	189
Standard	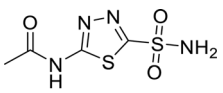 Acetazolamide (AAZ)	12.1	74	25.8	189

(K_i = 4.67 nM) compared to the standard AAZ (K_i = 25 nM for hCA-IX and 5.7 nM for hCA-XII). Molecular docking revealed that the sulfonamide moiety interacts with the Zn^{2+} ion in the CA active site, while the dual-tail extension engages with surrounding residues, enhancing the compounds' potency and selectivity (Fig. 101).[188]

Sharma *et al.* (2022) synthesized arylthiazolylhydrazono-1,2,3-triazoles incorporating sulfanilamide and metanilamide moieties using a tail-approach. Additionally, metanilamide analogues were better inhibitors of the hCA-IV and IX. Compounds **281**, **282**, **283**, and **284** potently inhibited hCA-II with K_i values of 18.1, 14.1, 14.9, and 17.8 nM, respectively, and **281–283** exhibited selectivity for hCA-II over hCA-I, IV, and IX isoforms by more than 15-fold. Compounds **282** and **285**, significant inhibition profiles against hCA-IX (K_i range of 0.113 μM-0.318 μM). Remarkably, **284** was the only compound in the series that effectively inhibited all the tested isoforms (Table 13). These findings can be leveraged to design novel inhibitors that incorporate both sulfanilamide and metanilamide moieties, offering enhanced potency and selectivity.[189]

Tawfik *et al.* (2022) designed featuring a benzenesulfonamide moiety for zinc binding, with hydrazone to interact with hydrophilic and hydrophobic regions of the active site, respectively. All synthesized compounds demonstrated inhibition of hCA-IX, with IC_{50} values ranging from 13.3 to 259 nM. Particularly, derivatives **286**, **287**, **288**, **289** and **290** showed high efficacy against the hCA-IX isoform, with K_i of 13.3, 22.6, 25.8, 26.9, and 27.2 nM, respectively (Fig. 102).[190]

Carradori *et al.* (2022) synthesized rhodamine-linked benzenesulfonamides and evaluated for their inhibitory activity against hCA-I, II, IX, and XII. All synthesized compounds exhibited good to excellent inhibition in the nanomolar range,

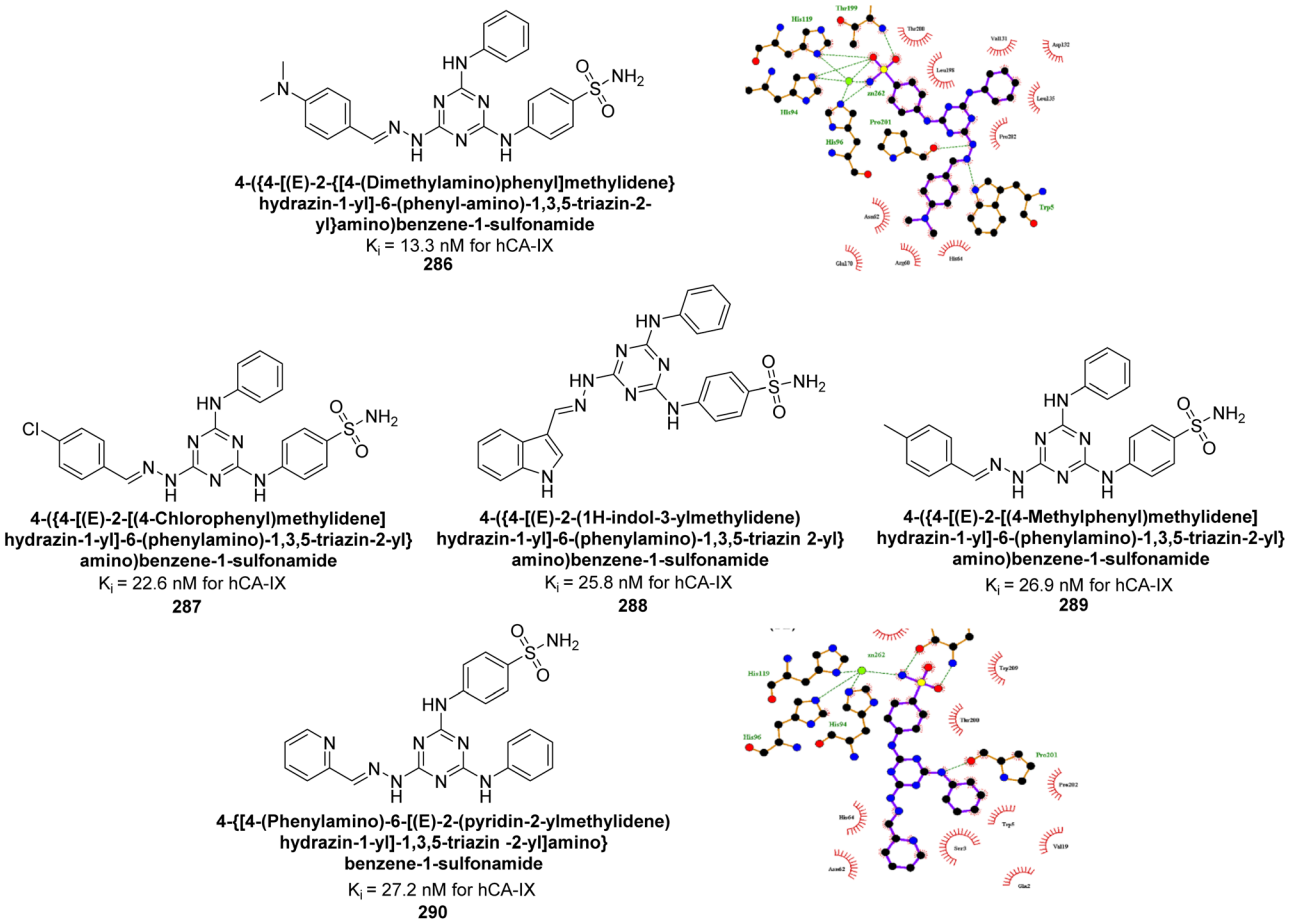

Fig. 102 Chemical structures of compounds **286–290**; their K_i values against hCA-IX along with docking images of **286** and **290**.

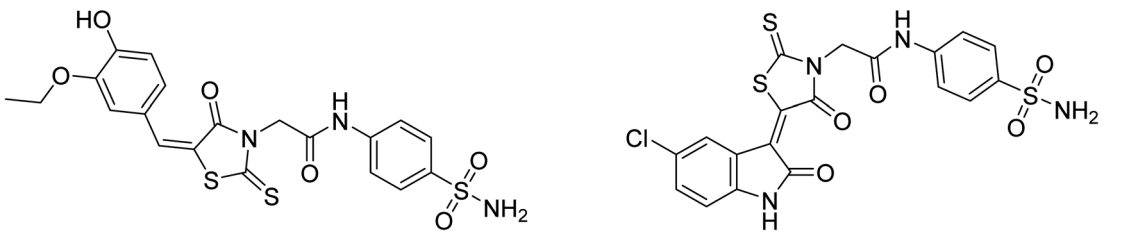

Fig. 103 Chemical structures of compounds **291** and **292**; their K_i values against hCA-I.

attributed to the sulfonamide moiety's zinc-binding properties. The most potent inhibitors of hCA-I were **291** ($K_i = 22.4$ nM) and **292** ($K_i = 35.8$ nM), significantly outperforming the standard drug AAZ ($K_i = 250.0$ nM) (Fig. 103). Both EWGs and EDGs on the aromatic ring significantly enhanced inhibition. The findings suggest that the newly synthesized benzenesulfonamide-linked rhodanine derivatives are promising candidates for developing isoform-selective inhibitors targeting CA isoforms.[191]

Supuran *et al.* (2022) synthesized isatin *N*-phenylacetamide-based sulfonamides and evaluated for their inhibitory activity against hCA isoforms. Among these, derivative **293** exhibited the most potent inhibition against hCA-I and hCA-II, with K_i values of 45.10 nM and 5.87 nM, respectively, surpassing the standard inhibitor AAZ. Additionally, **293** demonstrated significant inhibition of hCA-XII, with a K_i value of 7.91 nM, comparable to AAZ's K_i of 5.70 nM. Docking studies of the most active compound, **293** predicted their binding patterns and

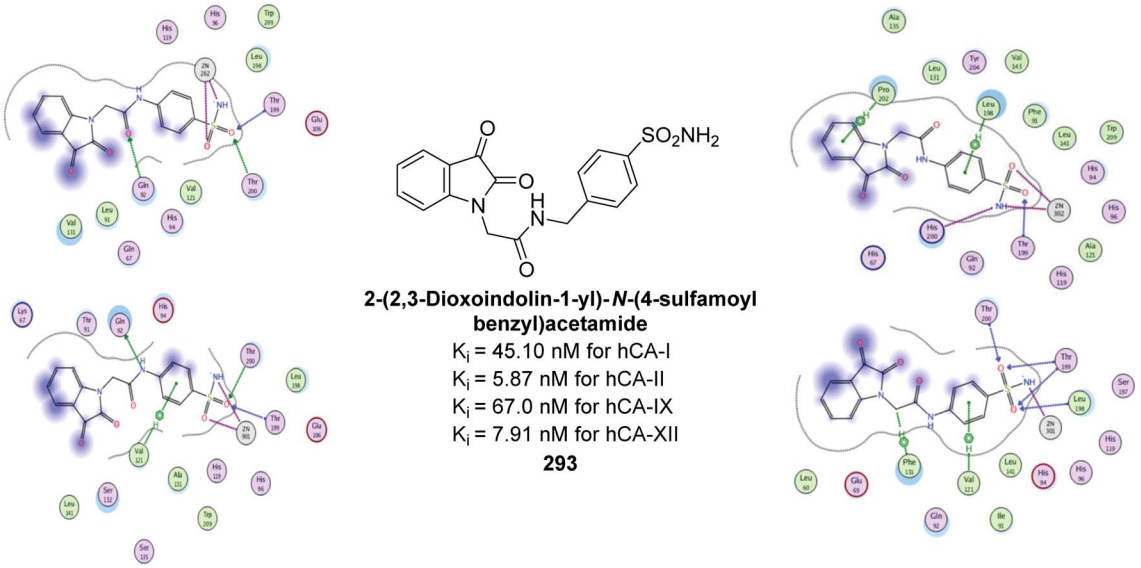

Fig. 104 Chemical structure of compound **293**; its K_i values against hCA-I, II, IX and XII along with its docking images.

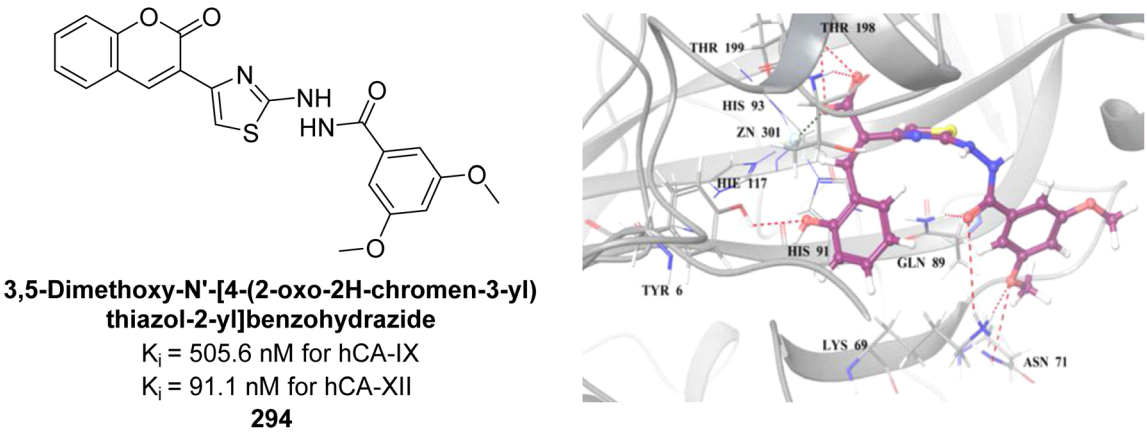

Fig. 105 Chemical structure of compound **294**; its K_i values against hCA-IX and XII along with its docking image against hCA-XII.

affinities to the active sites of all the investigated isoforms (Fig. 104).[192]

Thacker *et al.* (2022) synthesized coumarin-linked thiazole derivatives and assessed their inhibition of hCA-IX and XII. Remarkably, compound **294** showed the highest inhibition of hCA-XII with a K_i value of 91.1 nM (Fig. 105). The hydrolyzed form of compound **294** also demonstrated strong interactions and favorable docking scores with both isoforms, indicating its potential as a template for developing selective and potent hCA-XII inhibitors.[193]

Mohsen *et al.* (2022) synthesized 2-thioquinazoline-benzenesulfonamide hybrids and evaluated them as hCA inhibitors. Compounds **295** and **296** showed the highest potency across four hCA isoforms, with K_i values of 0.09 and 0.05 μM for hCA-II, 0.32 and 0.47 μM for hCA-IX, and 0.58 and 0.46 μM for hCA-XII, respectively. Compound **296** displayed distinguished selectivity for hCA-II. Molecular docking studies revealed that the benzenesulfonamide moiety binds deeply within the hCA-II active site, interacting with the Zn^{2+} ion and key residues Thr199 and Thr200, while the 2-substituted thioquinazoline moiety interacts with the hydrophilic region of the binding site (Fig. 106).[194]

Winum *et al.* (2022) designed and synthesized a series of novel *N*-triazolo-benzenesulfonamides-1,5-benzodiazepines using click chemistry. The synthesized compounds showed nanomolar affinity for various hCA isoforms, including hCA-I, II, IV, VII, IX, and XII. Remarkably, derivative **297** demonstrated exceptional inhibitory activity across all tested isoforms, outperforming AAZ and showing superior multivalent effects compared to previously reported divalent CA inhibitors (Fig. 107).[195]

Arslan *et al.* (2023) designed and synthesized a series of benzenesulfonamides featuring a 1,2,3-triazole moiety as inhibitors of α-hCAs using a tail approach. Among the synthesized derivatives, the naphthyl (**298**, $K_i = 68.6$ nM) and methyl (**299**, $K_i = 56.3$ nM) derivatives showed distinguished selectivity towards hCA-IX, while the propyl (**300**, $K_i = 95.6$ nM) and pentyl (**301**, $K_i = 51.1$ nM) derivatives were selective for hCA-XII.

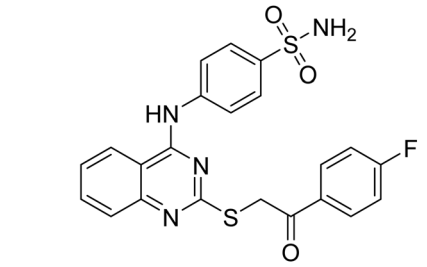

4-[(2-{[2-(4-Fluorophenyl)-2-oxoethyl]thio}quinazolin-4-yl)amino]-benzenesulfonamide

K_i = 0.09 nM for hCA-II
K_i = 0.32 nM for hCA-IX
K_i = 0.58 nM for hCA-XII

295

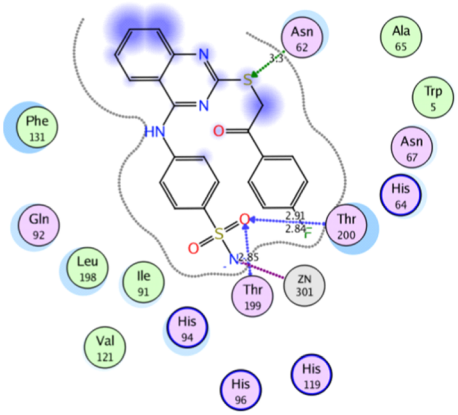

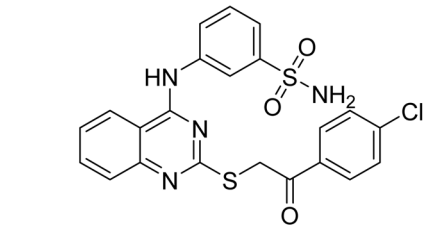

3-[(2-{[2-(4-Chlorophenyl)-2-oxoethyl]thio}quinazolin-4-yl)amino]-benzenesulfonamide

K_i = 0.05 nM for hCA-II
K_i = 0.47 nM for hCA-IX
K_i = 0.46 nM for hCA-XII

296

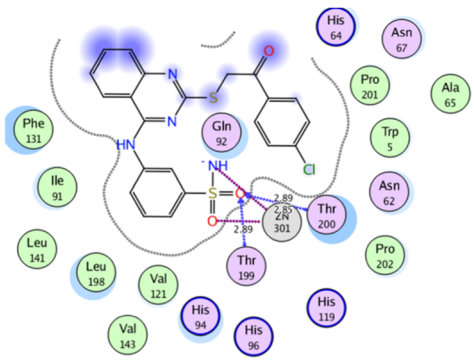

Fig. 106 Chemical structures of compounds **295** and **296**; their K_i values against hCA-II, IX and XII along with docking images.

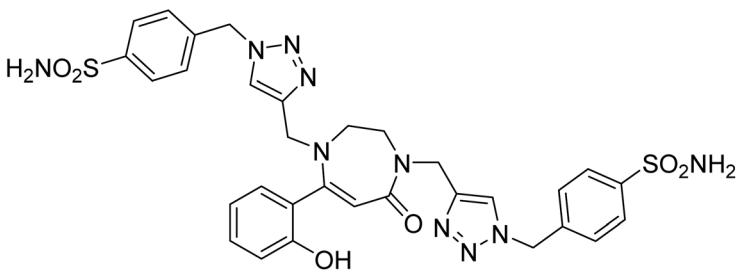

4,4'-((((7-(2-Hydroxyphenyl)-5-oxo-2,3-dihydro-1*H*-1,4-diazepine-1,4(5*H*)-diyl)bis(methylene))bis(1*H*-1,2,3-triazole-4,1-diyl))bis(methylene))dibenzenesulfonamide

K_i = 78.2 nM for hCA-I
K_i = 2.8 nM for hCA-II
K_i = 1013 nM for hCA-IV
K_i = 8.9 nM for hCA-VII
K_i = 13.2 nM for hCA-IX
K_i = 6.5 nM for hCA-XII

297

Fig. 107 Chemical structure of compound **297**; its K_i values against hCA-I, II, IV, VII, IX, and XII.

Derivative **302** exhibited strong inhibitory effects against hCA-I (K_i = 47.8 nM), hCA-IX and XII (K_i values of 195.9 and 116.9 nM, respectively), as compared to the reference drug AAZ with K_i values of 451.8, 437.2, and 338.9 nM, respectively. Additionally, derivative **303** demonstrated higher potency against hCA-II (K_i = 33.2 nM) compared to AAZ (K_i = 327.3 nM) (Fig. 108). The study also utilized molecular docking techniques to explore the binding interactions of the synthesized compounds within the active sites of hCAs.[196]

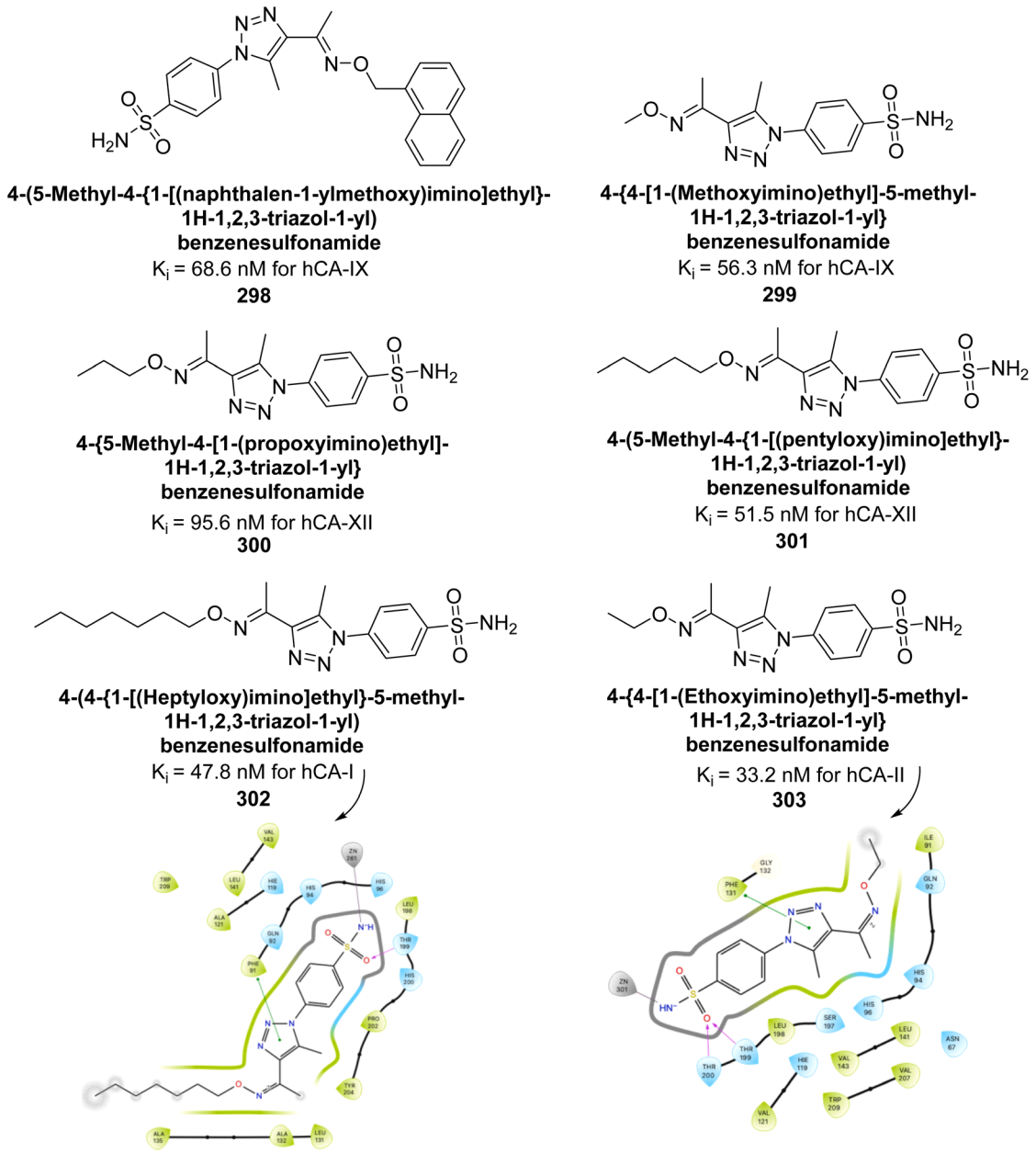

Fig. 108 Chemical structures of compounds **298**–**303**; their K_i values against hCA-I, II, IX and XII along with docking images of **302** and **303**.

Supuran *et al.* (2023) designed and synthesized pyrazole-based benzenesulfonamide with inhibitory activities against CA enzyme. Remarkably, hCA-IX and XII isoforms were potently inhibited by these compounds, exhibiting K_i values in the nanomolar range, between 13.0-82.1 nM for hCA-IX and 5.8–62.0 nM for hCA-XII. The study also utilized molecular docking techniques to explore the binding interactions of the synthesized compounds **304** and **305** within the active sites of hCA (Fig. 109).[197]

Türkeş *et al.* (2023) synthesized benzenesulfonamide derivatives and evaluated against CA isoforms. Among these, the 2-iodophenyl **306** and 2-naphthyl **307** derivatives showed notable selectivity for hCA-IX and XII over hCA-I, while the phenyl **308** and 2,6-dimethylphenyl **309** analogs were more selective for hCA-IX and XII over hCA-II. Compound **308** exhibited strong inhibition of hCA-IX (K_i = 18.29 nM), outperforming AAZ (K_i = 437.20 nM), and compound **307** showed superior potency against hCA-XII (K_i = 9.22 nM) compared to AAZ (K_i = 338.90 nM). Molecular docking indicated that the sulfonamide moiety binds well to the hCA active sites, interacting with the Zn^{2+} ion, while the tail extension engages in hydrophilic and hydrophobic interactions with surrounding amino acids, affecting the compounds' potency and selectivity (Fig. 110).[198]

Supuran *et al.* (2023) evaluated the inhibitory effects of quinazoline-based hydroxyl Schiff base derivatives against hCA isoforms. These quinazolines showed effective inhibition of hCA-I with K_i values ranging from 87.6 to 692.3 nM, comparable to or better than AAZ. For hCA-II, the inhibitors had K_i values

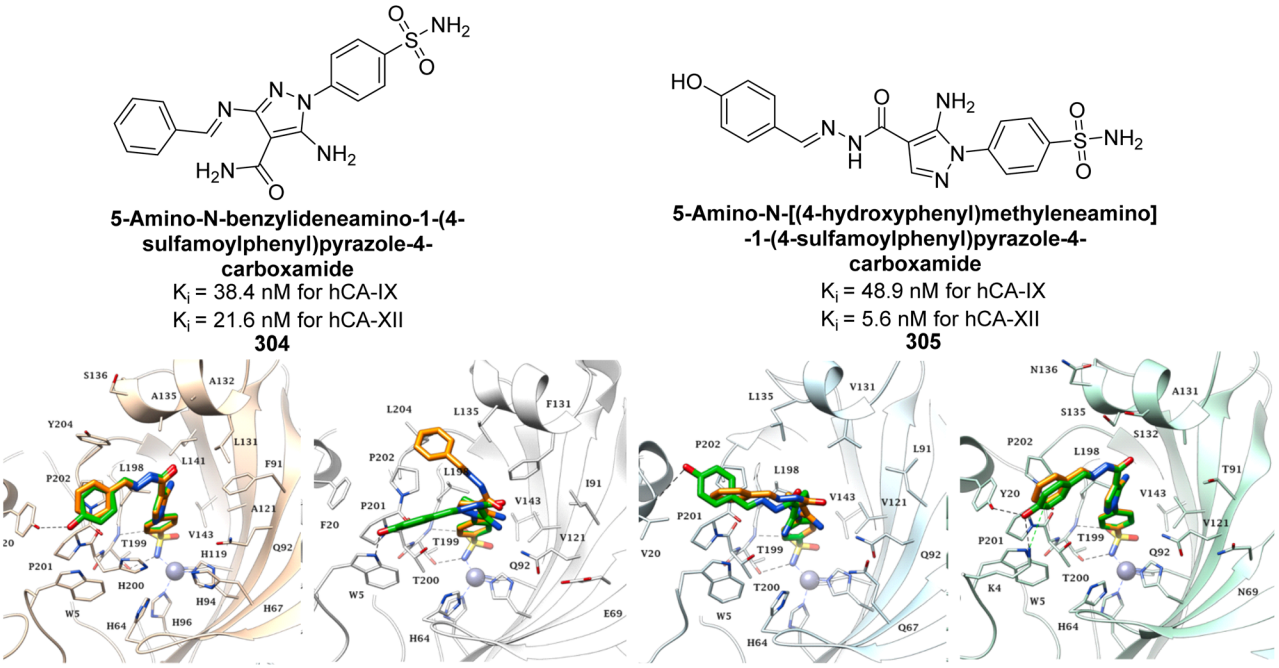

Fig. 109 Chemical structures of compounds **304** and **305**; their K_i values against hCA-I, II, IX and XII along with their docking images (predicted binding modes of compounds **304** (orange) and **305** (green)).

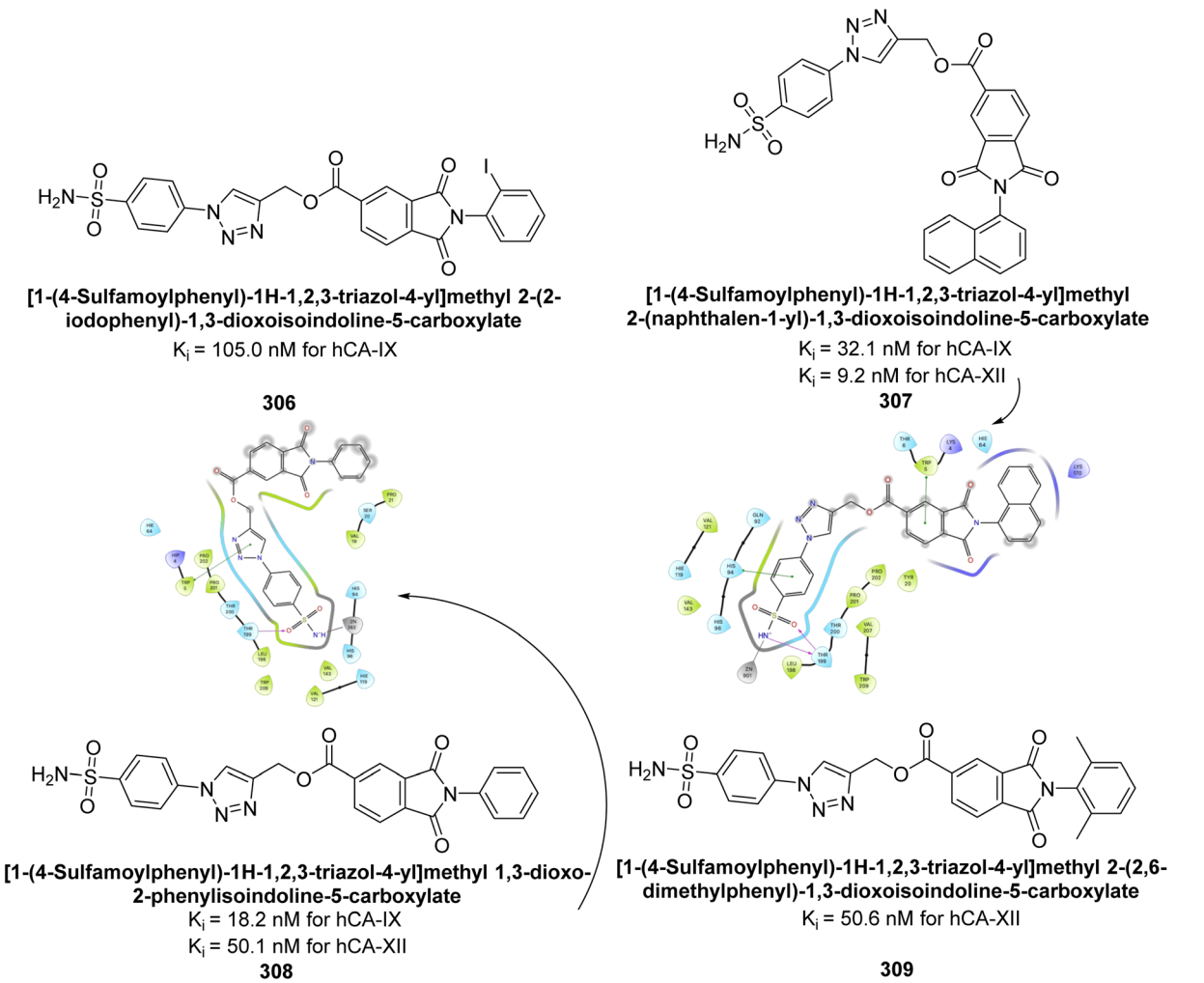

Fig. 110 Chemical structures of compounds **306–309**; their K_i values against hCA-I, IX and XII along with their docking images.

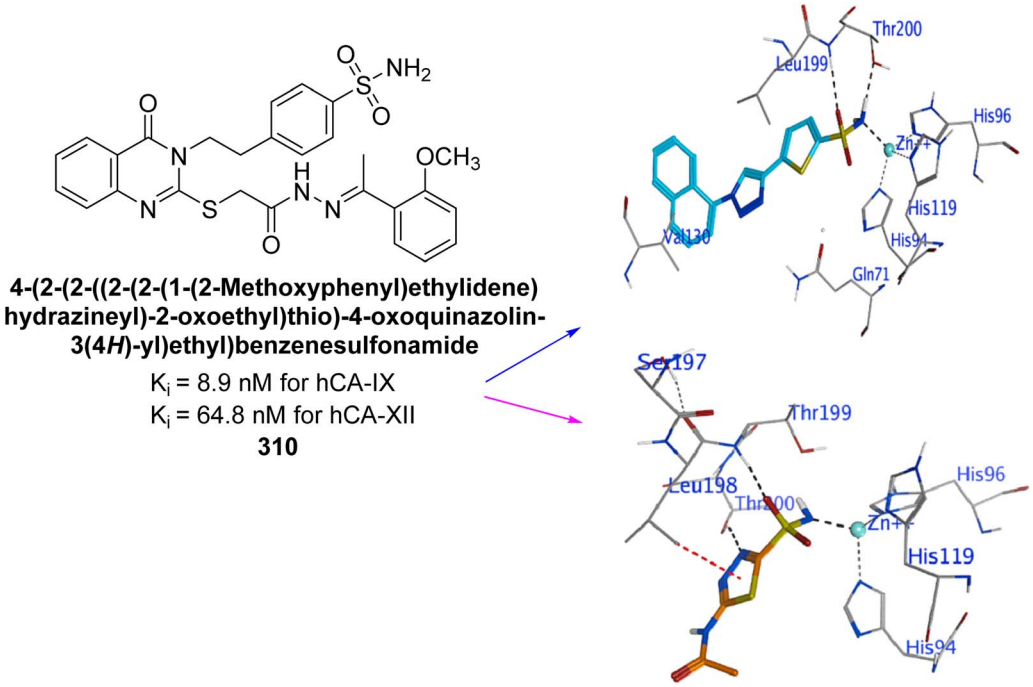

4-(2-(2-((2-(2-(1-(2-Methoxyphenyl)ethylidene) hydrazineyl)-2-oxoethyl)thio)-4-oxoquinazolin-3(4*H*)-yl)ethyl)benzenesulfonamide

K_i = 8.9 nM for hCA-IX

K_i = 64.8 nM for hCA-XII

310

Fig. 111 Chemical structure of compound **310**; its K_i values against hCA-IX and XII along with its docking images.

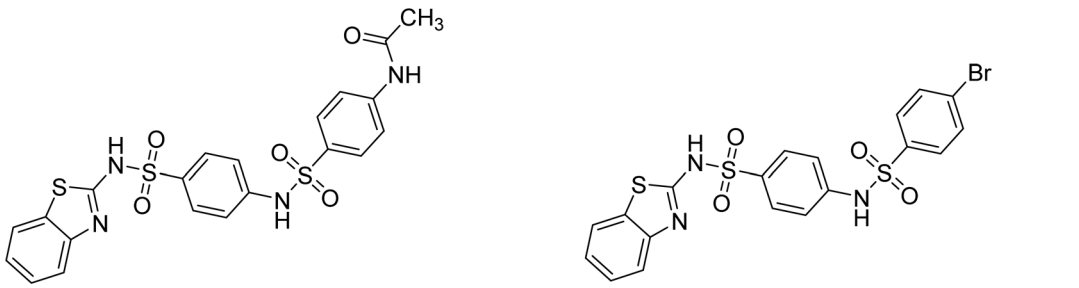

***N*-(4-(*N*-(4-(*N*-(Benzo[*d*]thiazol-2-yl)sulfamoyl)phenyl)sulfamoyl)phenyl)acetamide**

K_i = 0.112 nM for hCA-I

K_i = 0.025 nM for hCA-II

311

***N*-(Benzo[*d*]thiazol-2-yl)-4-((4-bromophenyl)sulfonamido)benzenesulfonamide**

K_i = 0.052 nM for hCA-I

K_i = 0.150 nM for hCA-II

312

Fig. 112 Chemical structures of compounds **311** and **312**; their K_i values against hCA-I and II.

between 16.9 and 29.7 nM, similar to AAZ. The compounds were particularly effective against hCA-IX, with K_i values from 8.9 to 88.3 nM, outperforming AAZ, and demonstrated strong inhibition of hCA-XII, with K_i values ranging from 5.4 to 19.5 nM. Molecular docking studies indicated that compound **310** binds strongly to hCA-IX and XII, highlighting its potential as a lead compound for developing hCA inhibitors (Fig. 111).[199]

Kalay *et al.* (2023) developed secondary sulfonamide derivatives with a benzothiazole scaffold and tested their inhibitory activity against hCA-I and II. The compounds exhibited K_i values from 0.052 to 0.971 μM for hCA-I and 0.025 to 0.682 μM for hCA-II. Remarkably, several of these compounds demonstrated more potent inhibition than the standard drug, AAZ, with compounds **311** and **312** showing the highest efficacy against hCA-I and II, respectively. In compound **311** ($K_i = 0.112$ μM), the presence of an EDG (amide group) in its tail was found to enhance the inhibitory activity. Furthermore, compound **312** ($K_i = 0.052$ μM) demonstrated significantly higher potency, being five times more active than the reference drug (AAZ, $K_i = 0.25$ μM) (Fig. 112).[200]

Bostancı *et al.* (2023) synthesized thiadiazole and hydrazone derivatives and assessed their inhibition of hCA-I, II, and IX. Compound **313** notably inhibited hCA-I with an $IC_{50} = 29.74$ μM, while compound **314** was a potent inhibitor of hCA-II with an $IC_{50} = 23.18$ μM. The *o*-fluoro substituent on the phenyl ring enhanced inhibition of hCA-II, while an *o*-methoxy group increased activity against hCA-I and showed anticancer potential. Molecular docking studies were performed for compounds

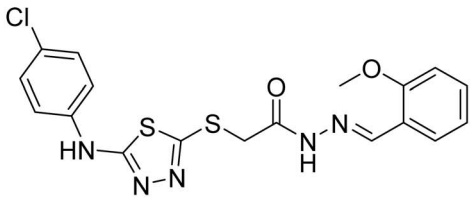

2-((5-((4-Chlorophenyl)amino)-1,3,4-thiadiazol-2-yl) thio)-N'-(2-methoxybenzylidene)acetohydrazide

IC_{50} = 29.74 μM for hCA-I

313

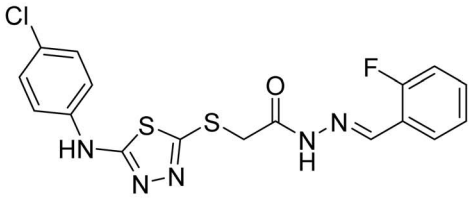

2-((5-((4-Chlorophenyl)amino)-1,3,4-thiadiazol-2-yl) thio)-N'-(2-fluorobenzylidene)acetohydrazide

IC_{50} = 23.18 μM for hCA-II

314

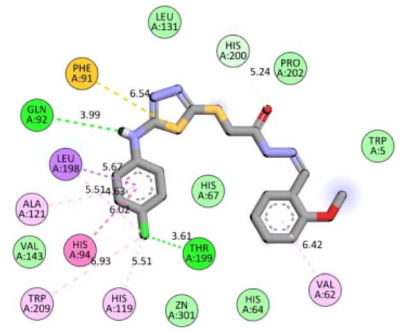

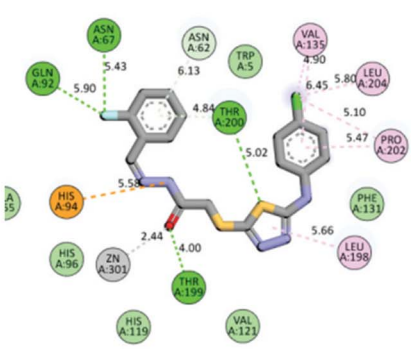

Fig. 113 Chemical structures of compounds **313** and **314**; their K_i values against hCA-I and II along with their docking images.

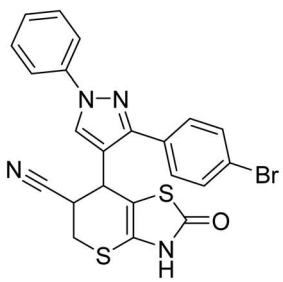

7-(3-(4-Bromophenyl)-1-phenyl-1H-pyrazol-4-yl)-2-oxo-3,5,6,7-tetrahydro-2H-thiopyrano-[2,3-d]thiazole-6-carbonitrile

IC_{50} = 0.067 μM for hCA-IX

315

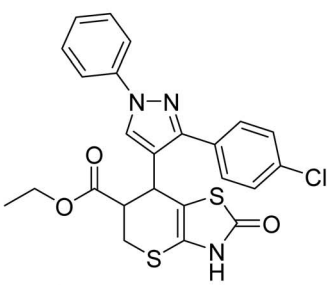

Ethyl 7-(3-(4-Chlorophenyl)-1-phenyl-1H-pyrazol-4-yl)-2-oxo-3,5,6,7-tetra-hydro-2H-thiopyrano[2,3-d]thiazole-6-carboxylate

IC_{50} = 0.123 μM for hCA-XII

316

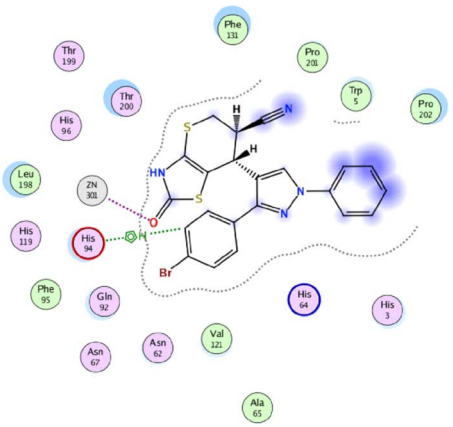

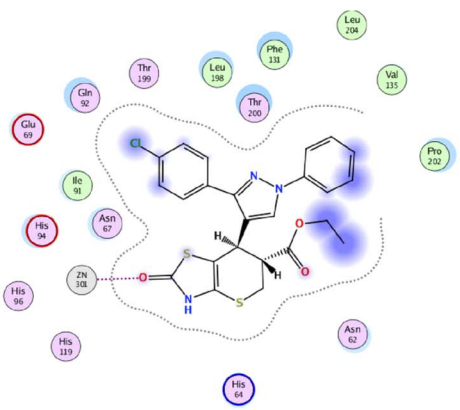

Fig. 114 Chemical structures of compounds **315** and **316**; their K_i values against hCA-IX and XII along with their docking images.

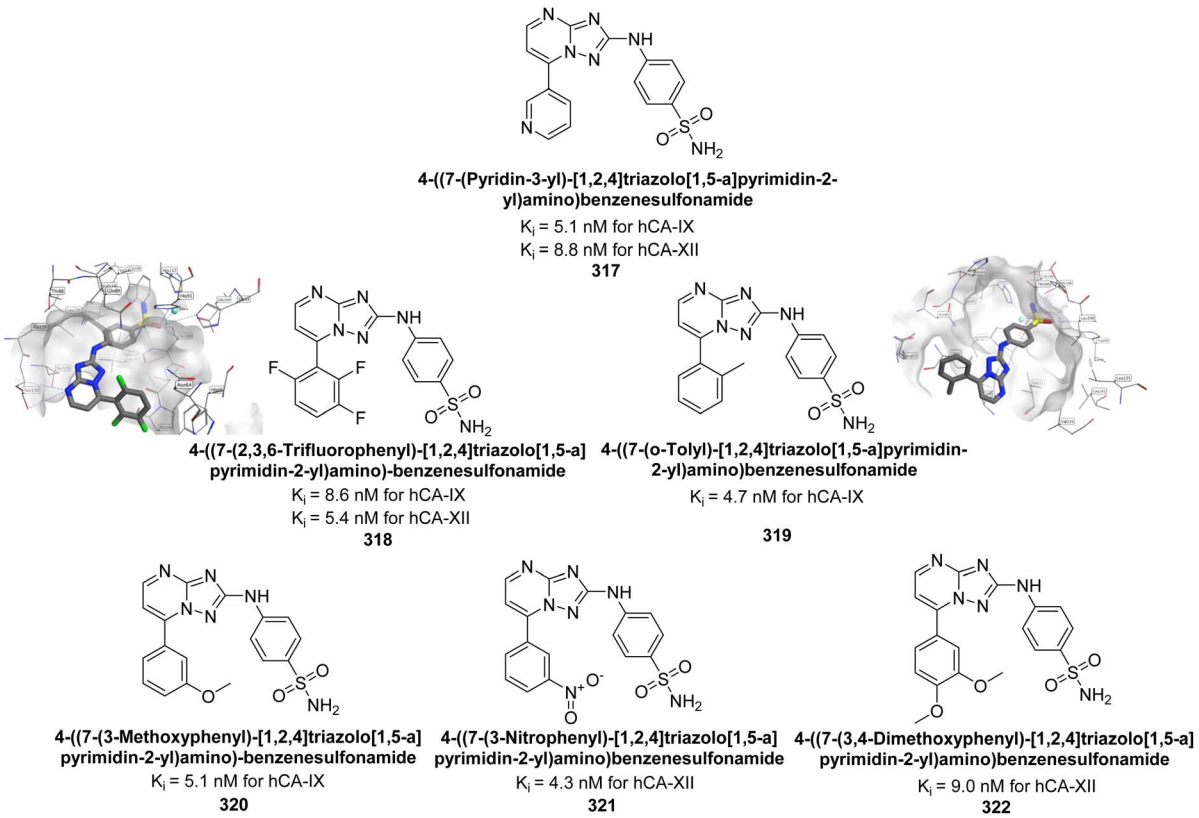

Fig. 115 Chemical structures of compounds **317**–**322**; their K_i values against hCA-IX and XII along with docking images of **318** and **319**.

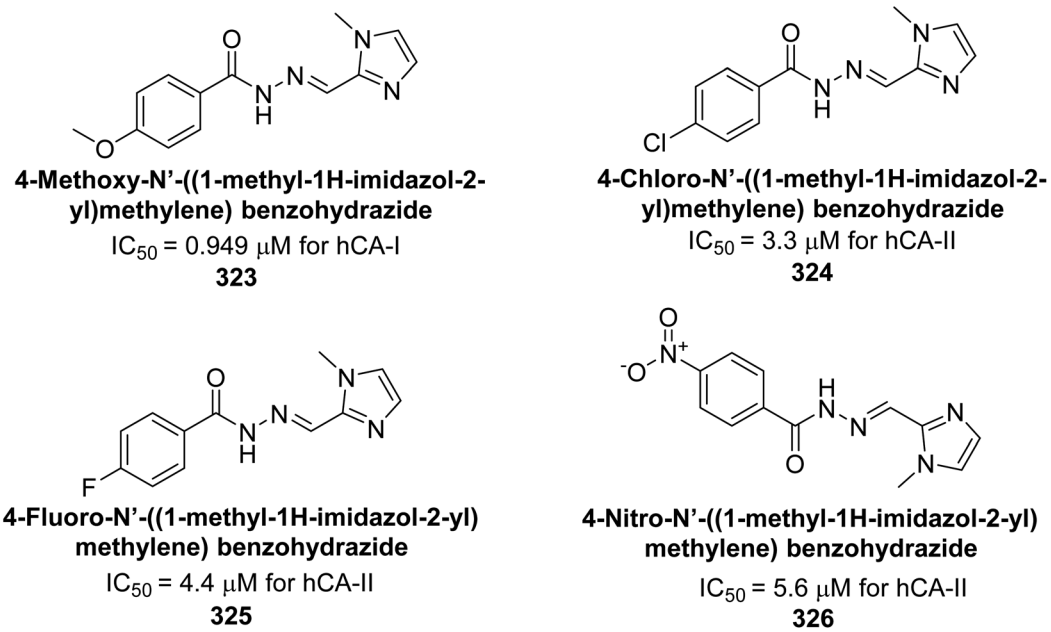

Fig. 116 Chemical structures of compounds **323**–**326**; their K_i values against hCA-I and II.

313 and **314** to investigate their biological interactions (Fig. 113). These compounds hold potential as promising lead candidates for further exploration against the CA target.[201]

Metwally *et al.* (2023) synthesized a series of thiopyrano[2,3-*d*]thiazoles linked to pyrazole moieties as potential anticancer agents through molecular hybridization. Remarkably, compound **315** exhibited an IC_{50} of 0.067 μM against hCA-IX, comparable to AAZ (0.059 μM). Similarly, compound **316** showed an IC_{50} of 0.123 μM against hCA-XII, close to AAZ's IC_{50} of 0.083 μM. Molecular docking studies further confirmed that

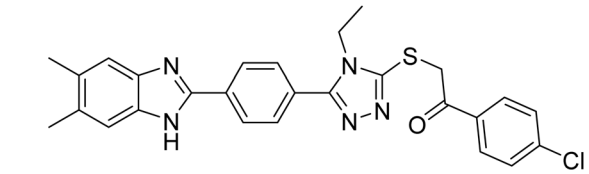

1-(4-Chlorophenyl)-2-((5-(4-(5,6-dimethyl-1*H*-benzo[*d*]imidazol-2-yl)phenyl)-4-ethyl-4*H*-1,2,4-triazol-3-yl)thio)ethan-1-one

IC_{50} = 1.28 μM for hCA-I

327

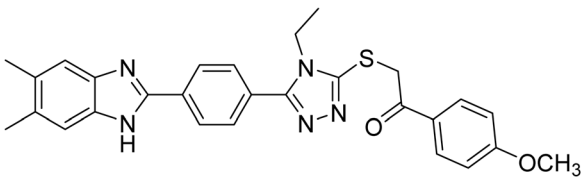

2-((5-(4-(5,6-Dimethyl-1*H*-benzo[*d*]imidazol-2-yl)phenyl)-4-ethyl-4*H*-1,2,4-triazol-3-yl)thio)-1-(4-methoxyphenyl)ethan-1-one

IC_{50} = 1.53 μM for hCA-II

328

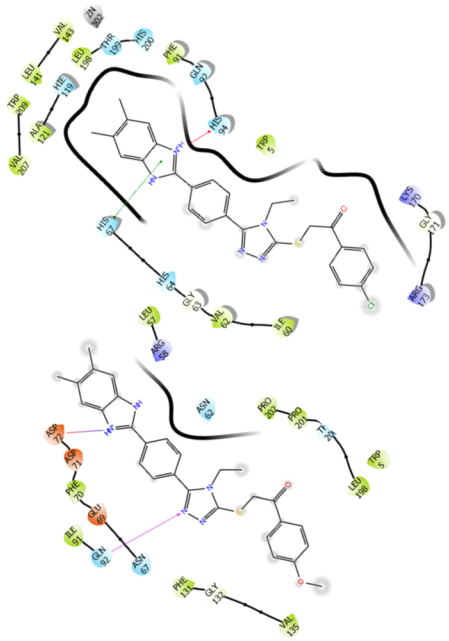

Fig. 117 Chemical structures of compounds **327** and **328**; their K_i values against hCA-I and II along with their docking images.

compounds **315** and **316** effectively occupied the active sites of hCA-IX and XII through various interactions (Fig. 114).[202]

Supuran *et al.* (2023) synthesized pyrimidines with modifications at the 7-position and evaluated their inhibition of hCA-IX and XII. The derivatives exhibited strong inhibition, with K_i values ranging from 5 to 96 nM for hCA-IX and 4 to 72 nM for hCA-XII. Especially, compounds **317**, **318**, **319**, and **320** showed potent inhibition of hCA-IX (K_i = 5.1, 8.6, 4.7, and 5.1 nM), while compounds **321** and **322** were effective against hCA-XII (K_i = 8.8, 5.4, 4.3, and 9.0 nM). Preliminary cytotoxicity tests indicated these compounds are not toxic to human non-tumor cells. The results suggest that small structural modifications at the 7-position of the triazolopyrimidine scaffold can enhance both inhibitory activity and isoform selectivity (Fig. 115).[203]

Ünver *et al.* (2023) synthesized imidazole-hydrazone Schiff base derivatives and evaluated their inhibitory effects against hCA-I and II. Compound **323** exhibited the highest inhibition of hCA-I, with an IC_{50} of 0.94 μM. Compounds **324**, **325**, and **326** showed notable inhibition of hCA-II, with IC50 values of 3.3, 4.4, and 5.6 μM, respectively (Fig. 116). Thus, compound **323** emerges as a potential lead for developing selective cytotoxic agents targeting hCA-I, while compound **324** holds promising for targeting hCA-II.[204]

Çevik *et al.* (2023) synthesized a series of benzimidazole-1,3,4-triazole derivatives with the objective of developing novel heterocyclic hybrids as potent enzyme inhibitors. Among them, compound **327** emerged as the most potent inhibitor of hCA-I, with an IC_{50} of 1.288 μM, while compound **328** was the most effective against hCA-II, with an IC_{50} of 1.532 μM. Enzyme inhibition kinetics revealed that all compounds act as non-competitive inhibitors. Molecular docking studies on compounds **327** and **328** confirmed their binding interactions within the enzyme's active site, corroborating the experimental results (Fig. 117).[205]

Kucukoglu *et al.* (2023) designed and synthesized a series of oxadiazoles synthesized and evaluated for their inhibitory activity against hCA-I and II. Many of the compounds demonstrated superior potency compared to AAZ. Remarkably, compounds **329** and **330** exhibited the strongest inhibition of hCA-I, with IC_{50} values of 0.68 and 0.96 μM, respectively. Additionally, compounds **329**, **330**, **331** and **332** showed significant inhibitory effects against hCA-II, with IC_{50} values of 0.65, 0.40, 0.40, and 0.71 μM, respectively. Molecular docking analysis indicated that compounds **329** and **330** engage in π–π stacking interactions with Phe91 in the active site of hCA-I. For hCA-II, these compounds formed π–π stacking interactions with His94 and π-cation interactions with Phe131 (Fig. 118). The alkylamino groups of both compounds played an essential role in their binding to hCA-II.[206]

Supuran *et al.* (2023) synthesized a series of biotin-conjugated sulfonamide derivatives to evaluate their potential as inhibitors of hCA-IX and XII. Particularly, in compound **333** inclusion of a 4-fluorophenyl (4-F-C_6H_4) group, resulted in high selectivity for hypoxia-induced hCA-XII, with a K_i value of 4.5 nM. Additionally, the 2-naphthyl derivative **334** emerged as the most potent inhibitor of hCA-IX, with a K_i of 6.2 nM—four times more effective than AAZ (K_i = 25 nM)—and exhibited excellent selectivity (Fig. 119).[207]

Taslimi *et al.* (2023) synthesized a series of new coumarin-dihydropyridine derivatives using a molecular hybridization

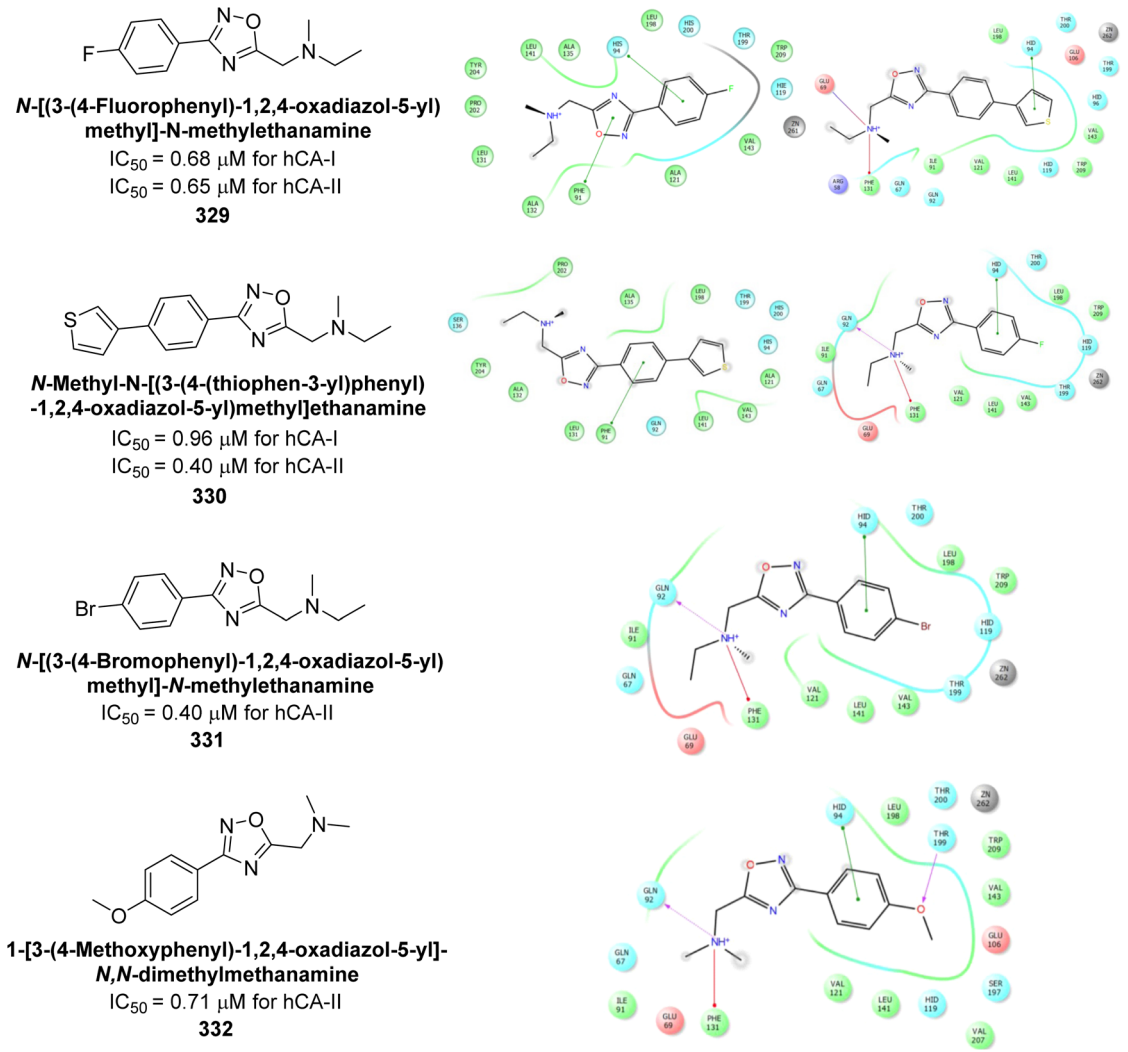

Fig. 118 Chemical structures of compounds 329–332; their IC_{50} values against hCA-I and II along with their docking images.

approach, combining key pharmacophore features. The synthesized derivatives were subsequently evaluated for their inhibitory activity against two key hCA isoforms, hCA-I and II. *In vitro* assays revealed that compounds **335**, **336**, and **337** were the most effective inhibitors of the studied hCA isoforms (Fig. 120). Compound **336**, belonging to the diethyl series and featuring a 4-fluorobenzyl substituent, was identified as the most selective inhibitor of hCA-I and II.[208]

Supuran *et al.* (2023) designed and synthesized furyl sulfonamides and tested for their inhibitory activity against hCA-I, II and IV. The findings indicated that compounds **338**, **339**, **340**, and **341** demonstrated strong inhibitory activity against the hCA-I and II isoforms, while compound **342** showed notable activity against the hCA-IV and IX isoforms. Additionally, molecular docking studies were conducted to explore potential interactions of these compounds with the active site of each isoform (Fig. 121). The most potent inhibitors exhibited favorable bioavailability and drug-likeness properties.[209]

Trippier *et al.* (2023) synthesized sulfonamides featuring a coumarin scaffold and evaluated as potent and selective CA inhibitors. Especially, compound **343** (K_i values: 21 nM for hCA-IX, and 5 nM for hCA-XII) was identified as a promising inhibitor of hCA-IX and XII, warranting further investigation (Fig. 122).[210]

Metwaly *et al.* (2024) designed and synthesized a series of novel substituted thiophene derivatives and their corresponding thiophene-pyrazole analogues incorporating a benzenesulfonamide moiety. The inhibitory effects of these synthesized analogues on hCA-IX and XII, were evaluated, with AAZ (IC_{50} = 0.065 μM for hCA-IX; 0.083 μM for hCA-XII) used as a reference compound. Compounds **344** (IC_{50} = 0.092 μM) and **345** (IC_{50} = 0.069 μM) demonstrated significant inhibitory activity against hCA-IX, while compounds **346** (IC_{50} = 0.173 μM) and **347** (IC_{50} = 0.146 μM) exhibited distinguished activity against hCA-XII (Fig. 123). The newly synthesized thiophene analogues were analyzed through molecular docking studies against the hCA-XII crystal structure to investigate their binding interactions.[211]

El-Messery *et al.* (2024) developed a series of coumarin sulfonate and sulfamate derivatives and evaluated their selectivity and inhibitory activity against hCA-II, IX, and XII, with AAZ as a reference. Derivatives with aryl or fluoroaryl sulfone groups favored cancer-related isoforms hCA-IX and XII. Markedly, the

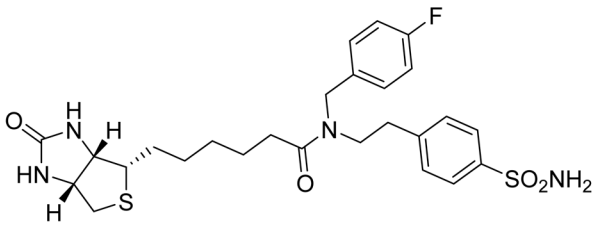

***N*-(4-Fluorobenzyl)-6-((3a*S*,4*S*,6a*R*)-2-oxo hexahydro-1*H*-thieno[3,4-*d*]imidazol-4-yl)-*N*-(4-sulfamoylphenethyl)hexanamide**

K_i = 4.5 nM for hCA-XII

333

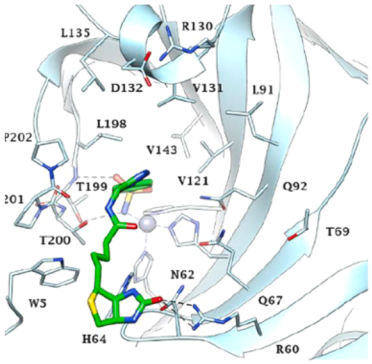

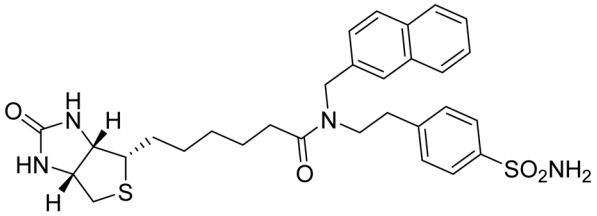

***N*-(Naphthalen-2-ylmethyl)-6-((3a*S*,4*S*,6a*R*)-2-oxo hexahydro-1*H*-thieno[3,4-*d*]imidazol-4-yl)-*N*-(4-sulfamoylphenethyl)hexanamide**

K_i = 6.2 nM for hCA-IX

334

Fig. 119 Chemical structures of compounds **333** and **334**; their K_i values against hCA-IX and XII along with docking image of **333**.

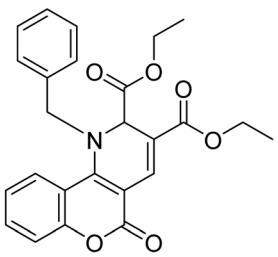

Diethyl 1-benzyl-5-oxo-1,5-dihydro-2H-chromeno[4,3-b]pyridine-2,3-dicarboxylate

IC_{50} = 1.47 μM for hCA-I

IC_{50} = 1.58 μM for hCA-II

335

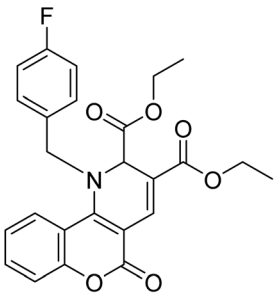

Diethyl 1-(4-fluorobenzyl)-5-oxo-1,5-dihydro-2H-chromeno[4,3-b]pyridine-2,3-dicarboxylate

IC_{50} = 0.88 μM for hCA-I

IC_{50} = 1.10 μM for hCA-II

336

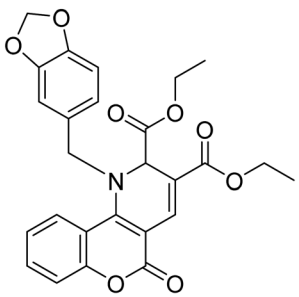

Diethyl 1-(benzo[d][1,3]dioxol-5-ylmethyl)-5-oxo-1,5-dihydro-2H-chromeno[4,3-b]pyridine-2,3-dicarboxylate

IC_{50} = 1.33 μM for hCA-I

IC_{50} = 1.53 μM for hCA-II

337

Fig. 120 Chemical structures of compounds **335–337**; their IC_{50} values against hCA-I and II.

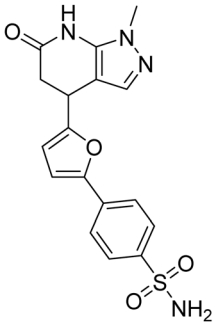

4-(5-(1-Methyl-6-oxo-4,5,6,7-tetrahydro-1H-pyrazolo[3,4-b]pyridin-4-yl)furan-2-yl)benzenesulfonamide

K_i = 20.0 nM for hCA-I
K_i = 5.5 nM for hCA-II

338

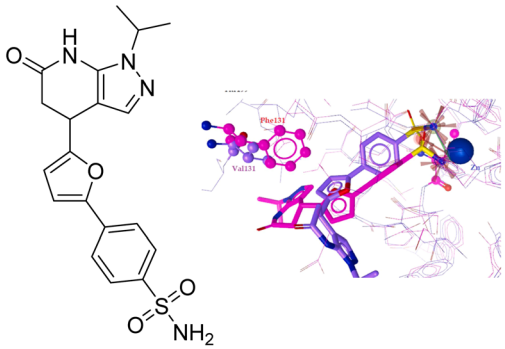

4-(5-(1-Isopropyl-6-oxo-4,5,6,7-tetrahydro-1H-pyrazolo[3,4-b]pyridin-4-yl)furan-2-yl)benzenesulfonamide

K_i = 6.30 nM for hCA-I
K_i = 4.00 nM for hCA-II

339

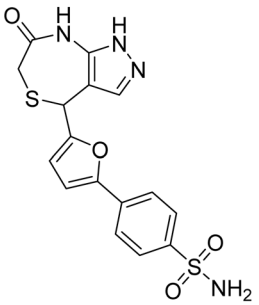

4-(5-(7-Oxo-4,6,7,8-tetrahydro-1H-pyrazolo [3,4-e][1,4]thiazepin- 4-yl)furan-2-yl) benzenesulfonamide

K_i = 17.5 nM for hCA-I
K_i = 5.8 nM for hCA-II

340

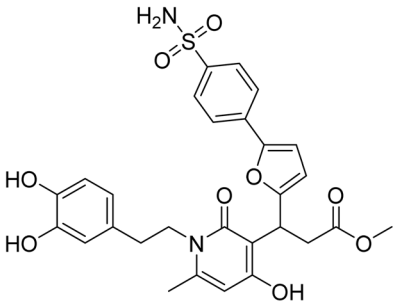

Methyl 3-(1-(3,4-dihydroxyphenethyl)-4-hydroxy-6-methyl-2-oxo-1,2- dihydropyridin-3-yl)-3-(5-(4-sulfamoylphenyl)furan-2-yl)propanoate

K_i = 23.2 nM for hCA-I
K_i = 5.9 nM for hCA-II

341

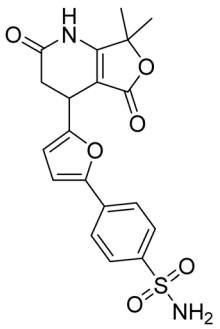

4-(5-(7,7-Dimethyl-2,5-dioxo-1,2,3,4,5,7-hexahydrofuro[3,4-b]pyridin-4-yl)furan-2-yl)benzenesulfonamide

K_i = 6.5 nM for hCA-IV
K_i = 16.8 nM for hCA-IX

342

Fig. 121 Chemical structures of compounds **338–342**; their K_i values against hCA-I, II and IV; docking image of compound **339**.

p-fluorine-substituted derivative **348** showed strong activity against hCA-IX (IC_{50} = 0.62 μM), while the benzene sulfone derivative **349** was selective for hCA-XII (IC_{50} = 0.56 μM). Coumarin derivatives with ethyl sulfone groups **350, 351, 352** were highly selective for hCA-II. Molecular docking studies indicated that these compounds interact with the hCA active site *via* various mechanisms (Fig. 124).[212]

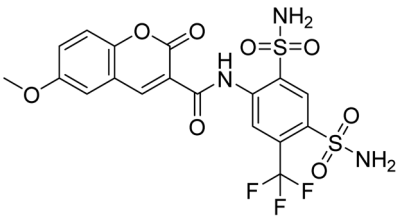

***N*-(2,4-disulfamoyl-5-(trifluoromethyl) phenyl)-6-methoxy-2-oxo-2H-chromene-3-carboxamide**

K_i = 21 nM for hCA-IX
K_i = 5 nM for hCA-XII
343

Fig. 122 Chemical structure of compound **343**; its K_i values against hCA-IX and XII.

Çevik *et al.* (2024) developed a series of benzimidazole-triazole derivatives and evaluated their inhibitory effects on hCA-I and II. The compounds showed IC_{50} values between 1.158 μM and 3.48 μM. Remarkably, compound **353** demonstrated the highest activity, with IC_{50} values of 1.288 μM for hCA-I and 1.619 μM for hCA-II. Kinetic studies indicated that these compounds act as non-competitive inhibitors. Molecular docking of compound **353** confirmed its interactions with the enzyme's active site, aligning with the experimental data (Fig. 125).[213]

Nural *et al.* (2024) developed naphthoquinone-thiazole hybrids and evaluated their inhibitory effects on hCA-I and II. The compounds exhibited significant inhibition, with K_i values ranging from 67.86 to 161.60 nM for hCA-I and 55.27 to 87.48 nM for hCA-II. The most potent compound, **354**, had K_i values of 67.86 nM for hCA-I and 56.8 nM for hCA-II. Molecular docking studies showed that in hCA-I, the naphthalene, thiazole, and difluorobenzene rings engaged in π–π stacking with residues His67, His94 and Phe91. For hCA-II, hydrogen bonds were formed with carbonyl groups at distances of 1.86, 2.11, and 2.15 Å, and π–π stacking occurred between His64 and the difluorobenzene ring (Fig. 126). These findings suggest that the compounds align well with the active sites of these enzymes.[214]

Mert *et al.* (2024) developed a series of novel pyrazole dicarboxylic acid derivatives. These derivatives were evaluated for their inhibitory activity against hCA-I and II, showing high potency. The compounds demonstrated significant inhibition, with K_i values ranging from 11.27 to 50.31 nM for hCA-I and 9.97 to 36.22 nM for hCA-II. Compound **355** (K_i = 11.27 nM) demonstrated exceptional activity against hCA-I. In contrast, compound **356** (K_i = 9.97 nM) exhibited excellent activity specifically against hCA-II. Molecular docking studies confirmed that these compounds effectively inhibit the target enzymes (Fig. 127).[215]

Supuran *et al.* (2024) synthesized coumarin analogues, incorporating a thiazole moiety and evaluated against hCAs. Particularly, compound **357**, featuring a 4-methoxy substitution, exhibited significant activity with a K_i of 90.9 nM against the hCA-XII isoform (Fig. 128). Significantly, all compounds showed selective inhibition against the hCA-IX and XII isoforms, with K_i values below 1000 nM. These findings suggest that the newly synthesized coumarin–thiazole hybrids have the potential to serve as selective lead candidates targeting hCA-IX and XII over hCA-I and II.[216]

Lamie *et al.* (2024) designed and synthesized a series of 1,2,3-triazole benzenesulfonamide derivatives to target hCA-IX and XII isoforms. Most of the synthesized compounds demonstrated significant inhibitory activity against these isoforms. Remarkably, compounds **358**, **359** and **360** exhibited exceptional inhibition of hCA-IX, with K_i values ranging from 0.03 to 0.06 μM, surpassing the potency of AAZ. Additionally, compounds **361** and **362** effectively inhibited the hCA-XII isoform, both with a K_i value of 0.02 μM, comparable to AAZ. ADME analysis indicated that compounds **358**, **360**, **361** and **362** complied with Lipinski's rule of five, suggesting they may be orally active, whereas compound **359** displayed lower oral bioavailability than AAZ. Molecular docking studies further elucidated the binding modes and stability of the target compounds within the active sites of hCA-IX and XII, particularly for compounds **360** and **362** (Fig. 129).[217]

Abouzid *et al.* (2024) synthesized a series of novel compounds incorporating the privileged thienopyrimidine scaffold. Among them, compounds **363**, **364**, **365** and **366** demonstrated the highest inhibition across all four isoforms. Particularly, compound **366** exhibited potent inhibitory activity against hCA-II, IX and XII, with K_i values of 8.6, 13.8, and 19 nM, respectively, comparing favorably to AAZ, which has K_i values of 12, 25, and 5.7 nM, respectively. Additionally, compound **365** showed significant activity against hCA-IX, with a K_i of 16.1 nM. Molecular docking studies were performed to predict the binding modes of these synthesized compounds within the active sites of the four CAIs. The results revealed that compounds **363–366** effectively mimicked the binding mode of AAZ, coordinating with the Zn^{2+} ion and interacting with critical amino acids Thr199, His96 and His94 essential for enzymatic activity (Fig. 130).[218]

Angeli *et al.* (2024) designed and synthesized dihydro-pyrrol-2-one compounds containing dual sulfonamide groups. Specifically, the ubiquitously expressed cytosolic hCA-I was inhibited with K_i values ranging from 3.9 (for compound **367**) to 870.9 nM, while hCA-II also showed significant inhibition. Importantly, all compounds demonstrated effective inhibition of the hCA-IX (K_i = 1.9 [for compound **368**] – 211.2 nM) and hCA-XII, with inhibition in the low nanomolar range (Fig. 131).[219]

Supuran *et al.* (2024) developed rhodanine-linked enamine-carbohydrazide derivatives and evaluated their effectiveness as inhibitors of mycobacterial carbonic anhydrase (mtCA). The results demonstrate their efficacy, with significant selectivity toward the mtCA-2 enzyme. Although these compounds exhibited moderate activity against hCA isoforms, their distinguished selectivity highlights their potential as antitubercular agents. Among the series, compound **369** emerged as the most potent, with a K_i value of 9.5 μM against mtCA-2. Molecular docking studies indicated that compounds **369** and **370** interact with the Zn^{2+} ion through metal coordination, similar to classical CAIs (Fig. 132).[220]

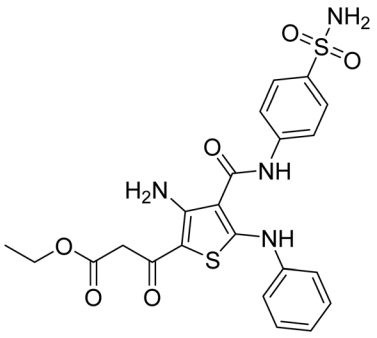

Ethyl 3-(3-amino-5-(phenylamino)-4-((4-sulfamoylphenyl)carbamoyl)thiophen-2-yl)-3-oxopropanoate

IC_{50} = 0.092 μM for hCA-IX

344

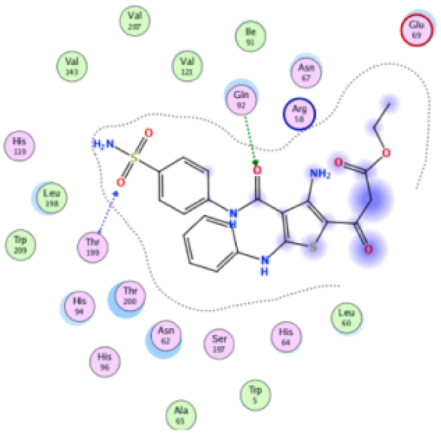

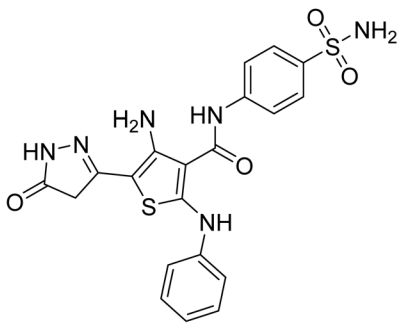

3-Amino-2-(5-oxo-4,5-dihydro-1H-pyrazol-3-yl)-5-(phenylamino)-N-(4-sulfamoylphenyl) thiophene-4-carboxamide

IC_{50} = 0.069 μM for hCA-IX

345

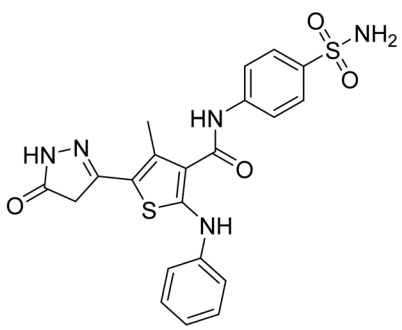

4-Methyl-5-(5-oxo-4,5-dihydro-1H-pyrazol-3-yl)-2-(phenylamino)-N-(4-sulfamoylphenyl) thiophene-3-carboxamide

IC_{50} = 0.173 μM for hCA-XII

346

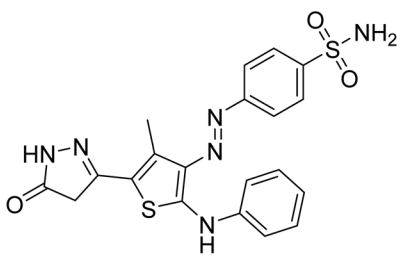

4-((4-Methyl-5-(5-oxo-4,5-dihydro-1H-pyrazol-3-yl) -2-(phenylamino)thiophen-3-yl)azo) benzenesulfonamide

IC_{50} = 0.146 μM for hCA-XII

347

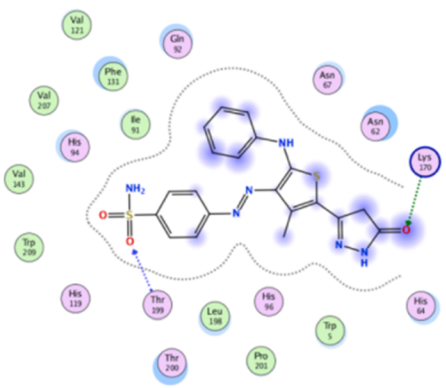

Fig. 123 Chemical structures of compounds **344**–**347**; their IC_{50} values against hCA-IX and XII along with docking images of **344** and **347**.

Žalubovskis *et al.* (2024) synthesized sulfonamide-incorporated bis(α-aminophosphonates) and evaluated against hCA-I, II, VII, IX, and XIII. The compounds showed notable activity and selectivity, particularly towards hCA-IX. Compound **371**, with a K_i of 15.1 nM, demonstrated high selectivity for hCA-IX. Additionally, these sulfonamides effectively inhibited hCA-XIII, with compound **372** showing the strongest inhibition (K_i = 17.2 nM), comparable to the well-known inhibitor AAZ but with greater selectivity (Fig. 133). We anticipate that this preliminary research will stimulate further exploration into the development of novel phosphorus-containing sulfonamide CAIs. Despite their promising inhibitory activities and selectivity, these compounds have been largely overlooked by researchers in this field.[221]

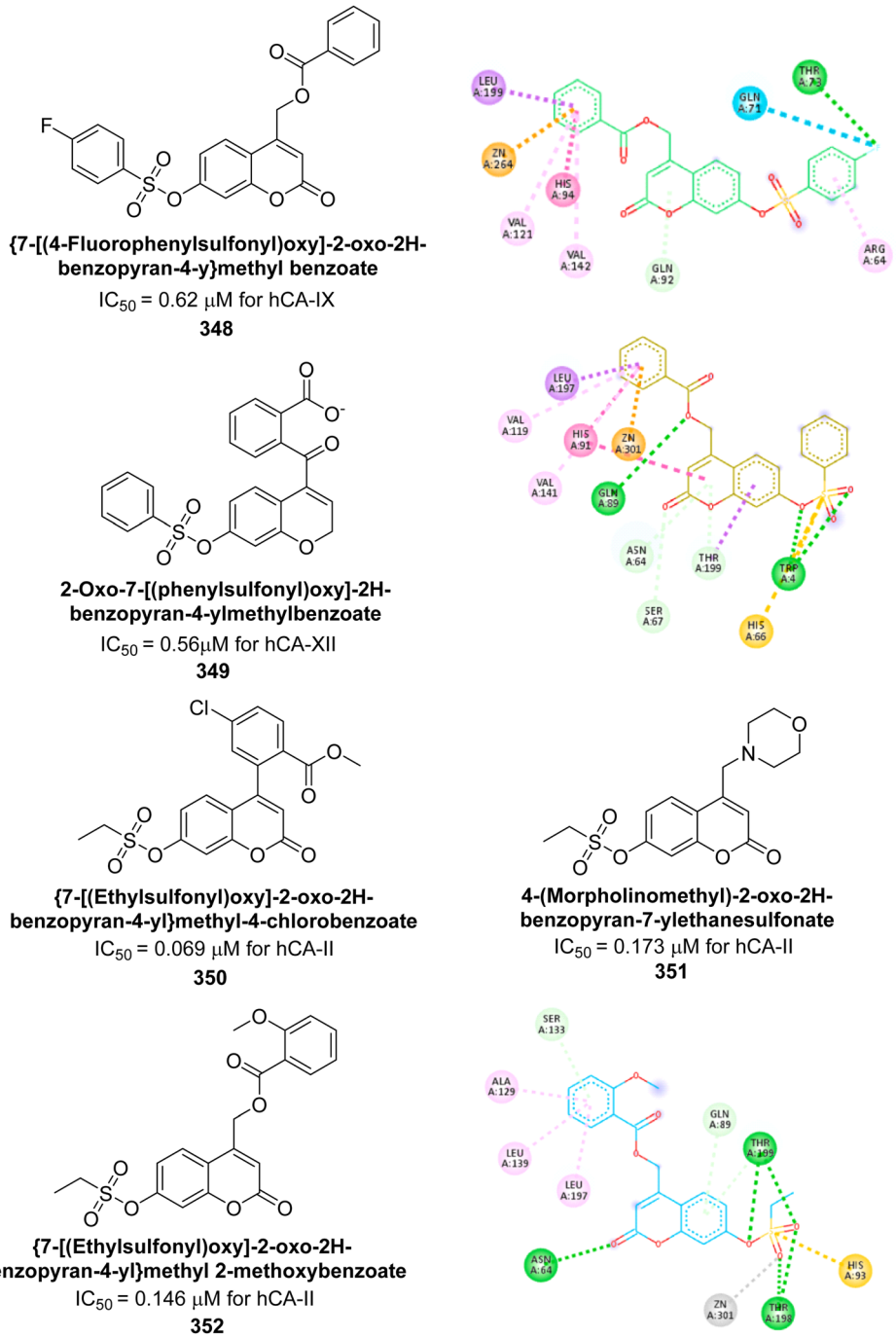

Fig. 124 Chemical structures of compounds **348–352**; their IC_{50} values against hCA-II, IX and XII along with their docking images.

Arifuddin *et al.* (2024) synthesized isatin-linked benzenesulfonamides and evaluated for their inhibitory potency against hCA-I, II, IX, and XII. Among the most potent were compounds **373** (435.8 nM) and **374** (956.4 nM) against hCA-I; compounds **375** (60.5 nM), **376** (95.6 nM), **377** (92.1 nM), and **378** (75.4 nM) against hCA-IX; and compound **379** (84.5 nM) against hCA-XII (Fig. 134). These derivatives showed greater selectivity towards hCA-IX over hCA-I, II, and XII, indicating their potential for further development as isoform-selective hCA-IX inhibitors through additional structural modifications.[222]

Göksu *et al.* (2024) designed and synthesized a series of benzene sulfonamides and assessed for their *in vitro* and *in silico* inhibitory activities against hCA-I and II. These compounds demonstrated significant inhibition of hCAs, with K_i ranging from 39.20 nM to 131.54 nM for hCA-I, and 50.96 nM to 147.94 nM for hCA-II. Compounds **380** and **381** proved to be potent inhibitors for hCA-I and II, respectively. The leucinate

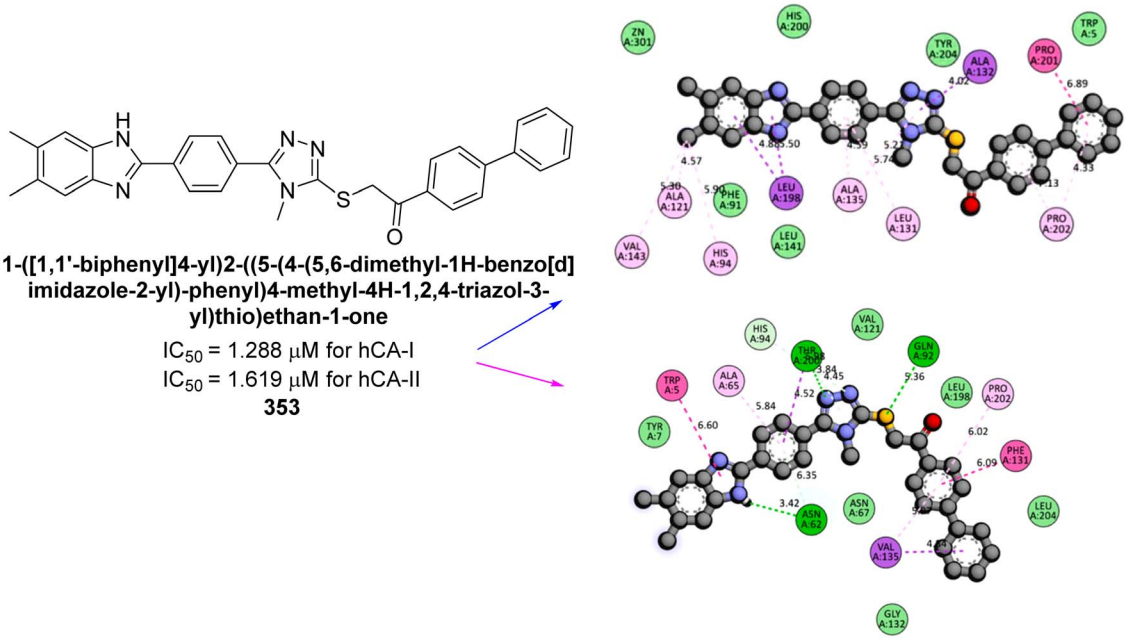

Fig. 125 Chemical structure of compound **353**; its IC_{50} values against hCA-I and II along with its docking images.

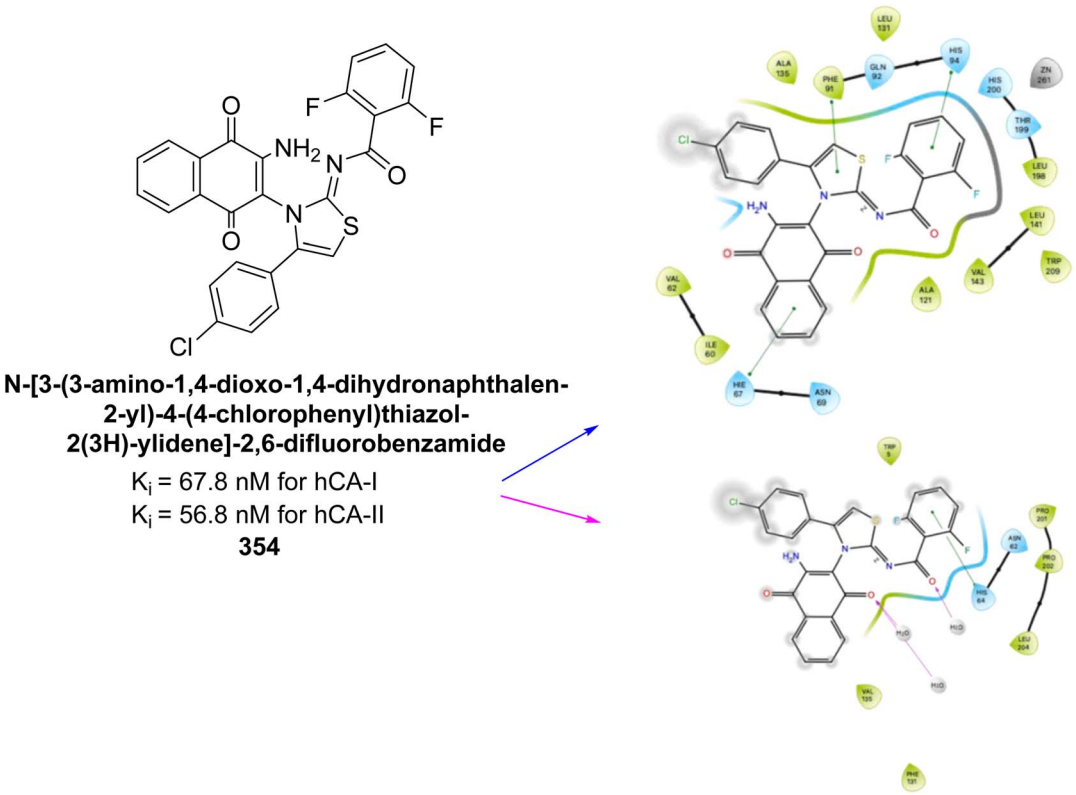

Fig. 126 Chemical structure of compound **354**; its K_i values against hCA-I and II along with its docking images.

group was particularly effective against hCA-I, while the *N*-butyl group showed greater efficacy for inhibiting hCA-II (Fig. 135).[223]

Moi *et al.* (2024) synthesized a series of piperidine-4-carboxamides and evaluated against hCA isoforms. Among the compounds, benzenesulfonamido carboxamides **382** and **383** emerged as the most potent in the piperazine- and benzylamine-based series, respectively. Shifting the 4-methyl group to the 2-position led to an approximately 10-fold decrease

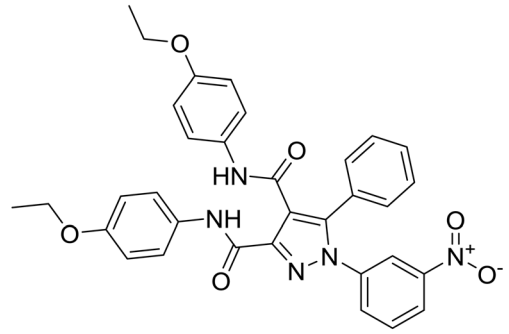

N^3,N^4-Bis(4-ethoxyphenyl)- 1-(3-nitrophenyl)-5-phenyl-1Hpyrazole-3,4-dicarboxamide

K_i = 11.27 nM for hCA-I

355

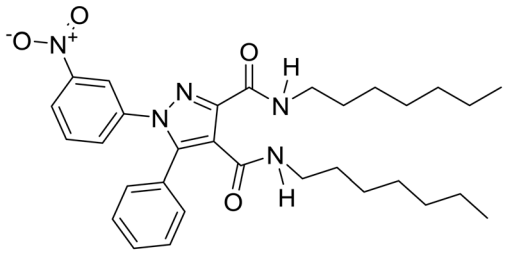

N^3,N^4-Diheptyl-1-(3-nitrophenyl)- 5-phenyl-1H-pyrazole-3,4-dicarboxamide

K_i = 9.97 nM for hCA-II

356

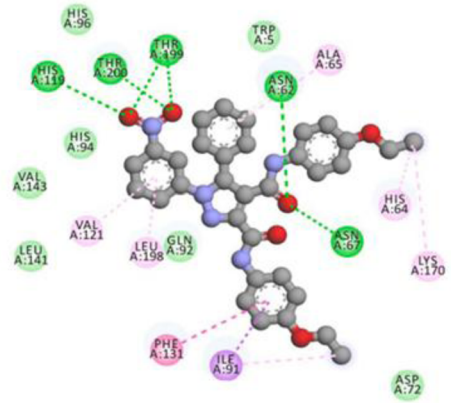

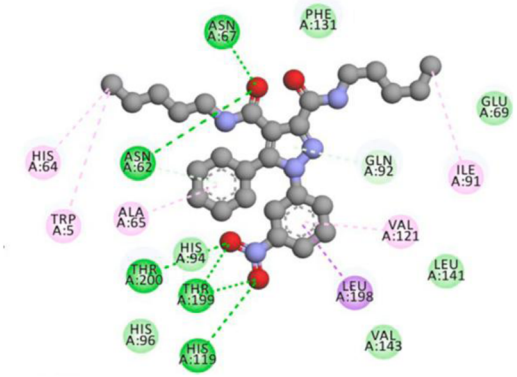

Fig. 127 Chemical structures of compounds **355** and **356**; their K_i values against hCA-I and II along with their docking images.

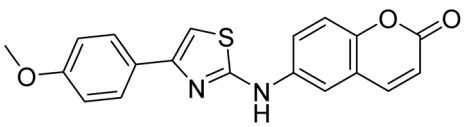

6-((4-(4-Methoxyphenyl)thiazol-2-yl) amino)-2H-chromen-2-one

K_i = 90.9 nM for hCA-XII

357

Fig. 128 Chemical structure of compound **357**; its K_i value against hCA-XII.

in activity against the target isoform, as demonstrated by compound **383**, which exhibited a K_i of 8.4 nM. Molecular docking studies revealed that compound **382** exhibited high selectivity for the tumor-associated hCA-IX and XII isoforms due to its ability to form favorable interactions within their active sites (Fig. 136). These initial findings highlighted the potential of piperidine-4-carboxamides as promising candidates for the continued development of therapies targeting cancer cell lines that express CA.[224]

Mert *et al.* (2024) designed and synthesized a series of novel pyrazole-dicarboxamides. The inhibition potency of the newly synthesized molecules against the hCA-I and II isoforms was evaluated, revealing K_i values ranging from 0.024 to 0.496 μM for hCA-I and 0.006 to 5.441 μM for hCA-II. Remarkably, compounds **384** and **386** exhibited nanomolar inhibition against hCA-II, demonstrating high selectivity for this isozyme. Molecular docking studies were conducted with the most active compounds, **385** and **386**, alongside the reference inhibitor AAZ, to elucidate their binding mechanisms with hCA-I and II. These compounds showed superior interactions with the isozymes compared to AAZ (Fig. 137). Consequently, these sulfonamide derivatives, demonstrating superior enzyme inhibition capabilities compared to the reference compound AAZ, hold promise as precursor molecules for further studies aimed at enzyme inhibition.[225]

Bagnoli *et al.* (2024) synthesized a diverse range of 3-selenylindoles through an eco-friendly method utilizing Oxone® as the oxidant with catalytic iodine. Additionally, several novel 3-selenylbenzenesulfonamide indoles were evaluated against hCAs. Particularly, 3-selenylbenzenesulfonamide indoles **387**, **388** and **389** exhibited strong and selective inhibition of hCA-II, while compounds **390** and **391** displayed selective inhibition of hCA-IX (Fig. 138). These results suggest that 3-selenylbenzenesulfonamide indoles hold promise as lead candidates for the development of more potent and selective hCA inhibitors.[226]

Durgun *et al.* (2024) synthesized a novel pyrazole carboxamide derivatives and evaluated their inhibitory effects on hCA-I and II. The compounds exhibited potential as inhibitors, with

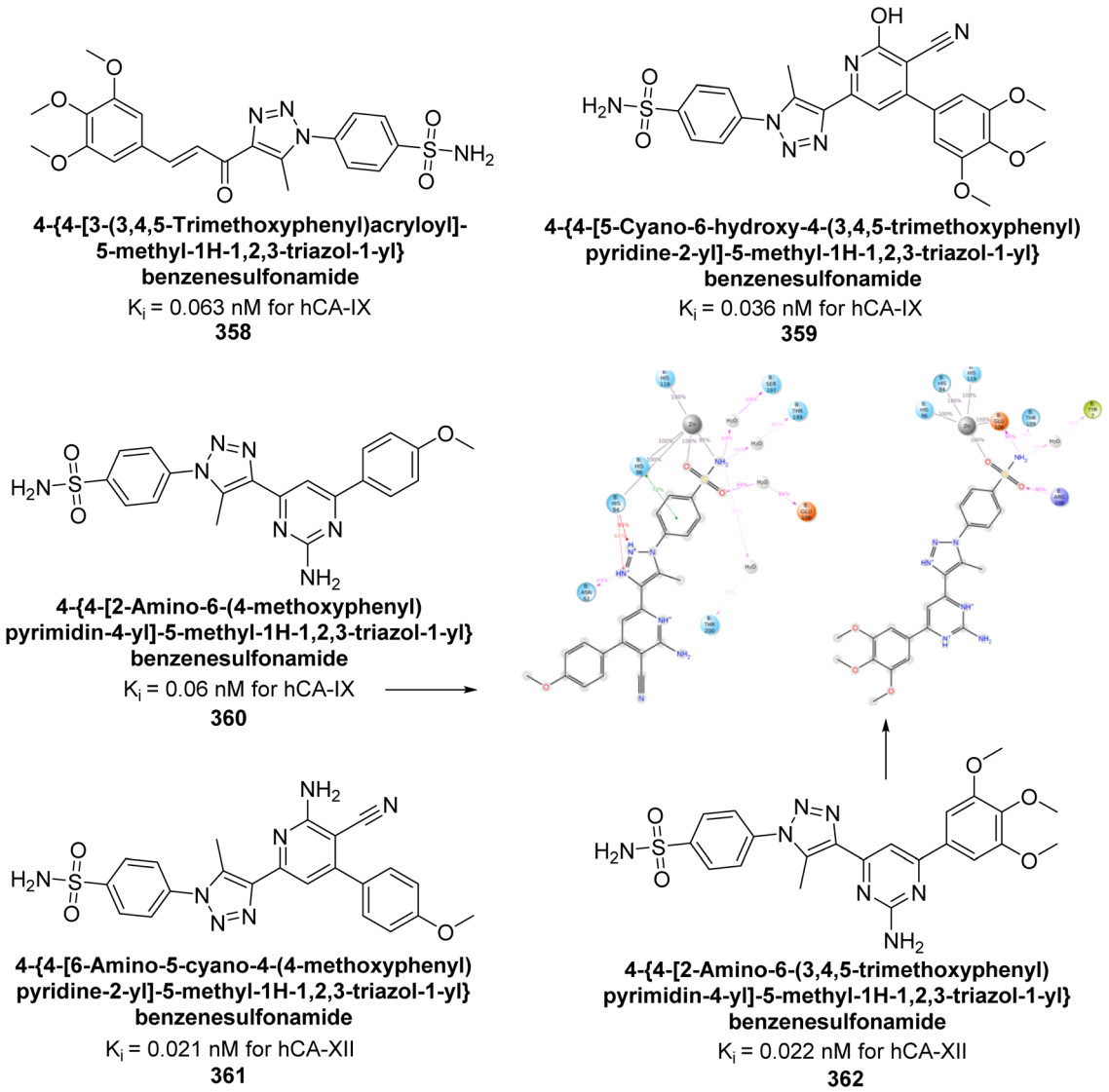

Fig. 129 Chemical structures of compounds **358–362**; their K_i values against hCA-XI and XII along with docking images of **360** and **362**.

K_i values ranging from 10.69 nM to 70.87 nM for hCA-I, and from 20.01 nM to 56.63 nM for hCA-II. Especially, compounds **392** and **393** showed competitive inhibition of hCA-I, while the other compounds demonstrated non-competitive inhibition. Additionally, compound **392** displayed competitive inhibition against hCA-II, forming an H-bond with the Thr200 residue and a water molecule within the active site of hCA-II, while Phe131 interacted through π–π stacking (Fig. 139). These docking scores and binding poses suggest that the compounds have significant potential as inhibitors of hCAs, and may serve as alternative therapeutic agents for the treatment of glaucoma.[227]

Angeli *et al.* (2024) synthesized a novel phthalazine derivatives and assessed for their inhibitory activity against hCA-II and IX. Markedly, several compounds displayed high selectivity, with a selectivity index reaching up to 13.8. The presence of a benzamide group at the 4′ position of the phthalazine ring was found to enhance hCA-IX inhibitory activity, similar to its effect on hCA-II inhibition. Replacing the benzamide group with a 4-hydroxybenzene moiety resulted in compound **394**, which was slightly less active than compound **395**. Among the compounds tested, **394** exhibited notable activity with a K_i value of 4.6 nM. Molecular docking studies were conducted to elucidate the interactions of these compounds within the active sites of hCA-II and IX isoforms (Fig. 140). These findings suggest that the developed phthalazine derivatives may offer valuable alternatives in anticancer therapy by addressing key challenges such as resistance development and lack of selectivity, which often lead to acute or chronic toxicity.[228]

Aslan *et al.* (2024) designed and synthesized a series of Biginelli products incorporating the benzenesulfonamide moiety known for inhibiting CA enzymes. The introduction of a carboxamide group at the 5-position of the 6-phenyl-tetrahydropyrimidine ring, as in compound **396**, resulted in significant and selective inhibition of hCA-IX and XII isoforms, with K_i values of 6.6 and 8.9 nM, respectively. Remarkably, compound **397** exhibited 1.7-fold higher potency against hCA-

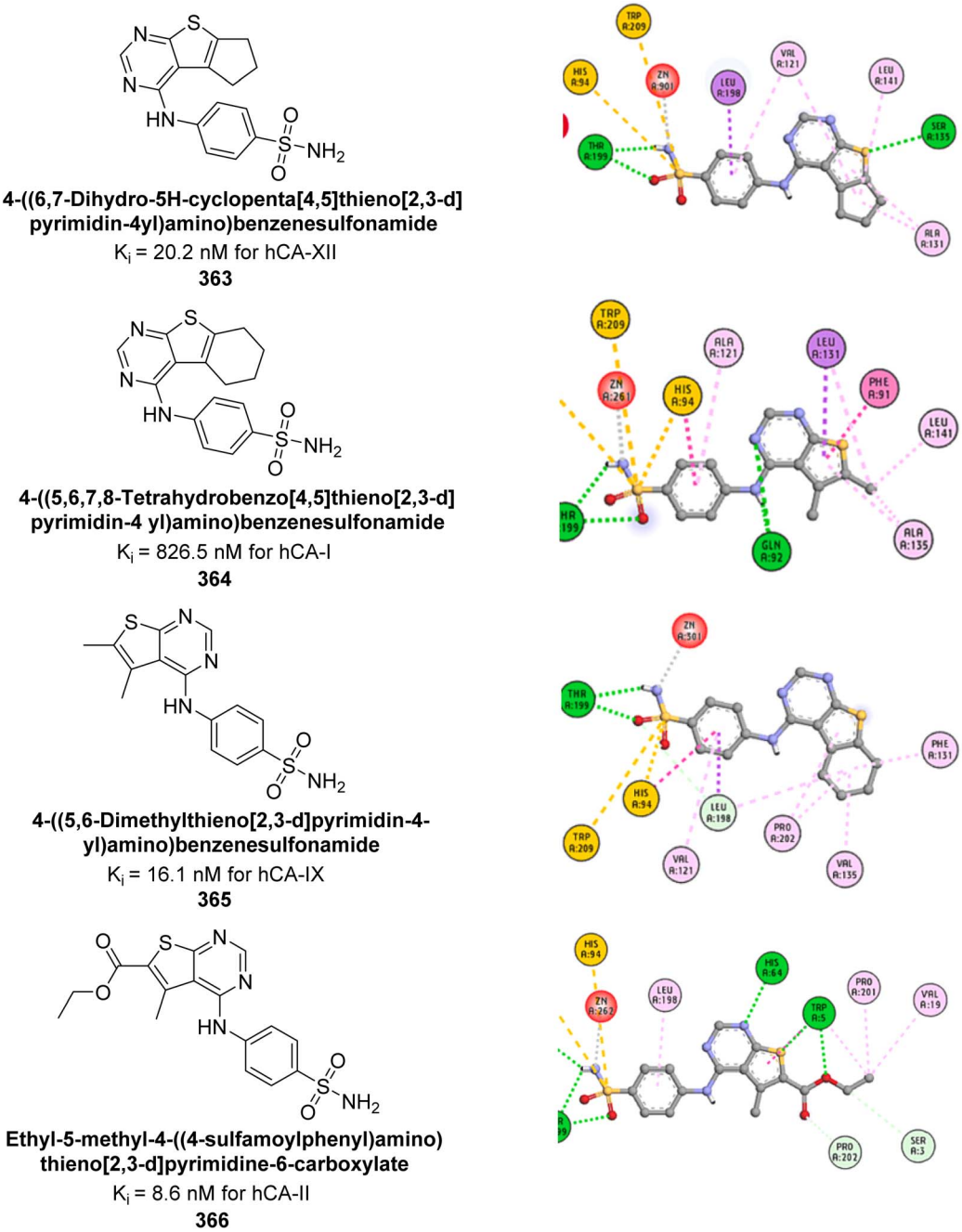

Fig. 130 Chemical structures of compounds **363–366**; their K_i values against hCA-I, II, XI and XII along with their docking images.

XII compared to hCA-IX, with K_i values of 5.3 and 8.9 nM, respectively (Fig. 141).[229]

Nafie *et al.* (2024) designed and synthesized a series of mono- and bis-1,2,3-triazoles and evaluated against hCA-IX. Compounds **398**, **399** and **400** demonstrated potent inhibition of hCA-IX, with IC_{50} values of 0.113, 0.134, and 0.214 μM. Molecular modeling studies revealed that compound **398**, in particular, shows a strong binding affinity for hCA-IX, which is a key target in PC-3 prostate cancer cells (Fig. 142). Future studies should investigate the anticancer activity of compound **398** *in vivo* to assess its efficacy and safety in experimental animal models, with the aim of clinical development.[230]

Kasımoğulları *et al.* (2024) synthesized a series of pyrazole-carboxamides and evaluated the inhibitory effects of these compounds on hCA-I and II, revealing K_i values ranging from 0.063 to 3.368 μM for hCA-I and from 0.007 to 4.235 μM for hCA-II. Compound **401** (IC_{50} = 0.420 μM for hCA-I & 0.310 μM for hCA-II) displayed non-competitive behavior. Compound **401**, which contains a primary $-SO_2NH_2$ group in the *para* position, is the most effective esterase inhibitor for both hCA-I and II. The compound **401** exhibited superior binding interactions relative to AAZ (Fig. 143).[231]

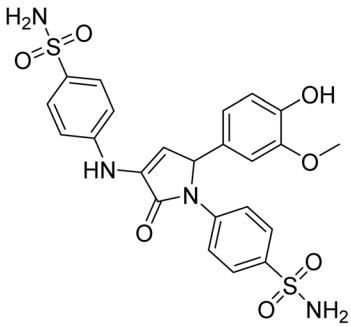

5-(4-Hydroxy-3-methoxyphenyl)-1-(4-sulfamoylphenyl)-3-((4-sulfamoylphenyl)amino)-1H-pyrrol-2(5H)-one

K_i = 3.9 nM for hCA-I

367

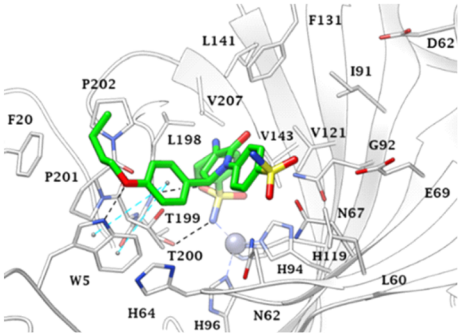

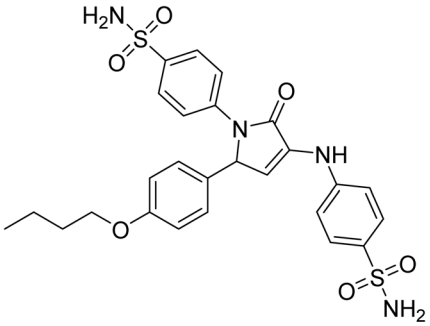

5-(4-Butoxyphenyl)-1-(4-sulfamoylphenyl)-3-((4-sulfamoylphenyl)amino)-1H-pyrrol-2(5H)-one

K_i = 1.9 nM for hCA-IX

368

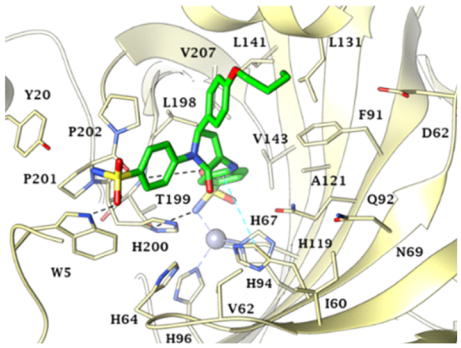

Fig. 131 Chemical structures of compounds **367** and **368**; their K_i values against hCA-I and IX along with their docking images.

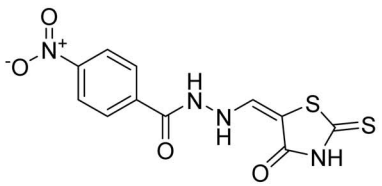

4-Nitro-N'-[(4-oxo-2-thioxothiazolidin-5-ylidene) methyl]benzohydrazide

K_i = 9.5 μM for mtCA-2

369

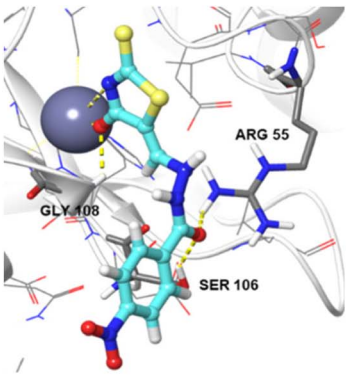

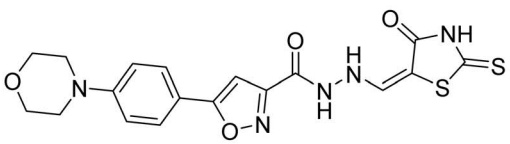

5-(4-Morpholinophenyl)-N'-[(4-oxo-2-thioxothiazolidin-5-ylidene)methyl]isoxazole-3-carbohydrazide

K_i = 63.9 μM for mtCA-2

370

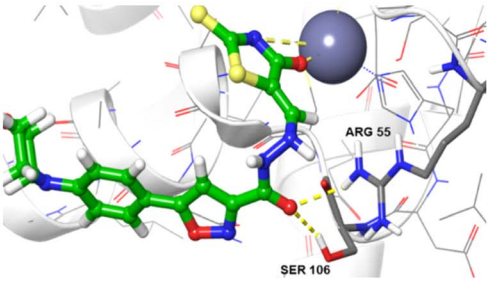

Fig. 132 Chemical structures of compounds **369** and **370**; their K_i values against mtCA-2 along with their docking images.

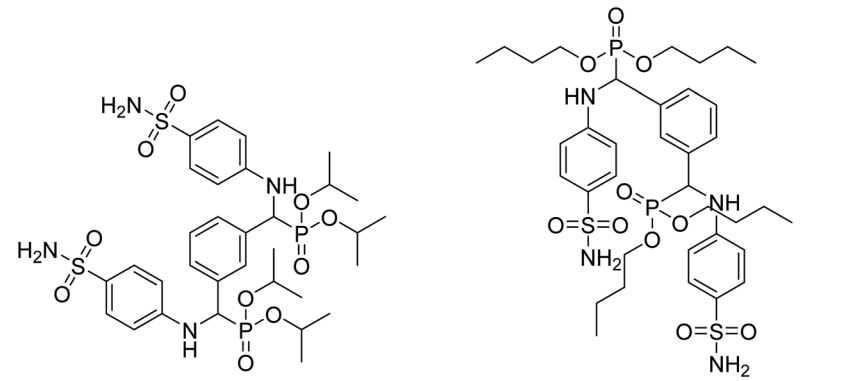

Tetraisopropyl (1,3-phenylenebis{[(4-sulfamoylphenyl)amino] methylene})bis(phosphonate)
K_i = 15.1 nM for hCA-IX
371

Tetrabutyl (1,3-phenylenebis{[(4-sulfamoylphenyl)amino]methylene}) bis(phosphonate)
K_i = 17.2 nM for hCA-XIII
372

Fig. 133 Chemical structures of compounds **371** and **372**; their K_i values against hCA-IX and XIII.

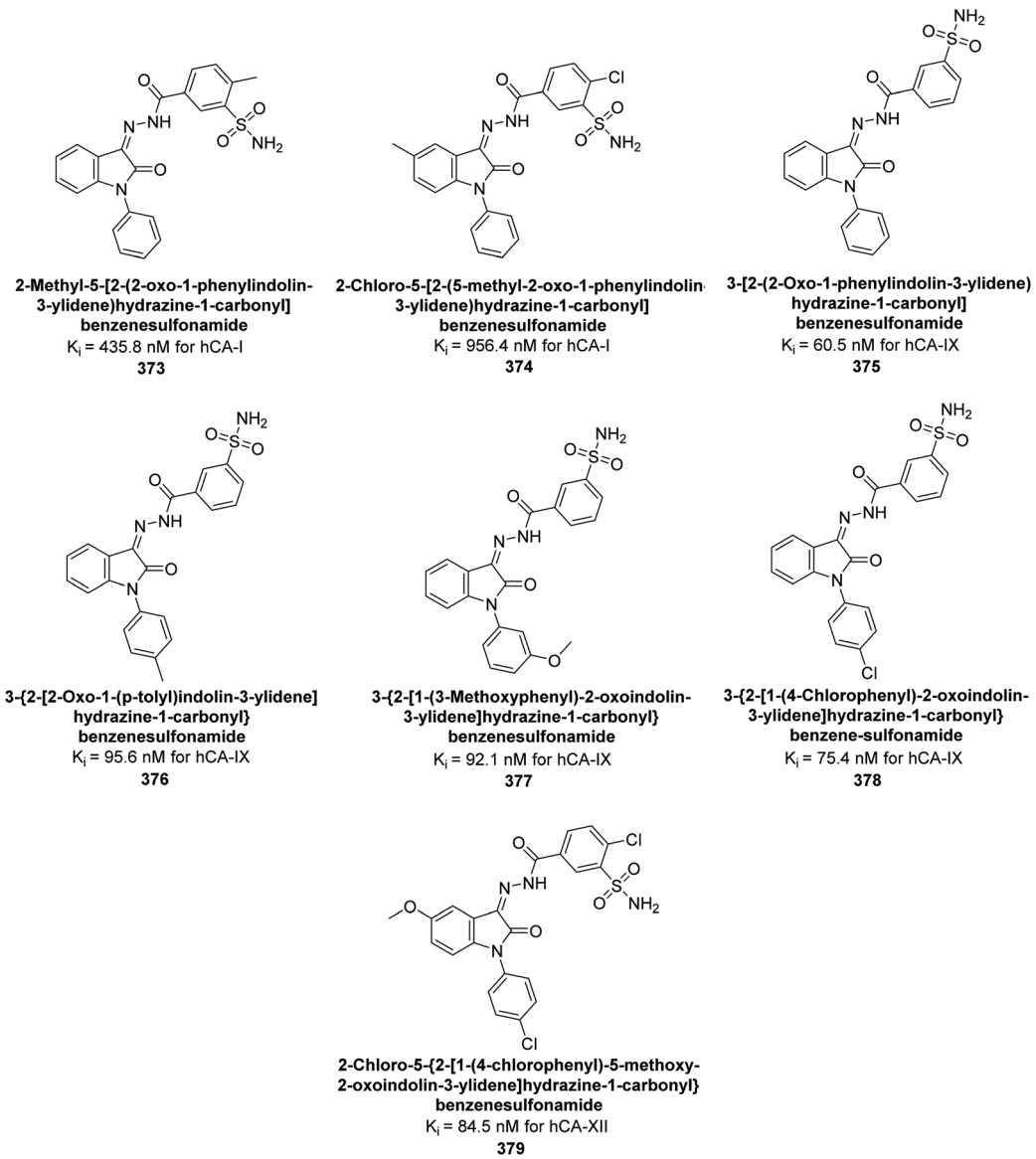

2-Methyl-5-[2-(2-oxo-1-phenylindolin-3-ylidene)hydrazine-1-carbonyl] benzenesulfonamide
K_i = 435.8 nM for hCA-I
373

2-Chloro-5-[2-(5-methyl-2-oxo-1-phenylindolin-3-ylidene)hydrazine-1-carbonyl] benzenesulfonamide
K_i = 956.4 nM for hCA-I
374

3-[2-(2-Oxo-1-phenylindolin-3-ylidene) hydrazine-1-carbonyl] benzenesulfonamide
K_i = 60.5 nM for hCA-IX
375

3-{2-[2-Oxo-1-(p-tolyl)indolin-3-ylidene] hydrazine-1-carbonyl} benzenesulfonamide
K_i = 95.6 nM for hCA-IX
376

3-{2-[1-(3-Methoxyphenyl)-2-oxoindolin-3-ylidene]hydrazine-1-carbonyl} benzenesulfonamide
K_i = 92.1 nM for hCA-IX
377

3-{2-[1-(4-Chlorophenyl)-2-oxoindolin-3-ylidene]hydrazine-1-carbonyl} benzene-sulfonamide
K_i = 75.4 nM for hCA-IX
378

2-Chloro-5-{2-[1-(4-chlorophenyl)-5-methoxy-2-oxoindolin-3-ylidene]hydrazine-1-carbonyl} benzenesulfonamide
K_i = 84.5 nM for hCA-XII
379

Fig. 134 Chemical structures of compounds **373–379**; their K_i values against hCA-I, IX and XII.

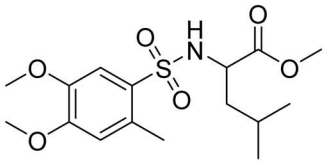

Methyl [(4,5-dimethoxy-2-methylphenyl)sulfonyl]-DL-leucinate

K_i = 39.2 nM for hCA-I

380

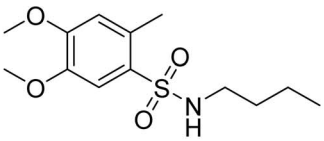

***N*-Butyl-4,5-dimethoxy-2-methylbenzenesulfonamide**

K_i = 50.9 nM for hCA-II

381

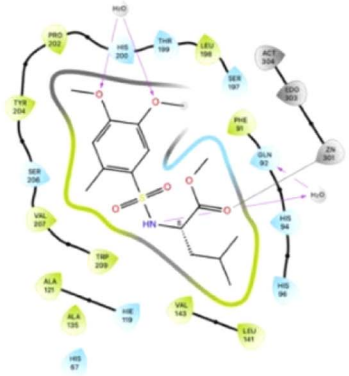

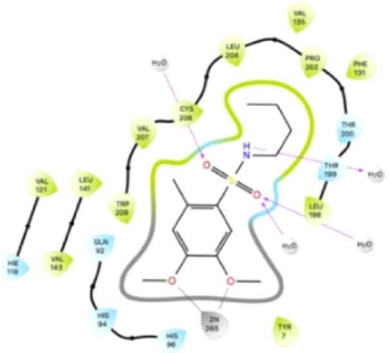

Fig. 135 Chemical structures of compounds **380** and **381**; their K_i values against hCA-I and II along with their docking images.

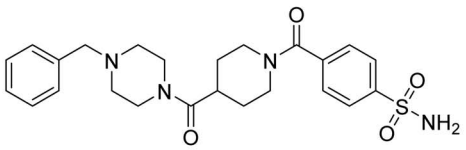

4-(4-(4-Benzylpiperazine-1-carbonyl)piperidine-1-carbonyl)benzenesulfonamide

K_i = 8.3 nM for hCA-IX

K_i = 2.7 nM for hCA-XII

382

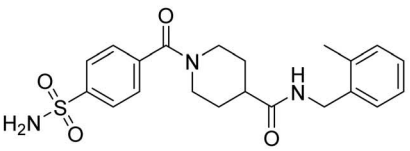

***N*-(2-Methylbenzyl)-1-(4-sulfamoylbenzoyl) piperidine-4-carboxamide**

K_i = 8.4 nM for hCA-IX

K_i = 6.9 nM for hCA-XII

383

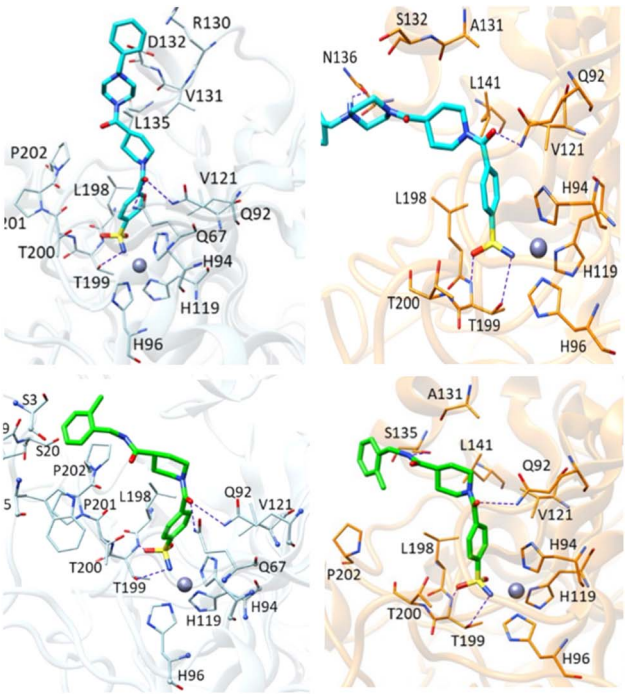

Fig. 136 Chemical structures of compounds **382** and **383**; their K_i values against hCA-IX and XII along with their docking images.

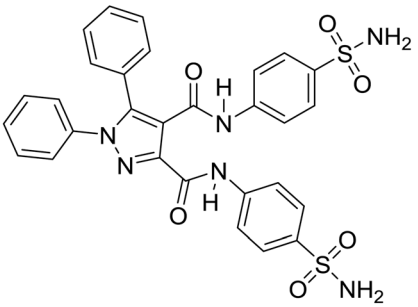

1,5-Diphenyl-N^3,N^4-bis(4-sulfamoylphenyl)-1H-pyrazole-3,4-dicarboxamide
K_i = 0.121 nM for hCA-II
384

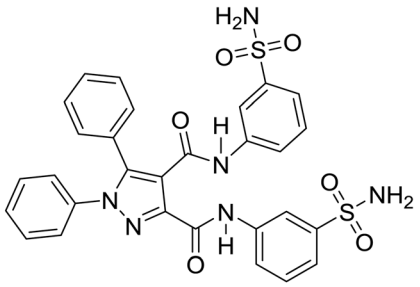

1,5-Diphenyl-N^3,N^4-bis(3-sulfamoylphenyl)-1H-pyrazole-3,4-dicarboxamide
K_i = 0.330 nM for hCA-I
K_i = 0.188 nM for hCA-II
385

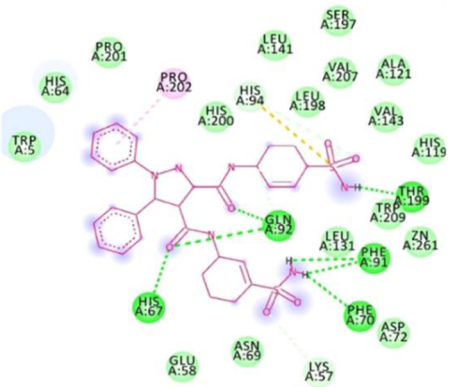

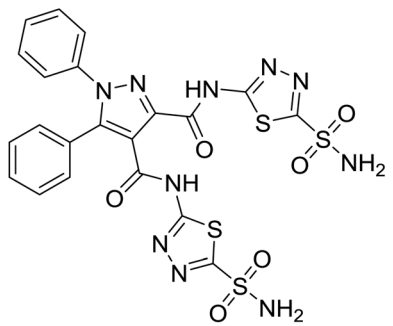

1,5-Diphenyl-N^3,N^4-bis(5-sulfamoyl-1,3,4-thiadiazol-2-yl)-1H-pyrazole-3,4-dicarboxamide
K_i = 0.332 nM for hCA-I
K_i = 0.032 nM for hCA-II
386

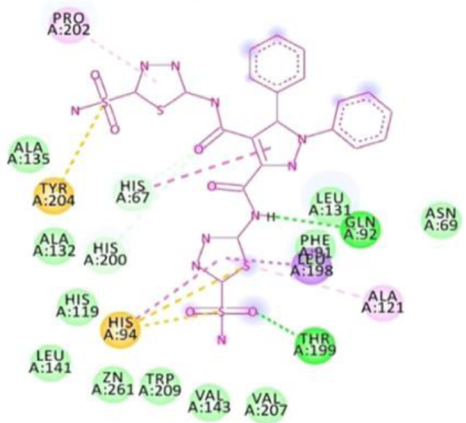

Fig. 137 Chemical structures of compounds **384–386**; their K_i values against hCA-I and II along with docking images of **385** and **386**.

6. Comparative analysis of the different heterocyclic scaffolds as CAIs against various isoforms based on IC_{50}/K_i values

The tabular data presents a comparative analysis of various heterocyclic scaffolds as CAIs based on their IC_{50} and K_i values against different CA isoforms (Table 14). This includes scaffolds such as pyrimidine, triazole, thiazole, phthalazine, imidazole, oxadiazole, indole, isatin, chalcone, coumarin, rhodanine, quinolines, and sulfonamides. Each scaffold's inhibitory performance is evaluated, showcasing its potency and selectivity towards different CA isoforms. The data serves to highlight the SAR and potential of each scaffold in CA inhibition for therapeutic applications.

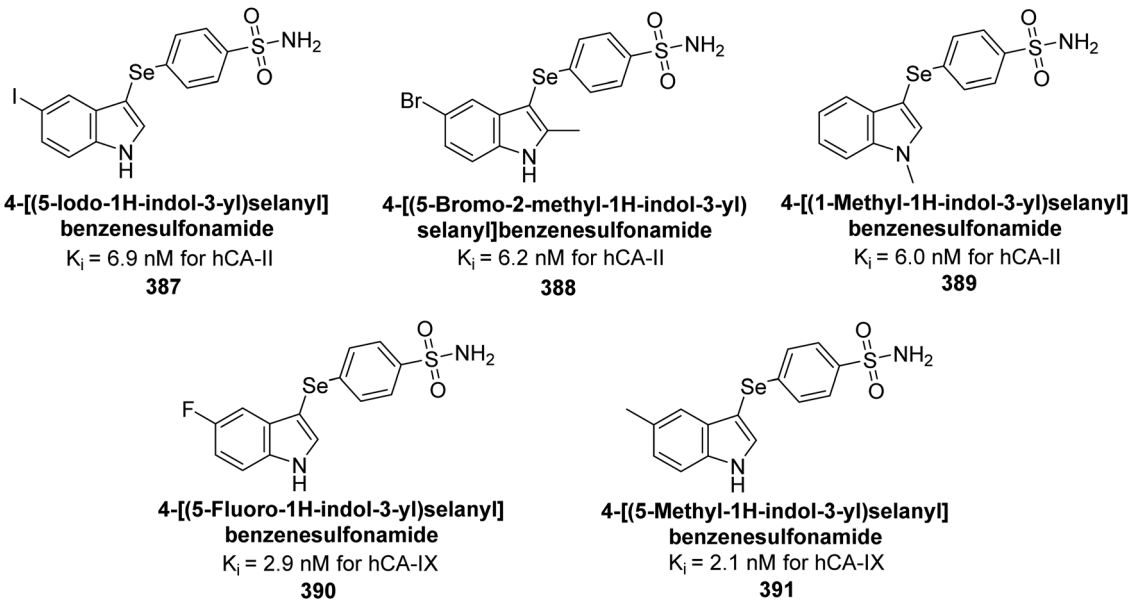

Fig. 138 Chemical structures of compounds 387–391; their K_i values against hCA-II and IX.

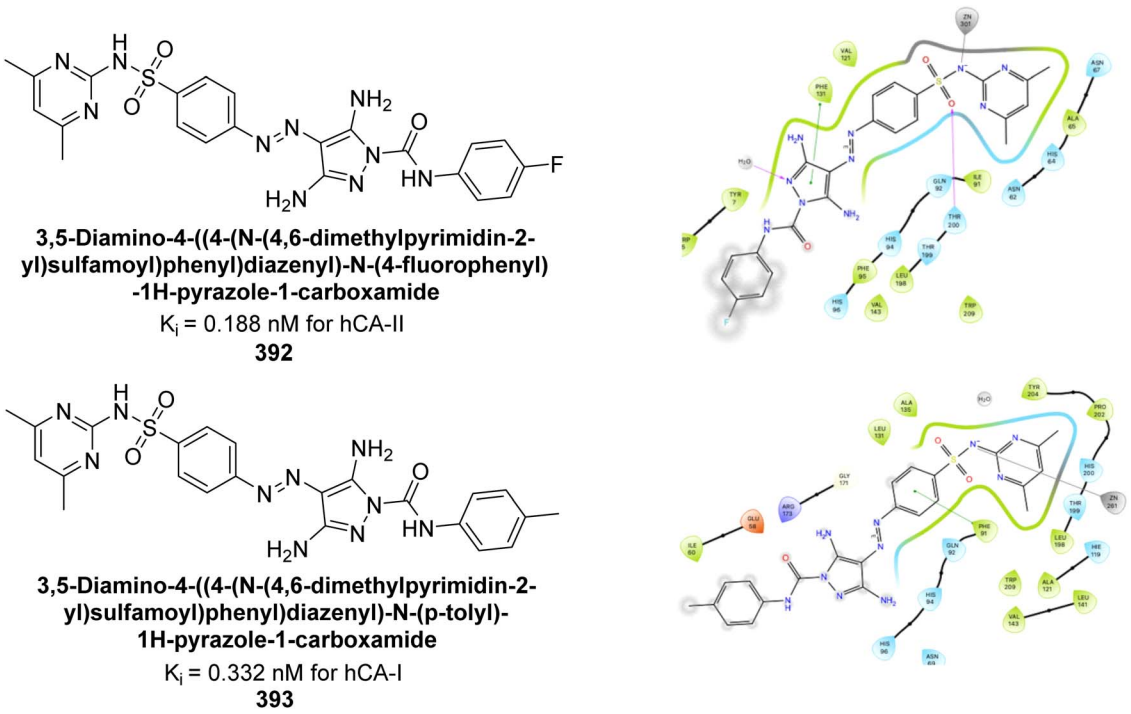

Fig. 139 Chemical structures of compounds 392 and 393; their K_i values against hCA-I and II along with their docking images.

Among the various heterocyclic scaffolds discussed, sulfonamide stand out as the most effective CAIs. Their established ability to coordinate directly with the zinc ion in the enzyme's active site contributes to their potent inhibitory activity, as reflected in low IC_{50}/K_i values across multiple CA isoforms. Sulfonamides benefit from a well-defined structure–activity relationship, allowing for strategic modifications to enhance both potency and selectivity. While other scaffolds such as phthalazine, pyrimidine, triazole, and thiazole also exhibit promising inhibitory activities, their variations in binding affinity and effectiveness often depend on specific substituents and structural characteristics.

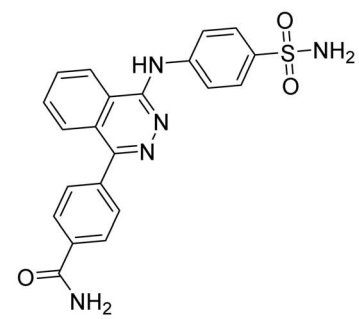

4-(4-((4-Sulfamoylphenyl)amino) phthalazin-1-yl)benzamide
K_i = 1.6 nM for hCA-II
K_i = 3.7 nM for hCA-IX
394

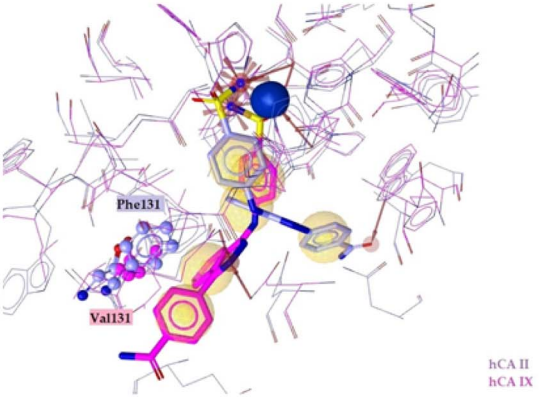

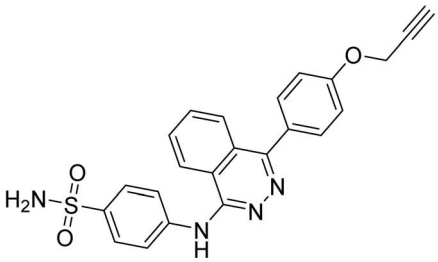

4-((4-(4-(Prop-2-yn-1-yloxy)phenyl)phthalazin-1-yl)amino)benzenesulfonamide
K_i = 52.8 nM for hCA-II
K_i = 8.9 nM for hCA-IX
395

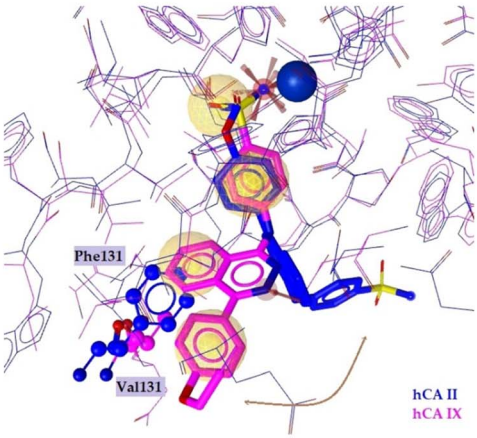

Fig. 140 Chemical structures of compounds **394** and **395**; their K_i values against hCA-II and IX along with their docking images.

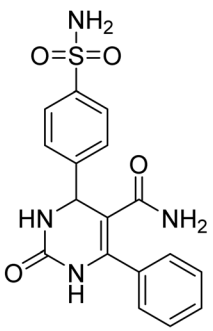

2-Oxo-6-phenyl-4-(4-sulfamoylphenyl)-1,2,3,4-tetrahydropyrimidine-5-carboxamide
K_i = 6.6 nM for hCA-IX
K_i = 8.9 nM for hCA-XII
396

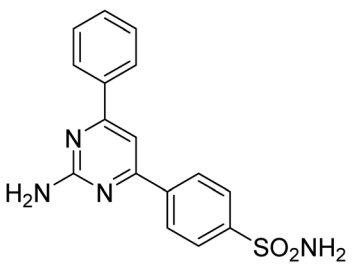

4-(2-Amino-6-phenylpyrimidin-4-yl) benzenesulfonamide
K_i = 8.9 nM for hCA-IX
K_i = 5.3 nM for hCA-XII
397

Fig. 141 Chemical structures of compounds **396** and **397**; their K_i values against hCA-IX and XII.

7. Structure–activity relationship based on different heterocyclic scaffolds

The SAR of different heterocyclic scaffolds-based CAIs can be extensively explored by considering the effects of various electron-donating (EDGs) and electron-withdrawing (EWGs) groups attached to the pyrazoline core. These substituents significantly impact the inhibitor's binding affinity, potency, and selectivity for different hCA isoforms. The interactions of these compounds with the active site of the enzyme can be further elucidated through molecular docking studies (Fig. 144).

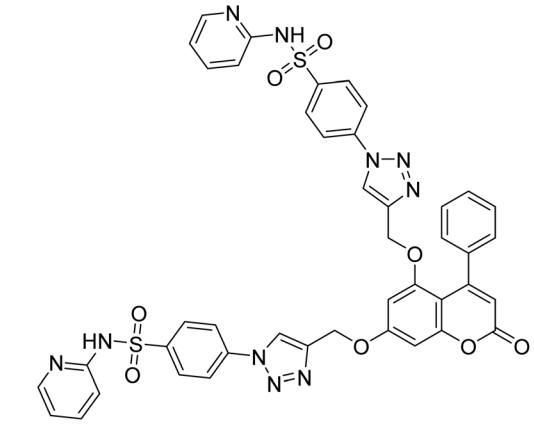

4,4'-((((2-Oxo-4-phenyl-2H-chromene-5,7 diyl)bis(oxy))bis(methylene))bis(1H-1,2,3-triazole-4,1-diyl))bis(N-(pyridin-2-yl)benzenesulfonamide)
IC_{50} = 0.113 μM for hCA-IX
398

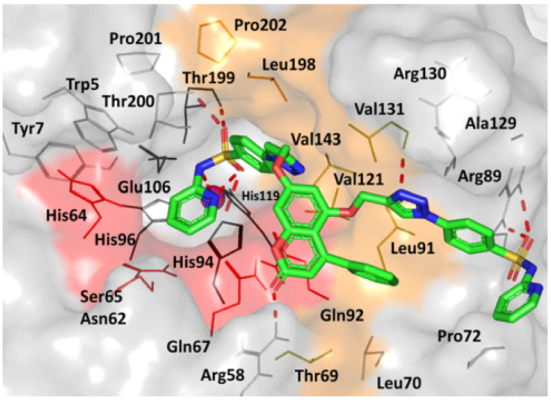

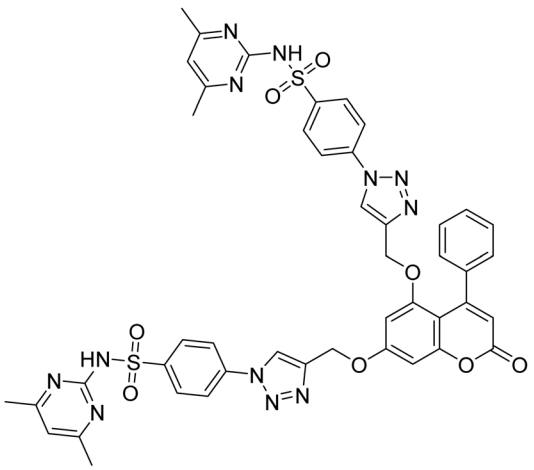

4,4'-((((2-Oxo-4-phenyl-2H-chromene-5,7-diyl)bis(oxy))bis(methylene))bis(1H-1,2,3-triazole-4,1-diyl))bis(N-(4,6-dimethylpyrimidin-2-yl)benzenesulfonamide)
IC_{50} = 0.134 μM for hCA-IX
399

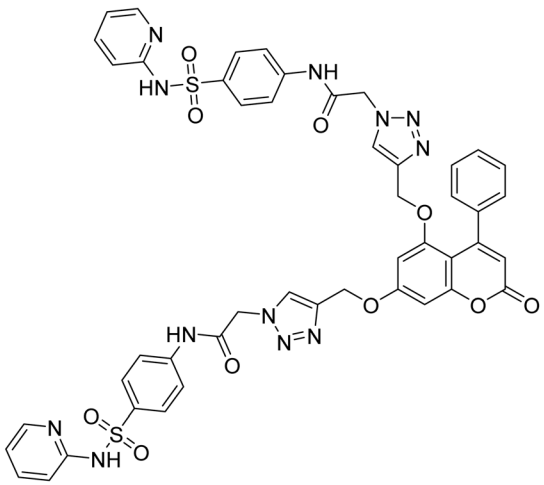

2,2'-((((2-Oxo-4-phenyl-2H-chromene-5,7-diyl)bis(oxy))bis(methylene))bis(1H-1,2,3-triazole-4,1-diyl))bis(N-(4-(N-(pyridin-2-yl)sulfamoyl)phenyl)acetamide)
IC_{50} = 0.214 μM for hCA-IX
400

Fig. 142 Chemical structures of compounds 398–400; their IC_{50} values against hCA-IX and docking image of 398.

7.1. Pyrazoline-based CAIs

7.1.1 Effect of electron-donating groups (EDGs). EDGs such as methyl ($-CH_3$) and methoxy ($-OCH_3$) on the phenyl ring attached to the pyrazoline scaffold generally enhance the electron density of the ring, which can increase the binding affinity of the compound towards the enzyme's active site. These groups typically favor interactions with the hydrophobic pockets of the enzyme, especially in hCA-I and hCA-II. For example, the methyl group at the *ortho* or *para* positions can enhance van der Waals interactions with amino acid residues such as Val121 and Phe131 in hCA-II, contributing to stronger binding. Docking studies reveal that EDGs may stabilize the compound within the active site by promoting favorable interactions with polar residues or water molecules near the zinc ion, leading to effective inhibition.

The presence of hydroxyl or amino groups increases the potential for hydrogen bonding with amino acids like Thr199 and His94 in hCA-II or His64 in hCA-I. Such groups often enhance the selectivity and potency of CAIs, as they can establish strong hydrogen bonds with the active site. In molecular docking simulations, hydroxyl groups frequently participate in forming stable hydrogen bonds with key active site residues, improving the inhibitor's binding stability. These interactions also contribute to the overall efficacy of the compounds.

7.1.2 Effect of electron-withdrawing groups (EWGs). EWGs like nitro ($-NO_2$) and halogens (chlorine, bromine, or fluorine) reduce the electron density of the pyrazoline scaffold, which can

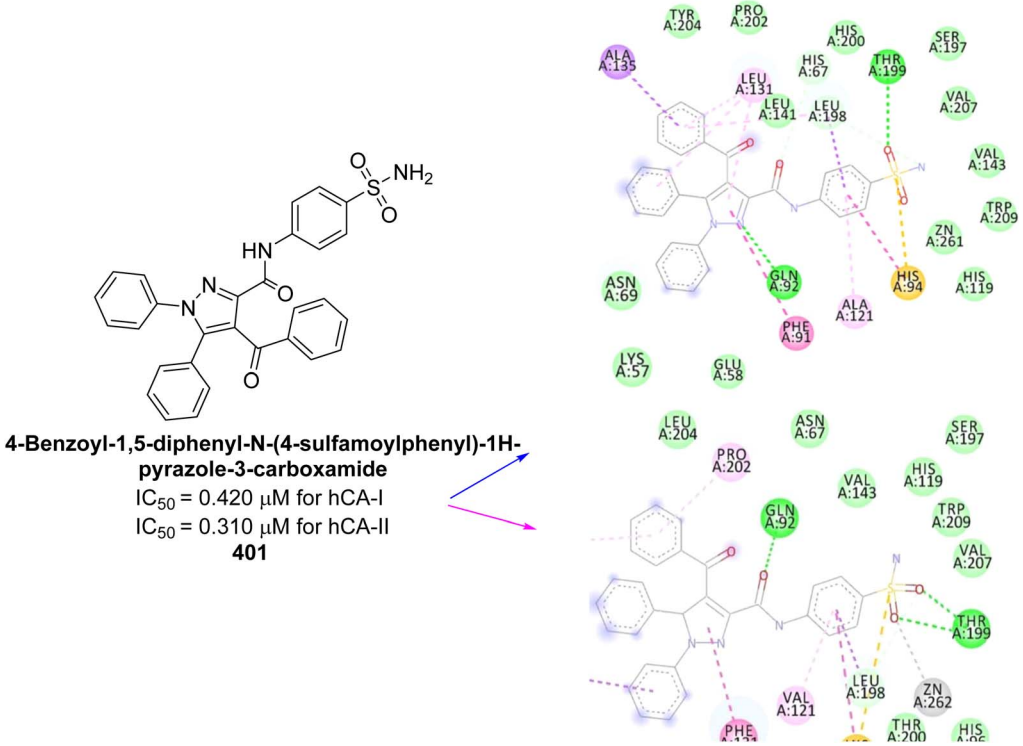

Fig. 143 Chemical structure of compound **401**; its IC_{50} values against hCA-I and II, and its docking images.

modulate the interaction between the compound and the enzyme. Halogen substituents, particularly fluorine, have been shown in docking studies to engage in halogen bonding with active site residues. For instance, halogen atoms can form interactions with residues like Thr199 or zinc-bound water molecules, stabilizing the compound in the active site and enhancing its inhibitory potency. Nitro groups, due to their strong electron-withdrawing nature, increase the affinity of the compound for the metal ion within the enzyme's catalytic pocket. Molecular docking studies reveal that the nitro group frequently participates in dipole–dipole interactions with residues like Glu106 or coordinates with the zinc ion, significantly increasing inhibition strength, particularly for hCA-IX and hCA-XII isoforms.

The carboxyl and sulfonamide groups are known to significantly improve binding affinity due to their ability to engage in both hydrogen bonding and ionic interactions with residues in the enzyme's active site. Sulfonamide derivatives are especially potent due to their ability to chelate the zinc ion, a key mechanism in CA inhibition. Molecular docking studies typically show that sulfonamide groups form strong coordinate bonds with the zinc ion, mimicking the interaction of classical CA inhibitors like AAZ. The sulfonamide group's interaction with the zinc ion is crucial for effective inhibition, especially for tumor-associated isoforms such as hCA-IX and XII.

7.1.3 Molecular docking studies. Molecular docking studies are instrumental in elucidating the interactions between pyrazoline-based CAIs and the enzyme's active site. These studies simulate how the inhibitor fits into the enzyme's active pocket, allowing for the analysis of key interactions such as hydrogen bonding, π–π stacking, van der Waals interactions, and coordination with the zinc ion.

7.1.3.1. Interaction with zinc ion. Most pyrazoline-based CAIs rely on functional groups such as sulfonamides or carboxylates to interact directly with the zinc ion in the active site. Docking studies frequently show that the sulfonamide moiety binds to the zinc ion *via* one of its oxygen atoms, displacing a water molecule and effectively inhibiting the enzyme's catalytic activity.

Compounds with carboxamide groups also demonstrate effective inhibition, with docking simulations revealing coordination between the carboxyl group and the zinc ion, enhancing the compound's inhibitory potency.

7.1.3.2. Hydrophobic interactions. Docking simulations illustrate that the hydrophobic interactions between EDGs like alkyl or alkoxy chains and hydrophobic residues (such as Val121, Leu198, and Phe131 in hCA-II) stabilize the pyrazoline scaffold within the active site. These interactions are particularly important for enhancing the selectivity of the compounds toward specific hCA isoforms. Pyrazoline derivatives with bulky substituents such as phenyl groups tend to occupy hydrophobic pockets within the enzyme, promoting favorable interactions that enhance the inhibitor's binding affinity and potency.

7.1.3.3. Hydrogen bonding. Hydrogen bonds formed between the inhibitor and active site residues are critical for stabilizing the inhibitor–enzyme complex. Pyrazoline CAIs with hydroxyl, amino, or carboxyl groups often form hydrogen bonds with residues such as Thr199, Glu106, or His94 in hCA-II. These

Table 14 Comparative analysis of heterocyclic scaffolds as CAIs

Compound no.	Chemical structure and IUPAC name	Isoform targeted, IC_{50} (μM)/K_i values (nM)							
		hCA-I	hCA-II	hCA-IV	hCA-VII	hCA-IX	hCA-XII	bCA-II	Ref.
1	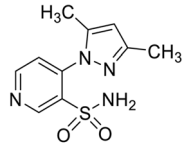 4-(3,5-Dimethyl-1*H*-pyrazol-1-yl) pyridine-3-sulfonamide	346	61.4	—	—	24.8	34.2	—	84
2	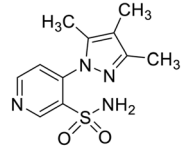 4-(3,4,5-Trimethyl-1*H*-pyrazol-1-yl) pyridine-3-sulfonamide	438	58.5	—	—	23.1	27.8	—	84
3	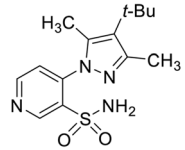 4-(*t*-Butyl-3,5-dimethyl-1*H*-pyrazol-1-yl) pyridine-3-sulfonamide	541	76.3	—	—	48.6	39.1	—	84
4	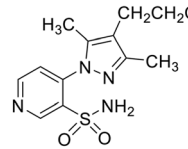 Ethyl 3-(3,5-dimethyl-1-(3-sulfamoyl pyridin-4-yl)-1*H*-pyrazol-4-yl)propanoate	397	134	—	—	19.5	22.6	—	84
5	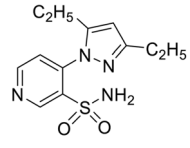 4-(3,5-Diethyl-1*H*-pyrazol-1-yl) pyridine-3-sulfonamide	278	87.1	—	—	31.7	16.8	—	84

Table 14 (*Contd.*)

Compound no.	Chemical structure and IUPAC name	Isoform targeted, IC_{50} (μM)/K_i values (nM)							Ref.
		hCA-I	hCA-II	hCA-IV	hCA-VII	hCA-IX	hCA-XII	bCA-II	
6	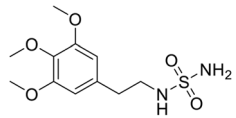 *N*-(3,4,5-Trimethoxyphenethyl) sulfamide	1.82	2.03	—	—	0.221	1.52	—	85
7	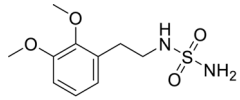 *N*-(2,3-Dimethoxyphenethyl) sulfamide	0.25	2.95	—	—	>50	0.047	—	85
8	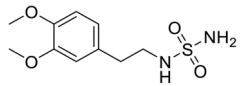 *N*-(3,4-Dimethoxyphenethyl) sulfamide	0.28	2.40	—	—	0.092	0.044	—	85
9	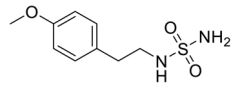 *N*-(4-Methoxyphenethyl) sulfamide	0.061	1.47	—	—	0.376	0.021	—	85
10	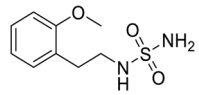 *N*-(2-Methoxyphenethyl) sulfamide	0.25	2.04	—	—	0.041	0.416	—	85
11	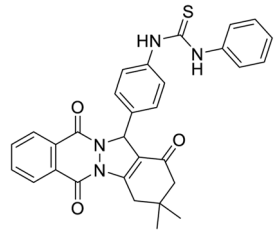 1-(4-(3,3-Dimethyl-1,6,11-trioxo-2,3,4,6,11,13-hexahydro-1*H*-indazolo[1,2-*b*]phthalazin-13-yl)phenyl)-3-phenylthiourea	IC_{50} = 6.40	IC_{50} = 6.13	—	—	—	—	—	86

Table 14 (*Contd.*)

Compound no.	Chemical structure and IUPAC name	Isoform targeted, IC_{50} (μM)/K_i values (nM)							Ref.
		hCA-I	hCA-II	hCA-IV	hCA-VII	hCA-IX	hCA-XII	bCA-II	
12	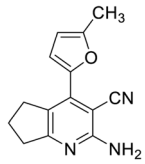 2-Amino-4-(5-methylfuran-2-yl)-6,7-dihydro-5*H*-cyclopenta[*b*] pyridine-3-carbonitrile	23.8	41	—	—	—	—	—	87
13	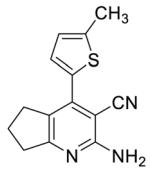 2-Amino-4-(5-methylthiophen-2-yl)-6,7-dihydro-5*H*-cyclopenta[*b*] pyridine-3-carbonitrile	31	182	—	—	—	—	—	87
14	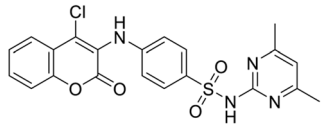 4-((4-Chloro-2-oxo-2*H*-chromen-3-yl)-methylene amino)-*N*-(4,6-dimethyl-pyrimidin-2-yl) benzenesulfonamide	—	23	—	—	—	124	—	88
15	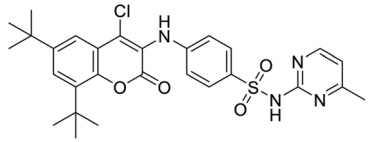 4-((6,8-Di-*tert*-butyl-4-chloro-2-oxo-2*H*-chromen-3-yl) methyleneamino)-*N*-(4-methylpyrimidin-2-yl) benzenesulfonamide	—	63	—	—	—	24	—	88

Table 14 (*Contd.*)

Compound no.	Chemical structure and IUPAC name	Isoform targeted, IC_{50} (μM)/K_i values (nM)							Ref.
		hCA-I	hCA-II	hCA-IV	hCA-VII	hCA-IX	hCA-XII	bCA-II	
16	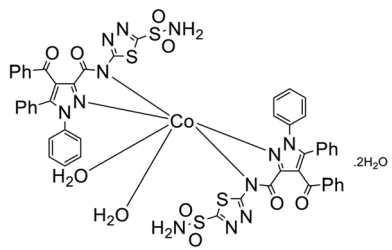 (Diaquabis (4-benzoyl-1,5-diphenyl-*N*-(5-sulfamoyl-1,3,4-thiadiazol-2-yl)-1*H*-pyrazole-3-carboxamide)cobalt(II) dihydrate	$IC_{50} = 0.058$	$IC_{50} = 0.110$	—	—	—	—	—	89
17	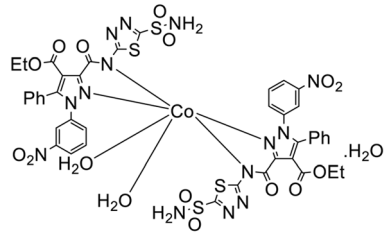 (Diaquabis(ethyl-1-(3-nitrophenyl)-5-phenyl-3-(5-sulfamoyl-1,3,4-thiadiazol-2-ylcarbamoyl)-1*H*-pyrazole-4-carboxylate)cobalt(II) monohydrate	$IC_{50} = 0.297$	$IC_{50} = 0.052$	—	—	—	—	—	89
18	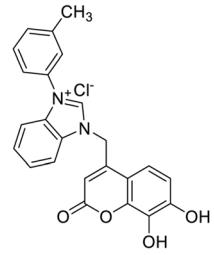 1-((7,8-Dihydroxy-2-oxo-2*H*-chromen-4-yl)methyl)-3-(*m*-tolyl)-1*H*-benzo[*d*]imidazol-3-ium chloride	$IC_{50} = 22.1$	$IC_{50} = 28.9$	—	—	—	—	—	90

Table 14 (*Contd.*)

Compound no.	Chemical structure and IUPAC name	Isoform targeted, IC_{50} (μM)/K_i values (nM)							Ref.
		hCA-I	hCA-II	hCA-IV	hCA-VII	hCA-IX	hCA-XII	bCA-II	
19	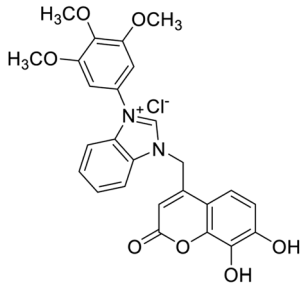 1-((7,8-Dihydroxy-2-oxo-2*H*-chromen-4-yl)methyl)-3-(3,4,5-trimethoxyphenyl)-1*H*-benzo[*d*]imidazol-3-ium chloride	IC_{50} = 33.1	IC_{50} = 23.3	—	—	—	—	—	90
20	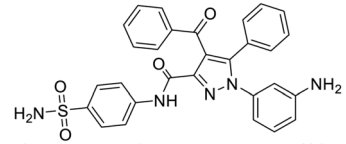 1-(3-Aminophenyl)-4-benzoyl-5-phenyl-*N*-(4-sulfamoylphenyl)-1*H*-pyrazole-3-carboxamide	0.108	0.055	—	—	—	—	—	91
21	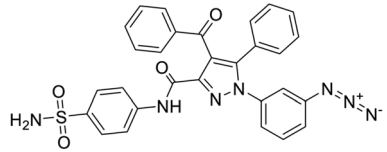 1-(3-Azidophenyl)-4-benzoyl-5-phenyl-*N*-(4-sulfamoylphenyl)-1*H*-pyrazole-3-carboxamide	0.129	0.064	—	—	—	—	—	91
22	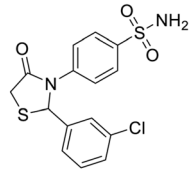 4-(2-(3-Chlorophenyl)-4-oxothiazolidin-3-yl) benzenesulfonamide	—	—	—	—	2.2	—	—	92

Table 14 (*Contd.*)

Compound no.	Chemical structure and IUPAC name	Isoform targeted, IC_{50} (μM)/K_i values (nM)							Ref.
		hCA-I	hCA-II	hCA-IV	hCA-VII	hCA-IX	hCA-XII	bCA-II	
23	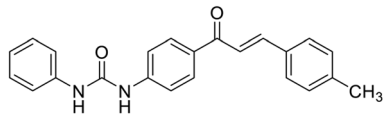 1-Phenyl-3-(4-(3-(*p*-tolyl)acryloyl)phenyl)urea	$IC_{50} = 25.4$	$IC_{50} = 27.2$	—	—	—	—	—	93
24	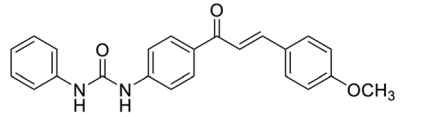 1-(4-(3-(4-Methoxyphenyl)acryloyl)phenyl)-3-phenylurea	$IC_{50} = 23.1$	$IC_{50} = 19.4$	—	—	—	—	—	93
25	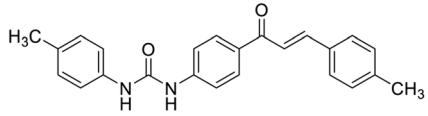 1-(*p*-Tolyl)-3-(4-(3-(*p*-tolyl)acryloyl)phenyl)urea	$IC_{50} = 27.9$	$IC_{50} = 14.4$	—	—	—	—	—	93
26	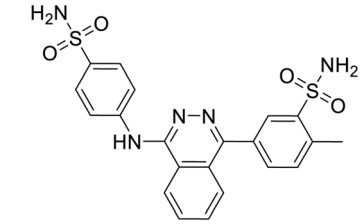 2-Methyl-5-(4-((4-sulfamoylphenyl)amino) phthalazin-1-yl)benzenesulfonamide	—	—	—	—	0.48	—	—	94
27	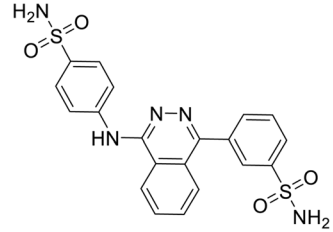 3-(4-((4-Sulfamoylphenyl)amino) phthalazin-1-yl)benzenesulfonamide	—	—	—	—	18.5	—	—	94

Table 14 (*Contd.*)

Compound no.	Chemical structure and IUPAC name	Isoform targeted, IC_{50} (μM)/K_i values (nM)							Ref.
		hCA-I	hCA-II	hCA-IV	hCA-VII	hCA-IX	hCA-XII	bCA-II	
28	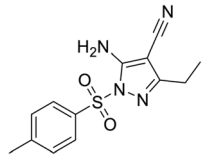 5-Amino-3-ethyl-1-(*p*-tosyl)-1*H*-pyrazole-4-carbonitrile	—	—	—	—	0.47	0.15	—	95
29	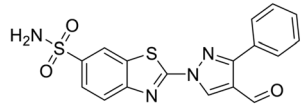 2-(4-Formyl-3-phenyl-1*H*-pyrazol-1-yl)-1,3-benzothiazole-6-sulfonamide	8806	10.9	—	—	1747	214	—	96
30	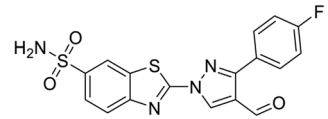 2-[3-(4-Fluorophenyl)-4-formyl-1*H*-pyrazol-1-yl]-1,3-benzothiazole-6-sulfonamide	15 690	10.4	—	—	1022	>10 000	—	96
31	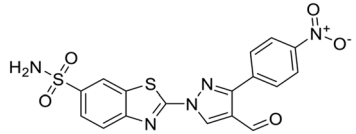 2-[4-Formyl-3-(4-nitrophenyl)-1*H*-pyrazol-1-yl]-1,3-benzothiazole-6-sulfonamide	2331	3.8	—	—	2109	74.5	—	96
32	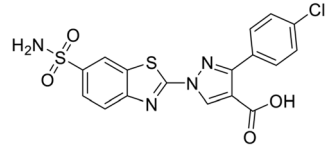 1-[6-(Aminosulfonyl)-1,3-benzothiazol-2-yl]-3-(4-chlorophenyl)-1*H*-pyrazole-4-carboxylic acid	407	7.3	—	—	2.8	5.5	—	96
33	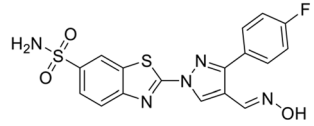 2-{3-(4-Fluorophenyl)-4-[(hydroxyimino)methyl]-1*H*-pyrazol-1-yl}-1,3-benzothiazole-6-sulfonamide	7161	8.5	—	—	224	83.8	—	96

Table 14 (*Contd.*)

Compound no.	Chemical structure and IUPAC name	Isoform targeted, IC_{50} (μM)/K_i values (nM)							Ref.
		hCA-I	hCA-II	hCA-IV	hCA-VII	hCA-IX	hCA-XII	bCA-II	
34	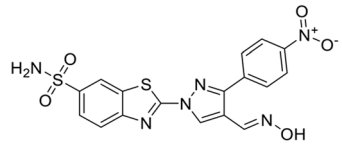 2-[4-[(Hydroxyimino)methyl]-3-(4-nitrophenyl)-1*H*-pyrazol-1-yl]-1,3-benzothiazole-6-sulfonamide	23 102	11.6	—	—	119	96.8	—	96
35	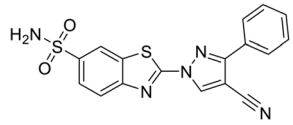 2-(4-Cyano-3-phenyl-1*H*-pyrazol-1-yl)-1,3-benzothiazole-6-sulfonamide	9819	139	—	—	81.6	6.6	—	96
36	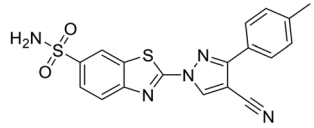 2-(4-Cyano-3-(4-methylphenyl)-1*H*-pyrazol-1-yl)-1,3-benzothiazole-6-sulfonamide	>50 000	48.1	—	—	186	7.2	—	96
37	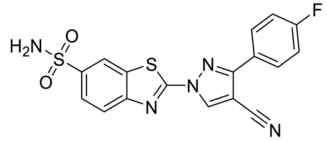 2-[4-Cyano-3-(4-fluorophenyl)-1*H*-pyrazol-1-yl]-1,3-benzothiazole-6-sulfonamide	12 108	27	—	—	739	7.4	—	96
38	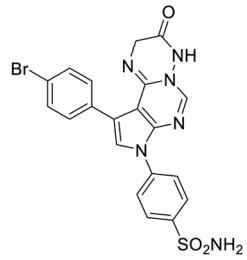 4-(10-(4-Bromophenyl)-3-oxo-3,4-dihydropyrrolo[2',3':4,5]pyrimido[1,6-*b*][1,2,4]triazin-8(2*H*)-yl) benzenesulfonamide	94.1	4.9	—	—	11.7	0.76	—	97

Table 14 (*Contd.*)

Compound no.	Chemical structure and IUPAC name	Isoform targeted, IC_{50} (μM)/K_i values (nM)							Ref.
		hCA-I	hCA-II	hCA-IV	hCA-VII	hCA-IX	hCA-XII	bCA-II	
39	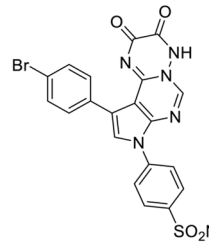 4-(10-(4-Bromophenyl)-2,3-dioxo-3,4-dihydropyrrolo [2',3':4,5]pyrimido[1,6-*b*][1,2,4]triazin-8(2*H*)-yl) benzenesulfonamide	69.1	64.3	—	—	325	0.912	—	97
40	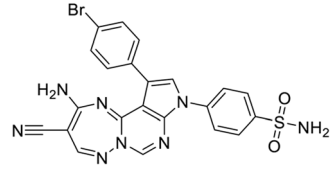 *p*-{13-Amino-3-(*p*-bromophenyl)-12-cyano-5,7,9,10,14-pentazatricyclo-[7.5.-0-.02,6]-tetradeca-1(14),2(6),3,7,10,12-hexaen-5-yl}benzenesulfonamide	80.4	5.2	—	—	3.1	0.9	—	97
41	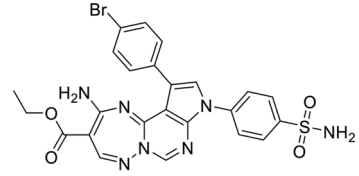 *p*-{13-Amino-3-(*p*-bromophenyl)-12-ethoxycarbonyl-5,7,9,10,14-pentazatricyclo [7.5.0.02,6]tetradeca-1(14),2(6),3,7, 10,12-hexaen-5-yl}benzenesulfonamide	126	7.3	—	—	3	0.83	—	97
42	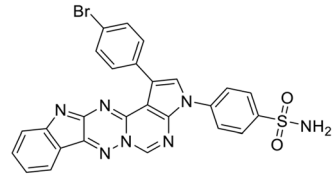 *p*-{5-(*p*-Bromophenyl)-2,7,9,11,12,20-hexazapenta cyclo-[11.7.0.03,11.04,8.014,19]-icosa-1(20), 2,4(8),5,9,12,14(19),15,17-nonaen-7-yl} benzenesulfonamide	498	8.5	—	—	2.7	0.72	—	97

Table 14 (*Contd.*)

Compound no.	Chemical structure and IUPAC name	Isoform targeted, IC_{50} (μM)/K_i values (nM)							Ref.
		hCA-I	hCA-II	hCA-IV	hCA-VII	hCA-IX	hCA-XII	bCA-II	
43	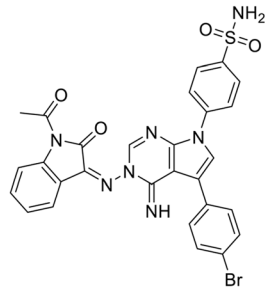 4-(3-(1-Acetyl-2-oxoindolin-3-ylideneamino)-5-(4-bromophenyl)-4-imino-3,4-dihydropyrrolo[2,3-*d*]pyrimidin-7-yl)benzenesulfonamide	25.1	5.6	—	—	3.1	0.81	—	97
44	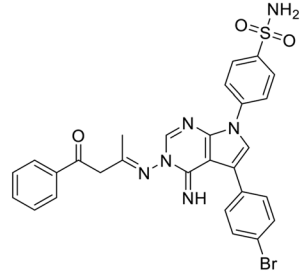 4-(5-(4-Bromophenyl)-4-imino-3-(4-oxo-4-phenylbutan-2-ylidene-amino)-3,4-dihydropyrrolo[2,3-*d*]pyrimidin-7-yl)benzenesulfonamide	16.3	3.9	—	—	2.8	0.94	—	97
45	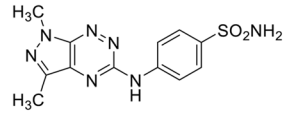 4-((1,3-Dimethyl-1*H*-pyrazolo[4,3-*e*][1,2,4]triazin-5-yl)amino)benzenesulfonamide	270	8	—	—	43.8	7.9	—	98
46	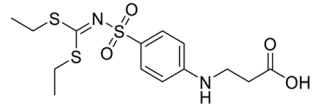 3-[(4-{[Bis(ethylthio)methylene]sulfamoyl}phenyl)amino]propanoic acid	—	40	—	—	—	>200	—	99

Table 14 (*Contd.*)

Compound no.	Chemical structure and IUPAC name	Isoform targeted, IC_{50} (μM)/K_i values (nM)							
		hCA-I	hCA-II	hCA-IV	hCA-VII	hCA-IX	hCA-XII	bCA-II	Ref.
47	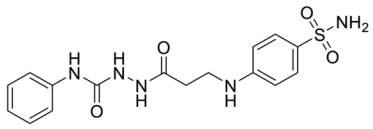 *N*-[(Phenylcarbamoyl)amino]-3-[(4-sulfamoyl phenyl)amino]propanamide	—	4.0	—	—	—	1.85	—	99
48	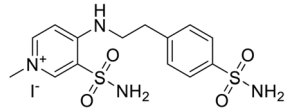 3-Sulfamoyl-4-[2-(4-sulfamoylphenyl) ethylamino]-1-methylpyridinium iodide	923	61.3	—	—	5.9	4.3	—	100
49	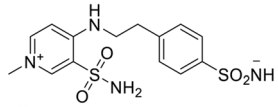 ((4-(2-((1-Methyl-3-sulfamoylpyridin-1-ium-4-yl)amino)ethyl)phenyl)sulfonyl)amide	887	60.1	—	—	6.2	4.0	—	100
50	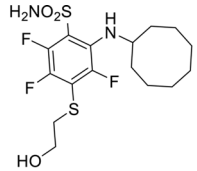 2-(Cyclooctyl-λ^4-azaneyl)-3,5,6-trifluoro-4-((2-hydroxyethyl)thio)benzenesulfonamide	—	—	—	—	—	1.1	—	101
51	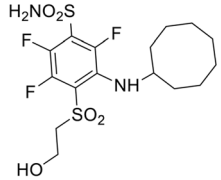 3-(Cyclooctylamino)-2,5,6-trifluoro-4-((2-hydroxyethyl)sulfonyl)benzenesulfonamide	—	—	—	—	—	0.05	—	101
52	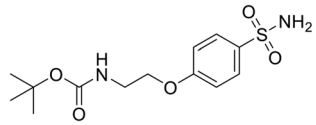 *tert*-Butyl 2-(4-sulfamoylphenoxy)-ethylcarbamate	5.3	5.0	—	—	8.3	7.2	—	102

Table 14 (*Contd.*)

Compound no.	Chemical structure and IUPAC name	Isoform targeted, IC_{50} (μM)/K_i values (nM)							Ref.
		hCA-I	hCA-II	hCA-IV	hCA-VII	hCA-IX	hCA-XII	bCA-II	
53	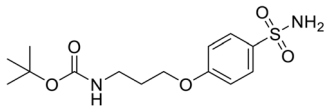 *tert*-Butyl 3-(4-sulfamoylphenoxy)-propylcarbamate	6.6	5.1	—	—	5.8	6.5	—	102
54	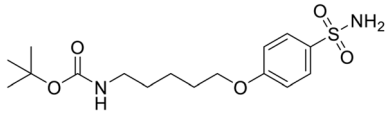 *tert*-Butyl 5-(4-sulfamoylphenoxy)-pentylcarbamate	7.9	5.5	—	—	7.1	5.7	—	102
55	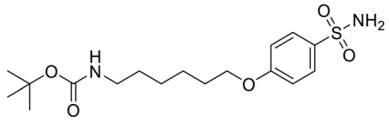 *tert*-Butyl 6-(4-sulfamoylphenoxy)-hexylcarbamate	6.1	5.2	—	—	6.9	6.4	—	102
56	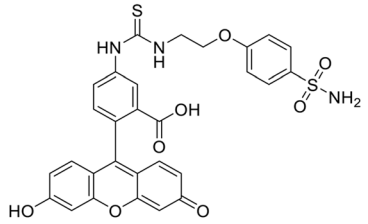 2-(6-Hydroxy-3-oxo-3*H*-xanthen-9-yl)-5-{3-[2-(4-sulfamoylphenoxy)-ethyl]-thioureido}-benzoic acid	18.0	5.0	—	—	8.5	8.6	—	102
57	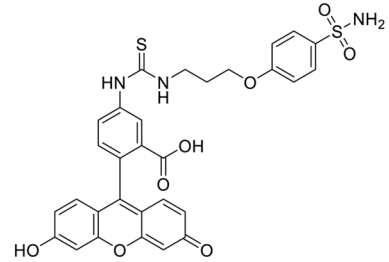 2-(6-Hydroxy-3-oxo-3*H*-xanthen-9-yl)-5-{3-[3-(4-sulfamoylphenoxy)-propyl]-thioureido}-benzoic acid	17.1	4.6	—	—	7.2	5.7	—	102

Table 14 (*Contd.*)

Compound no.	Chemical structure and IUPAC name	Isoform targeted, IC_{50} (μM)/K_i values (nM)							Ref.
		hCA-I	hCA-II	hCA-IV	hCA-VII	hCA-IX	hCA-XII	bCA-II	
58	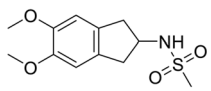 *N*-(5,6-Dimethoxy-2,3-dihydro-1*H*-inden-2-yl)methanesulfonamide	46	372	—	—	—	—	—	103
59	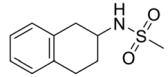 *N*-(1,2,3,4-Tetrahydronaphthalene-2-yl) methanesulfonamide	228	94	—	—	—	—	—	103
60	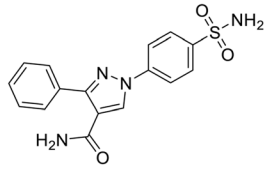 1-[4-(Aminosulfonyl)phenyl]-3-phenyl-1*H*-pyrazole-4-carboxamide	—	—	—	—	4.3	2.7	—	104
61	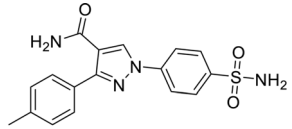 1-[4-(Aminosulfonyl)phenyl]-3-(4-methyl phenyl)-1*H*-pyrazole-4-carboxamide	—	—	—	—	4.2	3.1	—	104
62	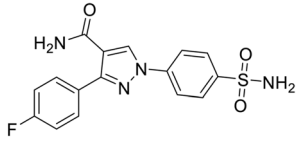 1-[4-(Aminosulfonyl)phenyl]-3-(4-fluoro phenyl)-1*H*-pyrazole-4-carboxamide	—	—	—	—	5.0	4.5	—	104
63	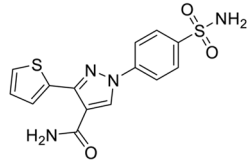 1-[4-(Aminosulfonyl)phenyl]-3-(2-thienyl)-1*H*-pyrazole-4-carboxamide	—	—	—	—	5.2	4.7	—	104

Table 14 (*Contd.*)

Compound no.	Chemical structure and IUPAC name	Isoform targeted, IC_{50} (μM)/K_i values (nM)							Ref.
		hCA-I	hCA-II	hCA-IV	hCA-VII	hCA-IX	hCA-XII	bCA-II	
64	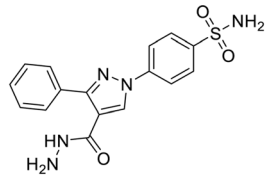 4-[4-(Hydrazinocarbonyl)-3-phenyl-1*H*-pyrazole-1-yl]benzenesulfonamide	—	—	—	—	2.3	1.9	—	104
65	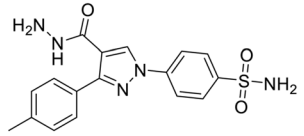 4-[4-(Hydrazinocarbonyl)-3-(4-methylphenyl)-1*H*-pyrazole-1-yl]benzenesulfonamide	—	—	—	—	2.8	12.9	—	104
66	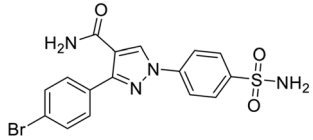 1-[4-(Aminosulfonyl)phenyl]-3-(4-bromophenyl)-1*H*-pyrazole-4-carboxamide	—	—	—	—	2.0	10.4	—	104
67	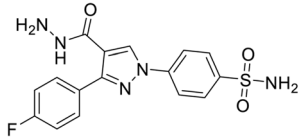 4-[3-(4-Fluorophenyl)-4-(hydrazinocarbonyl)-1*H*-pyrazole-1-yl]benzenesulfonamide	—	—	—	—	2.1	3.9	—	104
68	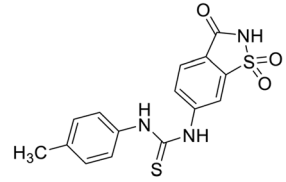 1-(1,1-Dioxido-3-oxo-2,3-dihydrobenzo[*d*]isothiazol-6-yl)-3-(*p*-tolyl)thiourea	IC_{50} = 13.67	IC_{50} = 11.54	—	—	—	—	—	105

Table 14 (*Contd.*)

Compound no.	Chemical structure and IUPAC name	Isoform targeted, IC_{50} (μM)/K_i values (nM)							Ref.
		hCA-I	hCA-II	hCA-IV	hCA-VII	hCA-IX	hCA-XII	bCA-II	
69	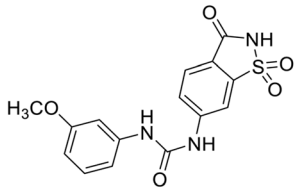 1-(1,1-Dioxido-3-oxo-2,3-dihydrobenzo[*d*]isothiazol-6-yl)-3-(3-methoxyphenyl)urea	IC_{50} = 41.67	IC_{50} = 6.54	—	—	—	—	—	105
70	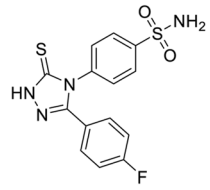 4-[3-(4-Fluorophenyl)-5-thioxo-1,5-dihydro-4*H*-1,2,4-triazol-4-yl]benzenesulfonamide	—	—	—	—	2.8	4.9	—	106
71	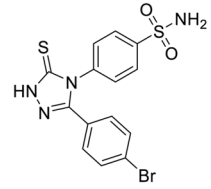 4-[3-(4-Bromophenyl)-5-thioxo-1,5-dihydro-4*H*-1,2,4-triazol-4-yl]benzenesulfonamide	—	—	—	—	7.6	1.3	—	106
72	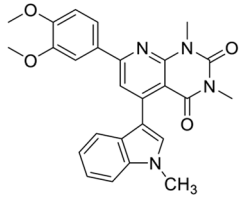 7-(3,4-Dimethoxyphenyl)-1,3-dimethyl-5-(1-methyl-1*H*-indol-3-yl)pyrido[2,3-*d*]pyrimidine-2,4(1*H*,3*H*)-dione	IC_{50} = 6.79	IC_{50} = 8.06	—	—	—	—	—	107

Table 14 (*Contd.*)

Compound no.	Chemical structure and IUPAC name	Isoform targeted, IC_{50} (μM)/K_i values (nM)							Ref.
		hCA-I	hCA-II	hCA-IV	hCA-VII	hCA-IX	hCA-XII	bCA-II	
73	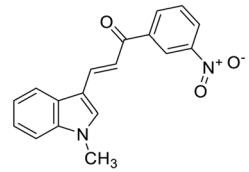 3-(1-Methyl-1*H*-indol-3-yl)-1-(3-nitrophenyl) prop-2-en-1-one	$IC_{50} = 8.38$	$IC_{50} = 7.22$	—	—	—	—	—	107
74	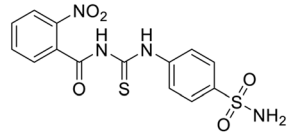 2-Nitro-*N*-((4-sulfamoylphenyl)carbamothioyl) benzamide	—	—	—	—	—	—	$IC_{50} = 0.261$	108
75	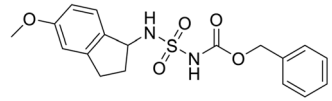 Benzyl *N*-(5-methoxy-2,3-dihydro-1*H*-inden-1-yl)sulfamoylcarbamate	153	306	—	—	—	—	—	109
76	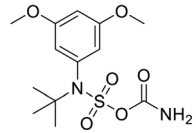 *t*-Butyl-*N*-(3,5-dimethoxyphenyl) sulfamoylcarbamate	262	117	—	—	—	—	—	109
77	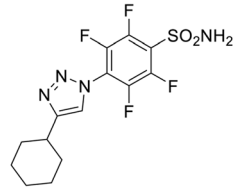 4-(4-Cyclohexyl-1*H*-1,2,3-triazol-1-yl)-2,3,5,6-tetrafluorobenzenesulfonamide	—	—	—	—	1.5	0.8	—	110

Table 14 (*Contd.*)

Compound no.	Chemical structure and IUPAC name	Isoform targeted, IC_{50} (μM)/K_i values (nM)							Ref.
		hCA-I	hCA-II	hCA-IV	hCA-VII	hCA-IX	hCA-XII	bCA-II	
78	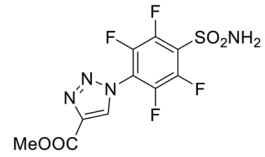 Methyl 1-(2,3,5,6-tetrafluoro-4-sulfamoyl phenyl)-1*H*-1,2,3-triazole-4-carboxylate	—	—	—	—	115	58.9	—	110
79	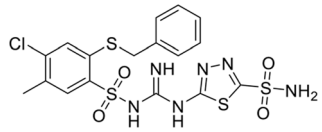 1-(2-Benzylthio-4-chloro-5-methylbenzenesulfonyl)-3-(2-sulfamoyl-1,3,4-thiadiazol-5-yl)guanidine	—	—	—	—	4.7	0.96	—	111
80	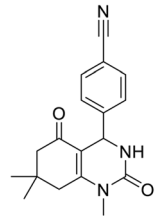 4-(1,7,7-Trimethyl-2,5-dioxo-1,2,3,4,5,6,7,8-octahydroquinazoline-4-yl)benzonitrile	$IC_{50} = 0.05$	—	—	—	—	—	—	112
81	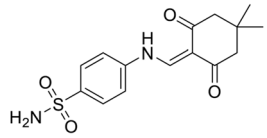 4-((4,4-Dimethyl-2,6-dioxocyclohexylidene) methylamino)benzene-sulfonamide	$IC_{50} = 2.12$	$IC_{50} = 6.41$	—	—	—	—	—	113
82	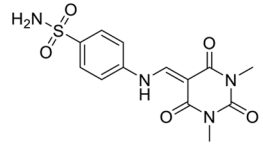 4-((1,3-Dimethyl-2,4,6-trioxo-tetrahydropyrimidin-5(6*H*)-ylidene)methylamino)benzene-sulfonamide	$IC_{50} = 5.20$	$IC_{50} = 2.52$	—	—	—	—	—	113

Table 14 (*Contd.*)

Compound no.	Chemical structure and IUPAC name	Isoform targeted, IC_{50} (μM)/K_i values (nM)							Ref.
		hCA-I	hCA-II	hCA-IV	hCA-VII	hCA-IX	hCA-XII	bCA-II	
83	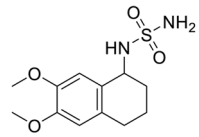 *N*-(6,7-Dimethoxy-1,2,3,4-tetrahydro naphthalen-1-yl)-sulphamide	0.71	0.69	—	—	—	—	—	114
84	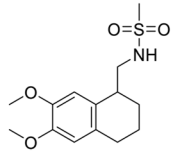 *N*-((6,7-Dimethoxy-1,2,3,4-tetrahydro naphthalen-1-yl)-methyl)methanesulphonamide	1.56	0.39	—	—	—	—	—	114
85	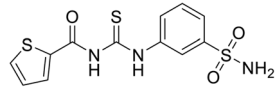 1-(2-Thienylcarbonyl)-3-(3-amino sulfonylphenyl)thiourea	—	—	—	—	—	—	$IC_{50} = 0.052$	115
86	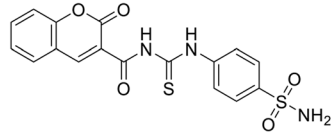 1-(-Oxo-2*H*-chromene-3-carbonyl)-3-(4-aminosulfonylphenyl)thiourea	—	—	—	—	—	—	$IC_{50} = 0.011$	115
87	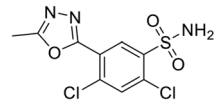 2,4-Dichloro-5-(5-methyl-1,3,4-oxadiazol-2-yl) benzenesulfonamide	718	8.7	—	—	2.8	6.3	—	116
88	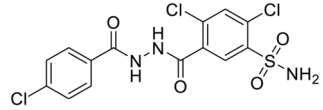 2,4-Dichloro-5-[2-(4-chlorobenzoyl)hydrazine carbonyl]benzenesulfonamide	3025	10.5	—	—	4.8	2.7	—	116

Table 14 (*Contd.*)

Compound no.	Chemical structure and IUPAC name	Isoform targeted, IC_{50} (μM)/K_i values (nM)							Ref.
		hCA-I	hCA-II	hCA-IV	hCA-VII	hCA-IX	hCA-XII	bCA-II	
89	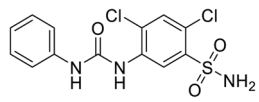 2,4-Dichloro-5-(3-phenylureido) benzenesulfonamide	2340	44	—	—	7.0	2.8	—	116
90	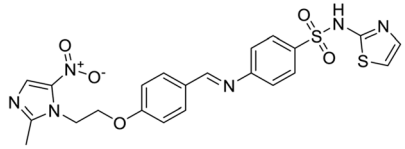 4-(4-(2-(2-Methyl-5-nitro-1*H*-imidazole-1-yl) ethoxy)benzylideneamino)-*N*-(thiazol-2-yl) benzenesulfonamide	—	16	—	—	93	—	—	117
91	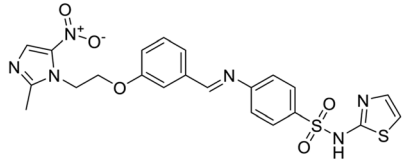 4-(3-(2-(2-Methyl-5-nitro-1*H*-imidazole-1-yl)ethoxy)benzylideneamino)-*N*-(thiazol-2-yl)benzenesulfonamide	—	89	—	—	38	—	—	117
92	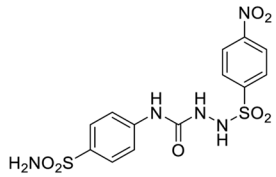 2-((4-Nitrophenyl)sulfonyl)-*N*-(4-sulfamoyl phenyl)hydrazine-1-carboxamide	—	6.0	—	—	0.79	—	—	118
93	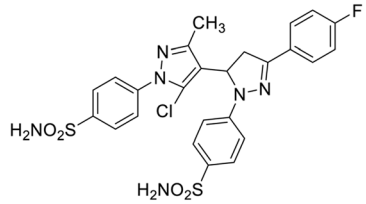 4,4'-(5'-Chloro-5-(4-fluorophenyl)-3'-methyl-3,4-dihydro-1'*H*,2*H*-[3,4'-bipyrazole]-1',2-diyl) dibenzenesulfonamide	1.4	—	—	3.0	—	—	—	119

Table 14 (*Contd.*)

Compound no.	Chemical structure and IUPAC name	Isoform targeted, IC_{50} (μM)/K_i values (nM)							Ref.
		hCA-I	hCA-II	hCA-IV	hCA-VII	hCA-IX	hCA-XII	bCA-II	
94	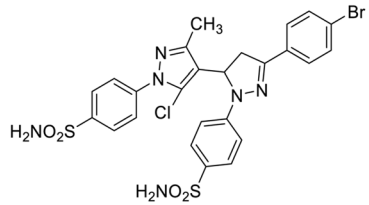 4,4'-(5-(4-Bromophenyl)-5'-chloro-3'-methyl-3,4-dihydro-1'*H*,2*H*-[3,4'-bipyrazole]-1',2-diyl) dibenzenesulfonamide	5.5	—	—	0.47	—	—	—	119
95	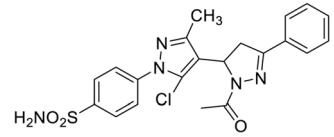 4-(2-Acetyl-5'-chloro-3'-methyl-5-phenyl-3,4-dihydro-1'*H*,2*H*-[3,4'-bipyrazol]-1'-yl) benzenesulfonamide	0.17	—	—	0.58	—	—	—	119
96	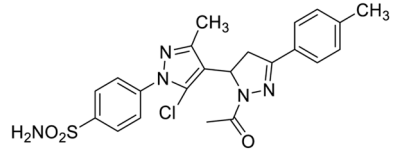 4-(2-Acetyl-5'-chloro-3'-methyl-5-(*p*-tolyl)-3,4-dihydro-1'*H*,2*H*-[3,4'-bipyrazol]-1'-yl) benzenesulfonamide	0.54	—	—	4.0	—	—	—	119
97	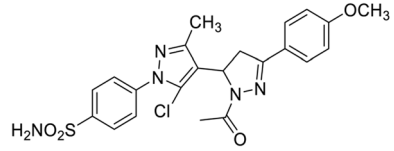 4-(2-Acetyl-5'-chloro-5-(4-methoxyphenyl)-3'-methyl-3,4-dihydro-1'*H*,2*H*-[3,4'-bipyrazol] -1'-yl)benzenesulfonamide	1.1	—	—	0.54	—	—	—	119
98	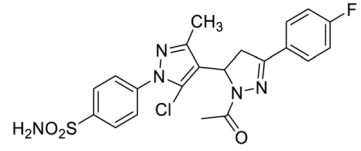 4-(2-Acetyl-5'-chloro-5-(4-fluorophenyl)-3'-methyl-3,4-dihydro-1'*H*,2*H*-[3,4'-bipyrazol]-1'-yl) benzenesulfonamide	1.7	—	—	0.57	—	—	—	119

Table 14 (*Contd.*)

Compound no.	Chemical structure and IUPAC name	Isoform targeted, IC_{50} (μM)/K_i values (nM)							Ref.
		hCA-I	hCA-II	hCA-IV	hCA-VII	hCA-IX	hCA-XII	bCA-II	
99	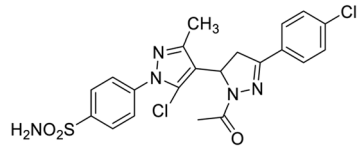 4-(2-Acetyl-5'-chloro-5-(4-chlorophenyl)-3'-methyl-3,4-dihydro-1'*H*,2*H*-[3,4'-bipyrazol]-1'-yl) benzenesulfonamide	0.26	—	—	3.9	—	—	—	119
100	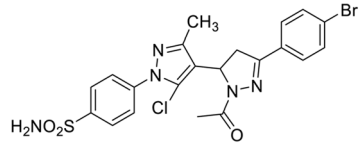 4-(2-Acetyl-5-(4-bromophenyl)-5'-chloro-3'-methyl-3,4-dihydro-1'*H*,2*H*-[3,4'-bipyrazol]-1'-yl) benzenesulfonamide	0.30	—	—	5.1	—	—	—	119
101	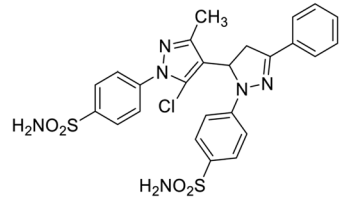 4,4'-(5'-Chloro-3'-methyl-5-phenyl-3,4-dihydro-1'*H*,2*H*-[3,4'-bipyrazole]-1',2-diyl) dibenzenesulfonamide	10.9	—	—	9.4	—	—	—	119
102	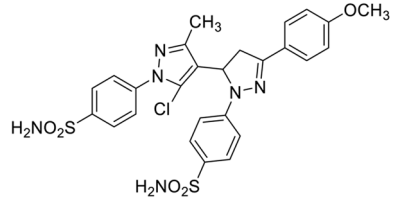 4,4'-(5'-Chloro-5-(4-methoxyphenyl)-3'-methyl-3,4-dihydro-1'*H*,2*H*-[3,4'-bipyrazole]-1',2-diyl) dibenzenesulfonamide	1.5	—	—	5.9	—	—	—	119

Table 14 (*Contd.*)

Compound no.	Chemical structure and IUPAC name	Isoform targeted, IC_{50} (μM)/K_i values (nM)							Ref.
		hCA-I	hCA-II	hCA-IV	hCA-VII	hCA-IX	hCA-XII	bCA-II	
103	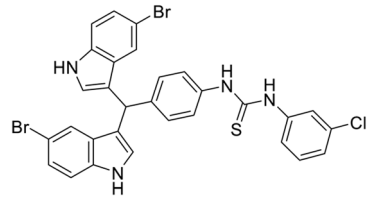 1-(4-(Bis(5-bromo-1*H*-indol-3-yl)methyl)phenyl)-3-(3-chlorophenyl)thiourea	—	IC_{50} = 42.9	—	—	—	—	—	120
104	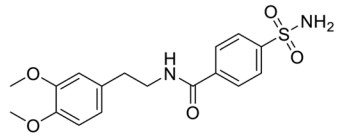 *N*-(3,4-Dimethoxyphenethyl)-4-sulfamoylbenzamide	—	—	—	—	3.8	—	—	121
105	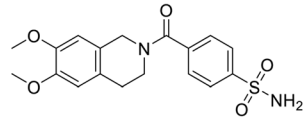 4-[(6,7-Dimethoxy-3,4-dihydroisoquinolin-2(1*H*)-yl)carbonyl]benzenesulfonamide	—	—	—	—	6.1	—	—	121
106	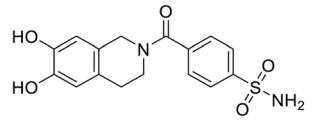 4-[(6,7-Dihydroxy-3,4-dihydroisoquinolin-2(1*H*)-yl)carbonyl]benzenesulfonamide	—	—	—	—	5.01	—	—	121
107	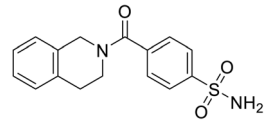 4-(3,4-Dihydroisoquinolin-2(1*H*)-ylcarbonyl)benzenesulfonamide	—	—	—	—	7.5	—	—	121
108	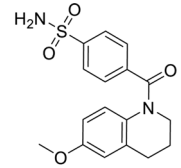 4-[(6-Methoxy-3,4-dihydroquinolin-1(2*H*)-yl)carbonyl]benzenesulfonamide	—	—	—	—	6.5	—	—	121

Table 14 (*Contd.*)

Compound no.	Chemical structure and IUPAC name	Isoform targeted, IC_{50} (μM)/K_i values (nM)							Ref.
		hCA-I	hCA-II	hCA-IV	hCA-VII	hCA-IX	hCA-XII	bCA-II	
109	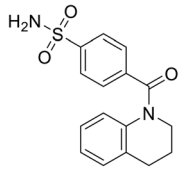 4-(3,4-Dihydroquinolin-1(2*H*)-yl carbonyl)benzenesulfonamide	—	—	—	—	9.4	—	—	121
110	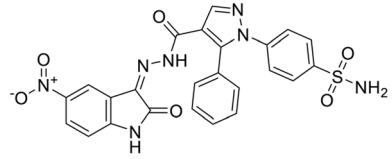 4-(4-(2-(5-Nitro-2-oxoindolin-3-ylidene)hydrazine-1-carbonyl)-5-phenyl-1*H*-pyrazol-1-yl)benzenesulfonamide	—	—	—	—	—	3.7	—	122
111	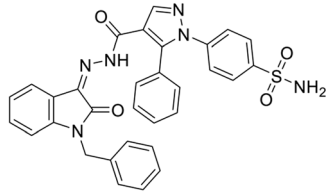 4-(4-(2-(1-Benzyl-2-oxoindolin-3-ylidene)hydrazine-1-carbonyl)-5-phenyl-1*H*-pyrazol-1-yl)benzenesulfonamide	—	—	—	—	—	6.5	—	122
112	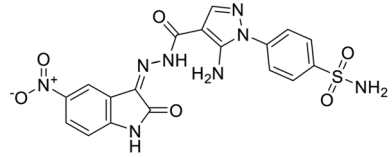 4-(5-Amino-4-(2-(5-Nitro-2-oxoindolin-3-ylidene)hydrazine-1-carbonyl)-1*H*-pyrazol-1-yl)benzenesulfonamide	—	—	—	—	—	5.4	—	122

Table 14 (*Contd.*)

Compound no.	Chemical structure and IUPAC name	Isoform targeted, IC_{50} (μM)/K_i values (nM)							Ref.
		hCA-I	hCA-II	hCA-IV	hCA-VII	hCA-IX	hCA-XII	bCA-II	
113	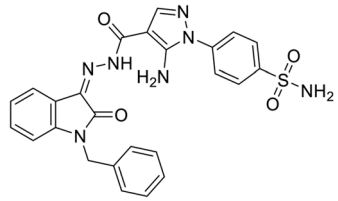 4-(5-Amino-4-(2-(1-benzyl-2-oxoindolin-3-ylidene)hydrazine-1-carbonyl)-1*H*-pyrazol-1-yl)benzenesulfonamide	—	—	—	—	—	7.2	—	122
114	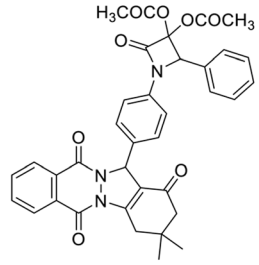 1-(4-(3,3-Dimethyl-1,6,11-trioxo-2,3,4,6,11,13-hexahydro-1*H*-indazolo[1,2-*b*]phthalazin-13-yl)phenyl)-2-oxo-4-phenylazetidine-3,3-diyl diacetate	IC_{50} = 6.97	IC_{50} = 8.48	—	—	—	—	—	123
115	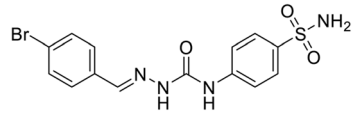 2-(4-Bromobenzylidene)-*N*-(4-sulfamoyl phenyl)hydrazinecarboxamide	95.2	6.2	—	—	90.4	92.3	—	124
116	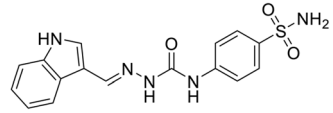 2-((1*H*-Indol-3-yl)methylene)-*N*-(4-sulfamoyl phenyl)hydrazinecarboxamide	71.2	4.0	—	—	103	63.1	—	124
117	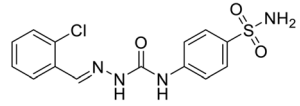 2-(2-Chlorobenzylidene)-*N*-(4-sulfamoyl phenyl)hydrazinecarboxamide	77.6	4.2	—	—	213	42.3	—	124

Table 14 (*Contd.*)

Compound no.	Chemical structure and IUPAC name	Isoform targeted, IC_{50} (μM)/K_i values (nM)							Ref.
		hCA-I	hCA-II	hCA-IV	hCA-VII	hCA-IX	hCA-XII	bCA-II	
118	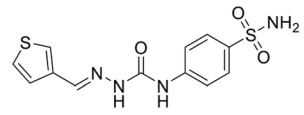 *N*-(4-Sulfamoylphenyl)-2-(thiophen-3-ylmethylene) hydrazine-1-carboxamide	79.3	4.6	—	—	395	23.8	—	124
119	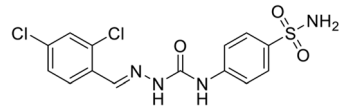 2-(2,4-Dichlorobenzylidene)-*N*-(4-sulfamoyl phenyl)hydrazinecarboxamide	6530	75.0	—	—	98.1	90.7	—	124
120	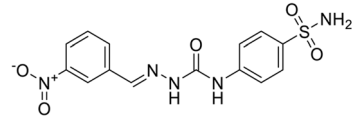 2-(3-Nitrobenzylidene)-*N*-(4-sulfamoyl phenyl)hydrazinecarboxamide	4930	51.6	—	—	415	83.9	—	124
121	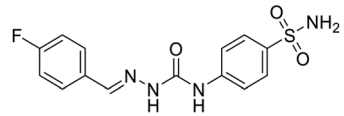 2-(4-Fluorobenzylidene)-*N*-(4-sulfamoylphenyl) hydrazinecarboxamide	675	5.6	—	—	27.3	95.8	—	124
122	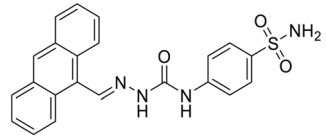 2-(Anthracen-9-ylmethylene)-*N*-(4-sulfamoyl phenyl)hydrazinecarboxamide	1640	19.5	—	—	381	21.5	—	124
123	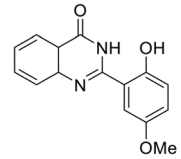 2-(2-Hydroxy-5-methoxyphenyl)-4*a*,8*a*-dihydroquinazolin-4(3*H*)-one	—	—	—	—	—	—	$IC_{50} = 61$	125

Table 14 (*Contd.*)

Compound no.	Chemical structure and IUPAC name	Isoform targeted, IC_{50} (μM)/K_i values (nM)							Ref.
		hCA-I	hCA-II	hCA-IV	hCA-VII	hCA-IX	hCA-XII	bCA-II	
124	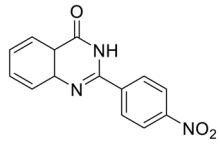 2-(4-Nitrophenyl)-4*a*,8*a*-dihydro quinazolin-4(3*H*)-one	—	—	—	—	—	—	$IC_{50} = 108$	125
125	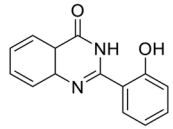 2-(2-Hydroxyphenyl)-4*a*,8*a*-dihydro quinazolin-4(3*H*)-one	—	—	—	—	—	—	$IC_{50} = 191$	125
126	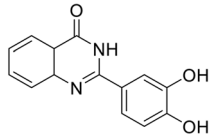 2-(3,4-Dihydroxyphenyl)-4*a*,8*a*-dihydroquinazolin-4(3*H*)-one	—	—	—	—	—	—	$IC_{50} = 20$	125
127	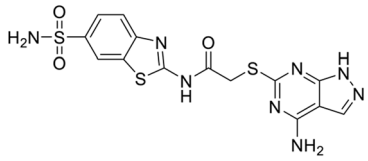 2-[(4-Amino-1*H*-pyrazolo[3,4-*d*]pyrimidin-6-yl)thio]-*N*-[6-(aminosulfonyl)-1,3-benzothiazol-2-yl]acetamide	—	—	—	9.5	—	—	—	126
128	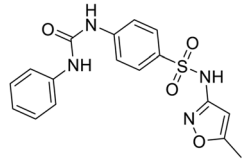 *N*-(5-Methyl-isoxazol-3-yl)-4–(3-phenyl-ureido)-benzenesulfonamide	73	—	—	85	—	—	—	127

Table 14 (*Contd.*)

Compound no.	Chemical structure and IUPAC name	Isoform targeted, IC_{50} (μM)/K_i values (nM)							Ref.
		hCA-I	hCA-II	hCA-IV	hCA-VII	hCA-IX	hCA-XII	bCA-II	
129	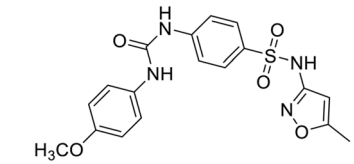 4-[3-(4-Methoxy-phenyl)-ureido]-*N*-(5-methyl-isoxazol-3-yl)-benzenesulfonamide	—	96	—	—	—	—	—	127
130	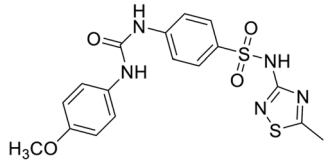 4-[3-(4-Methoxy-phenyl)-ureido]-*N*-(5-methyl-[1,3,4]thiadiazol-2-yl)-benzenesulfonamide	—	87	—	—	—	—	—	127
131	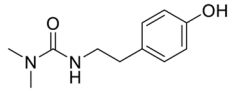 3-(4-Hydroxyphenethyl)-1,1-dimethylurea	—	0.307	—	—	—	—	—	128
132	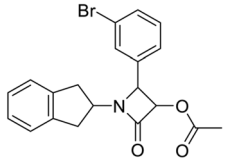 2-(3-Bromophenyl)-1-(2,3-dihydro-1*H*-inden-2-yl)-4-oxoazetidin-3-yl acetate	0.35	3.39	—	—	—	—	—	129
133	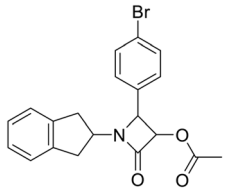 2-(4-Bromophenyl)-1-(2,3-dihydro-1*H*-inden-2-yl)-4-oxoazetidin-3-yl acetate	0.97	0.93	—	—	—	—	—	129

Table 14 (*Contd.*)

Compound no.	Chemical structure and IUPAC name	Isoform targeted, IC_{50} (μM)/K_i values (nM)							Ref.
		hCA-I	hCA-II	hCA-IV	hCA-VII	hCA-IX	hCA-XII	bCA-II	
134	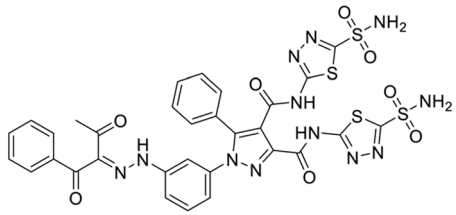 1-(3-(2-(1,3-Dioxo-1-phenylbutan-2-ylidene)hydrazinyl)phenyl)-5-phenyl-N^3,N^4-bis(5-sulfamoyl-1,3,4-thiadiazol-2-yl)-1*H*-pyrazole-3,4-dicarboxamide	0.119	—	—	—	—	—	—	130
135	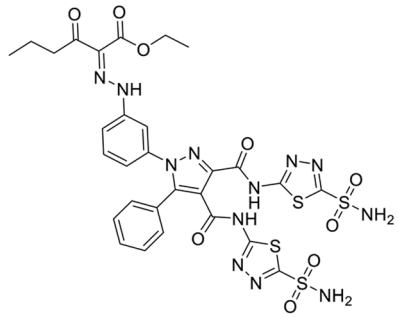 Ethyl 3-oxo-2-(2-(3-(5-phenyl-3,4-bis((5-sulfamoyl-1,3,4-thiadiazol-2-yl)carbamoyl)-1*H*-pyrazol-1-yl)phenyl)hydrazono) hexanoate	—	0.084	—	—	—	—	—	130
136	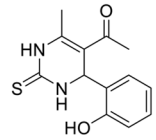 1-(4-(2-Hydroxyphenyl)-6-methyl-2-thioxo-1,2,3,4-tetrahydropyrimidin-5-yl)ethanone	47.40	76.06	—	—	—	—	—	131
137	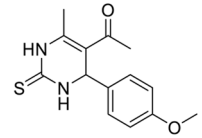 1-(4-(4-Methoxyphenyl)-6-methyl-2-thioxo-1,2,3,4-tetrahydropyrimidin-5-yl)ethanone	77.68	30.63	—	—	—	—	—	131

Table 14 (*Contd.*)

Compound no.	Chemical structure and IUPAC name	Isoform targeted, IC_{50} (μM)/K_i values (nM)							
		hCA-I	hCA-II	hCA-IV	hCA-VII	hCA-IX	hCA-XII	bCA-II	Ref.
138	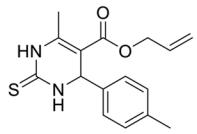 Allyl 6-methyl-2-thioxo-4-(*p*-tolyl)-1,2,3,4-tetrahydropyrimidine-5-carboxylate	218.5	155.4	—	—	—	—	—	132
139	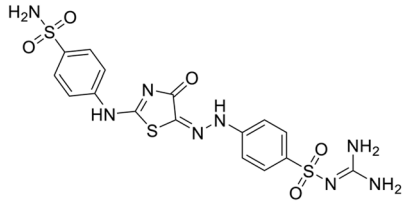 *N*-(Diaminomethylene)-4-(2-(4-oxo-2-((4-sulfamoylphenyl)amino)thiazol-5(4*H*)-ylidene)hydrazinyl)benzenesulfonamide	0.85	—	—	—	—	—	—	133
140	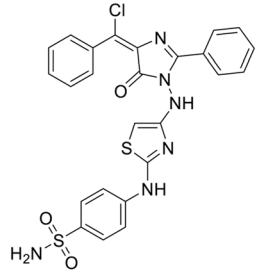 4-((4-((4-(Chlorobenzylidene)-5-oxo-2-phenyl-4,5-dihydro-1*H*-imidazol-1-yl)amino)thiazol-2-yl)amino)benzenesulfonamide	—	—	—	—	29.2	—	—	133
141	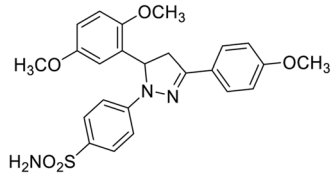 4-(5-(2,5-Dimethoxyphenyl)-3-(4-methoxyphenyl)-4,5-dihydro-1*H*-pyrazol-1-yl)benzenesulfonamide	26.5	18.9	—	—	—	—	—	134

Table 14 (*Contd.*)

Compound no.	Chemical structure and IUPAC name	Isoform targeted, IC_{50} (μM)/K_i values (nM)							Ref.
		hCA-I	hCA-II	hCA-IV	hCA-VII	hCA-IX	hCA-XII	bCA-II	
142	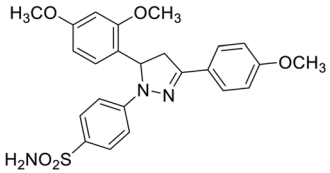 4-(5-(2,4-Dimethoxyphenyl)-3-(4-methoxyphenyl)-4,5-dihydro-1*H*-pyrazol-1-yl)benzenesulfonamide	39.7	20.5	—	—	—	—	—	134
143	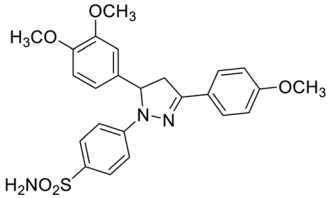 4-(5-(3,4-Dimethoxyphenyl)-3-(4-methoxyphenyl)-4,5-dihydro-1*H*-pyrazol-1-yl)benzenesulfonamide	55.5	28.8	—	—	—	—	—	134
144	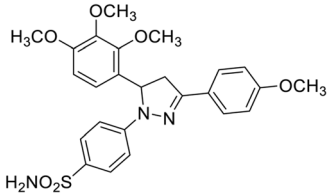 4-(3-(4-Methoxyphenyl)-5-(2,3,4-trimethoxyphenyl)-4,5-dihydro-1*H*-pyrazol-1-yl)benzenesulfonamide	31.4	19.9	—	—	—	—	—	134
145	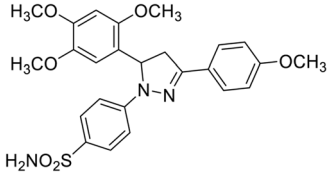 4-(3-(4-Methoxyphenyl)-5-(2,4,5-trimethoxyphenyl)-4,5-dihydro-1*H*-pyrazol-1-yl)benzenesulfonamide	29.9	25.9	—	—	—	—	—	134

Table 14 (*Contd.*)

Compound no.	Chemical structure and IUPAC name	Isoform targeted, IC_{50} (μM)/K_i values (nM)							
		hCA-I	hCA-II	hCA-IV	hCA-VII	hCA-IX	hCA-XII	bCA-II	Ref.
146	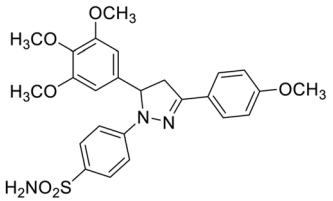 4-(3-(4-Methoxyphenyl)-5-(3,4,5-trimethoxyphenyl)-4,5-dihydro-1*H*-pyrazol-1-yl)benzenesulfonamide	34.1	20.2	—	—	—	—	—	134
147	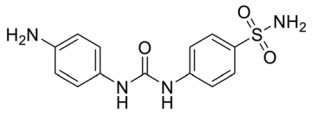 4-(3-(4-Aminophenyl)ureido)benzenesulfonamide	—	—	—	—	—	0.71	—	135
148	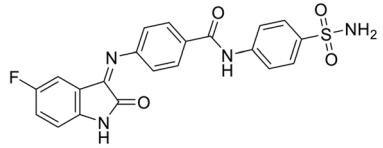 4-(5-Fluoro -2-oxoindolin-3-ylideneamino)-*N*-(4-sulfamoylphenyl)benzamide	—	—	—	—	—	0.69	—	135
149	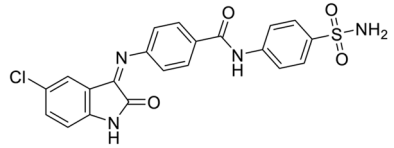 4-(5-Chloro-2-oxoindolin-3-ylideneamino)-*N*-(4-sulfamoylphenyl)benzamide	—	—	—	—	—	0.54	—	135
150	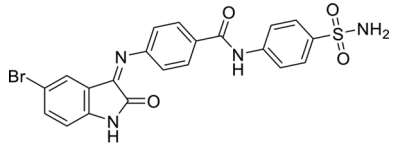 4-(5-Bromo-2-oxoindolin-3-ylideneamino)-*N*-(4-sulfamoylphenyl)benzamide	—	—	—	—	—	0.58	—	135

Table 14 (*Contd.*)

Compound no.	Chemical structure and IUPAC name	Isoform targeted, IC_{50} (μM)/K_i values (nM)							Ref.
		hCA-I	hCA-II	hCA-IV	hCA-VII	hCA-IX	hCA-XII	bCA-II	
151	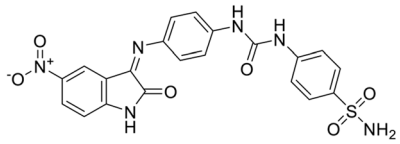 4-(3-(4-(5-Nitro-2-oxoindolin-3-ylideneamino)phenyl)ureido)benzenesulfonamide	—	—	—	—	—	0.67	—	135
152	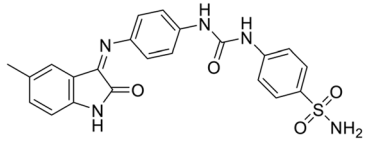 4-(3-(4-(5-Methyl-2-oxoindolin-3-ylideneamino)phenyl)ureido)benzenesulfonamide	—	—	—	—	—	0.64	—	135
153	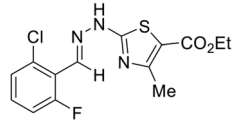 Ethyl-2-(2-(2-chloro-6-fluorobenzylidene) hydrazineyl)-4-methylthiazole-5-carboxylate	—	—	—	—	—	—	1.26	136
154	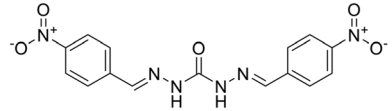 Bis[(4-nitrophenyl)methylidene]carbonic dihydrazide	—	—	—	—	—	—	$IC_{50} = 1.33$	137
155	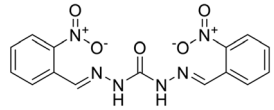 Bis[(2-nitrophenyl)methylidene]carbonic dihydrazide	—	—	—	—	—	—	$IC_{50} = 1.85$	137
156	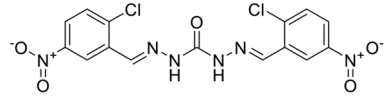 Bis[(2-chloro-5-nitrophenyl)methylidene]carbonic dihydrazide	—	—	—	—	—	—	$IC_{50} = 1.37$	137

Table 14 (*Contd.*)

Compound no.	Chemical structure and IUPAC name	Isoform targeted, IC_{50} (μM)/K_i values (nM)							Ref.
		hCA-I	hCA-II	hCA-IV	hCA-VII	hCA-IX	hCA-XII	bCA-II	
157	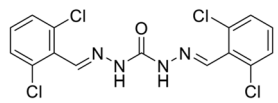 Bis[(*E*)-(2,6-dichlorophenyl)methylidene]carbonic dihydrazide	—	—	—	—	—	—	$IC_{50} = 1.46$	137
158	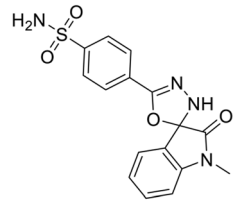 4-(1-Methyl-2-oxo-3′*H*-spiro[indoline-3,2′-[1,3,4]oxadiazole]-5′-yl)benzenesulphonamide	—	0.042	—	—	—	—	—	138
159	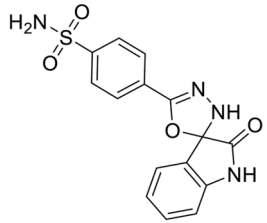 4-(2-Oxo-3′*H*-spiro[indoline-3,2′-[1,3,4] oxadiazole]-5′-yl) benzenesulphonamide	—	0.151	—	—	—	—	—	138
160	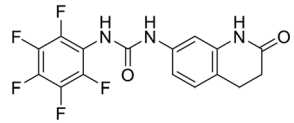 1-(2-Oxo-1,2,3,4-tetrahydroquinolin-7-yl)-3-(perfluorophenyl)urea	—	—	—	—	243.6	—	—	139
161	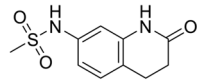 *N*-(2-oxo-1,2,3,4-tetrahydroquinolin-7-yl)methanesulfonamide	—	—	—	—	292.8	—	—	139

Table 14 (*Contd.*)

Compound no.	Chemical structure and IUPAC name	Isoform targeted, IC_{50} (μM)/K_i values (nM)							Ref.
		hCA-I	hCA-II	hCA-IV	hCA-VII	hCA-IX	hCA-XII	bCA-II	
162	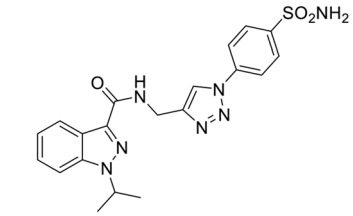 1-Isopropyl-*N*-((1-(4-sulfamoylphenyl)-1*H*-1,2,3-triazol-4-yl)methyl)-1*H*-indazole-3-carboxamide	—	—	—	—	1.8	—	—	140
163	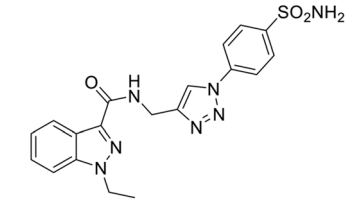 1-Ethyl-*N*-((1-(4-sulfamoylphenyl)-1*H*-1,2,3-triazol-4-yl)methyl)-1*H*-indazole-3-carboxamide	—	—	—	—	2.3	—	—	140
164	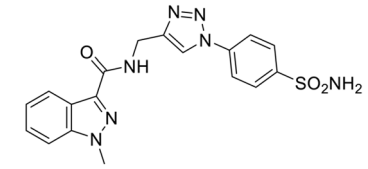 1-Methyl-*N*-((1-(4-sulfamoylphenyl)-1*H*-1,2,3-triazol-4-yl)methyl)-1*H*-indazole-3-carboxamide	—	—	—	—	2.0	—	—	140
165	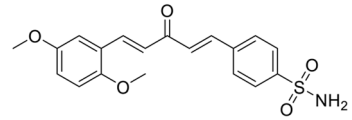 4-((1*E*,4*E*)-5-(2,5-dimethoxyphenyl)-3-oxopenta-1,4-dien-1-yl)benzenesulfonamide	0.89	—	—	—	—	—	—	141
166	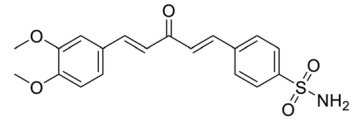 4-((1*E*,4*E*)-5-(3,4-dimethoxyphenyl)-3-oxopenta-1,4-dien-1-yl)benzenesulfonamide	0.75	—	—	—	—	—	—	141

Table 14 (*Contd.*)

Compound no.	Chemical structure and IUPAC name	Isoform targeted, IC_{50} (μM)/K_i values (nM)							Ref.
		hCA-I	hCA-II	hCA-IV	hCA-VII	hCA-IX	hCA-XII	bCA-II	
167	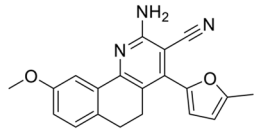 2-Amino-5,6-dihydro-9-methoxy-4-(5-methylfuran-2-yl)benzo[*h*]quinolin-3-carbonitrile	2.84	4.56	—	—	—	—	—	142
168	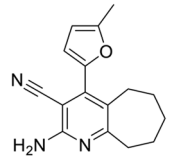 2-Amino-6,7,8,9-tetrahydro-4-(5-methylfuran-2-yl)-5*H*-cyclohepta[*b*]pyridine-3-carbonitrile	53.9	2.56	—	—	—	—	—	142
169	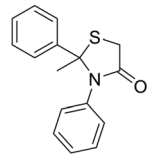 2-Phenyl-2-methyl-3-phenyl-thiazolidine-4-one	23.76	—	—	—	—	—	—	143
170	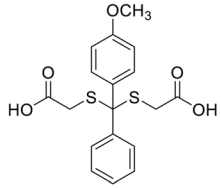 4-Methoxyanilide-1,1-bis-(hydroxycarbonyl methylthio)-1-phenylethane	—	58.92	—	—	—	—	—	143
171	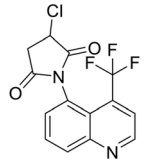 3-Chloro-1-(4-(trifluoromethyl)quinolin-5-yl) pyrrolidine-2,5-dione	23.27	—	—	—	—	—	—	144

Table 14 (*Contd.*)

Compound no.	Chemical structure and IUPAC name	Isoform targeted, IC_{50} (μM)/K_i values (nM)							Ref.
		hCA-I	hCA-II	hCA-IV	hCA-VII	hCA-IX	hCA-XII	bCA-II	
172	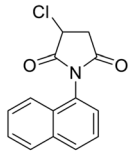 3-Chloro-1-(naphthalen-1-yl)pyrrolidine-2,5-dione	—	10.64	—	—	—	—	—	144
173	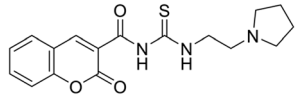 2-Oxo-*N*-((2-(pyrrolidin-1-yl)ethyl)carbamothioyl)-2*H*-chromene-3-carboxamide	—	—	—	—	107.9	—	—	145
174	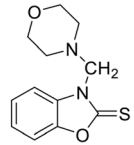 *N*-Morfolinomethylbenzoxazoline-2-thione	—	58	—	—	—	—	—	146
175	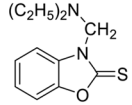 *N*-Diethylaminomethylbenzothiazoline-2-thione	—	70	—	—	—	—	—	146
176	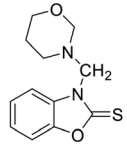 *N*-Oxazinomethylbenzothiazoline-2-thione	—	76	—	—	—	—	—	146
177	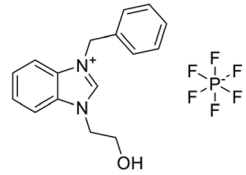 1-(2-Hydroxyethyl)-3-benzylbenzimidazolium hexafluorophosphate	13.90	12.82	—	—	—	—	—	147

Table 14 (*Contd.*)

Compound no.	Chemical structure and IUPAC name	Isoform targeted, IC_{50} (μM)/K_i values (nM)							Ref.
		hCA-I	hCA-II	hCA-IV	hCA-VII	hCA-IX	hCA-XII	bCA-II	
178	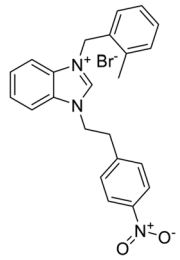 1-[2-(4-Nitrophenyl)ethyl]-3-(2-methylbenzyl) benzimidazolium bromide	17.33	45.31	—	—	—	—	—	148
179	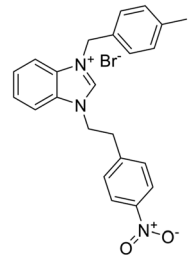 1-[2-(4-Nitrophenyl)ethyl]-3-(4-methylbenzyl) benzimidazolium bromide	54.48	33.98	—	—	—	—	—	148
180	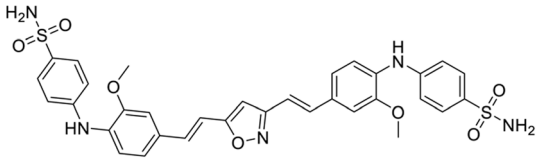 4,4'-{Isoxazole-3,5-diylbis[(*E*)ethene-2,1-diyl(2-methoxy-4,1-phenylene)imino]}dibenzenesulfonamide	0.99	—	—	—	—	—	0.71	149
181	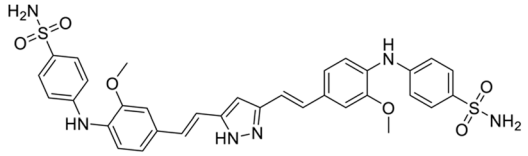 4,4'-{1*H*-pyrazole-3,5-diylbis[(*E*)ethene-2,1-diyl(2-methoxy-4,1-phenylene)imino]}dibenzenesulfonamide	—	0.67	—	—	—	—	—	149

Table 14 (*Contd.*)

Compound no.	Chemical structure and IUPAC name	Isoform targeted, IC_{50} (μM)/K_i values (nM)							Ref.
		hCA-I	hCA-II	hCA-IV	hCA-VII	hCA-IX	hCA-XII	bCA-II	
182	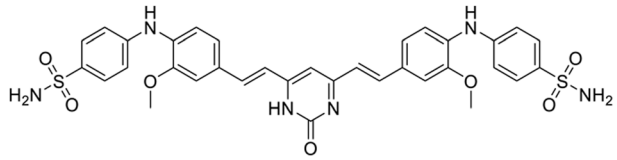 4,4'-{(2-Oxo-1,2-dihydropyrimidine-4,6-diyl)bis[(*E*)ethene-2,1-diyl(2-methoxy-4,1-phenylene)imino]}dibenzenesulfonamide	—	—	—	—	—	—	0.71	149
183	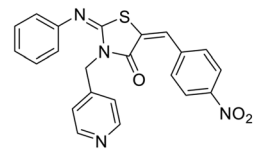 (*E*)-5-((*E*)-4-Nitrobenzylidene)-2-(phenylimino)-3-(pyridin-4-ylmethyl)thiazolidin-4-one	—	—	—	—	1.61	—	—	150
184	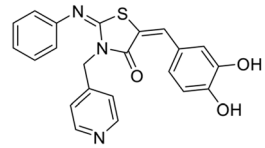 (*E*)-5-((*E*)-3,4-Dihydroxybenzylidene)-2-(phenylimino)-3-(pyridin-4-ylmethyl)thiazolidin-4-one	—	—	—	—	1.84	—	—	150
185	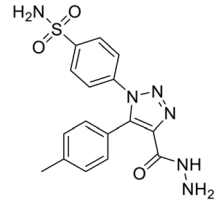 4-[4-(Hydrazinocarbonyl)-5-(p-tolyl)-1*H*-1,2,3-triazol-1-yl]benzenesulfonamide	27.2	—	—	—	—	—	—	151
186	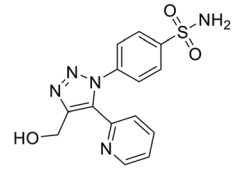 4-(4-(Hydroxymethyl)-5-(pyridin-2-yl)-1*H*-1,2,3-triazol-1-yl)benzenesulfonamide	—	—	—	—	14.3	—	—	151

Table 14 (*Contd.*)

Compound no.	Chemical structure and IUPAC name	Isoform targeted, IC_{50} (μM)/K_i values (nM)							Ref.
		hCA-I	hCA-II	hCA-IV	hCA-VII	hCA-IX	hCA-XII	bCA-II	
187	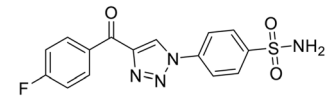 4-(4-(4-Fluorobenzoyl)-1*H*-1,2,3-triazol-1-yl) benzenesulfonamide	—	—	52.4	—	—	—	—	152
188	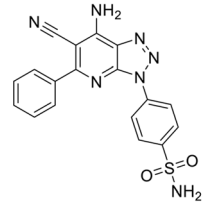 4-(7-Amino-6-cyano-5-phenyl-3*H*-[1,2,3] triazolo[4,5-*b*]pyridin-3-yl)benzenesulfonamide	—	—	—	—	46.4	—	—	153
189	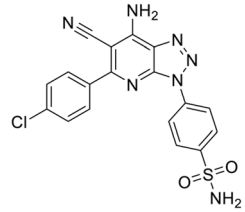 4-(7-Amino-5-(4-chlorophenyl)-6-cyano-3*H*-[1,2,3] triazolo[4,5-*b*]pyridin-3-yl)benzenesulfonamide	—	—	—	—	42.6	—	—	153
190	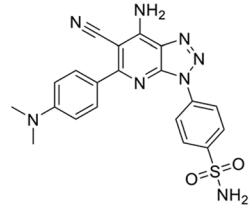 4-(7-Amino-6-cyano-5-(4-(dimethylamino)phenyl)-3*H*-[1,2,3] triazolo[4,5-*b*]pyridin-3-yl)benzenesulfonamide	—	—	—	—	35.1	—	—	153
191	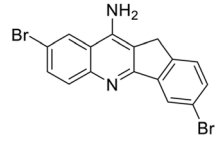 3,8-Dibromo-11*H*-indeno[1,2-*b*]quinolin-10-amine	120.9	267.5	—	—	—	—	—	154

Table 14 (*Contd.*)

Compound no.	Chemical structure and IUPAC name	Isoform targeted, IC_{50} (μM)/K_i values (nM)							Ref.
		hCA-I	hCA-II	hCA-IV	hCA-VII	hCA-IX	hCA-XII	bCA-II	
192	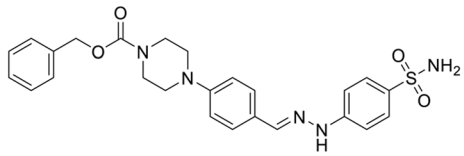 Benzyl 4-(4-((2-(4-sulfamoylphenyl)hydrazono)methyl) phenyl)piperazine-1-carboxylate	919.6	93.9	—	11.4	1631.4	—	—	155
193	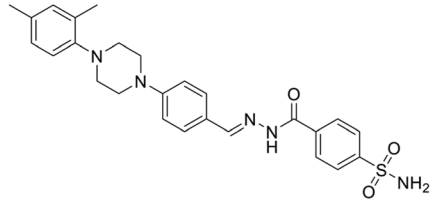 4-(2-(4-(4-(2,4-Dimethylphenyl)piperazin-1-yl)benzylidene) hydrazinecarbonyl)benzenesulfonamide	321.8	30.8	—	6.2	1788.6	—	—	155
194	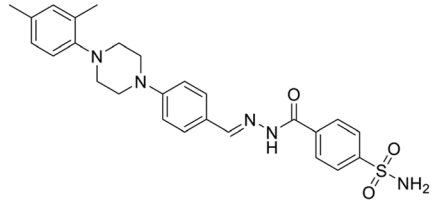 4-(2-(4-(4-(2,4-Dimethylphenyl)piperazin-1-yl)benzylidene) hydrazinecarbonyl)benzenesulfonamide	>10 000	9385.9	—	17.8	1660.9	—	—	155
195	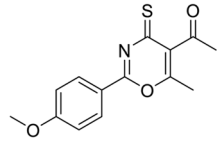 1-(2-[4-Methoxyphenyl]-6-methyl-4-thioxo- 4*H*-1,3-oxazin-5-yl)ethanone	—	—	—	—	—	—	0.144	156
196	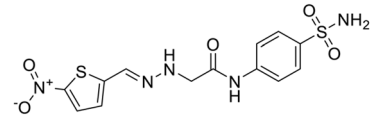 2-(2-((5-Nitrothiophen-2-yl)methylene)hydrazinyl) -*N*-(4-sulfamoylphenyl)acetamide	—	0.1676	—	—	—	—	—	157

Table 14 (*Contd.*)

Compound no.	Chemical structure and IUPAC name	Isoform targeted, IC_{50} (μM)/K_i values (nM)							Ref.
		hCA-I	hCA-II	hCA-IV	hCA-VII	hCA-IX	hCA-XII	bCA-II	
197	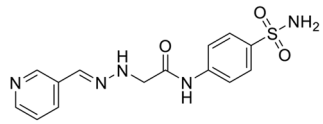 2-(2-(Pyridin-3-ylmethylene)hydrazinyl)-*N*-(4-sulfamoylphenyl)acetamide	—	0.2880	—	—	—	—	—	157
198	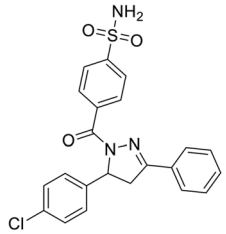 4-(5-(4-Chlorophenyl)-3-phenyl-4,5-dihydro-1*H*-pyrazole-1-carbonyl)benzenesulfonamide	195.0	—	—	—	7.9	34.0	—	158
199	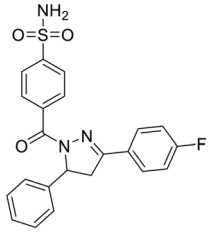 4-(3-(4-Fluorophenyl)-5-phenyl-4,5-dihydro-1*H*-pyrazole-1-carbonyl)benzenesulfonamide	102.9	—	—	—	23.1	10.1	—	158
200	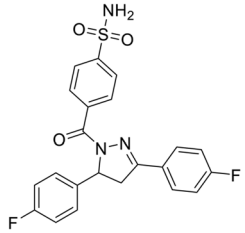 4-(3,5-Bis(4-fluorophenyl)-4,5-dihydro-1*H*-pyrazole-1-carbonyl)benzenesulfonamide	140.7	—	—	—	5.5	7.1	—	158

Table 14 (*Contd.*)

Compound no.	Chemical structure and IUPAC name	Isoform targeted, IC_{50} (μM)/K_i values (nM)							Ref.
		hCA-I	hCA-II	hCA-IV	hCA-VII	hCA-IX	hCA-XII	bCA-II	
201	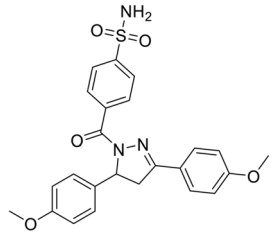 4-(3,5-Bis(4-methoxyphenyl)-4,5-dihydro-1*H*-pyrazole-1-carbonyl)benzenesulfonamide	875.9	—	—	—	37.0	18.8	—	158
202	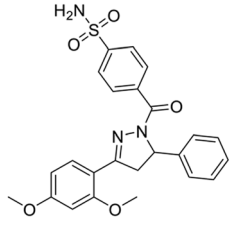 4-(3-(2,4-Dimethoxyphenyl)-5-phenyl-4,5-dihydro-1*H*-pyrazole-1-carbonyl)benzenesulfonamide	807.8	—	—	—	32.9	9.7	—	158
203	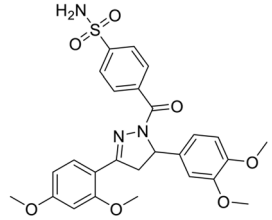 4-(3-(2,4-Dimethoxyphenyl)-5-(3,4-dimethoxy phenyl)-4,5-dihydro-1*H*-pyrazole-1-carbonyl)benzenesulfonamide	2961.3	—	—	—	36.3	28.9	—	158
204	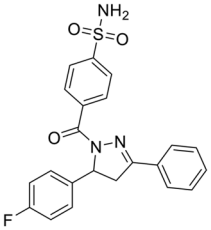 4-(5-(4-Fluorophenyl)-3-phenyl-4,5-dihydro-1*H*-pyrazole-1-carbonyl)benzenesulfonamide	87.8	—	—	—	44.5	9.4	—	158

Table 14 (*Contd.*)

Compound no.	Chemical structure and IUPAC name	Isoform targeted, IC_{50} (μM)/K_i values (nM)							Ref.
		hCA-I	hCA-II	hCA-IV	hCA-VII	hCA-IX	hCA-XII	bCA-II	
205	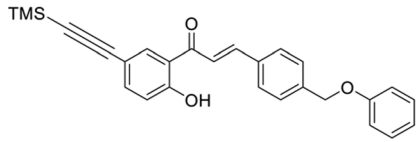 (1-(2-Hydroxy-5-(trimethylsilyl)phenyl)-3-(4-(phenoxymethyl)phenyl)prop-2-en-1-one	—	—	—	—	—	—	$IC_{50} = 0.054$	159
206	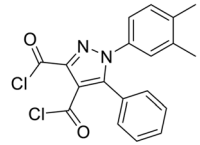 1-(3,4-Dimethylphenyl)-5-phenyl-1*H*-pyrazole-3,4-dicarbonyldichloride	1.03	1.82	—	—	—	—	—	160
207	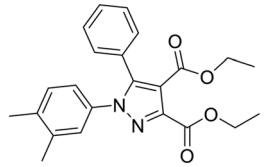 Diethyl 1-(3,4-dimethylphenyl)-5-phenyl-1*H*-pyrazole-3,4-dicarboxylate	6.58	8.93	—	—	—	—	—	160
208	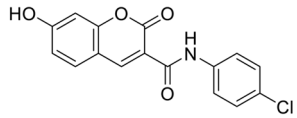 *N*-(4-Chlorophenyl)-7-hydroxy-2-oxo-2*H*-chromene-3-carboxamide	—	—	—	—	0.2	0.2	—	161
209	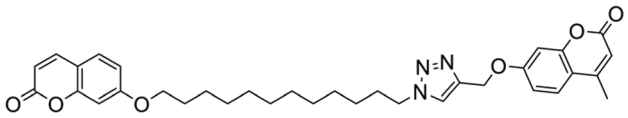 4-Methyl-7-((1-(12-((2-oxo-2*H*-chromen-7-yl)oxy) dodecyl)-1*H*-1,2,3-triazol-4-yl)methoxy)-2*H*-chromen-2-one	—	—	—	—	144.6	—	—	162

Table 14 (*Contd.*)

Compound no.	Chemical structure and IUPAC name	Isoform targeted, IC_{50} (μM)/K_i values (nM)							Ref.
		hCA-I	hCA-II	hCA-IV	hCA-VII	hCA-IX	hCA-XII	bCA-II	
210	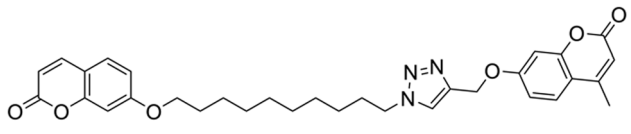 4-Methyl-7-((1-(10-((2-oxo-2*H*-chromen-7-yl)oxy) decyl)-1*H*-1,2,3-triazol-4-yl)methoxy)-2*H*-chromen-2-one	—	—	—	—	71.5	—	—	162
211	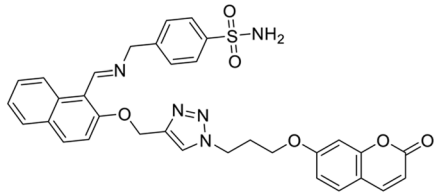 4-((((2-((1-(3-((2-oxo-2*H*-chromen-7-yl)oxy)propyl)-1*H*-1,2,3-triazol-4-yl)methoxy)naphthalen-1-yl)methylene)amino)methyl) benzenesulfonamide	—	—	—	—	45.5	—	—	163
212	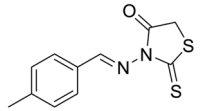 3-((4-Methylbenzylidene)amino)-2-thioxothiazolidin-4-one	47.7	52.8	—	—	—	—	—	164
213	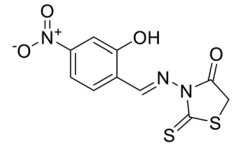 3-((2-Hydroxy-4-nitrobenzylidene)amino)-2-thioxothiazolidin-4-one	44.7	55.5	—	—	—	—	—	164
214	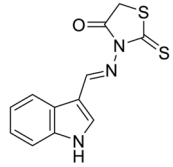 3-(((1*H*-Indol-3-yl)methylene)amino)-2-thioxothiazolidin-4-one	43.5	46.6	—	—	—	—	—	164

Table 14 (*Contd.*)

Compound no.	Chemical structure and IUPAC name	Isoform targeted, IC_{50} (μM)/K_i values (nM)							Ref.
		hCA-I	hCA-II	hCA-IV	hCA-VII	hCA-IX	hCA-XII	bCA-II	
215	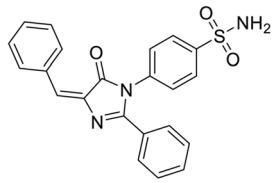 4-(4-Benzylidene-5-oxo-2-phenyl-4,5-dihydro-1*H*-imidazol-1-yl)benzenesulfonamide	—	—	—	—	58.7	76.5	—	165
216	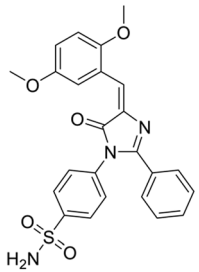 4-(4-(2,5-Dimethoxybenzylidene)-5-oxo-2-phenyl-4,5-dihydro-1*H*-imidazol-1-yl)benzenesulfonamide	—	—	—	—	23.0	54.8	—	165
217	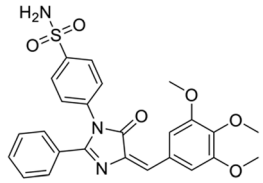 4-(5-Oxo-2-phenyl-4-(3,4,5-trimethoxybenzylidene)-4,5-dihydro-1*H*-imidazol-1-yl)benzenesulfonamide	—	—	—	—	68.2	179.6	—	165
218	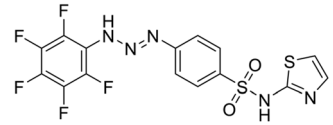 4-[3-(Perfluorophenyl)triaz-1-en-1-yl]-*N*-(thiazol-2-yl)-benzenesulfonamide	450.37	504.37	—	—	—	—	—	166

Table 14 (*Contd.*)

Compound no.	Chemical structure and IUPAC name	Isoform targeted, IC_{50} (μM)/K_i values (nM)							Ref.
		hCA-I	hCA-II	hCA-IV	hCA-VII	hCA-IX	hCA-XII	bCA-II	
219	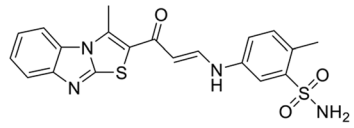 2-Methyl-5-((3-(3-methylbenzo[4,5]imidazo[2,1-*b*]thiazol-2-yl)-3-oxoprop-1-en-1-yl)amino)benzenesulfonamide	—	—	—	—	450.37	—	—	167
220	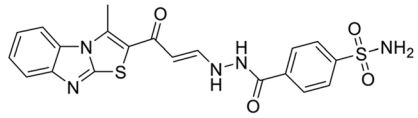 4-(2-(3-(3-Methylbenzo[4,5]imidazo[2,1-*b*]thiazol-2-yl)-3-oxoprop-1-en-1-yl)hydrazine-1-carbonyl)benzenesulfonamide	—	—	—	—	450.37	—	—	167
221	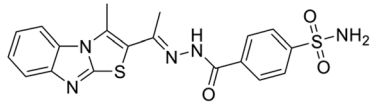 4-(2-(1-(3-Methylbenzo[4,5]imidazo[2,1-*b*]thiazol-2-yl)ethylidene)hydrazine-1-carbonyl)benzenesulfonamide	—	—	—	—	450.37	—	—	167
222	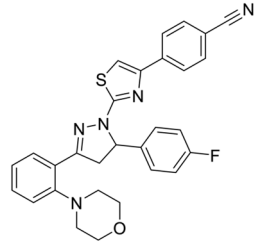 1-[4-(4-Cyanophenyl)thiazol-2-yl]-3-(4-morpholino phenyl)-5-(4-fluorophenyl)-2-pyrazoline	13.04	—	—	—	—	—	—	168
223	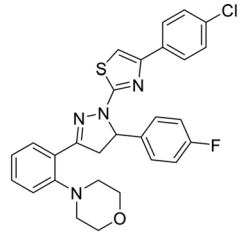 1-[4-(4-Chlorophenyl)thiazol-2-yl]-3-(4-morpholino phenyl)-5-(4-fluorophenyl)-2-pyrazoline	—	7.47	—	—	—	—	—	168

Table 14 (*Contd.*)

Compound no.	Chemical structure and IUPAC name	Isoform targeted, IC_{50} (μM)/K_i values (nM)							Ref.
		hCA-I	hCA-II	hCA-IV	hCA-VII	hCA-IX	hCA-XII	bCA-II	
224	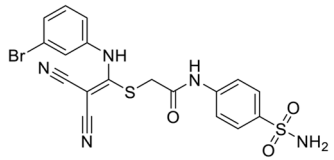 2-[1-(3-Bromophenylamino)-2,2-dicyanovinyl thio]-*N*-(4-sulfamoylphenyl)acetamide	9.01	—	—	—	—	—	—	169
225	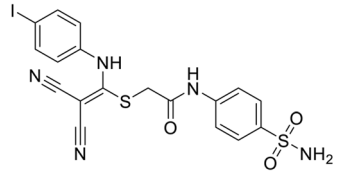 2-[2,2-Dicyano-1-(4-iodophenylamino)vinyl thio]-*N*-(4-sulfamoylphenyl)acetamide	—	7.41	—	—	—	—	—	169
226	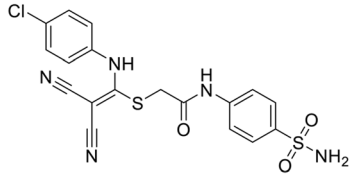 2-[1-(4-Chlorophenylamino)-2,2-dicyanovinyl thio]-*N*-(4-sulfamoylphenyl)acetamide	7.37	—	—	—	—	—	—	169
227	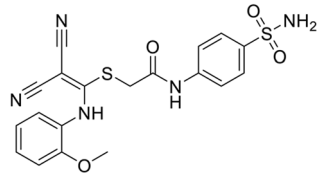 2-[2,2-Dicyano-1-(2-methoxyphenylamino)vinyl thio]-*N*-(4-sulfamoylphenyl)acetamide	48.28	—	—	—	—	—	—	169
228	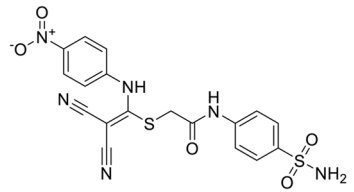 2-[2,2-Dicyano-1-(4-nitrophenylamino)vinyl thio]-*N*-(4-sulfamoylphenyl)acetamide	105.94	—	—	—	—	—	—	169

Table 14 (*Contd.*)

Compound no.	Chemical structure and IUPAC name	Isoform targeted, IC_{50} (μM)/K_i values (nM)							Ref.
		hCA-I	hCA-II	hCA-IV	hCA-VII	hCA-IX	hCA-XII	bCA-II	
229	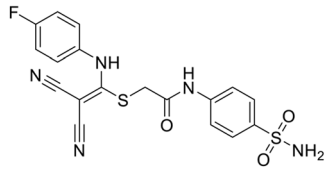 2-[2,2-Dicyano-1-(4-fluorophenylamino)vinyl thio]-*N*-(4-sulfamoylphenyl)acetamide	—	56.67	—	—	—	—	—	169
230	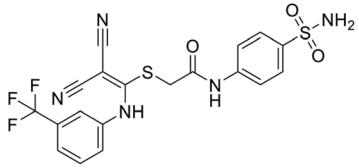 2-[2,2-Dicyano-1-(3-(trifluoromethyl)phenylamino)vinyl thio]-*N*-(4-sulfamoylphenyl)acetamide	—	49.92	—	—	—	—	—	169
231	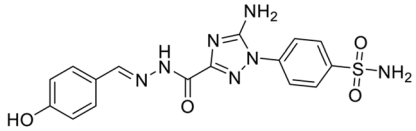 4-(5-Amino-3-(2-(4-hydroxybenzylidene)hydrazine-1-carbonyl)-1*H*-1,2,4-triazol-1-yl)benzenesulfonamide	—	—	—	—	8.3	7.8	—	170
232	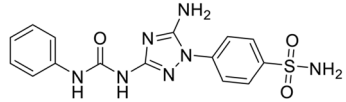 4-(5-Amino-3-(3-phenylureido)-1*H*-1,2,4-triazol-1-yl)benzenesulfonamide	—	—	—	—	8.2	8.1	—	170
233	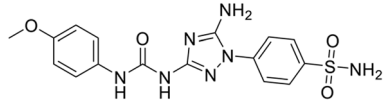 4-(5-Amino-3-(3-(4-methoxyphenyl)ureido)-1*H*-1,2,4-triazol-1-yl)benzenesulfonamide	—	—	—	—	3.3	—	—	170

Table 14 (*Contd.*)

Compound no.	Chemical structure and IUPAC name	Isoform targeted, IC_{50} (μM)/K_i values (nM)							Ref.
		hCA-I	hCA-II	hCA-IV	hCA-VII	hCA-IX	hCA-XII	bCA-II	
234	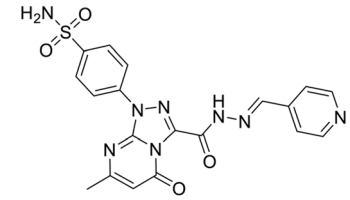 4-(7-Methyl-5-oxo-3-(2-(pyridin-4-ylmethylene) hydrazine-1-carbonyl)- [1,2,4]triazolo [4,3-*a*] pyrimidin-1(5*H*)-yl)benzenesulfonamide	—	—	—	—	24.6	—	—	170
235	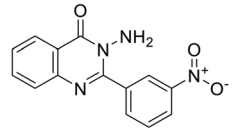 3-Amino-2-(3-nitrophenyl)quinazolin-4(3*H*)-one	—	$IC_{50} = 21.5$	—	—	—	—	$IC_{50} = 19.7$	171
236	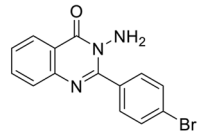 3-Amino-2-(4-bromophenyl)quinazolin-4(3*H*)-one	—	$IC_{50} = 14.0$	—	—	—	—	—	171
237	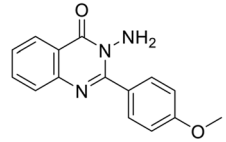 3-Amino-2-(4-methoxyphenyl)quinazolin-4(3*H*)-one	—	$IC_{50} = 22.0$	—	—	—	—	—	171
238	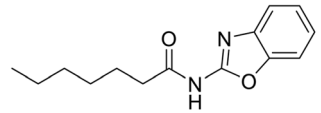 *N*-(Benzo[*d*]oxazol-2-yl)heptanamide	—	$IC_{50} = 0.00564$	—	—	—	—	—	172

Table 14 (*Contd.*)

Compound no.	Chemical structure and IUPAC name	Isoform targeted, IC_{50} (μM)/K_i values (nM)							Ref.
		hCA-I	hCA-II	hCA-IV	hCA-VII	hCA-IX	hCA-XII	bCA-II	
239	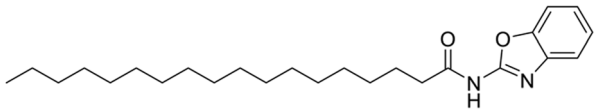 *N*-(Benzo[*d*]oxazol-2-yl)stearamide	—	IC_{50} = 0.00596	—	—	—	—	—	172
240	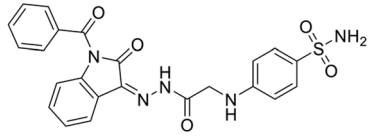 4-((2-(2-(1-Benzoyl-2-oxoindolin-3-ylidene)hydrazinyl)-2-oxoethyl)amino) benzenesulfonamide	—	—	—	—	—	21.5	—	173
241	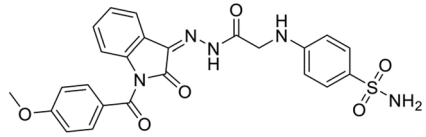 4-((2-(2-(1-(4-Methoxybenzoyl)-2-oxoindolin-3-ylidene) hydrazinyl)-2-oxoethyl) amino)benzenesulfonamide	—	—	—	—	—	22.3	—	173
242	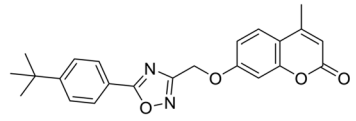 7-((5-(4-(*Tert*-butyl)phenyl)-1,2,4-oxadiazol-3-yl) methoxy)-4-methyl-2*H*-chromen-2-one	—	—	—	—	—	1.0	—	174
243	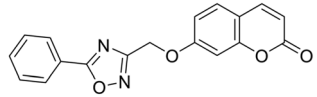 4-Methyl-7-((5-phenyl-1,2,4-oxadiazol-3-yl) methoxy)-2*H*-chromen-2-one	—	—	—	—	—	23.6	—	174
244	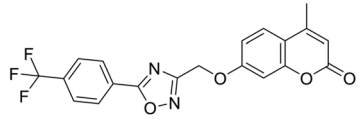 4-Methyl-7-((5-(4-(trifluoromethyl)phenyl)-1,2,4-oxadiazol-3-yl)methoxy)-2*H*-chromen-2-one	—	—	—	—	—	4.4	—	174

Table 14 (*Contd.*)

Compound no.	Chemical structure and IUPAC name	Isoform targeted, IC_{50} (μM)/K_i values (nM)							Ref.
		hCA-I	hCA-II	hCA-IV	hCA-VII	hCA-IX	hCA-XII	bCA-II	
245	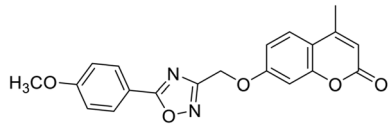 7-((5-(4-Methoxyphenyl)-1,2,4-oxadiazol-3-yl) methoxy)-4-methyl-2*H*-chromen-2-one	—	—	—	—	23.6	4.5	—	174
246	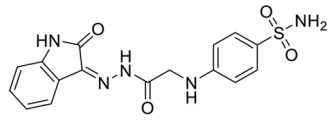 4-{2-Oxo-2-[2-(2-oxoindolin-3-ylidene)hydrazinyl] ethylamino}benzenesulfonamide	—	3.0	—	—	13.9	—	—	175
247	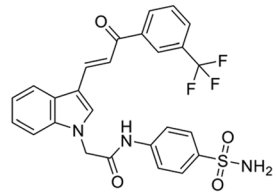 2-(3-(3-Oxo-3-(3-(trifluoromethyl)phenyl)prop-1-en-1-yl)-1*H*-indol-1-yl)-*N*-(4-sulfamoyl-phenyl)acetamide	—	2.3	—	—	—	—	—	176
248	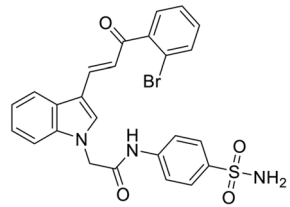 2-(3-(3-(2-Bromophenyl)-3-oxoprop-1-en-1-yl)-1*H*-indol-1-yl)-*N*-(4-sulfamoyl phenyl)acetamide	—	2.4	—	—	—	—	—	176
249	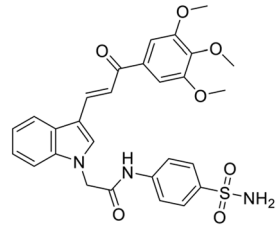 2-(3-(3-Oxo-3-(3,4,5-trimethoxyphenyl)prop-1-en-1-yl)-1*H*-indol-1-yl)-*N*-(4-sulfamoyl phenyl)acetamide	—	3.6	—	—	—	—	—	176

Table 14 (*Contd.*)

Compound no.	Chemical structure and IUPAC name	Isoform targeted, IC_{50} (μM)/K_i values (nM)							Ref.
		hCA-I	hCA-II	hCA-IV	hCA-VII	hCA-IX	hCA-XII	bCA-II	
250	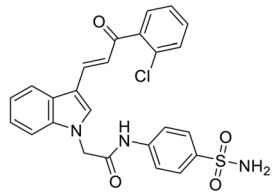 2-(3-(3-(2-Chlorophenyl)-3-oxoprop-1-en-1-yl)-1*H*-indol-1-yl)-*N*-(4-sulfamoylphenyl). acetamide	—	7.0	—	—	—	—	—	176
251	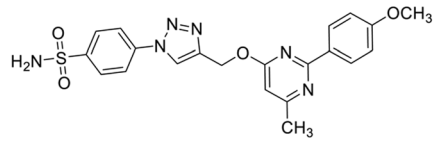 4-(4-(((2-(4-Methoxyphenyl)-6-methylpyrimidin-4-yl)oxy)methyl)-1*H*-1,2,3-triazol-1-yl)benzenesulfonamide	—	—	—	—	—	9.4	—	177
252	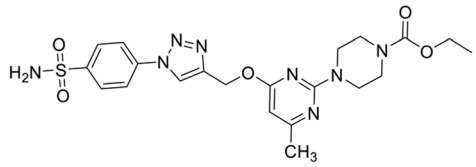 Ethyl 4-(4-methyl-6-((1-(4-sulfamoylphenyl)-1*H*-1,2,3-triazol-4-yl)methoxy)pyrimidin-2-yl)piperazine-1-carboxylate	—	—	—	—	—	1.8	—	177
253	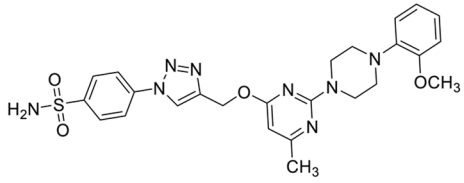 4-(4-(((2-(4-(2-Methoxyphenyl)piperazin-1-yl)-6-methylpyrimidin-4-yl)oxy)methyl)-1*H*-1,2,3-triazol-1-yl)benzenesulfonamide	—	—	—	—	—	0.82	—	177
254	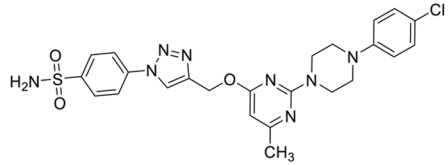 4-(4-(((2-(4-(4-Chlorophenyl)piperazin-1-yl)-6-methylpyrimidin-4-yl)oxy)methyl)-1*H*-1,2,3-triazol-1-yl)benzenesulfonamide	—	—	—	—	2.9	0.82	—	177

Table 14 (*Contd.*)

Compound no.	Chemical structure and IUPAC name	Isoform targeted, IC_{50} (μM)/K_i values (nM)							Ref.
		hCA-I	hCA-II	hCA-IV	hCA-VII	hCA-IX	hCA-XII	bCA-II	
255	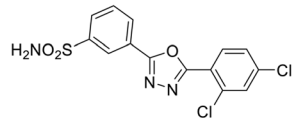 3-(5-(2,4-Dichlorophenyl)-1,3,4-oxadiazol-2-yl)benzenesulfonamide	75.8	—	—	—	—	15.4	—	178
256	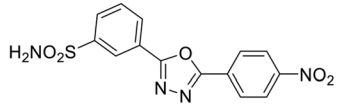 3-(5-(4-Nitrophenyl)-1,3,4-oxadiazol-2-yl)benzenesulfonamide	—	—	—	—	—	16.2	—	178
257	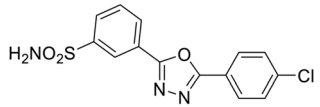 3-(5-(4-Chlorophenyl)-1,3,4-oxadiazol-2-yl)benzenesulfonamide	—	—	—	—	—	16.4	—	178
258	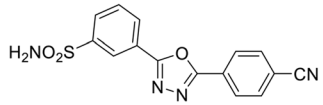 3-(5-(4-Cyanophenyl)-1,3,4-oxadiazol-2-yl)benzenesulfonamide	—	—	—	—	—	17.0	—	178
259	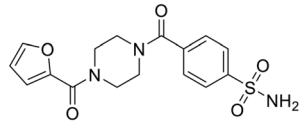 4-(4-(Furan-2-carbonyl)piperazine-1-carbonyl) benzenesulfonamide	—	—	4.3	—	—	—	—	179
260	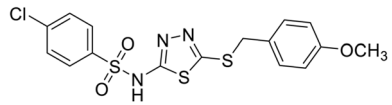 4-Chloro-*N*-(5-((4-methoxybenzyl)thio)-1,3,4-thiadiazol-2-yl)benzenesulfonamide	—	—	—	—	—	—	$IC_{50} = 0.60$	180

Table 14 (*Contd.*)

Compound no.	Chemical structure and IUPAC name	Isoform targeted, IC_{50} (μM)/K_i values (nM)							Ref.
		hCA-I	hCA-II	hCA-IV	hCA-VII	hCA-IX	hCA-XII	bCA-II	
261	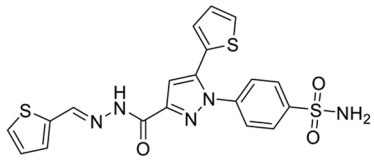 4-(3-(2-(Thiophene-2-yl-methylen)hydrazine-1-carbonyl)-5-(thiophene-2-yl)-1*H*-pyrazole-1-yl)benzenesulfonamide	—	—	—	—	7.0	—	—	181
262	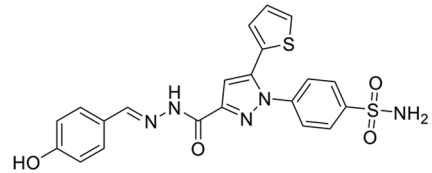 4-(3-(2-(4-Hydroxybenzylidene)hydrazine-1-carbonyl)-5-(thiophene-2-yl)-1*H*-pyrazole-1-yl)benzenesulfonamide	—	—	—	—	10.6	—	—	181
263	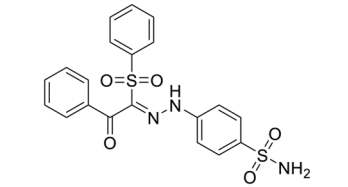 4-(2-(2-Oxo-2-phenyl-1(phenylsulfonyl) ethylidene)hydrazineyl)benzenesulfonamide	—	7.6	—	—	—	—	—	182
264	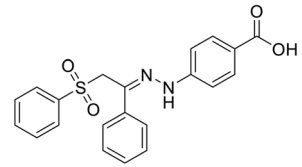 4-(2-(1-Phenyl-2-(phenylsulfonyl) ethylidene)hydrazineyl)benzoic acid	—	32 633	—	—	—	—	—	182
265	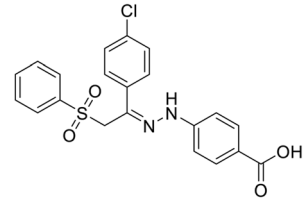 4-(2-(1-(4-Chlorophenyl)-2-(phenylsulfonyl) ethylidene)hydrazineyl)benzoic acid	—	9190	—	—	—	—	—	182

Table 14 (*Contd.*)

Compound no.	Chemical structure and IUPAC name	Isoform targeted, IC_{50} (μM)/K_i values (nM)							Ref.
		hCA-I	hCA-II	hCA-IV	hCA-VII	hCA-IX	hCA-XII	bCA-II	
266	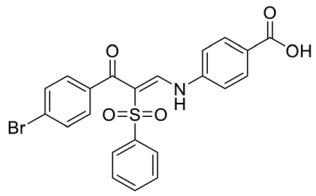 4-((3-(4-Bromophenyl)-3-oxo-2-(phenylsulfonyl) prop-1-en-1-yl)amino)benzoic acid	—	65 349	—	—	—	—	—	182
267	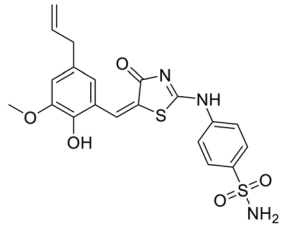 4-(5-(5-Allyl-2-hydroxy-3-methoxybenzylidene)-4-oxo-4,5-dihydrothiazol-2-ylamino)benzenesulfonamide	—	—	—	—	$IC_{50} = 0.011$	—	—	183
268	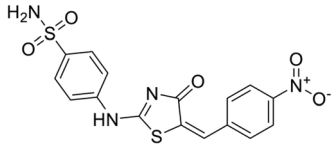 4-(5-(4-Nitrobenzylidene)-4-oxo-4,5-dihydrothiazol-2-ylamino)benzenesulfonamide	—	—	—	—	$IC_{50} = 0.017$	—	—	183
269	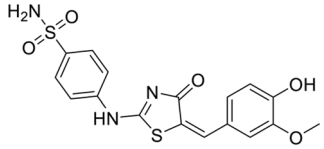 4-(5-(4-Hydroxy-3-methoxybenzylidene)-4-oxo-4,5-dihydrothiazol-2-ylamino)benzenesulfonamide	—	—	—	—	$IC_{50} = 0.026$	—	—	183
270	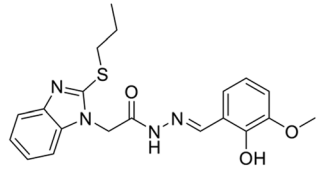 *N*′-(2-Hydroxy-3-methoxybenzylidene)-2-(2-(propylthio)-1*H*-benzo[*d*]imidazol-1-yl)acetohydrazide	—	—	—	—	—	—	$IC_{50} = 13.3$	184

Table 14 (*Contd.*)

Compound no.	Chemical structure and IUPAC name	Isoform targeted, IC_{50} (μM)/K_i values (nM)							Ref.
		hCA-I	hCA-II	hCA-IV	hCA-VII	hCA-IX	hCA-XII	bCA-II	
271	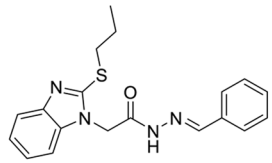 *N*′-Benzylidene-2-(2-(propylthio)-1*H*-benzo[*d*]imidazol-1-yl)acetohydrazide	—	—	—	—	—	—	$IC_{50} = 17.2$	184
272	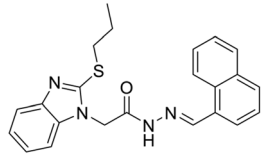 *N*′-(Naphthalen-1-ylmethylene)-2-(2-(propylthio)-1*H*-benzo[*d*]imidazol-1-yl)acetohydrazide	—	—	—	—	—	—	$IC_{50} = 14.6$	184
273	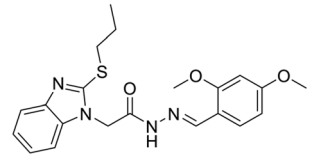 *N*′-(2,4-Dimethoxybenzylidene)-2-(2-(propylthio)-1*H*-benzo[*d*]imidazol-1-yl)acetohydrazide	—	—	—	—	—	—	$IC_{50} = 14.5$	184
274	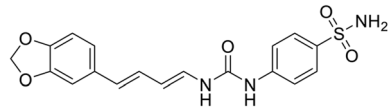 4-(3-((1*E*,3*E*)-4-(Benzo[*d*][1,3]dioxol-5-yl)buta-1,3-dien-1-yl)ureido)benzenesulfonamide	—	93.4	—	—	38.7	57.5	—	185
275	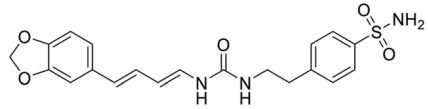 4-(2-(3-((1*E*,3*E*)-4-(Benzo[*d*][1,3]dioxol-5-yl)buta-1,3-dien-1-yl) ureido) ethyl) benzenesulfonamide	—	88.6	—	—	68.2	45.6	—	185

Table 14 (*Contd.*)

Compound no.	Chemical structure and IUPAC name	Isoform targeted, IC_{50} (μM)/K_i values (nM)							Ref.
		hCA-I	hCA-II	hCA-IV	hCA-VII	hCA-IX	hCA-XII	bCA-II	
276	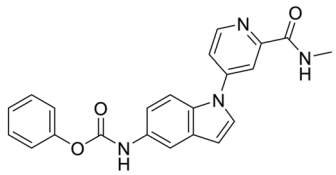 Phenyl 1-(2-(methylcarbamoyl)pyridin-4-yl)-1*H*-indol-5-ylcarbamate	—	—	—	—	—	—	IC_{50} = 0.0440	186
277	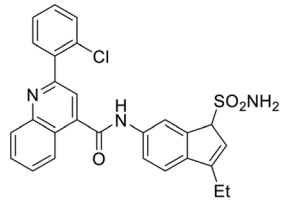 2-(2-Chlorophenyl)-*N*-(3-ethyl-1-sulfamoyl-1*H*-inden-6-yl)quinoline-4-carboxamide	—	—	—	—	1.57	—	—	187
278	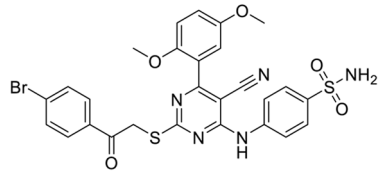 4-((2-((2-(4-Bromophenyl)-2-oxoethyl)thio)-5-cyano-6-(2,5-dimethoxyphenyl)pyrimidin-4-yl)amino)benzenesulfonamide	—	1.72	—	—	—	—	—	188
279	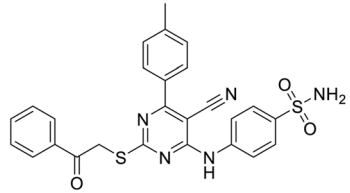 4-((5-Cyano-2-((2-oxo-2-phenylethyl)thio)-6-(*p*-tolyl)pyrimidin-4-yl)amino) benzene sulfonamide	—	—	—	—	7.4	—	—	188

Table 14 (*Contd.*)

Compound no.	Chemical structure and IUPAC name	Isoform targeted, IC_{50} (μM)/K_i values (nM)							Ref.
		hCA-I	hCA-II	hCA-IV	hCA-VII	hCA-IX	hCA-XII	bCA-II	
280	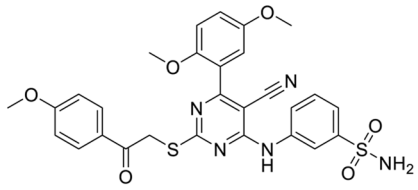 3-((5-Cyano-6-(2,5-dimethoxyphenyl)-2-((2-(4methoxy phenyl)-2-oxoethyl)thio)pyrimidin-4-yl) amino)benzenesulfonamide	—	—	—	—	7.0	4.67	—	188
281	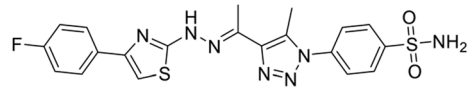 4-(4-(1-(2-(4-(4-Fluorophenyl)thiazol-2-yl)hydrazono)ethyl)-5-methyl-1*H*-1,2,3-triazol-1-yl)benzenesulfonamide	—	18.1	5416	—	279.8	—	—	189
282	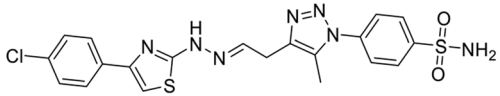 4-(4-(1-(2-(4-(4-Chlorophenyl)thiazol-2-yl)hydrazono) ethyl)-5-methyl-1*H*-1,2,3-triazol-1-yl)benzenesulfonamide	—	14.1	8871	—	7893	—	—	189
283	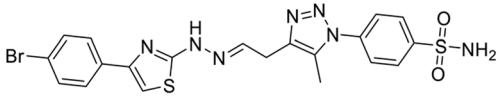 4-(4-(1-(2-(4-(4-Bromophenyl)thiazol-2-yl)hydrazono) ethyl)-5-methyl-1*H*-1,2,3-triazol-1-yl)benzenesulfonamide	—	14.9	8717	—	270.2	—	—	189
284	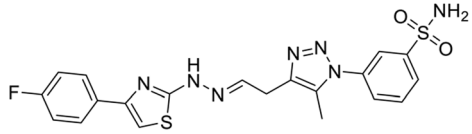 3-(4-(1-(2-(4-(4-Fluorophenyl)thiazol-2-yl)hydrazono) ethyl)-5-methyl-1*H*-1,2,3-triazol-1-yl)benzenesulfonamide	—	17.8	88	—	113	—	—	189
285	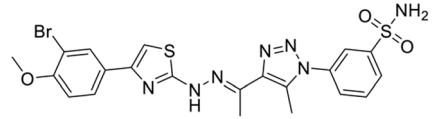 3-(4-(1-(2-(4-(3-Bromo-4-methoxyphenyl)thiazol-2-yl)hydrazono) ethyl)-5-methyl-1*H*-1,2,3-triazol-1-yl)benzenesulfonamide	—	810.4	5667	—	856	—	—	189

Table 14 (*Contd.*)

Compound no.	Chemical structure and IUPAC name	Isoform targeted, IC_{50} (μM)/K_i values (nM)							Ref.
		hCA-I	hCA-II	hCA-IV	hCA-VII	hCA-IX	hCA-XII	bCA-II	
286	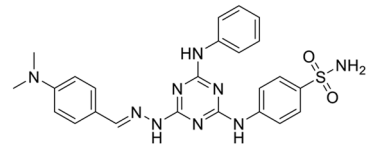 4-({4-[(*E*)-2-{[4-(Dimethylamino)phenyl]methylidene} hydrazin-1-yl]-6-(phenyl-amino)-1,3,5-triazin-2-yl}amino)benzene-1-sulfonamide	—	—	—	—	13.3	—	—	190
287	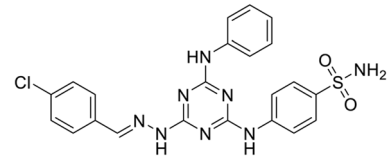 4-({4-[(*E*)-2-[(4-Chlorophenyl)methylidene] hydrazin-1-yl]-6-(phenylamino)-1,3,5-triazin-2-yl} amino)benzene-1-sulfonamide	—	—	—	—	22.6	—	—	190
288	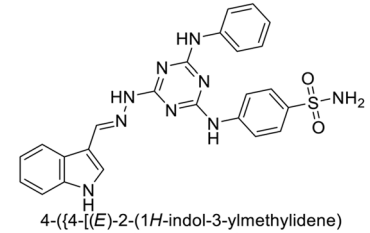 4-({4-[(*E*)-2-(1*H*-indol-3-ylmethylidene) hydrazin-1-yl]-6-(phenylamino)-1,3,5-triazin 2-yl} amino)benzene-1-sulfonamide	—	—	—	—	25.8	—	—	190
289	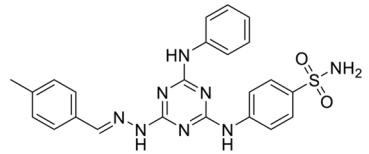 4-({4-[(*E*)-2-[(4-Methylphenyl)methylidene] hydrazin-1-yl]-6-(phenylamino)-1,3,5-triazin-2-yl} amino)benzene-1-sulfonamide	—	—	—	—	26.9	—	—	190

Table 14 (*Contd.*)

Compound no.	Chemical structure and IUPAC name	Isoform targeted, IC_{50} (μM)/K_i values (nM)							Ref.
		hCA-I	hCA-II	hCA-IV	hCA-VII	hCA-IX	hCA-XII	bCA-II	
290	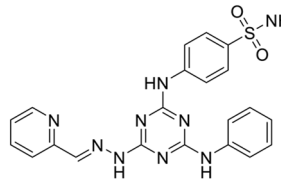 4-{[4-(Phenylamino)-6-[(*E*)-2-(pyridin-2-ylmethylidene) hydrazin-1-yl]-1,3,5-triazin -2-yl]amino} benzene-1-sulfonamide	—	—	—	—	27.2	—	—	190
291	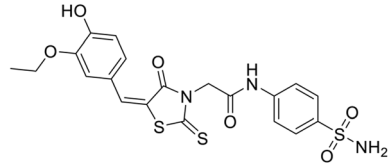 2-(5-(3-Ethoxy-4-hydroxybenzylidene)-4-oxo-2-thioxothiazolidin-3-yl)-*N*-(4-sulfamoylphenyl)acetamide	22.4	—	—	—	—	—	—	191
292	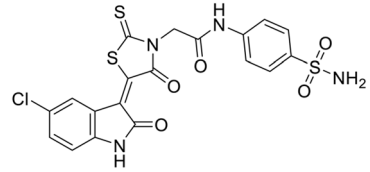 2-(5-(5-Chloro-2-oxoindolin-3-ylidene)-4-oxo-2-thioxothiazolidin-3-yl)-*N*-(4-sulfamoylphenyl) acetamide	35.8	—	—	—	—	—	—	191
293	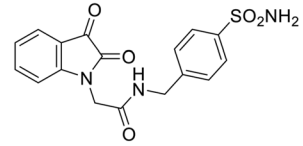 2-(2,3-Dioxoindolin-1-yl)-*N*-(4-sulfamoyl benzyl)acetamide	45.10	5.87	—	—	67.0	7.91	—	192

Table 14 (*Contd.*)

Compound no.	Chemical structure and IUPAC name	Isoform targeted, IC_{50} (μM)/K_i values (nM)							Ref.
		hCA-I	hCA-II	hCA-IV	hCA-VII	hCA-IX	hCA-XII	bCA-II	
294	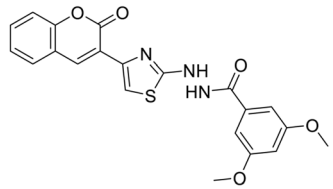 3,5-Dimethoxy-*N*'-[4-(2-oxo-2*H*-chromen-3-yl) thiazol-2-yl]benzohydrazide	—	—	—	—	505.6	91.1	—	193
295	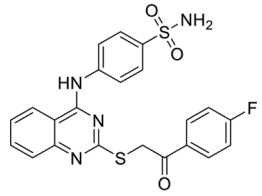 4-[(2-{[2-(4-Fluorophenyl)-2-oxoethyl]thio} quinazolin-4-yl)amino]-benzenesulfonamide	—	0.09	—	—	0.32	0.58	—	194
296	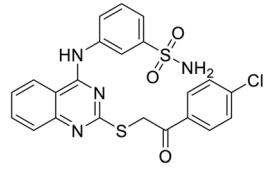 3-[(2-{[2-(4-Chlorophenyl)-2-oxoethyl]thio} quinazolin-4-yl)amino]-benzenesulfonamide	—	0.05	—	—	0.47	0.46	—	194
297	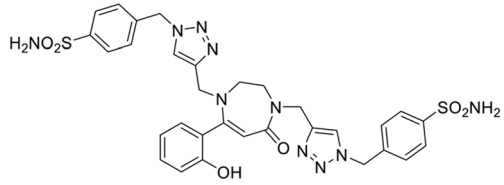 4,4'-((((7-(2-Hydroxyphenyl)-5-oxo-2,3-dihydro-1*H*-1,4-diazepine-1,4(5*H*)-diyl) bis(methylene))bis(1*H*-1,2,3-triazole-4,1-diyl)) bis(methylene))dibenzenesulfonamide	78.2	2.8	1013	8.9	13.2	6.5	—	195

Table 14 (*Contd.*)

Compound no.	Chemical structure and IUPAC name	Isoform targeted, IC_{50} (μM)/K_i values (nM)							Ref.
		hCA-I	hCA-II	hCA-IV	hCA-VII	hCA-IX	hCA-XII	bCA-II	
298	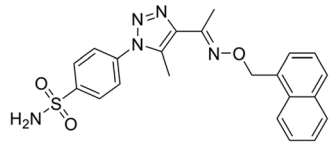 4-(5-Methyl-4-{1-[(naphthalen-1-ylmethoxy)imino]ethyl}-1*H*-1,2,3-triazol-1-yl) benzenesulfonamide	—	—	—	—	68.6	—	—	196
299	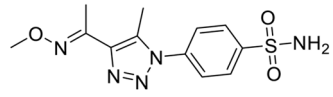 4-{4-[1-(Methoxyimino)ethyl]-5-methyl-1*H*-1,2,3-triazol-1-yl} benzenesulfonamide	—	—	—	—	56.3	—	—	196
300	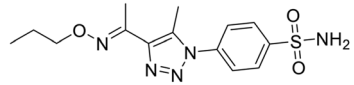 4-{5-Methyl-4-[1-(propoxyimino)ethyl]-1*H*-1,2,3-triazol-1-yl} benzenesulfonamide	—	—	—	—	—	95.6	—	196
301	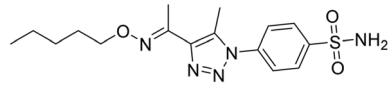 4-(5-Methyl-4-{1-[(pentyloxy)imino]ethyl}-1*H*-1,2,3-triazol-1-yl) benzenesulfonamide	—	—	—	—	—	51.5	—	196
302	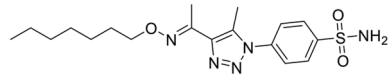 4-(4-{1-[(Heptyloxy)imino]ethyl}-5-methyl-1*H*-1,2,3-triazol-1-yl) benzenesulfonamide	47.8	—	—	—	—	—	—	196
303	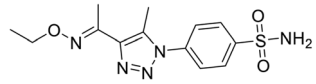 4-{4-[1-(Ethoxyimino)ethyl]-5-methyl-1*H*-1,2,3-triazol-1-yl} benzenesulfonamide	—	33.2	—	—	—	—	—	196

Table 14 (*Contd.*)

Compound no.	Chemical structure and IUPAC name	Isoform targeted, IC_{50} (μM)/K_i values (nM)							Ref.
		hCA-I	hCA-II	hCA-IV	hCA-VII	hCA-IX	hCA-XII	bCA-II	
304	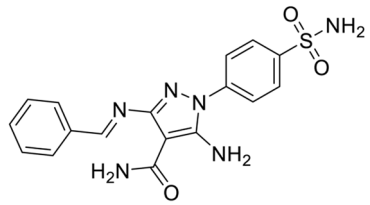 5-Amino-*N*-benzylideneamino-1-(4-sulfamoylphenyl)pyrazole-4-carboxamide	—	—	—	—	38.4	21.6	—	197
305	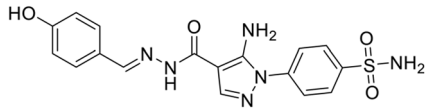 5-Amino-*N*-[(4-hydroxyphenyl)methyleneamino]-1-(4-sulfamoylphenyl)pyrazole-4-carboxamide	—	—	—	—	48.9	5.6	—	197
306	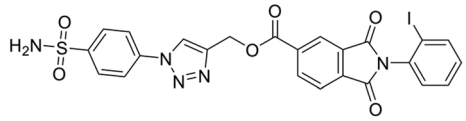 [1-(4-Sulfamoylphenyl)-1*H*-1,2,3-triazol-4-yl]methyl 2-(2-iodophenyl)-1,3-dioxoisoindoline-5-carboxylate	—	—	—	—	105.0	—	—	198
307	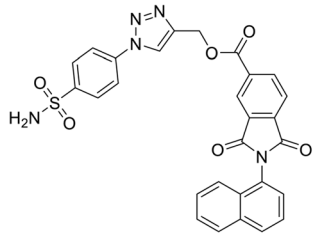 [1-(4-Sulfamoylphenyl)-1*H*-1,2,3-triazol-4-yl]methyl 2-(naphthalen-1-yl)-1,3-dioxoisoindoline-5-carboxylate	—	—	—	—	32.1	9.2	—	198

Table 14 (*Contd.*)

Compound no.	Chemical structure and IUPAC name	Isoform targeted, IC_{50} (μM)/K_i values (nM)							Ref.
		hCA-I	hCA-II	hCA-IV	hCA-VII	hCA-IX	hCA-XII	bCA-II	
308	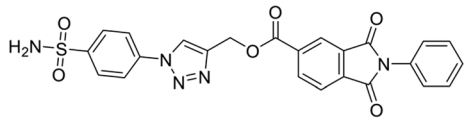 [1-(4-Sulfamoylphenyl)-1*H*-1,2,3-triazol-4-yl] methyl-1,3-dioxo-2-phenylisoindoline-5-carboxylate	—	—	—	—	18.2	50.1	—	198
309	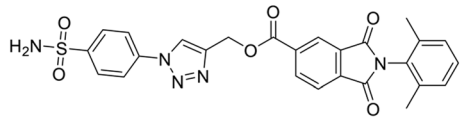 [1-(4-Sulfamoylphenyl)-1*H*-1,2,3-triazol-4-yl]methyl 2-(2,6-dimethylphenyl)-1,3-dioxoisoindoline-5-carboxylate	—	—	—	—	—	50.6	—	198
310	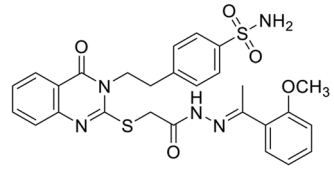 4-(2-(2-((2-(2-(1-(2-Methoxyphenyl)ethylidene) hydrazineyl)-2-oxoethyl)thio)-4-oxoquinazolin-3(4*H*)-yl)ethyl)benzenesulfonamide	—	—	—	—	8.9	64.8	—	199
311	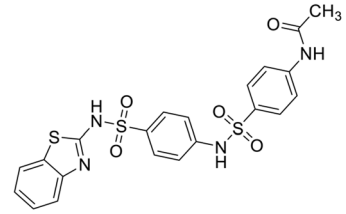 *N*-(4-(*N*-(4-(*N*-(Benzo[*d*]thiazol-2-yl)sulfamoyl)phenyl)sulfamoyl)phenyl)acetamide	0.112	0.025	—	—	—	—	—	200
312	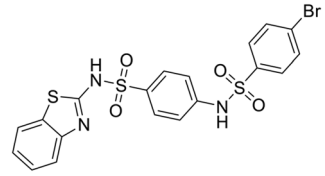 *N*-(Benzo[*d*]thiazol-2-yl)-4-((4-bromophenyl)sulfonamido)benzenesulfonamide	0.052	0.150	—	—	—	—	—	200

Table 14 (*Contd.*)

Compound no.	Chemical structure and IUPAC name	Isoform targeted, IC_{50} (μM)/K_i values (nM)							Ref.
		hCA-I	hCA-II	hCA-IV	hCA-VII	hCA-IX	hCA-XII	bCA-II	
313	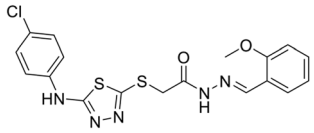 2-((5-((4-Chlorophenyl)amino)-1,3,4-thiadiazol-2-yl) thio)-*N*′-(2-methoxybenzylidene)acetohydrazide	IC_{50} = 29.74	—	—	—	—	—	—	201
314	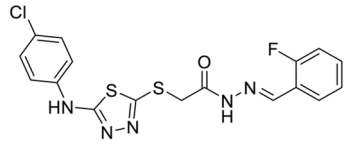 2-((5-((4-Chlorophenyl)amino)-1,3,4-thiadiazol-2-yl) thio)-*N*′-(2-fluorobenzylidene)acetohydrazide	—	IC_{50} = 23.18	—	—	—	—	—	201
315	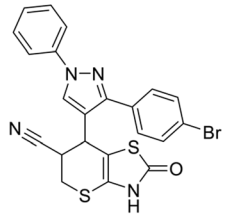 7-(3-(4-Bromophenyl)-1-phenyl-1*H*-pyrazol-4-yl)-2-oxo-3,5,6,7-tetrahydro-2*H*-thiopyrano-[2,3-*d*]thiazole-6-carbonitrile	—	—	—	—	IC_{50} = 0.067	—	—	202
316	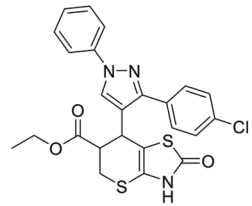 Ethyl 7-(3-(4-Chlorophenyl)-1-phenyl-1*H*-pyrazol-4-yl)-2-oxo-3,5,6,7-tetra-hydro-2*H*-thiopyrano[2,3-*d*]thiazole-6-carboxylate	—	—	—	—	—	IC_{50} = 0.123	—	202

Table 14 (*Contd.*)

Compound no.	Chemical structure and IUPAC name	Isoform targeted, IC_{50} (μM)/K_i values (nM)							Ref.
		hCA-I	hCA-II	hCA-IV	hCA-VII	hCA-IX	hCA-XII	bCA-II	
317	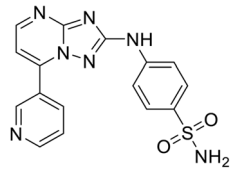 4-((7-(Pyridin-3-yl)-[1,2,4]triazolo[1,5-*a*]pyrimidin-2-yl)amino)benzenesulfonamide	—	—	—	—	5.1	8.8	—	203
318	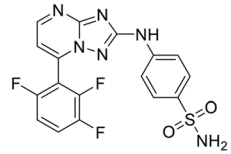 4-((7-(2,3,6-Trifluorophenyl)-[1,2,4]triazolo[1,5-*a*]pyrimidin-2-yl)amino)-benzenesulfonamide	—	—	—	—	8.6	5.4	—	203
319	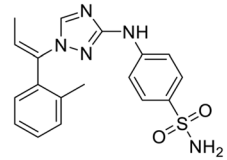 4-((7-(*o*-Tolyl)-[1,2,4]triazolo[1,5-*a*]pyrimidin-2-yl)amino)benzenesulfonamide	—	—	—	—	4.7	—	—	203
320	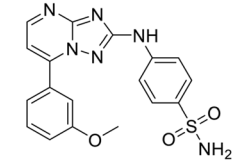 4-((7-(3-Methoxyphenyl)-[1,2,4]triazolo[1,5-*a*]pyrimidin-2-yl)amino)-benzenesulfonamide	—	—	—	—	5.1	—	—	203
321	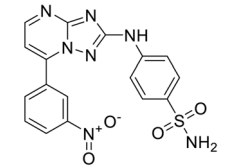 4-((7-(3-Nitrophenyl)-[1,2,4]triazolo[1,5-*a*]pyrimidin-2-yl)amino)benzenesulfonamide	—	—	—	—	—	4.3	—	203

Table 14 (*Contd.*)

Compound no.	Chemical structure and IUPAC name	Isoform targeted, IC_{50} (μM)/K_i values (nM)							Ref.
		hCA-I	hCA-II	hCA-IV	hCA-VII	hCA-IX	hCA-XII	bCA-II	
322	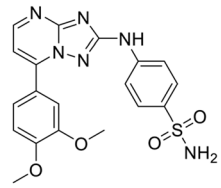 4-((7-(3,4-Dimethoxyphenyl)-[1,2,4]triazolo[1,5-*a*] pyrimidin-2-yl)amino)benzenesulfonamide	—	—	—	—	—	9.0	—	203
323	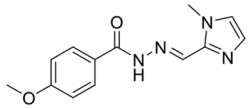 4-Methoxy-*N*′-((1-methyl-1*H*-imidazol-2-yl)methylene) benzohydrazide	0.949	—	—	—	—	—	—	204
324	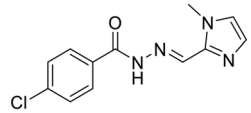 4-Chloro-*N*′-((1-methyl-1*H*-imidazol-2-yl)methylene) benzohydrazide	—	$IC_{50} = 3.3$	—	—	—	—	—	204
325	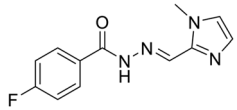 4-Fluoro-*N*′-((1-methyl-1*H*-imidazol-2-yl) methylene) benzohydrazide	—	$IC_{50} = 4.4$	—	—	—	—	—	204
326	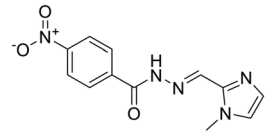 4-Nitro-*N*′-((1-methyl-1*H*-imidazol-2-yl) methylene) benzohydrazide	—	$IC_{50} = 5.6$	—	—	—	—	—	204
327	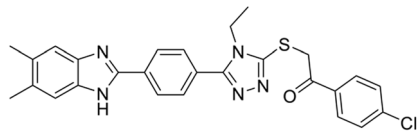 1-(4-Chlorophenyl)-2-((5-(4-(5,6-dimethyl-1*H*-benzo[*d*]imidazol-2-yl)phenyl)-4-ethyl-4*H*-1,2,4-triazol-3-yl)thio)ethan-1-one	$IC_{50} = 1.28$	—	—	—	—	—	—	205

Table 14 (*Contd.*)

Compound no.	Chemical structure and IUPAC name	Isoform targeted, IC_{50} (μM)/K_i values (nM)							Ref.
		hCA-I	hCA-II	hCA-IV	hCA-VII	hCA-IX	hCA-XII	bCA-II	
328	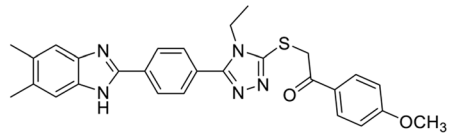 2-((5-(4-(5,6-Dimethyl-1*H*-benzo[*d*]imidazol-2-yl)phenyl)-4-ethyl-4*H*-1,2,4-triazol-3-yl)thio)-1-(4-methoxyphenyl)ethan-1-one	—	$IC_{50} = 1.53$	—	—	—	—	—	205
329	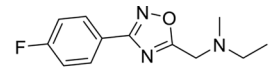 *N*-[(3-(4-Fluorophenyl)-1,2,4-oxadiazol-5-yl)methyl]-*N*-methylethanamine	$IC_{50} = 0.68$	$IC_{50} = 0.65$	—	—	—	—	—	206
330	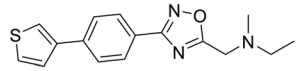 *N*-Methyl-*N*-[(3-(4-(thiophen-3-yl)phenyl)-1,2,4-oxadiazol-5-yl)methyl]ethanamine	$IC_{50} = 0.96$	$IC_{50} = 0.40$	—	—	—	—	—	206
331	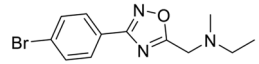 *N*-[(3-(4-Bromophenyl)-1,2,4-oxadiazol-5-yl)methyl]-*N*-methylethanamine	—	$IC_{50} = 0.40$	—	—	—	—	—	206
332	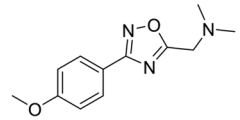 1-[3-(4-Methoxyphenyl)-1,2,4-oxadiazol-5-yl]-*N*,*N*-dimethylmethanamine	—	$IC_{50} = 0.71$	—	—	—	—	—	206
333	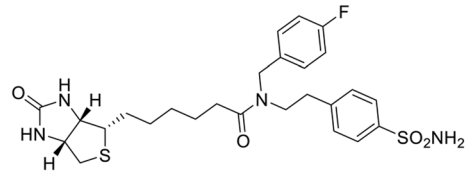 *N*-(4-Fluorobenzyl)-6-((3*aS*,4*S*,6*aR*)-2-oxohexahydro-1*H*-thieno[3,4-*d*]imidazol-4-yl)-*N*-(4-sulfamoylphenethyl)hexanamide	—	—	—	—	—	4.5	—	207

Table 14 (*Contd.*)

Compound no.	Chemical structure and IUPAC name	Isoform targeted, IC_{50} (μM)/K_i values (nM)							Ref.
		hCA-I	hCA-II	hCA-IV	hCA-VII	hCA-IX	hCA-XII	bCA-II	
334	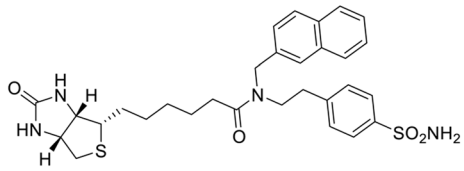 *N*-(Naphthalen-2-ylmethyl)-6-((3*aS*,4*S*,6*aR*)-2-oxo hexahydro-1*H*-thieno[3,4-*d*]imidazol-4-yl)-*N*-(4-sulfamoylphenethyl)hexanamide	—	—	—	—	6.2	—	—	207
335	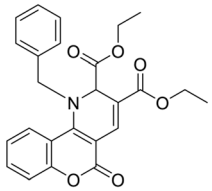 Diethyl 1-benzyl-5-oxo-1,5-dihydro-2*H*-chromeno[4,3-*b*]pyridine-2,3-dicarboxylate	$IC_{50} = 1.47$	$IC_{50} = 1.58$	—	—	—	—	—	208
336	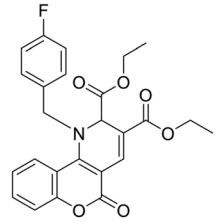 Diethyl 1-(4-fluorobenzyl)-5-oxo-1,5-dihydro-2*H*-chromeno[4,3-*b*]pyridine-2,3-dicarboxylate	$IC_{50} = 0.88$	$IC_{50} = 1.10$	—	—	—	—	—	208
337	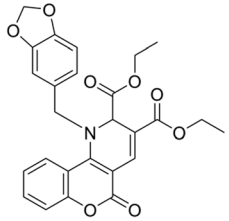 Diethyl 1-(benzo[*d*][1,3]dioxol-5-ylmethyl)-5-oxo-1,5-dihydro-2*H*-chromeno[4,3-*b*]pyridine-2,3-dicarboxylate	$IC_{50} = 1.33$	$IC_{50} = 1.53$	—	—	—	—	—	208

Table 14 (*Contd.*)

Compound no.	Chemical structure and IUPAC name	Isoform targeted, IC_{50} (μM)/K_i values (nM)							Ref.
		hCA-I	hCA-II	hCA-IV	hCA-VII	hCA-IX	hCA-XII	bCA-II	
338	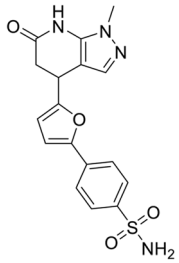 4-(5-(1-Methyl-6-oxo-4,5,6,7-tetrahydro-1*H*-pyrazolo[3,4-*b*]pyridin-4-yl)furan-2-yl)benzenesulfonamide	20.0	5.5	—	—	—	—	—	209
339	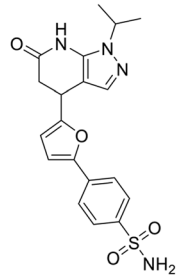 4-(5-(1-Isopropyl-6-oxo-4,5,6,7-tetrahydro-1*H*-pyrazolo[3,4-*b*]pyridin-4-yl)furan-2-yl)benzenesulfonamide	6.30	4.00	—	—	—	—	—	209
340	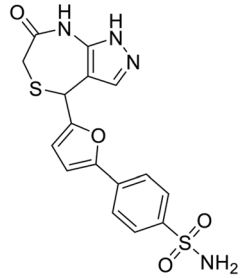 4-(5-(7-Oxo-4,6,7,8-tetrahydro-1*H*-pyrazolo [3,4-*e*][1,4]thiazepin- 4-yl)furan-2-yl) benzenesulfonamide	17.5	5.8	—	—	—	—	—	209

Table 14 (*Contd.*)

Compound no.	Chemical structure and IUPAC name	Isoform targeted, IC_{50} (μM)/K_i values (nM)							Ref.
		hCA-I	hCA-II	hCA-IV	hCA-VII	hCA-IX	hCA-XII	bCA-II	
341	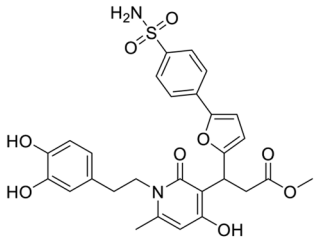 Methyl 3-(1-(3,4-dihydroxyphenethyl)-4-hydroxy-6-methyl-2-oxo-1,2- dihydropyridin-3-yl)-3-(5-(4-sulfamoylphenyl)furan-2-yl)propanoate	23.2	5.9	—	—	—	—	—	209
342	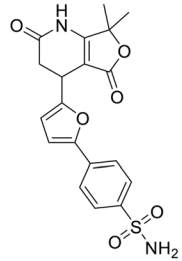 4-(5-(7,7-Dimethyl-2,5-dioxo-1,2,3,4,5,7-hexahydrofuro[3,4-*b*]pyridin-4-yl)furan-2-yl)benzenesulfonamide	—	—	6.5	16.8	—	—	—	209
343	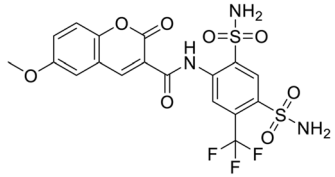 *N*-(2,4-disulfamoyl-5-(trifluoromethyl) phenyl)-6-methoxy-2-oxo-2*H*-chromene-3-carboxamide	—	—	—	—	21	5	—	210

Table 14 (*Contd.*)

Compound no.	Chemical structure and IUPAC name	Isoform targeted, IC_{50} (μM)/K_i values (nM)							Ref.
		hCA-I	hCA-II	hCA-IV	hCA-VII	hCA-IX	hCA-XII	bCA-II	
344	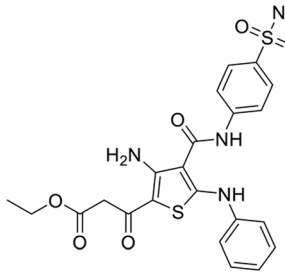 Ethyl 3-(3-amino-5-(phenylamino)-4-((4-sulfamoylphenyl)carbamoyl)thiophen-2-yl)-3-oxopropanoate	—	—	—	—	0.092	—	—	211
345	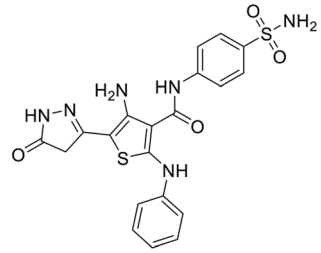 3-Amino-2-(5-oxo-4,5-dihydro-1*H*-pyrazol-3-yl)-5-(phenylamino)-*N*-(4-sulfamoylphenyl) thiophene-4-carboxamide	—	—	—	—	0.069	—	—	211
346	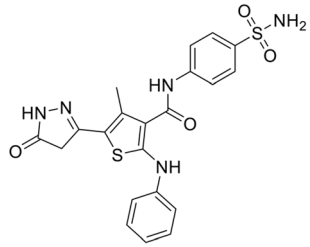 4-Methyl-5-(5-oxo-4,5-dihydro-1*H*-pyrazol-3-yl)-2-(phenylamino)-*N*-(4-sulfamoylphenyl) thiophene-3-carboxamide	—	—	—	—	—	IC_{50} = 0.173	—	211

Table 14 (*Contd.*)

Compound no.	Chemical structure and IUPAC name	Isoform targeted, IC_{50} (μM)/K_i values (nM)							Ref.
		hCA-I	hCA-II	hCA-IV	hCA-VII	hCA-IX	hCA-XII	bCA-II	
347	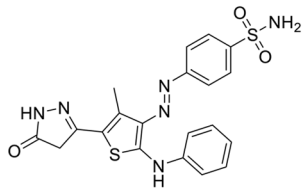 4-((4-Methyl-5-(5-oxo-4,5-dihydro-1*H*-pyrazol-3-yl) -2-(phenylamino)thiophen-3-yl)azo) benzenesulfonamide	—	—	—	—	—	$IC_{50} = 0.146$	—	211
348	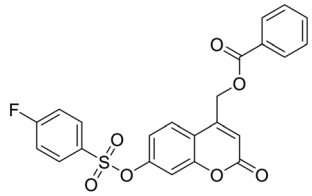 {7-[(4-Fluorophenylsulfonyl)oxy]-2-oxo-2*H*- benzopyran-4-y}methyl benzoate	—	$IC_{50} = 0.62$	—	—	—	—	—	212
349	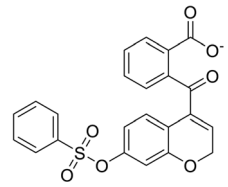 2-Oxo-7-[(phenylsulfonyl)oxy]-2*H*- benzopyran-4-ylmethylbenzoate	—	—	—	—	—	$IC_{50} = 0.56$	—	212
350	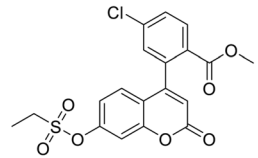 {7-[(Ethylsulfonyl)oxy]-2-oxo-2*H*- benzopyran-4-yl}methyl-4-chlorobenzoate	—	$IC_{50} = 0.069$	—	—	—	—	—	212

Table 14 (*Contd.*)

Compound no.	Chemical structure and IUPAC name	Isoform targeted, IC_{50} (μM)/K_i values (nM)							Ref.
		hCA-I	hCA-II	hCA-IV	hCA-VII	hCA-IX	hCA-XII	bCA-II	
351	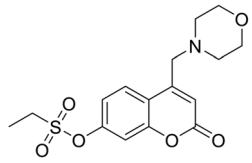 4-(Morpholinomethyl)-2-oxo-2*H*-benzopyran-7-ylethanesulfonate	—	$IC_{50} = 0.173$	—	—	—	—	—	212
352	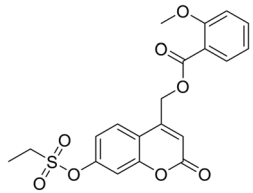 {7-[(Ethylsulfonyl)oxy]-2-oxo-2*H*-benzopyran-4-yl}methyl 2-methoxybenzoate	—	$IC_{50} = 0.146$	—	—	—	—	—	212
353	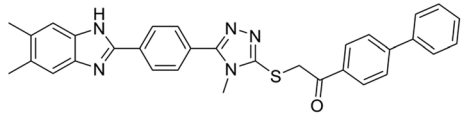 1-([1,1'-biphenyl]4-yl)2-((5-(4-(5,6-dimethyl-1*H*-benzo[*d*]imidazole-2-yl)-phenyl)4-methyl-4*H*-1,2,4-triazol-3-yl)thio)ethan-1-one	1.288	1.699	—	—	—	—	—	213
354	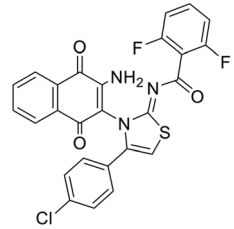 *N*-[3-(3-amino-1,4-dioxo-1,4-dihydronaphthalen-2-yl)-4-(4-chlorophenyl)thiazol-2(3*H*)-ylidene]-2,6-difluorobenzamide	67.8	56.8	—	—	—	—	—	214

Table 14 (*Contd.*)

Compound no.	Chemical structure and IUPAC name	Isoform targeted, IC_{50} (μM)/K_i values (nM)							Ref.
		hCA-I	hCA-II	hCA-IV	hCA-VII	hCA-IX	hCA-XII	bCA-II	
355	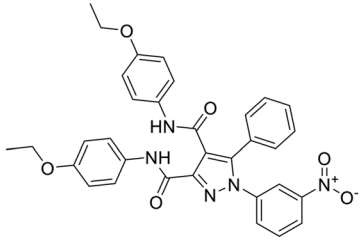 N^3,N^4-Bis(4-ethoxyphenyl)- 1-(3-nitrophenyl)-5-phenyl-1*H*-pyrazole-3,4-dicarboxamide	11.27	—	—	—	—	—	—	215
356	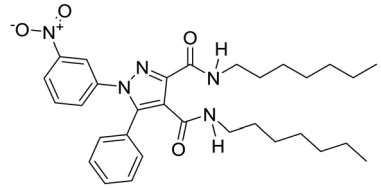 N^3,N^4-Diheptyl-1-(3-nitrophenyl)-5-phenyl-1*H*-pyrazole-3,4-dicarboxamide	—	9.97	—	—	—	—	—	215
357	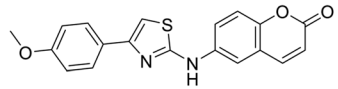 6-((4-(4-Methoxyphenyl)thiazol-2-yl) amino)-2*H*-chromen-2-one	—	—	—	—	—	90.9	—	216
358	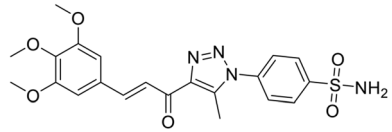 4-{4-[3-(3,4,5-Trimethoxyphenyl)acryloyl]-5-methyl-1*H*-1,2,3-triazol-1-yl} benzenesulfonamide	—	—	—	—	0.063	—	—	217
359	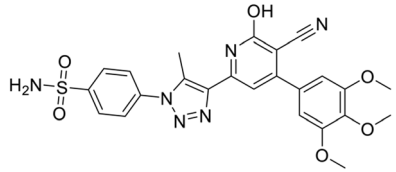 4-{4-[5-Cyano-6-hydroxy-4-(3,4,5-trimethoxyphenyl) pyridine-2-yl]-5-methyl-1*H*-1,2,3-triazol-1-yl} benzenesulfonamide	—	—	—	—	0.036	—	—	217

Table 14 (*Contd.*)

Compound no.	Chemical structure and IUPAC name	Isoform targeted, IC_{50} (μM)/K_i values (nM)							Ref.
		hCA-I	hCA-II	hCA-IV	hCA-VII	hCA-IX	hCA-XII	bCA-II	
360	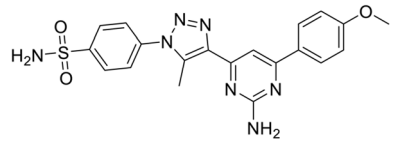 4-{4-[2-Amino-6-(4-methoxyphenyl) pyrimidin-4-yl]-5-methyl-1*H*-1,2,3-triazol-1-yl} benzenesulfonamide	—	—	—	—	0.06	—	—	217
361	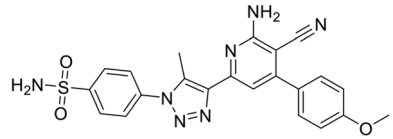 4-{4-[6-Amino-5-cyano-4-(4-methoxyphenyl) pyridine-2-yl]-5-methyl-1*H*-1,2,3-triazol-1-yl} benzenesulfonamide	—	—	—	—	—	0.021	—	217
362	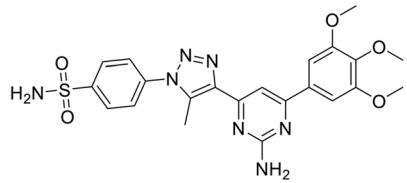 4-{4-[2-Amino-6-(3,4,5-trimethoxyphenyl) pyrimidin-4-yl]-5-methyl-1*H*-1,2,3-triazol-1-yl} benzenesulfonamide	—	—	—	—	—	0.022	—	217
363	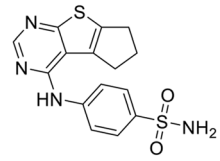 4-((6,7-Dihydro-5*H*-cyclopenta[4,5]thieno[2,3-*d*] pyrimidin-4yl)amino)benzenesulfonamide	—	—	—	—	—	20.2	—	218
364	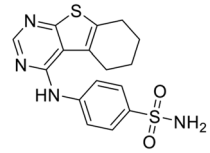 4-((5,6,7,8-Tetrahydrobenzo[4,5]thieno[2,3-*d*] pyrimidin-4 yl)amino)benzenesulfonamide	826.5	—	—	—	—	—	—	218

Table 14 (*Contd.*)

Compound no.	Chemical structure and IUPAC name	Isoform targeted, IC_{50} (μM)/K_i values (nM)							Ref.
		hCA-I	hCA-II	hCA-IV	hCA-VII	hCA-IX	hCA-XII	bCA-II	
365	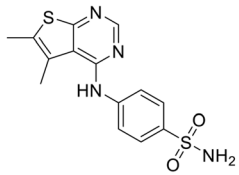 4-((5,6-Dimethylthieno[2,3-*d*]pyrimidin-4-yl)amino)benzenesulfonamide	—	—	—	—	16.9	—	—	218
366	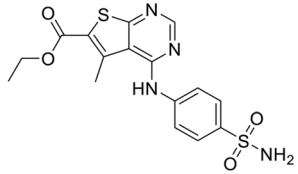 Ethyl-5-methyl-4-((4-sulfamoylphenyl)amino) thieno[2,3-*d*]pyrimidine-6-carboxylate	—	8.6	—	—	—	—	—	218
367	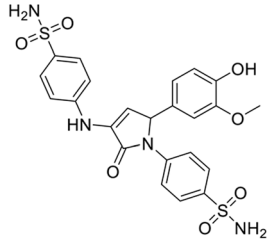 5-(4-Hydroxy-3-methoxyphenyl)-1-(4-sulfamoylphenyl)-3-((4-sulfamoylphenyl)amino)-1*H*-pyrrol-2(5*H*)-one	3.9	—	—	—	—	—	—	219
368	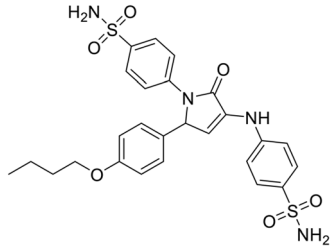 5-(4-Butoxyphenyl)-1-(4-sulfamoylphenyl)-3-((4-sulfamoylphenyl)amino)-1*H*-pyrrol-2(5*H*)-one	—	—	—	—	1.9	—	—	219

Table 14 (*Contd.*)

Compound no.	Chemical structure and IUPAC name	Isoform targeted, IC_{50} (μM)/K_i values (nM)							Ref.
		hCA-I	hCA-II	hCA-IV	hCA-VII	hCA-IX	hCA-XII	bCA-II	
369	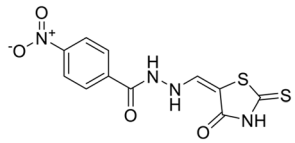 4-Nitro-*N*'-[(4-oxo-2-thioxothiazolidin-5-ylidene) methyl]benzohydrazide	—	9.5	—	—	—	—	—	220
370	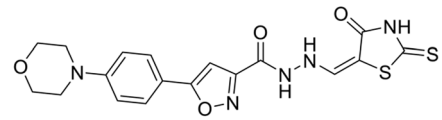 5-(4-Morpholinophenyl)-*N*'-[(4-oxo-2-thioxothiazolidin-5-ylidene)methyl]isoxazole-3-carbohydrazide	—	63.9	—	—	—	—	—	220
371	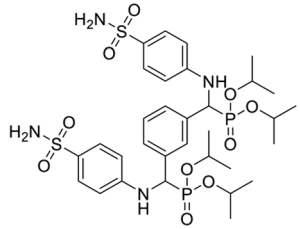 Tetraisopropyl (1,3-phenylenebis{[(4-sulfamoylphenyl)amino] methylene})bis(phosphonate)	—	—	—	—	15.1	—	—	221
372	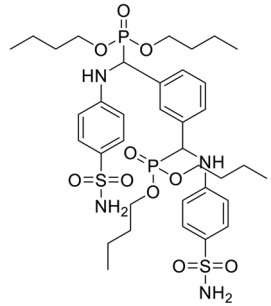 Tetrabutyl (1,3-phenylenebis{[(4-sulfamoylphenyl)amino]methylene}) bis(phosphonate)	—	—	—	—	—	17.2	—	221

Table 14 (*Contd.*)

Compound no.	Chemical structure and IUPAC name	Isoform targeted, IC_{50} (μM)/K_i values (nM)							Ref.
		hCA-I	hCA-II	hCA-IV	hCA-VII	hCA-IX	hCA-XII	bCA-II	
373	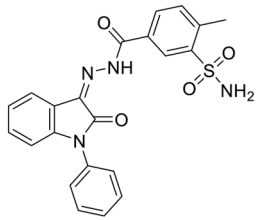 2-Methyl-5-[2-(2-oxo-1-phenylindolin-3-ylidene)hydrazine-1-carbonyl] benzenesulfonamide	435.8	—	—	—	—	—	—	222
374	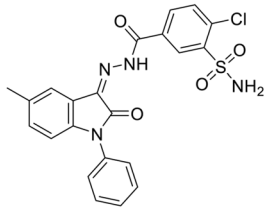 2-Chloro-5-[2-(5-methyl-2-oxo-1-phenylindolin-3-ylidene)hydrazine-1-carbonyl] benzenesulfonamide	956.4	—	—	—	—	—	—	222
375	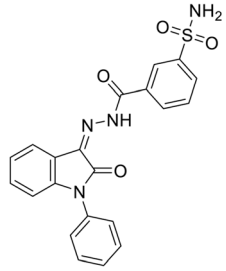 3-[2-(2-Oxo-1-phenylindolin-3-ylidene) hydrazine-1-carbonyl] benzenesulfonamide	—	—	—	—	60.5	—	—	222

Table 14 (*Contd.*)

Compound no.	Chemical structure and IUPAC name	Isoform targeted, IC_{50} (μM)/K_i values (nM)							Ref.
		hCA-I	hCA-II	hCA-IV	hCA-VII	hCA-IX	hCA-XII	bCA-II	
376	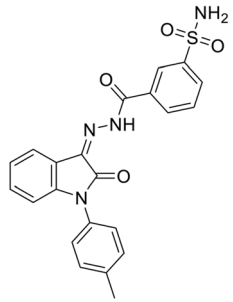 3-{2-[2-Oxo-1-(*p*-tolyl)indolin-3-ylidene] hydrazine-1-carbonyl} benzenesulfonamide	—	—	—	—	95.6	—	—	222
377	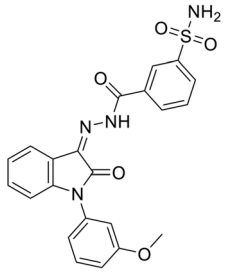 3-{2-[1-(3-Methoxyphenyl)-2-oxoindolin-3-ylidene]hydrazine-1-carbonyl} benzenesulfonamide	—	—	—	—	92.1	—	—	222
378	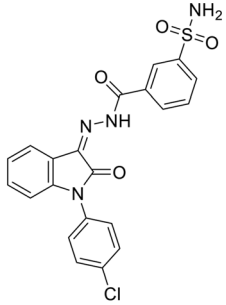 3-{2-[1-(4-Chlorophenyl)-2-oxoindolin-3-ylidene]hydrazine-1-carbonyl} benzene-sulfonamide	—	—	—	—	75.4	—	—	222

Table 14 (*Contd.*)

Compound no.	Chemical structure and IUPAC name	Isoform targeted, IC_{50} (μM)/K_i values (nM)							Ref.
		hCA-I	hCA-II	hCA-IV	hCA-VII	hCA-IX	hCA-XII	bCA-II	
379	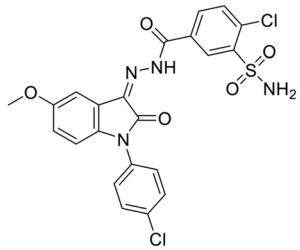 2-Chloro-5-{2-[1-(4-chlorophenyl)-5-methoxy-2-oxoindolin-3-ylidene]hydrazine-1-carbonyl} benzenesulfonamide	—	—	—	—	—	84.5	—	222
380	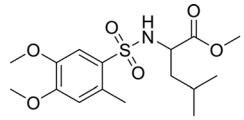 Methyl [(4,5-dimethoxy-2-methylphenyl)sulfonyl]-DL-leucinate	—	39.2	—	—	—	—	—	223
381	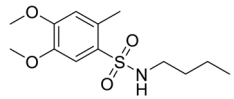 *N*-Butyl-4,5-dimethoxy-2-methylbenzenesulfonamide	—	50.9	—	—	—	—	—	223
382	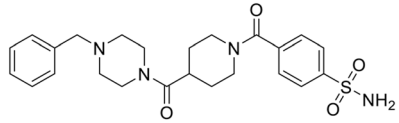 4-(4-(4-Benzylpiperazine-1-carbonyl)piperidine-1-carbonyl)benzenesulfonamide	—	—	—	—	8.3	2.7	—	224
383	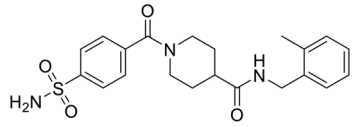 *N*-(2-Methylbenzyl)-1-(4-sulfamoylbenzoyl) piperidine-4-carboxamide	—	—	—	—	8.4	6.9	—	224

Table 14 (*Contd.*)

Compound no.	Chemical structure and IUPAC name	Isoform targeted, IC_{50} (μM)/K_i values (nM)							Ref.
		hCA-I	hCA-II	hCA-IV	hCA-VII	hCA-IX	hCA-XII	bCA-II	
384	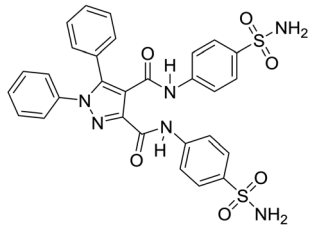 1,5-Diphenyl-N^3,N^4-bis(4-sulfamoylphenyl)-1H-pyrazole-3,4-dicarboxamide	—	0.121	—	—	—	—	—	225
385	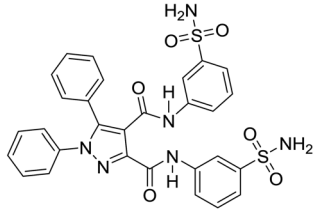 1,5-Diphenyl-N^3,N^4-bis(3-sulfamoylphenyl) -1H-pyrazole-3,4-dicarboxamide	0.330	0.188	—	—	—	—	—	225
386	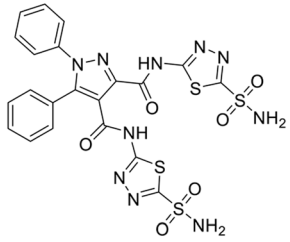 1,5-Diphenyl-N^3,N^4-bis(5-sulfamoyl-1,3,4-thiadiazol-2-yl)-1*H*-pyrazole-3,4-dicarboxamide	0.332	0.032	—	—	—	—	—	225
387	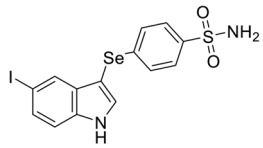 4-[(5-Iodo-1*H*-indol-3-yl)selanyl] benzenesulfonamide	—	6.9	—	—	—	—	—	226

Table 14 (*Contd.*)

Compound no.	Chemical structure and IUPAC name	Isoform targeted, IC_{50} (μM)/K_i values (nM)							Ref.
		hCA-I	hCA-II	hCA-IV	hCA-VII	hCA-IX	hCA-XII	bCA-II	
388	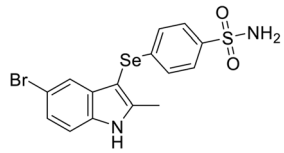 4-[(5-Bromo-2-methyl-1*H*-indol-3-yl) selanyl]benzenesulfonamide	—	6.2	—	—	—	—	—	226
389	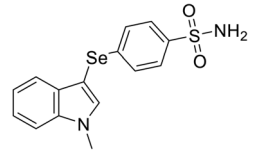 4-[(1-Methyl-1*H*-indol-3-yl)selanyl] benzenesulfonamide	—	6.0	—	—	—	—	—	226
390	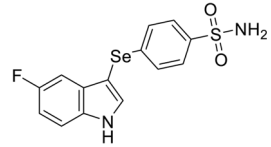 4-[(5-Fluoro-1*H*-indol-3-yl)selanyl] benzenesulfonamide	—	—	—	—	2.9	—	—	226
391	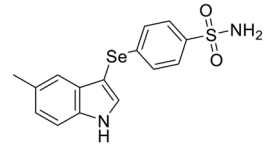 4-[(5-Methyl-1*H*-indol-3-yl)selanyl] benzenesulfonamide	—	—	—	—	2.1	—	—	226
392	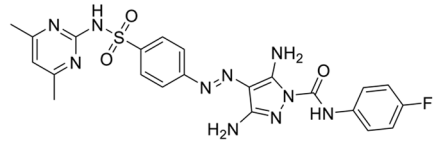 3,5-Diamino-4-((4-(*N*-(4,6-dimethylpyrimidin-2-yl)sulfamoyl)phenyl)diazenyl)-*N*-(4-fluorophenyl) -1*H*-pyrazole-1-carboxamide	—	0.188	—	—	—	—	—	227

Table 14 (*Contd.*)

Compound no.	Chemical structure and IUPAC name	Isoform targeted, IC_{50} (μM)/K_i values (nM)							Ref.
		hCA-I	hCA-II	hCA-IV	hCA-VII	hCA-IX	hCA-XII	bCA-II	
393	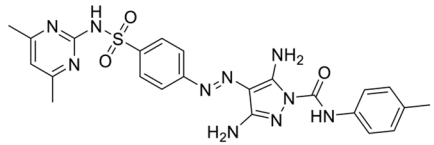 3,5-Diamino-4-((4-(*N*-(4,6-dimethylpyrimidin-2-yl)sulfamoyl)phenyl)diazenyl)-*N*-(p-tolyl)-1*H*-pyrazole-1-carboxamide	0.332	—	—	—	—	—	—	227
394	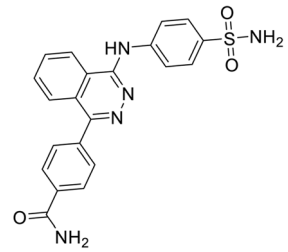 4-(4-((4-Sulfamoylphenyl)amino) phthalazin-1-yl)benzamide	—	1.6	—	—	3.7	—	—	228
395	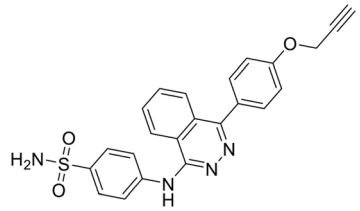 4-((4-(4-(Prop-2-yn-1-yloxy)phenyl)phthalazin-1-yl)amino)benzenesulfonamide	—	52.8	—	—	8.9	—	—	228
396	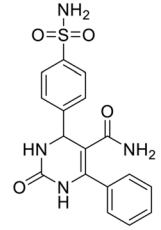 2-Oxo-6-phenyl-4-(4-sulfamoylphenyl)-1,2,3,4-tetrahydropyrimidine-5-carboxamide	—	—	—	—	6.6	8.9	—	229

Table 14 (*Contd.*)

Compound no.	Chemical structure and IUPAC name	Isoform targeted, IC_{50} (μM)/K_i values (nM)							Ref.
		hCA-I	hCA-II	hCA-IV	hCA-VII	hCA-IX	hCA-XII	bCA-II	
397	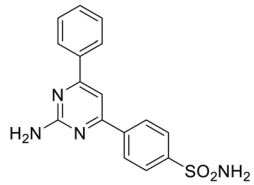 4-(2-Amino-6-phenylpyrimidin-4-yl) benzenesulfonamide	—	—	—	—	8.9	5.3	—	229
398	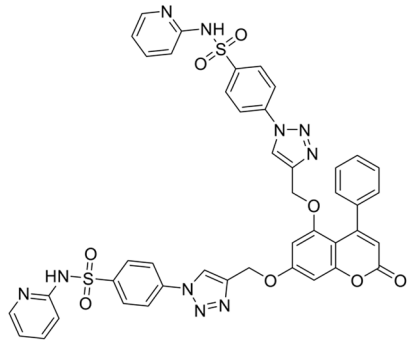 4,4'-((((2-Oxo-4-phenyl-2*H*-chromene-5,7 diyl)bis(oxy))bis(methylene))bis(1*H*-1,2,3-triazole-4,1-diyl))bis(*N*-(pyridin-2-yl)benzenesulfonamide)	—	—	—	—	$IC_{50} = 0.113$	—	—	230
399	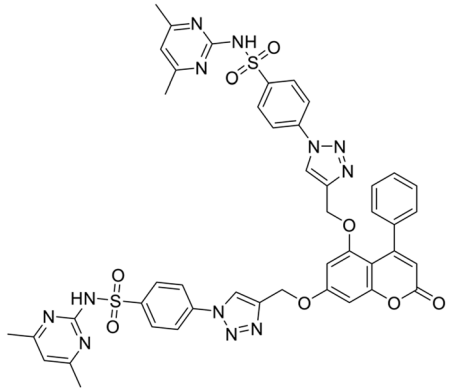 4,4'-((((2-Oxo-4-phenyl-2*H*-chromene-5,7-diyl)bis(oxy))bis(methylene))bis(1*H*-1,2,3-triazole-4,1-diyl))bis(*N*-(4,6-dimethylpyrimidin-2-yl)benzenesulfonamide)	—	—	—	—	$IC_{50} = 0.134$	—	—	230

Table 14 (*Contd.*)

Compound no.	Chemical structure and IUPAC name	Isoform targeted, IC_{50} (μM)/K_i values (nM)							Ref.
		hCA-I	hCA-II	hCA-IV	hCA-VII	hCA-IX	hCA-XII	bCA-II	
400	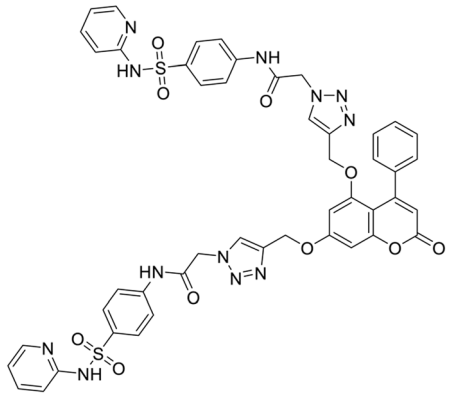 2,2'-((((2-Oxo-4-phenyl-2*H*-chromene-5,7-diyl)bis(oxy))bis(methylene))bis(1*H*-1,2,3-triazole-4,1-diyl))bis(*N*-(4-(*N*-(pyridin-2-yl)sulfamoyl)phenyl)acetamide)	—	—	—	—	$IC_{50} = 0.214$	—	—	230
401	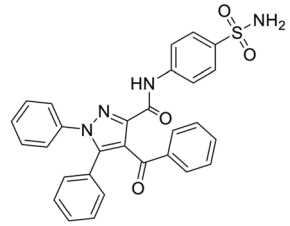 4-Benzoyl-1,5-diphenyl-*N*-(4-sulfamoylphenyl)-1*H*-pyrazole-3-carboxamide	$IC_{50} = 0.420$	$IC_{50} = 0.310$	—	—	—	—	—	231

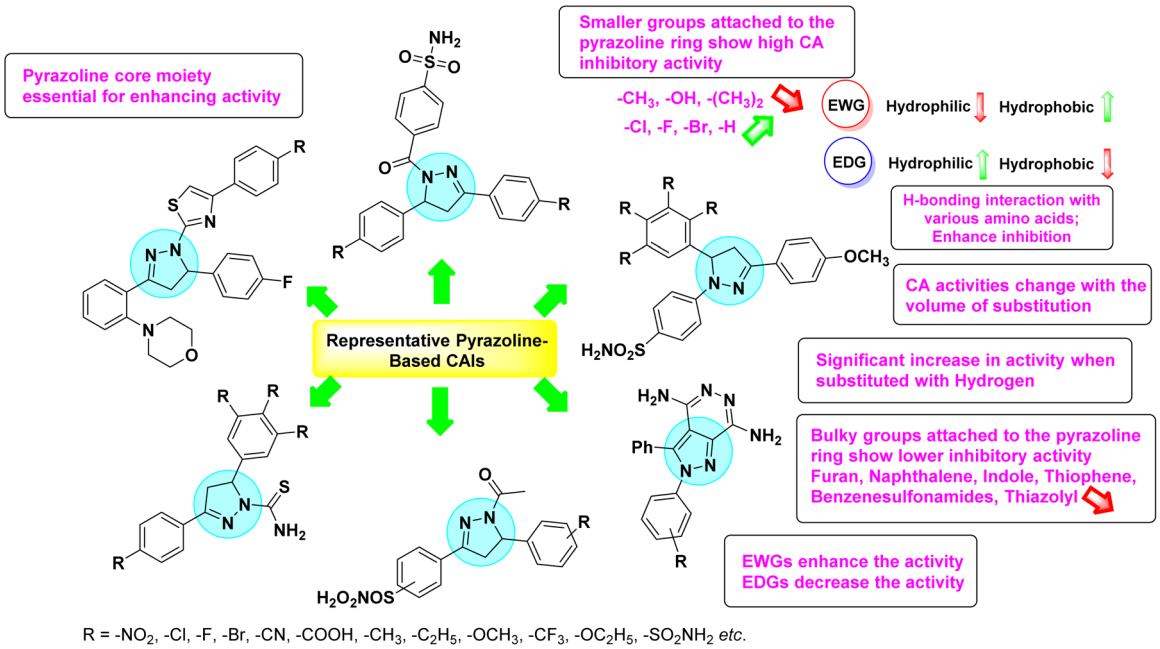

Fig. 144 SAR of pyrazoline-based CAIs.

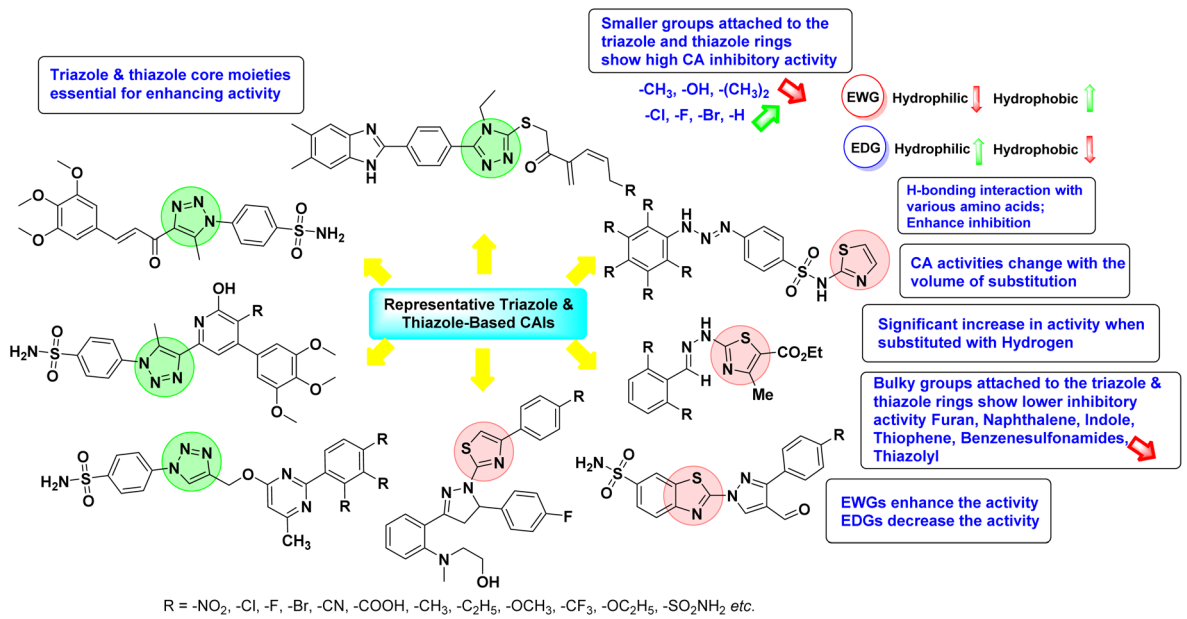

Fig. 145 SAR of triazole and thiazole-based CAIs.

bonds are observed in docking studies to significantly increase binding affinity. The positioning of electron-donating or withdrawing groups in relation to the hydrogen bonding residues in the enzyme is a determining factor in the compound's inhibitory efficiency.

7.2. Triazole and thiazole-based CAIs

7.2.1 Triazole CAIs. Triazole rings, due to their aromatic and heterocyclic nature, are frequently utilized as scaffolds in the design of CAIs. The presence of different substituents on the triazole ring can significantly alter the compound's interaction with the enzyme's active site (Fig. 145).

7.2.1.1. Electron-donating groups. Alkyl groups such as methyl ($-CH_3$) or ethyl ($-C_2H_5$) attached to the triazole ring tend to increase the electron density of the ring, enhancing hydrophobic interactions with the enzyme's active site. These interactions typically involve nonpolar residues in the enzyme, such as Val121 and Leu198 in hCA-II. Docking studies often show that these EDGs stabilize the triazole ring within the

hydrophobic pocket of the enzyme, improving the binding affinity and selectivity of the inhibitor, particularly for isoforms like hCA-I and hCA-II.

The presence of hydroxyl or amino groups introduces the possibility of forming hydrogen bonds with key active site residues, such as Thr199 and His94 in hCA-II. These interactions are critical for enhancing the binding affinity and specificity of the inhibitor. Molecular docking simulations often reveal that these groups engage in strong hydrogen bonds, leading to enhanced stabilization of the inhibitor within the active site. This interaction is particularly beneficial for improving selectivity towards certain hCA isoforms.

7.2.1.2. Electron-withdrawing groups. Halogens, particularly fluorine (–F) and chlorine (–Cl), when attached to the triazole ring, decrease the electron density, which can strengthen interactions with the zinc ion at the enzyme's active site. These substituents also contribute to enhanced van der Waals interactions with hydrophobic residues. Docking studies often show that halogen atoms participate in halogen bonding with residues such as Thr199 or zinc-bound water molecules, which stabilizes the inhibitor and increases its potency against isoforms like hCA-IX and hCA-XII.

Strong EWGs like nitro (–NO_2) and cyano (–CN) enhance the affinity of triazole-based CAIs for the zinc ion by creating a more favorable electronic environment for interaction with the metal center. Docking studies demonstrate that these groups often form electrostatic interactions with the zinc ion or polar residues near the active site, such as His64 or His94. This leads to stronger inhibition, particularly against tumor-associated hCA isoforms, where the zinc ion plays a crucial role in enzymatic activity.

7.2.2 Thiazole-based CAIs. Thiazole rings, like triazoles, are valuable scaffolds in CAI design due to their aromaticity and the presence of both sulfur and nitrogen atoms, which can engage in various types of interactions with the enzyme.

7.2.2.1. Electron-donating groups. The addition of alkyl groups (methyl and isopropyl) to the thiazole ring increases hydrophobic character, which can enhance the interaction of the inhibitor with nonpolar residues in the enzyme's active site. Docking studies often show that alkyl-substituted thiazoles engage in van der Waals interactions with hydrophobic residues such as Leu198 and Val121 in hCA-II, contributing to better stabilization within the active site.

These groups hydroxyl (–OH) and alkoxy (–OR) can form hydrogen bonds with polar residues in the active site, enhancing the binding affinity of the inhibitor. The presence of a hydroxyl group on the thiazole ring may allow interaction with residues such as Thr199 or Glu106 in hCA-II, enhancing specificity. Docking simulations suggest that these groups stabilize the inhibitor through hydrogen bonding and may also participate in water-mediated interactions with the zinc ion, leading to improved inhibitory potency.

7.2.2.2. Electron-withdrawing groups. Halogen atoms (–Cl, –Br), when attached to the thiazole ring, can participate in both halogen bonding and electrostatic interactions with residues near the zinc ion. This is particularly true for fluorine, which can increase binding affinity by forming stable interactions with polarizable residues or the zinc ion. Molecular docking studies frequently reveal that halogenated thiazoles exhibit stronger binding affinities due to these interactions, particularly with hCA-IX and XII, where halogen atoms can enhance the inhibitor's potency by stabilizing the compound in the active site.

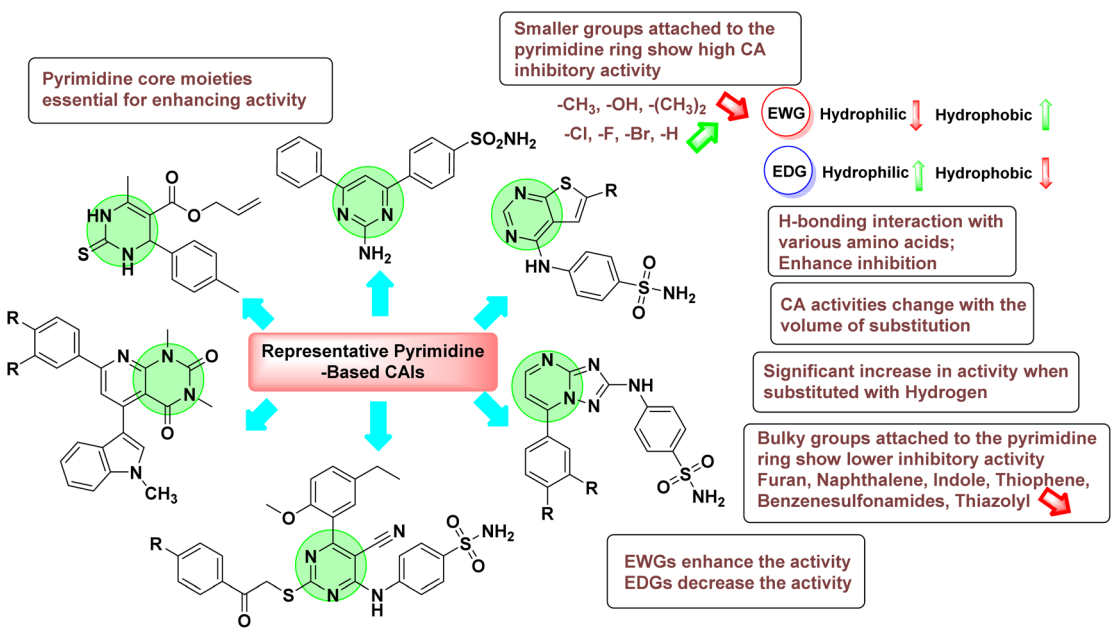

Fig. 146 SAR of pyrimidine-based CAIs.

The introduction of nitro or sulfonamide groups enhances the binding affinity of thiazole-based CAIs by facilitating strong interactions with the zinc ion in the active site. The sulfonamide group, in particular, is well-known for its ability to chelate the zinc ion, which is a key mechanism of action for many CAIs. Docking studies show that these EWGs enhance the inhibitory activity by forming coordinate bonds with the zinc ion and additional hydrogen bonds with surrounding amino acid residues. This is especially effective against hCA-IX and XII isoforms, where such interactions are critical for potent inhibition.

7.2.3 Molecular docking studies. Molecular docking studies provide detailed insights into how triazole- and thiazole-based CAIs interact with the active site of hCA isoforms. These studies simulate the binding process and allow the identification of key interactions that contribute to the inhibitor's potency and selectivity.

7.2.3.1. Interaction with zinc ion. Both triazole and thiazole derivatives, particularly those with EWGs like sulfonamide or nitro, demonstrate strong interactions with the zinc ion. The binding mechanism typically involves the coordination of these groups with the zinc ion, leading to effective inhibition of enzymatic activity.

7.2.3.2. Hydrophobic and van der Waals interactions. The hydrophobic nature of alkyl-substituted triazoles and thiazoles allows these inhibitors to fit snugly within the enzyme's hydrophobic pocket, enhancing binding affinity. Docking simulations reveal that these interactions are crucial for stabilizing the inhibitor within the active site, particularly in isoforms like hCA-I and hCA-II.

7.2.3.3. Hydrogen bonding and π–π stacking. Triazoles and thiazoles with hydroxyl, amino, or carboxyl groups are often involved in hydrogen bonding with key residues such as Thr199, His94, and Glu106. These interactions are crucial for enhancing the binding affinity and selectivity of the inhibitors, as demonstrated by docking studies. π–π Stacking interactions, particularly with aromatic residues within the active site, also play a significant role in stabilizing the inhibitor, contributing to its overall potency.

7.3. Pyrimidine-based CAIs

Pyrimidine rings are commonly employed in CAI design due to their aromatic nature and nitrogen atoms, which can engage in various interactions with the active site of hCA isoforms. The substitution patterns on the pyrimidine ring play a crucial role in determining the activity and selectivity of the inhibitors (Fig. 146).

7.3.1 Electron-donating groups. Alkyl substituents such as methyl ($-CH_3$) or ethyl ($-C_2H_5$) increase the electron density of the pyrimidine ring, which can enhance hydrophobic interactions within the enzyme's active site. These interactions are typically with nonpolar residues, leading to improved binding affinity and inhibitory activity. Molecular docking studies often show that alkyl-substituted pyrimidines fit well into hydrophobic pockets within the active site, particularly those of hCA-I and II, stabilizing the inhibitor and increasing potency.

The introduction of amino or hydroxyl groups on the pyrimidine ring allows for the formation of hydrogen bonds with key active site residues, such as Thr199, His94, and His64. These interactions are crucial for enhancing the binding affinity and selectivity of the inhibitor. Docking simulations reveal that these groups can participate in hydrogen bonding with the enzyme, leading to better stabilization of the inhibitor within the active site. This is particularly important for selective inhibition of hCA isoforms like hCA-IX and XII.

7.3.2 Electron-withdrawing groups. Halogen atoms, such as fluorine (–F) and chlorine (–Cl), decrease the electron density on the pyrimidine ring, which can strengthen interactions with the zinc ion at the enzyme's active site. Additionally, these substituents can enhance van der Waals interactions with hydrophobic residues. Molecular docking studies often show that halogenated pyrimidines exhibit increased binding affinity due to these interactions, particularly with isoforms such as hCA-IX and XII, where halogen bonding and electrostatic interactions play a significant role.

Strong EWGs like $-NO_2$ and –CN groups enhance the pyrimidine ring's ability to interact with the zinc ion by creating a more favorable electronic environment. These interactions are essential for the potent inhibition of hCA isoforms. Docking studies demonstrate that these EWGs often participate in electrostatic interactions with the zinc ion or with polar residues near the active site, leading to stronger inhibition. This is particularly effective in isoforms like hCA-IX and XII, where the zinc ion is crucial for enzymatic activity.

7.3.3 Molecular docking studies. Molecular docking studies provide a detailed understanding of how pyrimidine-based CAIs interact with the active site of hCA isoforms. These studies simulate the binding process and help identify key interactions that contribute to the inhibitor's potency and selectivity.

7.3.3.1. Interaction with zinc ion. Pyrimidine derivatives, especially those with strong EWGs like sulfonamide or nitro groups, demonstrate robust interactions with the zinc ion. The binding mechanism often involves coordination with the zinc ion, which is a critical step in inhibiting the enzyme's activity.

7.3.3.2. Hydrophobic and van der Waals interactions. Alkyl and halogen-substituted pyrimidines tend to occupy hydrophobic pockets within the enzyme's active site, where they engage in van der Waals interactions. These interactions are crucial for stabilizing the inhibitor and enhancing binding affinity, particularly in hCA-I and II.

7.3.3.3. Hydrogen bonding and π–π stacking. Pyrimidine derivatives with hydroxyl, amino, or carboxyl groups often form hydrogen bonds with active site residues such as Thr199, His94, and Glu106. These interactions significantly enhance binding affinity and selectivity. π–π Stacking interactions, especially with aromatic residues in the active site, also contribute to the stabilization of the inhibitor, thus increasing its potency.

7.3.4 SAR of pyrimidine-based CAIs w.r.t. specific functional groups

7.3.4.1. Substitutions at the 2-position. The 2-position of the pyrimidine ring is commonly substituted with groups like amines, which can interact with zinc-bound water molecules in

the active site. This interaction enhances the inhibitor's binding affinity. Molecular docking studies reveal that amine groups at this position can form hydrogen bonds with key residues, improving selectivity for hCA-II over other isoforms.

7.3.4.2. Substitutions at the 4-position. The 4-position is often substituted with EWGs like sulfonamides, which are known to chelate the zinc ion effectively. This chelation is critical for inhibition, especially in tumor-associated isoforms like hCA-IX and XII. Docking simulations show that sulfonamide groups form stable interactions with the zinc ion, making them crucial for high inhibitory potency.

7.3.4.3. Substitutions at the 5-position. The 5-position is frequently modified with hydrophobic groups that engage in van der Waals interactions with the enzyme's active site. Alkyl or halogen substituents at this position can enhance the inhibitor's affinity by stabilizing the compound within the hydrophobic pocket. Molecular docking studies indicate that these interactions are essential for maintaining the inhibitor's orientation within the active site, contributing to its overall potency.

7.4. Phthalazine-based CAIs

Phthalazine derivatives have been explored as potential inhibitors of various hCA isoforms, with modifications at different positions of the scaffold offering insights into how electron-donating and EWGs affect activity and selectivity. The substitution pattern significantly influences the pharmacological profile of these compounds, as demonstrated by various molecular docking studies (Fig. 147).

7.4.1 Electron-donating groups. Amino groups are strong EDGs that can enhance the nucleophilicity of the phthalazine ring. When placed at strategic positions on the scaffold, amino groups can facilitate hydrogen bonding with key residues in the enzyme's active site, such as Thr199, His94, and His64. Molecular docking studies reveal that amino-substituted phthalazines exhibit strong interactions with the zinc-bound water molecule, leading to improved inhibition of isoforms like hCA-II and IX. This hydrogen bonding interaction increases the binding affinity and selectivity for these isoforms, making amino groups effective at improving potency.

Alkyl substituents increase the electron density on the phthalazine ring, which can strengthen hydrophobic interactions with the non-polar residues in the enzyme's active site. These interactions help stabilize the inhibitor within the active site, enhancing its inhibitory activity. In docking simulations, alkyl-substituted phthalazines are observed to occupy hydrophobic pockets within the active site, contributing to stronger van der Waals interactions. This is particularly effective for inhibiting hCA-II, where such hydrophobic interactions play a significant role in enzyme inhibition.

7.4.2 Electron-withdrawing groups. Halogen atoms such as fluorine and chlorine are EWGs that reduce the electron density on the phthalazine ring, enhancing interactions with polar residues and the zinc ion in the enzyme's active site. The introduction of halogen atoms often leads to an increase in binding affinity, particularly toward hCA-IX and XII isoforms, which are relevant in cancer therapy. Docking studies frequently show that halogenated phthalazine derivatives engage in halogen bonding with active site residues and form strong electrostatic interactions with the zinc ion. This increases the stability of the inhibitor within the active site, particularly for tumor-associated isoforms like hCA-IX.

Strong EWGs like nitro and cyano groups decrease the electron density of the phthalazine ring, making the compound

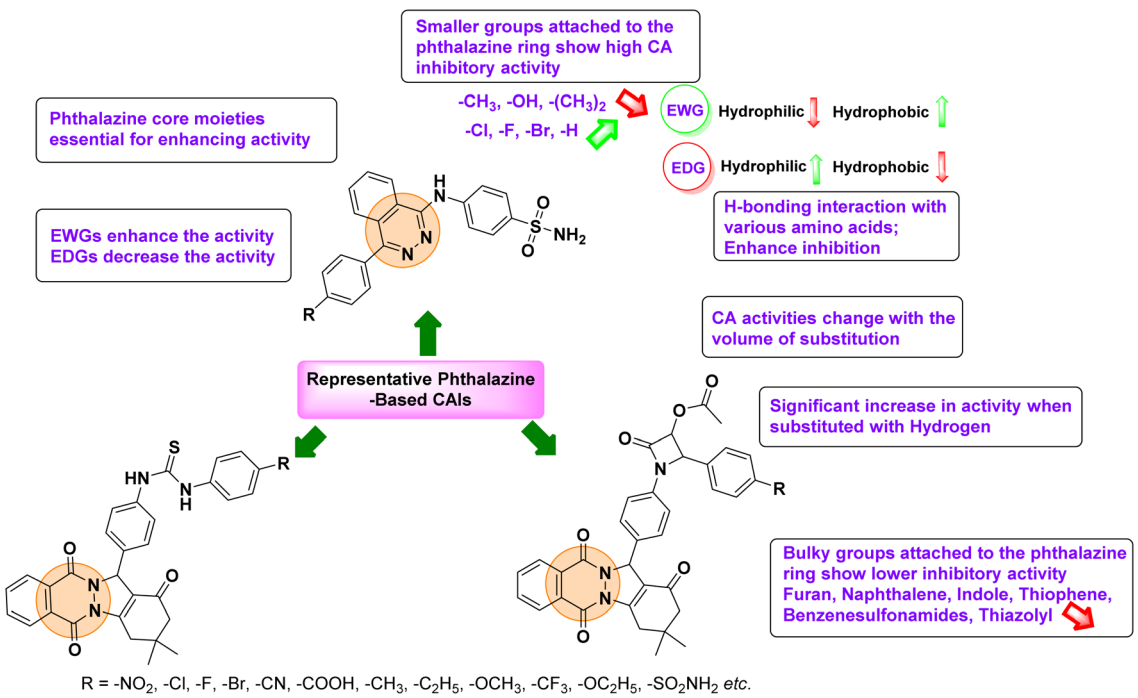

Fig. 147 SAR of phthalazine-based CAIs.

more electrophilic and enhancing its ability to interact with the zinc ion at the core of the enzyme's active site. Molecular docking simulations show that phthalazine derivatives with nitro or cyano groups form robust interactions with the zinc ion, contributing to potent inhibition of hCA-IX and XII isoforms. These EWGs also engage in electrostatic interactions with nearby residues, further stabilizing the inhibitor within the enzyme's active site.

7.4.3 Molecular docking studies. Molecular docking studies play a crucial role in understanding how phthalazine-based CAIs interact with the active site of hCA isoforms. These studies provide insights into the binding mechanisms and the influence of different substituents on the binding affinity, selectivity, and overall inhibitory potency of the compounds.

7.4.3.1. Interaction with zinc ion. The zinc ion located at the active site of carbonic anhydrases is critical for catalysis. Phthalazine-based CAIs, particularly those with strong EWGs like sulfonamides, nitro, or cyano groups, exhibit strong coordination with the zinc ion. This interaction is essential for inhibiting the enzyme's activity, as it disrupts the catalytic cycle. Docking studies show that sulfonamide-substituted phthalazines, for instance, coordinate directly with the zinc ion, leading to a significant reduction in enzymatic activity. This is especially effective for isoforms like hCA-IX and XII, which are targeted in anticancer therapies.

7.4.3.2. Hydrophobic interactions. Phthalazine derivatives with alkyl or halogen substituents often engage in hydrophobic interactions with nonpolar residues within the enzyme's active site, such as Val121, Leu198, and Phe131. These interactions help stabilize the inhibitor within the active site, enhancing its inhibitory potency. Docking studies demonstrate that these hydrophobic interactions are particularly important for hCA-II inhibition, where the enzyme's active site contains a number of hydrophobic pockets that can accommodate alkyl or halogenated substituents.

7.4.3.3. Hydrogen bonding and π–π stacking. Phthalazine derivatives with amino or hydroxyl groups often participate in hydrogen bonding with key active site residues, such as Thr199, Glu106, and His64. These interactions significantly enhance the binding affinity and selectivity of the inhibitors, especially for isoforms like hCA-II and IX. π–π Stacking interactions between the aromatic phthalazine ring and aromatic residues within the enzyme's active site, such as Phe131 and Trp209, also contribute to the stabilization of the inhibitor. Molecular docking studies frequently highlight these interactions as critical for the potent inhibition of hCA isoforms.

7.4.4 SAR of phthalazine-based CAIs in relation to specific functional groups

7.4.4.1. Substitutions at the 2-position. Substituents at the 2-position of the phthalazine ring, such as alkyl or halogen groups, can significantly influence the inhibitor's interaction with hydrophobic pockets in the enzyme's active site. These groups enhance the hydrophobic interactions, leading to increased binding affinity and inhibition potency, particularly for hCA-II.

7.4.4.2. Substitutions at the 4-position. EWGs such as sulfonamides or nitro groups at the 4-position can enhance the interaction with the zinc ion in the enzyme's active site. These groups are essential for inhibiting hCA-IX and XII, as they engage in strong electrostatic interactions with the zinc ion, which is critical for the enzyme's catalytic activity.

7.4.4.3. Substitutions at the 6-position. The 6-position of the phthalazine ring is often substituted with hydrophilic groups, such as amino or hydroxyl groups, which can form hydrogen bonds with polar residues within the enzyme's active site. These interactions increase the binding affinity and selectivity for hCA-II, which has several polar residues near the active site.

7.5. Imidazole and oxadiazole-based CAIs

7.5.1 Imidazole-based CAIs. Imidazole is a five-membered heterocyclic ring with two nitrogen atoms. Its derivatives have been extensively studied as potential CAIs due to their ability to coordinate with the zinc ion in the enzyme's active site (Fig. 148).

7.5.1.1. Electron-donating groups. Amino groups are strong electron donors and can enhance the nucleophilicity of the imidazole ring. When substituted at various positions on the imidazole ring, amino groups can engage in hydrogen bonding with the enzyme's active site residues, such as Thr199 and His94. Molecular docking studies often show that imidazole derivatives with amino groups exhibit strong interactions with the active site, improving binding affinity and selectivity for isoforms like hCA-II. The amino group can form a hydrogen bond with the carbonyl group of Thr199, stabilizing the inhibitor.

Hydroxyl groups are also electron-donating and can form hydrogen bonds with key residues in the enzyme's active site. This interaction can increase the inhibitor's binding affinity. Hydroxyl-substituted imidazoles are effective in forming hydrogen bonds with residues like Glu106 and His64. Docking studies reveal that these interactions contribute to the improved inhibition of isoforms such as hCA-I and IX.

7.5.1.2. Electron-withdrawing groups. Nitro group is strong EWG that reduce the electron density on the imidazole ring. This can enhance the interaction of the ring with the zinc ion in the enzyme's active site. Nitro-substituted imidazoles often show strong binding affinity due to their ability to interact electrostatically with the zinc ion and other polar residues. Docking studies highlight their effective inhibition of isoforms like hCA-IX, where the nitro group stabilizes the binding through electrostatic interactions with the zinc ion.

Chloro group is mild EWG that can alter the electronic environment of the imidazole ring, influencing its interaction with the enzyme. Chlorinated imidazoles can increase the hydrophobic interactions with non-polar residues in the enzyme's active site. Molecular docking studies show that these compounds bind effectively to isoforms like hCA-II, where the chloro group enhances the hydrophobic interactions.

7.5.2 Molecular docking studies

7.5.2.1. Binding interactions. Imidazole-based CAIs often coordinate with the zinc ion at the active site, a crucial interaction for inhibition. EDGs like amino and hydroxyl groups can

enhance this coordination through hydrogen bonding with nearby residues. EWGs like nitro group strengthen the binding through electrostatic interactions with the zinc ion and other polar residues.

7.5.2.2. Binding affinity. Docking studies reveal that imidazoles with EDGs generally exhibit higher binding affinity due to their ability to form hydrogen bonds and stabilize the inhibitor in the active site. EWGs improve binding through electrostatic and hydrophobic interactions.

7.5.3 Oxadiazole-based CAIs. Oxadiazole is a five-membered heterocyclic ring containing two nitrogen atoms and one oxygen atom. Its derivatives are also explored as potential CAIs due to their interaction with the enzyme's active site.

7.5.3.1. Electron-donating groups. Amino groups enhance the electron density on the oxadiazole ring, improving its nucleophilicity and ability to interact with the enzyme's active site. Compounds with amino substitutions often show increased inhibition due to their ability to form hydrogen bonds with active site residues such as Thr199 and Glu106. Molecular docking studies indicate that amino-substituted oxadiazoles bind effectively to isoforms like hCA-I and hCA-IX.

Methoxy groups are electron-donating and can increase the electron density on the oxadiazole ring. They can also participate in hydrogen bonding. Methoxy groups enhance the binding of oxadiazoles by forming hydrogen bonds with polar residues in the enzyme's active site. Docking studies show that these compounds have improved inhibition profiles for isoforms like hCA-II.

7.5.3.2. Electron-withdrawing groups. Nitro groups decrease the electron density on the oxadiazole ring and increase its electrophilicity. This enhances interactions with the enzyme's active site. Nitro-substituted oxadiazoles exhibit strong binding affinity due to their electrostatic interactions with the zinc ion. Docking studies demonstrate that these compounds are potent inhibitors of isoforms such as hCA-IX and XII.

Cyano groups are strong EWGs that can stabilize the oxadiazole ring through electrostatic interactions. Cyano-substituted oxadiazoles bind effectively to the enzyme's active site through electrostatic interactions with the zinc ion. Molecular docking studies reveal their high potency against isoforms like hCA-XII.

7.5.4 Molecular docking studies

7.5.4.1. Binding interactions. Oxadiazole-based CAIs often interact with the zinc ion in the enzyme's active site. EDGs like amino and methoxy groups improve binding through hydrogen bonding and increased electron density. EWGs like nitro and cyano groups enhance binding through electrostatic interactions with the zinc ion and other active site residues.

7.5.4.2. Binding affinity. Docking studies show that oxadiazole derivatives with EDGs generally exhibit higher binding affinity due to favorable hydrogen bonding interactions. EWGs improve binding through electrostatic interactions and stabilization of the enzyme–inhibitor complex.

7.6. Indole and isatin-based CAIs

7.6.1 Indole-based CAIs. Indole is a privileged scaffold in medicinal chemistry, offering a versatile framework for the development of CAIs. The structural activity of indole-based CAIs can be significantly influenced by the nature and position of various substituents, particularly electron-donating and EWGs (Fig. 149).

7.6.1.1. Electron-donating groups. When –OH and –OCH_3 groups positioned at the C5 or C6 of the indole ring, these EDGs enhance the electron density on the indole nitrogen, increasing its ability to form hydrogen bonds with amino acid residues in the active site of carbonic anhydrase enzymes. For instance,

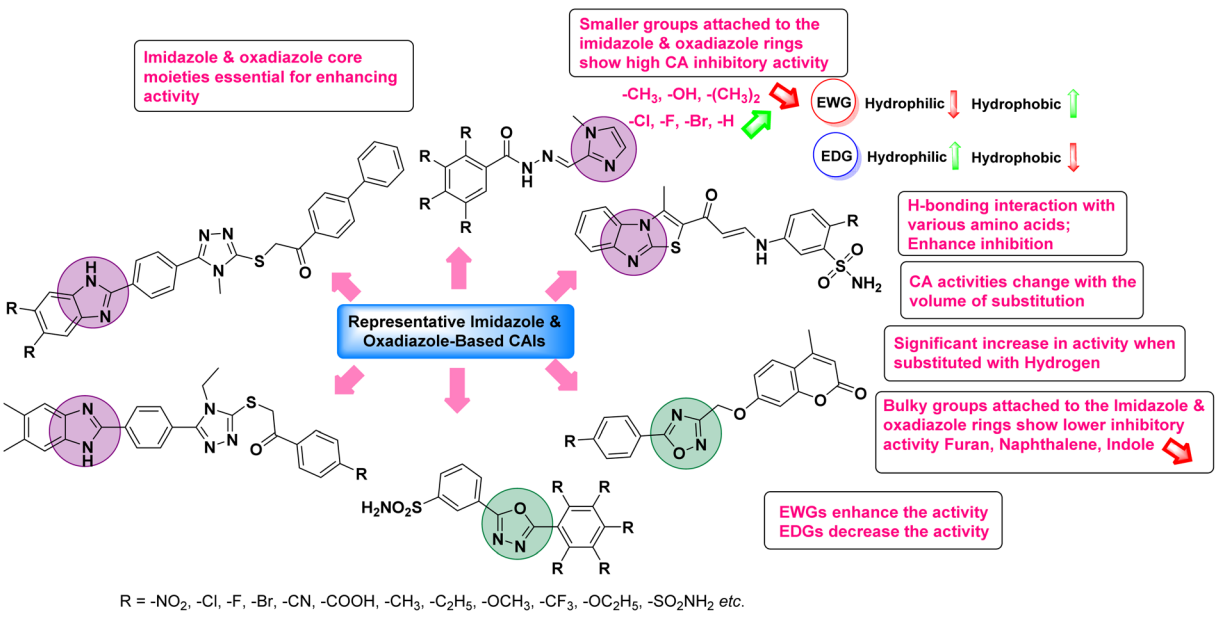

Fig. 148 SAR of imidazole and oxadiazole-based CAIs.

hydroxyl groups can form hydrogen bonds with residues such as Thr199 and Glu106, contributing to stronger binding affinity and improved inhibitory activity. Methoxy groups also enhance the interaction through van der Waals forces, increasing the overall stability of the enzyme–inhibitor complex.

The introduction of an amino group, particularly at the C2 or C3 position, enhances the inhibitor's ability to form hydrogen bonds, which can significantly improve the binding affinity towards hCA-I and II. Additionally, the amino group can participate in electrostatic interactions, further stabilizing the complex within the active site.

7.6.1.2. Electron-withdrawing groups. EWGs like nitro groups and halogens, when placed at the C5 or C7 positions, reduce the electron density on the indole ring, thereby enhancing π–π stacking interactions with aromatic residues in the enzyme's active site, such as Phe131 and Trp209. The nitro group, in particular, can participate in strong dipole interactions, enhancing the overall binding affinity.

Substituting carbonyl groups at C3 or C5 positions can increase the affinity of the inhibitor for the enzyme by forming additional hydrogen bonds with key residues in the active site, such as His94 and His119. This interaction is critical for the stabilization of the inhibitor within the enzyme's active site, leading to improved inhibitory potency.

7.6.1.3. Molecular docking studies. Molecular docking studies of indole-based CAIs typically show that inhibitors with EDGs exhibit enhanced hydrogen bonding interactions with active site residues, leading to a higher binding affinity. In contrast, inhibitors with EWGs tend to rely more on electrostatic interactions and π–π stacking, which also contribute to high binding affinity, albeit through a different mechanism. Docking studies have highlighted that indole derivatives with appropriately positioned EDGs and EWGs can achieve a fine balance between binding affinity and selectivity for different hCA isoforms, particularly hCA-IX and XII.

7.6.2 Isatin-based CAIs. Isatin, another privileged scaffold, provides a rich platform for the development of CAIs. Its unique structure, with a keto group at position 2 and a lactam ring, allows for versatile modifications that can enhance enzyme binding and selectivity.

7.6.2.1. Electron-donating groups. When –OH and $–OCH_3$ groups introduced at the N1 position or the aromatic ring, these EDGs can increase the electron density on the isatin scaffold, thereby enhancing the interaction with zinc ions and nearby amino acid residues in the active site. Hydroxyl groups often form hydrogen bonds with key residues such as Thr200 and His119, which are critical for potent inhibition.

Alkyl substitutions at the N1 or C5 position of the isatin scaffold can improve hydrophobic interactions with non-polar regions of the enzyme's active site, such as the hydrophobic pocket near Val121, thereby enhancing binding affinity and inhibitory potency.

7.6.2.2. Electron-withdrawing groups. Substitution of halogens or nitro groups at the C5 or C7 position can enhance the binding affinity through increased dipole–dipole interactions and the stabilization of the enzyme–inhibitor complex. These EWGs can also increase the binding strength by facilitating π–π stacking interactions with aromatic residues such as Phe131 and Trp209.

The –COOH and –CN groups, when introduced at the C3 or C7 positions, can increase the inhibitor's ability to coordinate with the zinc ion in the active site. The carboxyl group, in particular, can form salt bridges with positively charged residues, such as Lys67, enhancing the inhibitory effect.

7.6.2.3. Molecular docking studies. Docking studies of isatin-based CAIs have demonstrated that the presence of EWGs

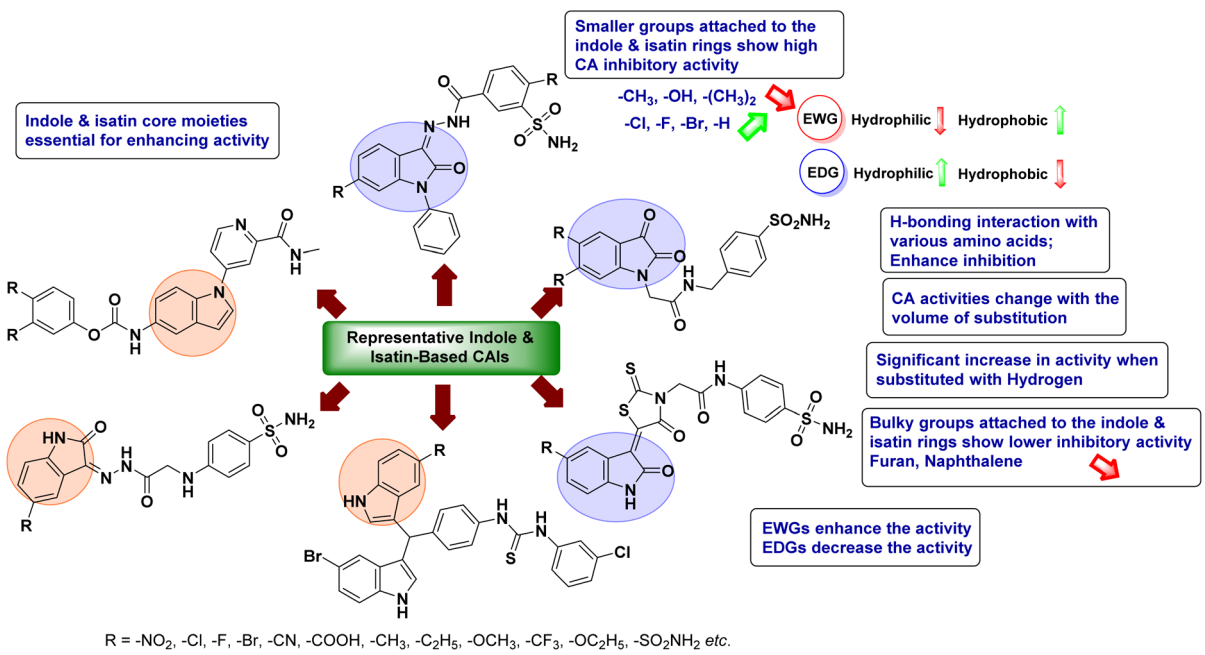

Fig. 149 SAR of indole and isatin-based CAIs.

significantly enhances the binding affinity by stabilizing the inhibitor within the enzyme's active site. These studies reveal that isatin derivatives with appropriately placed EWGs tend to have a higher selectivity for hCA-IX and XII due to their stronger interactions with zinc ion and nearby residues. Conversely, derivatives with EDGs often show enhanced hydrogen bonding capabilities, contributing to higher overall binding affinity but with a potential reduction in selectivity.

7.7. Chalcone and coumarin-based CAIs

7.7.1 Chalcone-based CAIs. Chalcones are a class of compounds characterized by the presence of an α,β-unsaturated carbonyl system, which serves as a versatile platform for structural modification. The activity of chalcone-based CAIs is influenced by various substituents on the aromatic rings, and their interactions with CA enzymes largely depend on the nature of these substituents (Fig. 150).

7.7.1.1. Electron-donating groups. When –OH and –OCH_3 groups are attached to the A or B ring of the chalcone, especially at the *ortho* or *para* positions, they enhance hydrogen bonding interactions with amino acid residues in the active site of CA enzymes. Hydroxyl groups increase the polar character of the molecule, allowing strong hydrogen bonds with residues like Thr199 and His94 in the hCA-IX or XII isoforms, improving binding affinity.

The presence of amino groups enhances the electrostatic interactions and hydrogen bonding with CA residues. For example, amino-substituted chalcones have shown increased binding affinity towards hCA-IX due to stronger interactions with the zinc-bound water molecule and surrounding residues.

7.7.1.2. Electron-withdrawing groups. Halogen substitutions, particularly at the *para* position of the B ring, tend to enhance inhibitory activity through halogen bonding and hydrophobic interactions with residues like Val121 and Leu198 in the active site. Halogen groups also contribute to the stabilization of the π–π stacking interactions with aromatic amino acids like Phe131.

EWGs like nitro and cyano groups increase the binding affinity by forming dipole–dipole interactions with polar residues in the enzyme's active site. These groups enhance the inhibitor's interaction with residues near the zinc ion, promoting stronger binding and better inhibition.

7.7.1.3. Molecular docking studies. Molecular docking studies of chalcone-based CAIs reveal that the introduction of EDGs leads to enhanced hydrogen bonding with active site residues, resulting in improved binding affinity. Chalcones with EWGs, on the other hand, show better interaction with the hydrophobic regions and aromatic residues through halogen bonding and π–π stacking interactions, leading to effective enzyme inhibition. Chalcone derivatives generally show moderate selectivity towards hCA-IX and XII isoforms, with structural modifications fine-tuning the potency and selectivity.

7.7.2 Coumarin-based CAIs. Coumarin derivatives possess a benzopyrone structure that offers a rigid scaffold for structural modifications. Coumarins act as non-classical CAIs, typically undergoing hydrolysis to form active species that inhibit CA isoforms by binding at the entrance of the active site rather than directly coordinating with the zinc ion.

7.7.2.1. Electron-donating groups. Substituting hydroxyl or alkoxy groups at positions 6, 7, or 8 on the coumarin ring significantly enhances the binding affinity through hydrogen bonding with residues at the entrance of the active site. These groups facilitate interactions with residues like Asn67 and His119, promoting strong and stable enzyme inhibition, particularly against hCA-IX and XII. The introduction of amino

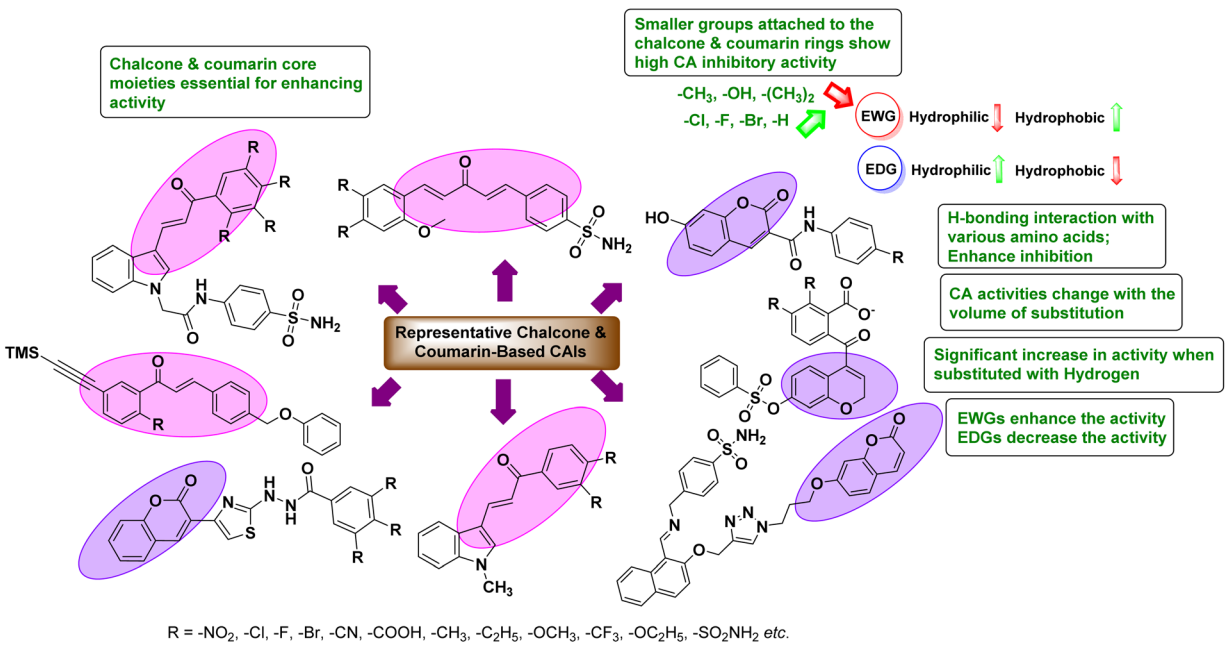

Fig. 150 SAR of chalcone and coumarin-based CAIs.

groups at positions 6 or 7 on the coumarin ring increases the inhibitor's polar character and enhances hydrogen bonding with residues near the enzyme's active site entrance. This modification generally leads to better inhibition of hCA isoforms, particularly membrane-bound isoforms such as hCA-IX.

7.7.2.2. Electron-withdrawing groups. Halogenation at positions 3 or 6 on the coumarin ring improves inhibitory activity by increasing the hydrophobic interactions with the enzyme's active site entrance. Halogenated coumarins interact with hydrophobic pockets within the enzyme, leading to improved binding stability. The EWGs (–COOH, –C═O), when introduced at position 3, enhance the interaction with polar residues at the active site entrance, such as Arg64 and His200. The presence of carbonyl groups further strengthens the inhibitor's ability to stabilize within the active site, contributing to a stronger inhibition profile.

7.7.2.3. Molecular docking studies. Molecular docking studies of coumarin-based CAIs reveal that EDGs enhance hydrogen bonding interactions with residues at the entrance of the active site, leading to higher binding affinity. EWGs improve the inhibitor's interaction with hydrophobic and polar regions of the enzyme, particularly with residues near the zinc ion. Coumarins exhibit moderate activity, and their effectiveness is highly dependent on the substituent pattern. Modifications with EDGs and EWGs can fine-tune the inhibitory potency, with most coumarins displaying higher selectivity for hCA-IX and XII.

7.8. Rhodanine-based CAIs

Rhodanine-based scaffolds have attracted considerable attention in medicinal chemistry, particularly for their role as CAIs. These molecules are characterized by a five-membered ring structure containing sulfur, nitrogen, and a ketone group, making them versatile in terms of functionalization and interactions with enzyme active sites (Fig. 151).

7.8.1 Electron-donating groups. Introduction of EDGs (–CH_3, –OCH_3) at various positions on the rhodanine ring can enhance the binding affinity of the molecule towards CA enzymes, particularly hCA-IX and hCA-XII, which are relevant in cancer therapy. These groups can increase the electron density on the molecule, facilitating better hydrogen bonding and van der Waals interactions within the enzyme's active site.

The presence of amino groups further enhances the electron density, allowing for strong interaction with amino acid residues in the active site, such as histidines and zinc ion coordination, crucial for CA inhibition.

7.8.2 Electron-withdrawing groups. The groups (–NO_2, –CN), when attached to the rhodanine scaffold, typically increase the molecule's electrophilicity, improving its interaction with nucleophilic residues in the CA active site. This often results in stronger binding and increased inhibitory activity. However, excessive electron withdrawal might reduce overall binding affinity if the molecule becomes too electrophilic, leading to non-specific interactions.

Halogen substitution can significantly enhance binding affinity due to their size and ability to form halogen bonds. Fluorine, due to its small size and high electronegativity, often provides the best balance between binding affinity and selectivity for specific CA isoforms.

7.8.3 Molecular docking insights. Molecular docking studies of rhodanine derivatives typically reveal the following interactions:

7.8.3.1. Zinc coordination. The sulfur atom in the rhodanine ring often coordinates with the zinc ion present in the active site of the CA enzyme, a critical interaction that is a hallmark of potent CAIs.

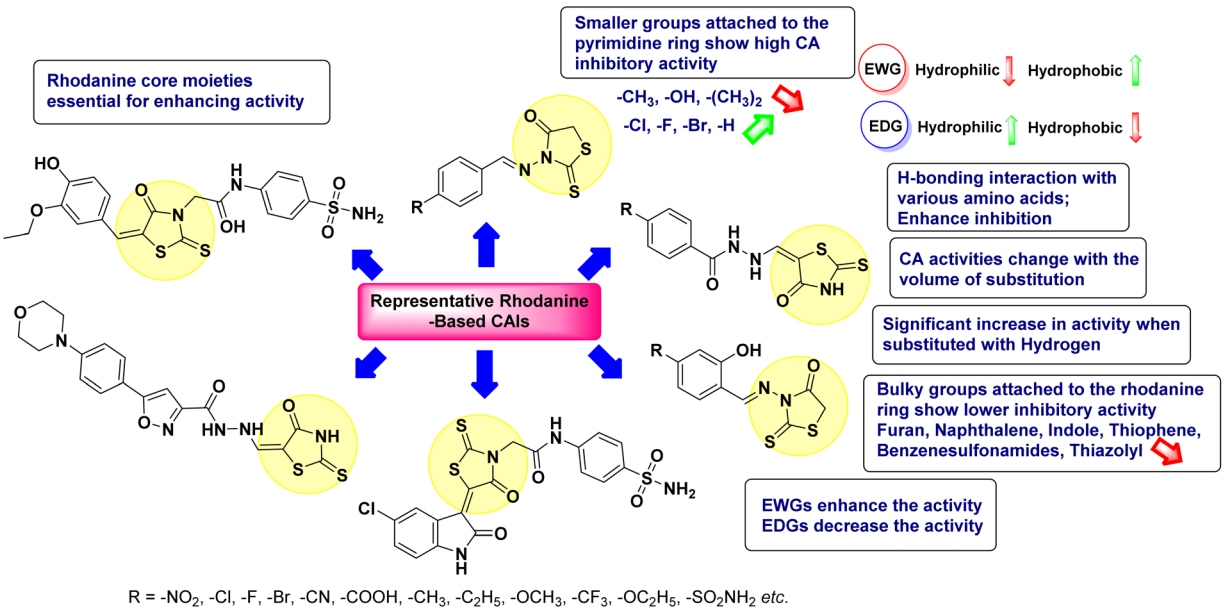

Fig. 151 SAR of rhodanine-based CAIs.

7.8.3.2. Hydrogen bonding. Functional groups like amines, hydroxyls, or carboxylates can form hydrogen bonds with key residues in the active site, such as Thr199, His94, and His119. These interactions are vital for high-affinity binding and selective inhibition of specific CA isoforms.

7.8.3.3. π–π Stacking and hydrophobic interactions. The rhodanine ring can participate in π–π stacking interactions with aromatic residues like Phe131 or hydrophobic interactions within the enzyme's active site, further stabilizing the inhibitor–enzyme complex.

7.9. Quinolines-based CAIs

Quinoline-based scaffolds are an important class of CAIs due to their ability to interact with various CA isoforms. The quinoline ring system, a fused bicyclic structure with a benzene ring fused to a pyridine, offers a versatile platform for chemical modifications that can significantly influence the inhibitory activity against CA enzymes (Fig. 152).

7.9.1 Electron-donating groups. Introducing alkyl groups at specific positions on the quinoline ring can increase the electron density, enhancing the interaction with amino acid residues in the CA active site. These groups can improve the hydrophobic interactions with the enzyme's binding pocket, leading to increased inhibitory activity, particularly against hCA-IX and XII.

The groups (OH, $-OCH_3$) further increase the electron density, which can enhance hydrogen bonding with active site residues like Thr199, His94, and His119. The position of these substituents on the quinoline ring is crucial, as certain positions may favor stronger binding interactions, thus improving potency and selectivity.

7.9.2 Electron-withdrawing groups. EWGs decrease the electron density on the quinoline ring, making the molecule more electrophilic. This property can enhance interactions with nucleophilic residues within the CA active site, such as those coordinating with the zinc ion. However, excessive electron withdrawal can reduce the overall binding affinity if the interaction becomes too strong and leads to off-target effects.

Halogen atoms, especially fluorine, can be strategically placed on the quinoline ring to enhance binding affinity through halogen bonding and hydrophobic interactions. Fluorine, due to its small size and high electronegativity, often provides a good balance, leading to potent CA inhibition.

7.9.3 Molecular docking insights. Molecular docking studies of quinoline-based CAIs typically reveal the following interactions:

7.9.3.1. Zinc coordination. Although the quinoline scaffold itself does not directly coordinate with the zinc ion in the CA active site, functional groups attached to the scaffold can facilitate this interaction. For example, a sulfonamide group attached to the quinoline ring can coordinate with the zinc ion, which is a key interaction for potent CA inhibition.

7.9.3.2. Hydrogen bonding. Substituents such as hydroxyl or amino groups on the quinoline ring can form hydrogen bonds with key residues in the CA active site. These interactions are crucial for stabilizing the inhibitor within the enzyme's binding pocket, thereby enhancing selectivity and potency.

7.9.3.3. π–π Stacking and hydrophobic interactions. The planar structure of the quinoline ring allows for π–π stacking interactions with aromatic residues like Phe131, as well as hydrophobic interactions within the active site. These interactions contribute to the overall binding affinity and specificity of quinoline-based inhibitors.

7.10. Sulfonamides-based CAIs

Sulfonamides are a cornerstone class of CAIs due to their ability to effectively coordinate with the zinc ion in the active site of CA enzymes. The sulfonamide group ($-SO_2NH_2$) is essential for binding to the zinc ion and is a critical pharmacophore for CA inhibition. Modifying the surrounding structural elements,

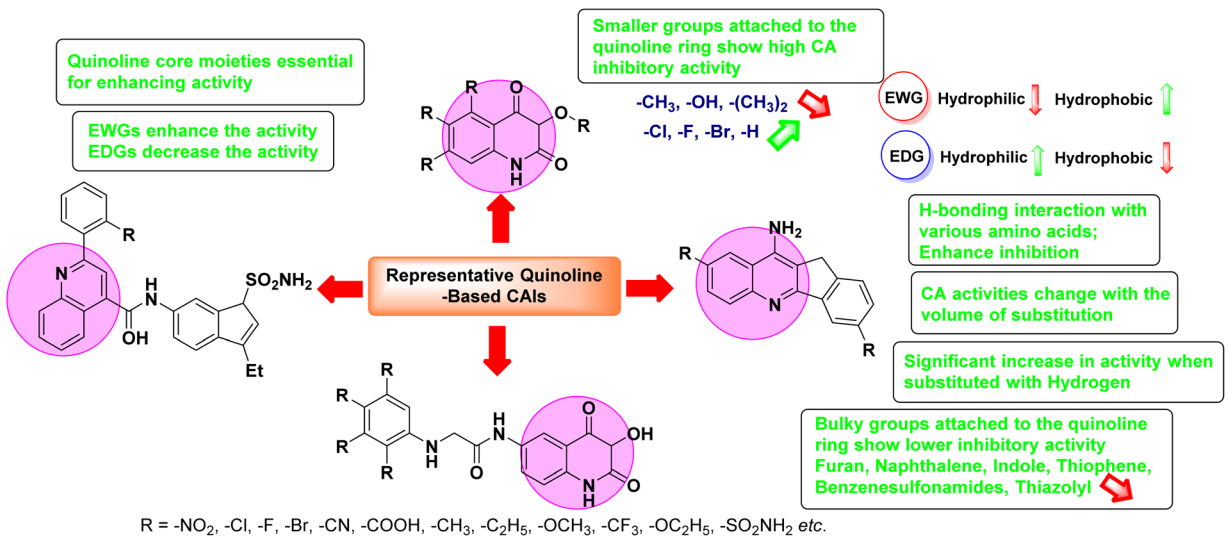

Fig. 152 SAR of quinoline-based CAIs.

including electron-donating and EWGs, significantly influences their potency and selectivity across different CA isoforms (Fig. 153).

7.10.1 Electron-donating groups. Incorporation of alkyl groups (–CH_3, –C_2H_5) adjacent to the sulfonamide moiety can increase hydrophobic interactions with the CA binding pocket. These modifications often lead to enhanced inhibitory activity due to improved stabilization of the inhibitor within the enzyme's active site, particularly against cytosolic isoforms such as hCA-I and II.

These groups (–OH, –OCH_3) can increase the electron density around the sulfonamide scaffold, which may enhance hydrogen bonding with key residues in the CA active site (*e.g.*, Thr199 or Glu106). In addition, the hydroxyl group can form water-mediated interactions, further stabilizing the inhibitor in the enzyme pocket.

7.10.2 Electron-withdrawing groups. The substituents (–NO_2, –CN) reduce the electron density on the sulfonamide scaffold, increasing the electrophilicity of the molecule. This can enhance binding through electrostatic interactions with residues in the CA active site, such as the zinc-coordinating histidines (His94 and His119). However, strong EWGs can sometimes reduce overall affinity by destabilizing the inhibitor within the enzyme pocket.

Halogen atoms (–Cl, –F, –Br), especially fluorine, when placed on the aryl ring of sulfonamides, tend to increase the potency of CA inhibition by enhancing both hydrophobic and electrostatic interactions. Fluorine is often favored due to its ability to enhance lipophilicity while maintaining a good balance between binding affinity and isoform selectivity.

7.10.3 Molecular docking insights. Molecular docking studies of sulfonamide-based CAIs consistently demonstrate the following key interactions:

7.10.3.1. Zinc ion coordination. The sulfonamide nitrogen forms a crucial interaction with the zinc ion in the CA active site. This coordination is the primary mechanism by which sulfonamides exert their inhibitory effect. The binding of the sulfonamide group displaces the water molecule coordinated to the zinc ion, thereby inhibiting the enzyme's catalytic activity.

7.10.3.2. Hydrogen bonding. The sulfonamide's nitrogen and oxygen atoms can form hydrogen bonds with surrounding active site residues, such as Thr199 and Glu106. The presence of EDGs on the sulfonamide scaffold can enhance this hydrogen bonding interactions, improving binding affinity and selectivity.

7.10.3.3. Electrostatic and hydrophobic interactions. Substituents on the sulfonamide scaffold, such as halogens or alkyl groups, can engage in hydrophobic interactions with non-polar residues lining the active site, such as Val121 and Phe131. Additionally, EWGs can improve electrostatic interactions with the enzyme's active site, further stabilizing the inhibitor.

7.11. Overall ranking based on CA inhibitory activity

Phthalazine and sulfonamides-based CAIs show the highest activity due to their strong binding interactions with the enzyme, especially against hCA-IX and hCA-I. Imidazole, oxadiazole, and triazole scaffolds also demonstrate significant potential, with their effectiveness stemming from their ability to engage in diverse interactions within the enzyme's active site. Other scaffolds like thiazole, pyrimidine, and indole/isatin offer

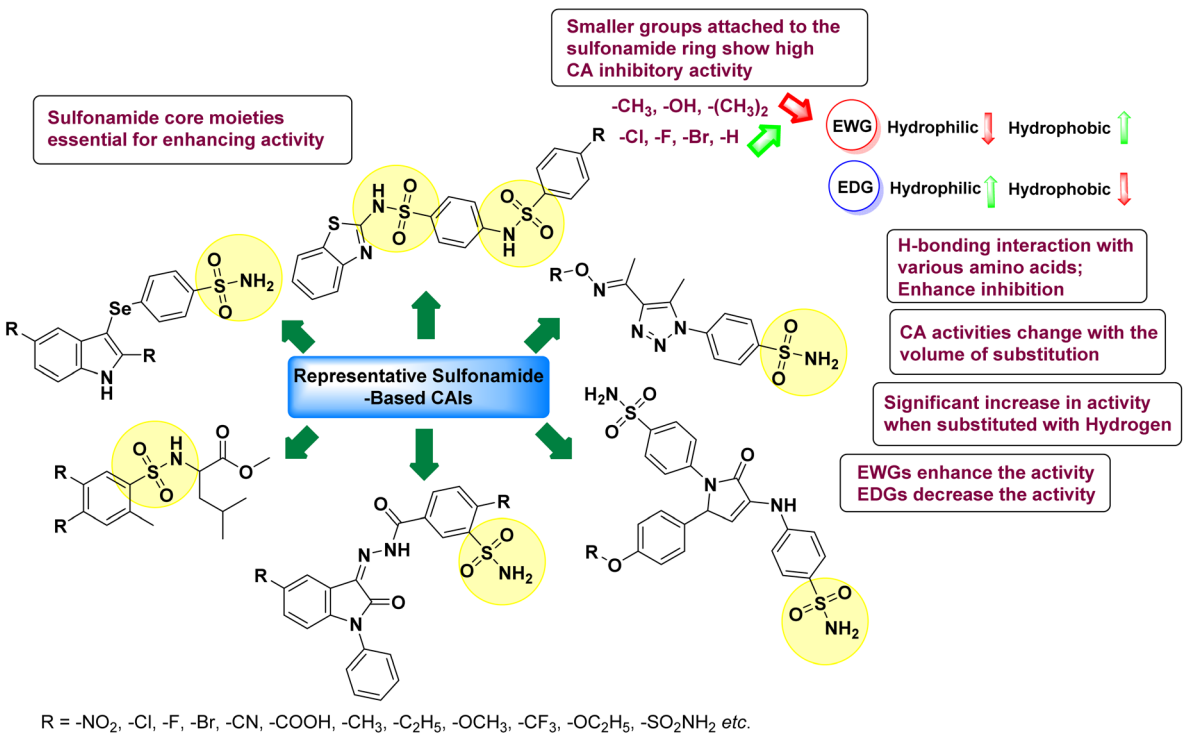

Fig. 153 SAR of sulfonamide-based CAIs.

moderate to high activity, influenced by their substitution patterns. Chalcone, coumarin, rhodanine, and quinolines show more variable effectiveness, highlighting the importance of functional group selection in optimizing inhibitory potential.

In the context of CA inhibition, small molecules that form hydrogen bonds with the target protein typically interact with specific amino acid residues in or near the enzyme's active site. CA enzymes, particularly the human isoforms have a highly conserved active site containing a Zn^{2+} coordinated by three histidine residues. The small molecule inhibitors usually form key interactions around this zinc-binding region.

Here's a breakdown of important binding regions and how small molecules form H-bonds:

7.11.1 Zinc ion coordination. The inhibitors often have a sulfonamide ($-SO_2NH_2$) or related moiety that can coordinate with the zinc ion. This interaction is crucial for inhibition but does not involve H-bonding itself.

7.11.2 Thr199 (threonine 199). This residue, conserved in CA-II and other isoforms, is critical for forming hydrogen bonds with inhibitors. The hydroxyl group of Thr199 can participate in H-bonding with the sulfonamide group or other electronegative atoms on the inhibitor.

7.11.3 Glu106 (glutamate 106). Another important residue that can form hydrogen bonds with the inhibitor. The carboxyl group in Glu106 often interacts with the sulfonamide nitrogen or other donor/acceptor groups in heterocyclic inhibitors.

7.11.4 Water network. Water molecules in the active site, especially those near the zinc ion, can mediate hydrogen bonds between the inhibitor and the protein residues. These water molecules form a dynamic H-bonding network with both the protein and the inhibitor.

7.11.5 Other residues. In addition to Thr199 and Glu106, other residues such as Gln92, Asn67, and Asn62 may form hydrogen bonds depending on the specific inhibitor and isoform of CA being studied.

During a docking study, hydrogen bonds between the inhibitor and these residues or water molecules can contribute significantly to the binding affinity and specificity of the inhibitor toward the CA active site. Understanding these interactions helps in rationalizing the structure–activity relationship (SAR) of carbonic anhydrase inhibitors.

Moreover, the installation of EWGs or EDGs on various scaffolds plays a critical role in modulating CA inhibition. EWGs are often placed in positions that enhance hydrophobic interactions within the enzyme's active site, while EDGs are placed to improve hydrogen bonding or solubility. The exact placement depends on the scaffold and the target isoform, allowing for fine-tuning of inhibitor activity and selectivity.

8. Key positions for EWG/EDG introduction

8.1. *Meta*- or *para*-positions on aromatic rings or heterocyclic scaffolds

Substitutions at these positions generally have the most profound impact on the electronic and physicochemical properties of the molecule, influencing how the inhibitor interacts with both the hydrophobic and polar regions of CA.

8.2. Nitrogen-containing heterocycles

In scaffolds like imidazole, thiazole, or triazole, substituents at key positions (such as C-2 or C-5) modulate the molecule's electron density, thereby affecting both zinc coordination and interactions with surrounding residues.

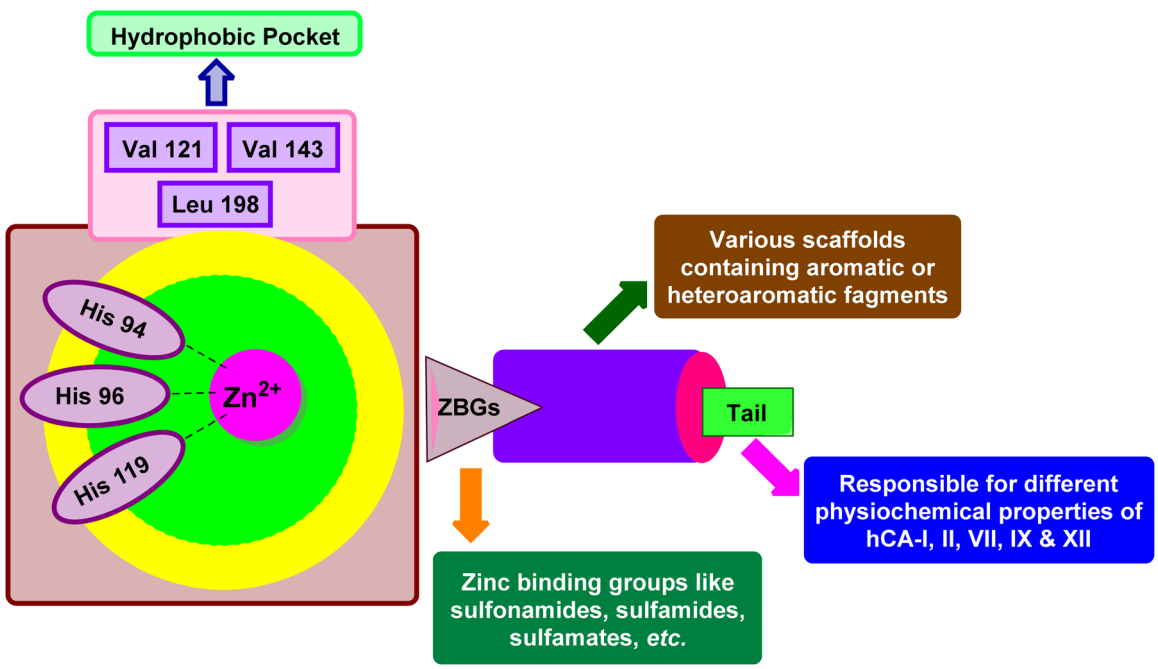

Fig. 154 SAR of different heterocyclic scaffolds against hCA isoforms based on docking study.

8.3. Sulfonamide group modification

While the sulfonamide group itself is conserved for binding to the zinc ion, modifications at the periphery of this group can introduce EWGs or EDGs that affect the molecule's overall hydrophobicity or polarity.

Each scaffold class has a unique SAR profile when it comes to CA inhibition. The effects of EWGs, EDGs, steric factors, and binding modes vary from one scaffold to another. While some general principles apply (*e.g.*, EWGs increasing hydrophobicity and EDGs enhancing hydrogen bonding),[13,232–235] the specific SAR for each scaffold has been discussed earlier w.r.t enzyme's active site, the targeted isoform, and the scaffold's binding interactions.

The SAR of CAIs reveals that both EDGs and EWGs significantly impact inhibitory activity. Scaffolds with strong EDGs tend to show enhanced binding through hydrogen bonding, while those with EWGs often improve binding through electrostatic interactions. Overall, phthalazine and sulfonamides-based CAIs exhibit the highest activity, with other scaffolds like imidazole, oxadiazole, and triazole also demonstrating significant potential (Fig. 154).

9. Conclusions

The inhibition of CA isoforms remains a validated therapeutic approach for treating various disorders such as glaucoma, cancer, retinopathy, hemolytic anemia, and edema, due to the enzymes' diverse cellular roles and physiological functions. Recent advancements in medicinal chemistry, particularly over the past eleven years (2013–2024), have led to the development of structurally diverse CAIs from synthetic compounds and rational design. These efforts have produced inhibitors with enhanced isoform selectivity, improved pharmacological profiles, and better physicochemical properties. Additionally, this review highlights the significant advancements in the development of CAIs across various chemical scaffolds, including phthalazine, sulfonamides, imidazole, oxadiazole, triazole, and others. Despite substantial progress, isoform selectivity remains a key challenge, limiting further clinical development of potent inhibitors due to the difficulty in balancing inhibitory activity and selectivity. A critical structural feature of potent CAIs, particularly against hCA-IX and XII, is the presence of a sulfonamide group, which coordinates with the zinc ion in the enzyme's active site and interacts with residues like His94 and His119. To address isoform selectivity, the "tail approach" has been extensively explored. This strategy involves attaching various molecular scaffolds to the core sulfonamide-bearing aromatic or heterocyclic ring to fine-tune binding interactions within the active site, enhancing both potency and selectivity. The SAR studies discussed emphasize the critical role of functional groups, particularly the balance between electron-donating and electron-withdrawing properties, in enhancing the inhibitory potency and selectivity of CAIs. Phthalazine and sulfonamide-based CAIs, in particular, have demonstrated exceptional efficacy, especially against cancer-related isoforms such as hCA-IX and hCA-XII. Targeting these isoforms (hCA-IX and XII) presents a promising strategy for cancer therapy. Benzenesulfonamides are commonly used in clinical applications. However, these compounds face two significant challenges: their lack of selectivity, as they tend to inhibit multiple isoforms indiscriminately, and their association with "sulfa allergies" in susceptible individuals. To address these issues, research has shifted towards exploring alternative scaffolds that offer both selectivity and safety. Coumarin and its derivatives have emerged as highly selective and potent inhibitors of hCA-IX and XII, and they have been combined with various pharmacophores, such as pyrazole, 1,2,3-triazole, 4-thiazolidinone, and thiourea, to enhance specificity and potency. The findings underscore the potential of CAIs as versatile therapeutic agents, with promising applications in oncology and other disease areas where carbonic anhydrases play a pivotal role.

10. Future perspectives for CAIs

The promising results observed with various CAIs, including phthalazine, sulfonamides, imidazole, oxadiazole, and triazole-based scaffolds, underscore the potential for further advancements in this field. Based on the current findings and SAR,

Table 15 Future directions and challenges in CAIs research

Research area	Key focus	Challenges
Isoform selectivity	Designing selective inhibitors for specific CA isoforms	Minimizing off-target effects and improving specificity
Resistance mechanisms	Addressing molecular mechanisms of CAI resistance	Developing novel scaffolds to overcome resistance
Pharmacokinetics and bioavailability	Optimizing ADME properties of CAIs	Ensuring adequate bioavailability and systemic exposure
Non-classical CAIs	Exploring novel heterocyclic frameworks	Discovering unique mechanisms with reduced side effects
Tumor-associated isoforms (CA-IX and CA-XII)	Targeting CA-IX and XII for cancer therapy	Minimizing inhibition of essential isoforms like CA-I, II
Combination therapies	Synergistic effects with other therapeutic agents	Optimizing dosing regimens and overcoming resistance
Clinical translation	Advancing promising candidates to clinical trials	Overcoming formulation, synthesis, and scalability issues

several future directions can be envisaged to enhance the development of CAIs (Table 15):

(i) Enhancing isoform selectivity: one of the key challenges in CAI research is achieving selective inhibition of specific CA isoforms, particularly those implicated in disease. While significant progress has been made, future research should focus on designing inhibitors with greater selectivity to minimize off-target effects and improve therapeutic outcomes. Advanced computational modeling and structure-based drug design (SBDD) approaches could play a pivotal role in achieving this goal.

One of the primary challenges arises from the high degree of conservation in the active site among different carbonic anhydrase (CA) isoforms. The core structure of the active site is largely similar across these isoforms, which is essential for their catalytic function. Although individual isoforms may have variations in adjacent amino acid residues, these differences are often insufficient to create distinct binding pockets that could be targeted selectively by inhibitors. As a result, many potential inhibitors exhibit similar affinities for multiple isoforms, leading to off-target effects that diminish therapeutic efficacy.

Moreover, the structural plasticity of CA isoforms plays a significant role in this challenge. These enzymes can adopt various conformations depending on the presence of substrates, inhibitors, or changes in environmental conditions. Such conformational flexibility can result in unexpected binding interactions that are difficult to predict using static structural models. Consequently, inhibitors designed to target specific isoforms may inadvertently interact with others due to this dynamic nature, complicating the achievement of selectivity.

Additionally, the potential for allosteric regulation introduces another layer of complexity. While targeting allosteric sites offers a pathway to enhance isoform selectivity, the identification and characterization of these sites can be challenging. The subtle differences in the allosteric sites among isoforms may not always be apparent, making it difficult to design inhibitors that are both effective and selective.

Future research should focus on utilizing advanced techniques such as computational modeling, molecular dynamics simulations, and structural biology to gain deeper insights into the isoform-specific interactions of potential inhibitors. By addressing these challenges, the development of CAIs with improved selectivity and reduced off-target effects can become more attainable.

(ii) Overcoming resistance mechanisms: with long-term therapeutic use, resistance to CAIs may emerge, limiting their effectiveness. Investigating the underlying molecular mechanisms of resistance and developing CAIs that can overcome these barriers is an area that requires attention. This could involve exploring novel heterocyclic scaffolds or hybrid molecules that incorporate multiple mechanisms of action.

(iii) Optimizing pharmacokinetics and bioavailability: many potent CAIs suffer from suboptimal pharmacokinetics, leading to poor bioavailability or rapid metabolism. Future research should prioritize optimizing the physicochemical properties of CAIs to enhance their pharmacokinetic profiles, ensuring better systemic exposure and prolonged therapeutic efficacy. This includes improving absorption, distribution, metabolism, and excretion (ADME) characteristics of lead compounds.

(iv) Exploring non-classical CAIs: although sulfonamides remain the most widely studied CAIs, non-classical inhibitors based on different heterocyclic frameworks offer a promising avenue for future research. These scaffolds may provide unique mechanisms of action, potentially leading to the development of novel therapeutics with reduced side effects or improved efficacy.

(v) Targeting tumor-associated CA isoforms: CA-IX and CA-XII have been identified as key targets in cancer therapy due to their overexpression in hypoxic tumor environments. Future studies should focus on developing CAIs specifically targeting these isoforms while ensuring minimal inhibition of other physiologically essential isoforms such as CA-I and CA-II. This could enhance the therapeutic index and reduce toxicity in cancer treatments.

(vi) Exploring combination therapies: given the complexity of diseases involving carbonic anhydrases, there is growing interest in combining CAIs with other therapeutic agents to achieve synergistic effects. Research into combination therapies, particularly in oncology, may reveal new strategies for overcoming resistance or enhancing the efficacy of existing treatments.

(vii) Clinical translation of promising candidates: finally, while numerous CAIs have demonstrated efficacy in preclinical studies, the translation of these findings into clinical practice remains a challenge. Addressing formulation issues, scaling up synthesis, and conducting comprehensive clinical trials will be essential to bring new CAIs into therapeutic use.

(viii) Expanding therapeutic applications: exploring the potential of CAIs beyond cancer, such as in the treatment of glaucoma, epilepsy, and metabolic disorders, can broaden their clinical applications and improve patient outcomes.

One major challenge is the gap between preclinical efficacy and clinical outcomes. Preclinical studies often rely on *in vitro* assays or animal models that do not fully capture the complexity of human diseases, leading to discrepancies in therapeutic effects when tested in humans. This highlights the need for more advanced models that better mimic human pathophysiology, ensuring that findings from preclinical studies are more predictive of clinical success.

Another key challenge is optimizing the pharmacokinetic and pharmacodynamic profiles of CAIs for human use. Many compounds with excellent activity *in vitro* may suffer from poor bioavailability, rapid metabolism, or short half-lives *in vivo*, which reduces their efficacy. Developing formulations or delivery systems that improve the absorption, distribution, metabolism, and excretion (ADME) properties of CAIs is essential for translating preclinical candidates into viable clinical drugs.

Additionally, toxicity and off-target effects represent significant hurdles. While CAIs may selectively inhibit specific isoforms in controlled laboratory conditions, they may also inhibit non-target isoforms in clinical use, leading to adverse effects. Achieving isoform selectivity with minimal off-target activity is

critical for improving the therapeutic index and minimizing side effects.

Lastly, scaling up the synthesis of promising CAIs from laboratory-scale to commercial-scale production can pose significant challenges. The complexity of certain synthetic pathways or the cost of raw materials may hinder large-scale manufacturing, impacting the overall feasibility of clinical development.

Addressing these challenges requires an integrated approach, combining advancements in drug design, formulation strategies, and more predictive preclinical models to facilitate the successful clinical translation of CAIs.

Data availability

All the data is provided in manuscript file.

Conflicts of interest

Authors have no conflict of interests to declare.

Acknowledgements

The authors extend their appreciation to the Deanship of Research and Graduate Studies at King Khalid University for funding this work through Large Research Project under grant number RGP2/255/45.

References

1 T. Qadir, A. Amin, P. K. Sharma, I. Jeelani and H. Abe, *Open Med. Chem. J.*, 2022, **16**, 1–34.
2 E. Kabir and M. Uzzaman, *Results Chem.*, 2022, **4**, 100606.
3 R. S. Jassas, N. Naeem, A. Sadiq, R. Mehmood, N. A. Alenazi, M. M. Al-Rooqi, E. U. Mughal, R. I. Alsantali and S. A. Ahmed, *RSC Adv.*, 2023, **13**, 16413–16452.
4 R. J. Obaid, N. Naeem, E. U. Mughal, M. M. Al-Rooqi, A. Sadiq, R. S. Jassas, Z. Moussa and S. A. Ahmed, *RSC Adv.*, 2022, **12**, 19764–19855.
5 P. N. Kalaria, S. C. Karad and D. K. Raval, *Eur. J. Med. Chem.*, 2018, **158**, 917–936.
6 V. Srivastava, P. K. Singh, S. Tivari and P. P. Singh, *Org. Chem. Front.*, 2022, **9**, 1485–1507.
7 M. H. A. Al-Jumaili, A. A. Hamad, H. E. Hashem, A. D. Hussein, M. J. Muhaidi, M. A. Ahmed, A. H. A. Albanaa, F. Siddique and E. A. Bakr, *J. Mol. Struct.*, 2023, **1271**, 133970.
8 M. M. Heravi and V. Zadsirjan, *RSC Adv.*, 2020, **10**, 44247–44311.
9 A. Husain and D. Madhesia, *J. Enzyme Inhib. Med. Chem.*, 2012, **27**, 773–783.
10 A. Al-Mulla, *Der Pharma Chem.*, 2017, **9**, 141–147.
11 R. J. Obaid, E. U. Mughal, N. Naeem, M. M. Al-Rooqi, A. Sadiq, R. S. Jassas, Z. Moussa and S. A. Ahmed, *Process Biochem.*, 2022, **120**, 250–259.
12 P. Arora, V. Arora, H. Lamba and D. Wadhwa, *Int. J. Pharm. Sci. Res.*, 2012, **3**, 2947.
13 C. T. Supuran, *Bioorg. Med. Chem. Lett.*, 2010, **20**, 3467–3474.
14 C. T. Supuran and A. Scozzafava, *Expert Opin. Ther. Pat.*, 2000, **10**, 575–600.
15 J. Zhu, X. Jiang, X. Luo, R. Zhao, J. Li, H. Cai, X. Y. Ye, R. Bai and T. Xie, *Drug Dev. Res.*, 2023, **84**, 718–735.
16 C. T. Supuran, *J. Enzyme Inhib. Med. Chem.*, 2012, **27**, 759–772.
17 W. Zuo, L. Zuo, X. Geng, Z. Li and L. Wang, *Org. Chem. Front.*, 2023, **10**, 6112–6116.
18 R. Jing, Z. Jiang and X. Tang, *Int. J. Mol. Sci.*, 2024, **25**, 8638.
19 C. T. Supuran, *Expert Opin. Ther. Pat.*, 2018, **28**, 709–712.
20 A. Thiry, C. T. Supuran, B. Masereel and J.-M. Dogné, *J. Med. Chem.*, 2008, **51**, 3051–3056.
21 S. Kumar, S. Rulhania, S. Jaswal and V. Monga, *Eur. J. Med. Chem.*, 2021, **209**, 112923.
22 E. Masini, F. Carta, A. Scozzafava and C. T. Supuran, *Expert Opin. Ther. Pat.*, 2013, **23**, 705–716.
23 G. De Simone and C. T. Supuran, *Curr. Top. Med. Chem.*, 2007, **7**, 879–884.
24 A. Thiry, J.-M. Dogne, C. T. Supuran and B. Masereel, *Curr. Top. Med. Chem.*, 2007, **7**, 855–864.
25 C. T Supuran, *Future Med. Chem.*, 2021, **13**, 1935–1937.
26 C. T. Supuran, *J. Enzyme Inhib. Med. Chem.*, 2016, **31**, 345–360.
27 S. Lindskog, *Pharmacol. Ther.*, 1997, **74**, 1–20.
28 C. T. Supuran, *Expert Opin. Drug Discovery*, 2017, **12**, 61–88.
29 C. T. Supuran and A. Scozzafava, *Expert Opin. Ther. Pat.*, 2002, **12**, 217–242.
30 R. McKenna and C. T. Supuran, *Carbonic Anhydrase: Mechanism, Regulation, Links to Disease, and Industrial Applications*, 2013, pp. 291–323.
31 M. Aggarwal and R. McKenna, *Expert Opin. Ther. Pat.*, 2012, **22**, 903–915.
32 K. M. Merz Jr, R. Hoffmann and M. J. Dewar, *J. Am. Chem. Soc.*, 1989, **111**, 5636–5649.
33 C. T. Supuran, in *Carbonic Anhydrase*, CRC press, 2004, pp. 13–36.
34 C. T. Supuran, *Clin. Sci.*, 2021, **135**, 1233–1249.
35 A. Angeli, F. Carta and C. T. Supuran, *Catalysts*, 2020, **10**, 1008.
36 R. J. DiMario, M. C. Machingura, G. L. Waldrop and J. V. Moroney, *Plant Sci.*, 2018, **268**, 11–17.
37 M. Carter, *Biol. Rev.*, 1972, **47**, 465–513.
38 A. Nocentini and C. T. Supuran, *Carbonic Anhydrases*, 2019, 3–16.
39 L. Chen, Z. Jiang, L. Yang, Y. Fang, S. Lu, O. U. Akakuru, S. Huang, J. Li, S. Ma and A. Wu, *Chin. J. Chem.*, 2023, **41**, 199–206.
40 C. Zhao, X. Tang, X. Chen and Z. Jiang, *ACS Nano*, 2024, **18**, 17852–17868.
41 P. Xu, C. Li, J. Yuan, Z. Bao and W. Liu, *Front. Genet.*, 2024, **15**, 1388015.
42 M. I. Hassan, B. Shajee, A. Waheed, F. Ahmad and W. S. Sly, *Bioorg. Med. Chem.*, 2013, **21**, 1570–1582.
43 K. Gilmour, *Comp. Biochem. Physiol., Part A: Mol. Integr. Physiol.*, 2010, **157**, 193–197.

44 C. T. Supuran, A. Scozzafava and A. Casini, *Med. Res. Rev.*, 2003, **23**, 146–189.
45 C. T. Supuran and A. Scozzafava, *Bioorg. Med. Chem.*, 2007, **15**, 4336–4350.
46 C. T. Supuran and C. Capasso, *Metabolites*, 2017, **7**, 56.
47 V. Alterio, A. Di Fiore, K. D'Ambrosio, C. T. Supuran and G. De Simone, *X-Ray Crystallography of Carbonic Anhydrase Inhibitors and its Importance in Drug Design*, Wiley, Hoboken, New Jersey, 2009.
48 C. T. Supuran, *Biochem. J.*, 2016, **473**, 2023–2032.
49 L. Baranauskienė and D. Matulis, *Carbonic Anhydrase as Drug Target: Thermodynamics and Structure of Inhibitor Binding*, 2019, pp. 3–14.
50 M. Aggarwal, C. D. Boone, B. Kondeti and R. McKenna, *J. Enzyme Inhib. Med. Chem.*, 2013, **28**, 267–277.
51 D. W. Christianson and C. A. Fierke, *Acc. Chem. Res.*, 1996, **29**, 331–339.
52 C. T. Supuran, in *Metalloenzymes*, Elsevier, 2024, pp. 139–156.
53 J.-Y. Winum and C. T. Supuran, *J. Enzyme Inhib. Med. Chem.*, 2015, **30**, 321–324.
54 S. Zamanova, A. M. Shabana, U. K. Mondal and M. A. Ilies, *Expert Opin. Ther. Pat.*, 2019, **29**, 509–533.
55 S. Pastorekova, S. Parkkila and J. Zavada, *Adv. Clin. Chem.*, 2006, **42**, 167–216.
56 L. Ciccone, C. Cerri, S. Nencetti and E. Orlandini, *Molecules*, 2021, **26**, 6380.
57 C. T. Supuran, *Expert Opin. Ther. Pat.*, 2003, **13**, 1545–1550.
58 C. T. Supuran, *J. Enzyme Inhib. Med. Chem.*, 2022, **37**, 2478–2488.
59 S. Bibi, T. Javed, F. Alam, A. Ali, S. Ali, M. Ullah, H. B. Asad, M. Hassham, F. Hasan and S. Muhammad, *Pak. J. Pharm. Sci.*, 2019, **32**, 709–720.
60 E. Berrino and F. Carta, in *Carbonic Anhydrases*, Elsevier, 2019, pp. 311–329.
61 J. Haapasalo, K. Nordfors, H. Haapasalo and S. Parkkila, *Cancers*, 2020, **12**, 1723.
62 E. Ruusuvuori and K. Kaila, *Carbonic Anhydrase: Mechanism, Regulation, Links to Disease, and Industrial Applications*, 2014, 271–290.
63 F. Carta and C. T. Supuran, *Expert Opin. Ther. Pat.*, 2013, **23**, 681–691.
64 S. Bua, A. Nocentini and C. T. Supuran, in *Carbonic Anhydrases*, Elsevier, 2019, pp. 287–309.
65 M. Pandey, A. Singh, N. Agnihotri, R. Kumar, P. Saha, R. P. Pandey and A. Kumar, *J. Res. Appl. Sci. Biotechnol.*, 2022, **1**, 11–20.
66 C. T. Supuran, *Expert Opin. Drug Metab. Toxicol.*, 2016, **12**, 423–431.
67 P. Challa and D. L. Epstein, in *Chandler and Grant's Glaucoma*, CRC Press, 2024, pp. 159–164.
68 G. Durand-Cavagna, R. Owen, L. Gordon, C. Peter and C. Boussiquet-Leroux, *Toxicol. Sci.*, 1992, **18**, 137–143.
69 L. Ambrosio, J. S. Williams, A. Gutierrez, E. A. Swanson, R. J. Munro, R. D. Ferguson, A. B. Fulton and J. D. Akula, *Exp. Eye Res.*, 2021, **202**, 108344.
70 A. Lafuma and G. Berdeaux, *Curr. Med. Res. Opin.*, 2008, **24**, 1519–1527.
71 N. A. Sharif, *Exp. Eye Res.*, 2023, **232**, 109444.
72 M. L. Shahsuvaryan, *Med. Hypothesis, Discovery Innovation Ophthalmol.*, 2022, **11**, 34.
73 M. F. Syed, A. Rehmani and M. Yang, *Med. Clin.*, 2021, **105**, 425–444.
74 F. Mincione, L. Menabuoni and C. T. Supuran, in *Carbonic Anhydrase*, CRC Press, 2004, pp. 255–266.
75 J. C. Clapham, J. R. Arch and M. Tadayyon, *Pharmacol. Ther.*, 2001, **89**, 81–121.
76 G. D. Simone, A. D. Fiore and C. T. Supuran, *Curr. Pharm. Des.*, 2008, **14**, 655–660.
77 M. Y. Mboge, R. McKenna and S. C. Frost, *Topics in Anti-Cancer Research*, 2015, 5, 3.
78 S. G. Nerella, P. Singh, M. Arifuddin and C. T. Supuran, *Expert Opin. Ther. Pat.*, 2022, **32**, 833–847.
79 M. Y. Mboge, B. P. Mahon, R. McKenna and S. C. Frost, *Metabolites*, 2018, **8**, 19.
80 W. M. Dr. Pierce Jr, G. F. Nardin, M. F. Fuqua, E. Sabah-Maren and S. H. Stern, *J. Bone Miner. Res.*, 1991, **6**, 347–354.
81 Z. Alkhayal, Z. Shinwari, A. Gaafar and A. Alaiya, *Curr. Issues Mol. Biol.*, 2023, **45**, 1373–1386.
82 X. Chang, Y. Zheng, Q. Yang, L. Wang, J. Pan, Y. Xia, X. Yan and J. Han, *Arthritis Res. Ther.*, 2012, **14**, 1–14.
83 M. A. Hayward and T. J. Caggiano, in *Annual Reports in Medicinal Chemistry*, Elsevier, 1987, vol. 22, pp. 169–178.
84 J. Sławiński, K. Szafrański, D. Vullo and C. T. Supuran, *Eur. J. Med. Chem.*, 2013, **69**, 701–710.
85 K. Aksu, M. Nar, M. Tanc, D. Vullo, İ. Gülçin, S. Göksu, F. Tümer and C. T. Supuran, *Bioorg. Med. Chem.*, 2013, **21**, 2925–2931.
86 N. Berber, M. Arslan, E. Yavuz, C. Bilen and N. Gencer, *Arthritis Res. Ther.*, 2013, **2013**, 1–8.
87 S. Ayvaz, M. Çankaya, A. Atasever and A. Altuntas, *J. Enzyme Inhib. Med. Chem.*, 2013, **28**, 305–310.
88 Z.-C. Wang, Y.-J. Qin, P.-F. Wang, Y.-A. Yang, Q. Wen, X. Zhang, H.-Y. Qiu, Y.-T. Duan, Y.-T. Wang, Y.-L. Sang and H.-L. Zhu, *Eur. J. Med. Chem.*, 2013, **66**, 1–11.
89 N. Büyükkidan, B. Büyükkidan, M. Bülbül, R. Kasimoğullari, M. Serdar and S. Mert, *J. Pharm. Pharmacol.*, 2013, **65**, 363–369.
90 M. O. Karatas, B. Alici, U. Cakir, E. Cetinkaya, D. Demir, A. Ergün, N. Gençer and O. Arslan, *J. Enzyme Inhib. Med. Chem.*, 2013, **28**, 299–304.
91 E. Şen, Z. Alım, H. Duran, M. M. İşgör, Ş. Beydemir, R. Kasımoğulları and S. Ok, *J. Enzyme Inhib. Med. Chem.*, 2013, **28**, 328–336.
92 S. K. Suthar, S. Bansal, S. Lohan, V. Modak, A. Chaudhary and A. Tiwari, *Eur. J. Med. Chem.*, 2013, **66**, 372–379.
93 N. Gençer, Ç. Bilen, D. Demir, A. Atahan, M. Ceylan and M. Küçükislamoğlu, *Artif. Cells, Nanomed., Biotechnol.*, 2013, **41**, 384–388.
94 R. Gao, S. Liao, C. Zhang, W. Zhu, L. Wang, J. Huang, Z. Zhao, H. Li, X. Qian and Y. Xu, *Eur. J. Med. Chem.*, 2013, **62**, 597–604.

95 F. Allouche, F. Chabchoub, F. Carta and C. T. Supuran, *J. Enzyme Inhib. Med. Chem.*, 2013, **28**, 343–349.
96 M. Ceruso, P. Khloya, C. T. Supuran and P. K. Sharma, *Bioorg. Med. Chem.*, 2014, **22**, 6945–6952.
97 M. M. Ghorab, M. S. Alsaid, M. Ceruso, Y. M. Nissan and C. T. Supuran, *Bioorg. Med. Chem.*, 2014, **22**, 3684–3695.
98 M. Mojzych, A. Bielawska, K. Bielawski, M. Ceruso and C. T. Supuran, *Bioorg. Med. Chem.*, 2014, **22**, 2643–2647.
99 K. Rutkauskas, A. Zubrienė, I. Tumosienė, K. Kantminienė, M. Kažemėkaitė, A. Smirnov, J. Kazokaitė, V. Morkūnaitė, E. Čapkauskaitė, E. Manakova, S. Gražulis, Z.-J. Beresnevičius and D. Matulis, *Molecules*, 2014, **19**, 17356–17380.
100 J. Sławiński, Z. Brzozowski, B. Żołnowska, K. Szafrański, A. Pogorzelska, D. Vullo and C. T. Supuran, *Eur. J. Med. Chem.*, 2014, **84**, 59–67.
101 V. Dudutiene, J. Matuliene, A. Smirnov, D. D. Timm, A. Zubriene, L. Baranauskiene, V. Morkunaite, J. Smirnoviene, V. Michailoviene, V. Juozapaitiene and D. Matulis, *J. Med. Chem.*, 2014, **57**, 9435–9446.
102 M. Bozdag, M. Pinard, F. Carta, E. Masini, A. Scozzafava, R. McKenna and C. T. Supuran, *J. Med. Chem.*, 2014, **57**, 9673–9686.
103 Y. Akbaba, A. Akıncıoğlu, H. Göçer, S. Göksu, İ. Gülçin and C. T. Supuran, *J. Enzyme Inhib. Med. Chem.*, 2014, **29**, 35–42.
104 P. Khloya, G. Celik, D. Vullo, C. T. Supuran and P. K. Sharma, *Eur. J. Med. Chem.*, 2014, **76**, 284–290.
105 F. Sonmez, C. Bilen, S. Sumersan, N. Gençer, S. Isik, O. Arslan and M. Kucukislamoglu, *J. Enzyme Inhib. Med. Chem.*, 2014, **29**, 118–123.
106 G. Celik, P. Khloya, D. Vullo, C. T. Supuran and P. K. Sharma, *Bioorg. Med. Chem.*, 2014, **22**, 1873–1882.
107 H. Kuday, F. Sonmez, C. Bilen, E. Yavuz, N. Gençer and M. Kucukislamoglu, *BioMed Res. Int.*, 2014, **1**, 594879–594885.
108 A. Saeed, M. Al-Rashida, M. Hamayoun, A. Mumtaz and J. Iqbal, *J. Enzyme Inhib. Med. Chem.*, 2014, **29**, 901–905.
109 Y. Akbaba, E. Bastem, F. Topal, İ. Gülçin, A. Maraş and S. Göksu, *Arch. Pharm.*, 2014, **347**, 950–957.
110 N. Pala, L. Micheletto, M. Sechi, M. Aggarwal, F. Carta, R. McKenna and C. T. Supuran, *ACS Med. Chem. Lett.*, 2014, **5**, 927–930.
111 B. Żołnowska, J. Sławiński, A. Pogorzelska, J. Chojnacki, D. Vullo and C. T. Supuran, *Eur. J. Med. Chem.*, 2014, **71**, 135–147.
112 F. Celik, M. Arslan, M. O. Kaya, E. Yavuz, N. Gençer and O. Arslan, *Artif. Cells, Nanomed., Biotechnol.*, 2014, **42**, 58–62.
113 T. Demirci, M. Arslan, Ç. Bilen, D. Demir, N. Gençer and O. Arslan, *J. Enzyme Inhib. Med. Chem.*, 2014, **29**, 132–136.
114 A. Akıncıoğlu, M. Topal, İ. Gülçin and S. Göksu, *Arch. Pharm.*, 2014, **347**, 68–76.
115 S. Zaib, A. Saeed, K. Stolte, U. Flörke, M. Shahid and J. Iqbal, *Eur. J. Med. Chem.*, 2014, **78**, 140–150.
116 J. Sławiński, A. Pogorzelska, B. Żołnowska, K. Brożewicz, D. Vullo and C. T. Supuran, *Eur. J. Med. Chem.*, 2014, **82**, 47–55.
117 Z.-C. Wang, Y.-T. Duan, H.-Y. Qiu, W.-Y. Huang, P.-F. Wang, X.-Q. Yan, S.-F. Zhang and H.-L. Zhu, *RSC Adv.*, 2014, **4**, 33029–33038.
118 J. Pichake, P. S. Kharkar, M. Ceruso, C. T. Supuran and M. P. Toraskar, *ACS Med. Chem. Lett.*, 2014, **5**, 793–796.
119 P. Khloya, M. Ceruso, S. Ram, C. T. Supuran and P. K. Sharma, *Bioorg. Med. Chem. Lett.*, 2015, **25**, 3208–3212.
120 S. Imran, M. Taha, N. H. Ismail, S. Fayyaz, K. M. Khan and M. I. Choudhary, *Bioorg. Chem.*, 2015, **62**, 83–93.
121 M. R. Buemi, L. De Luca, S. Ferro, E. Bruno, M. Ceruso, C. T. Supuran, K. Pospíšilová, J. Brynda, P. Řezáčová and R. Gitto, *Eur. J. Med. Chem.*, 2015, **102**, 223–232.
122 H. S. Ibrahim, S. M. Abou-Seri, M. Tanc, M. M. Elaasser, H. A. Abdel-Aziz and C. T. Supuran, *Eur. J. Med. Chem.*, 2015, **103**, 583–593.
123 N. Berber, M. Arslan, Ç. Bilen, Z. Sackes, N. Gençer and O. Arslan, *Russ. J. Bioorg. Chem.*, 2015, **41**, 414–420.
124 N. Singasane, P. S. Kharkar, M. Ceruso, C. T. Supuran and M. P. Toraskar, *J. Enzyme Inhib. Med. Chem.*, 2015, **30**, 901–907.
125 S. Muhammad Saad, M. Saleem, S. Perveen, M. Tanveer Alam, K. Mohammed Khan and M. Iqbal Choudhary, *Med. Chem.*, 2015, **11**, 336–341.
126 D. A. Ibrahim, D. S. Lasheen, M. Y. Zaky, A. W. Ibrahim, D. Vullo, M. Ceruso, C. T. Supuran and D. A. Abou El Ella, *Bioorg. Med. Chem.*, 2015, **23**, 4989–4999.
127 C. B. Mishra, S. Kumari, A. Angeli, S. M. Monti, M. Buonanno, A. Prakash, M. Tiwari and C. T. Supuran, *J. Enzyme Inhib. Med. Chem.*, 2016, **31**, 174–179.
128 K. Aksu, B. Özgeriş, P. Taslimi, A. Naderi, İ. Gülçin and S. Göksu, *Arch. Pharm.*, 2016, **349**, 944–954.
129 H. Genç, R. Kalin, Z. Köksal, N. Sadeghian, U. M. Kocyigit, M. Zengin, İ. Gülçin and H. Özdemir, *Int. J. Mol. Sci.*, 2016, **17**, 1736.
130 S. Mert, Z. Alım, M. M. İşgör, Ş. Beydemir and R. Kasımoğulları, *Bioorg. Chem.*, 2016, **68**, 64–71.
131 E. Garibov, P. Taslimi, A. Sujayev, Z. Bingol, S. Çetinkaya, İ. Gulçin, S. Beydemir, V. Farzaliyev, S. H. Alwasel and C. T. Supuran, *J. Enzyme Inhib. Med. Chem.*, 2016, **31**, 1–9.
132 A. Sujayev, L. Polat Kose, E. Garibov, İ. Gülçin, V. Farzaliev, S. H. Alwasel and C. T. Supuran, *J. Enzyme Inhib. Med. Chem.*, 2016, **31**, 1192–1197.
133 N. M. A. Gawad, N. H. Amin, M. T. Elsaadi, F. M. Mohamed, A. Angeli, V. De Luca, C. Capasso and C. T. Supuran, *Bioorg. Med. Chem.*, 2016, **24**, 3043–3051.
134 K. Kucukoglu, F. Oral, T. Aydin, C. Yamali, O. Algul, H. Sakagami, I. Gulcin, C. T. Supuran and H. I. Gul, *J. Enzyme Inhib. Med. Chem.*, 2016, **31**, 20–24.
135 W. M. Eldehna, M. Fares, M. Ceruso, H. A. Ghabbour, S. M. Abou-Seri, H. A. Abdel-Aziz, D. A. Abou El Ella and C. T. Supuran, *Eur. J. Med. Chem.*, 2016, **110**, 259–266.
136 A. Saeed, S. U. Khan, P. A. Mahesar, P. A. Channar, G. Shabir and J. Iqbal, *Biochem. Biophys. Res. Commun.*, 2017, **482**, 176–181.
137 S. Iqbal, M. Saleem, M. K. Azim, M. Taha, U. Salar, K. M. Khan, S. Perveen and M. I. Choudhary, *Bioorg. Chem.*, 2017, **72**, 89–101.

138 Ö. Güleç, M. Arslan, N. Gencer, A. Ergun, C. Bilen and O. Arslan, *Arch. Physiol. Biochem.*, 2017, **123**, 306–312.
139 M. Bozdag, S. Bua, S. M. Osman, Z. AlOthman and C. T. Supuran, *J. Enzyme Inhib. Med. Chem.*, 2017, **32**, 885–892.
140 S. Angapelly, P. Sri Ramya, A. Angeli, C. T. Supuran and M. Arifuddin, *ChemMedChem*, 2017, **12**, 1578–1584.
141 P. S. Ramya, S. Angapelly, A. Angeli, C. S. Digwal, M. Arifuddin, B. N. Babu, C. T. Supuran and A. Kamal, *J. Enzyme Inhib. Med. Chem.*, 2017, **32**, 1274–1281.
142 A. Altundas, B. Gül, M. Çankaya, A. Atasever and İ. Gülçin, *J. Biochem. Mol. Toxicol.*, 2017, **31**, e21998.
143 P. Taslimi, S. Osmanova, İ. Gulçin, S. Sardarova, V. Farzaliyev, A. Sujayev, R. Kaya, F. Koc, S. Beydemir and S. H. Alwasel, *J. Biochem. Mol. Toxicol.*, 2017, **31**, e21931.
144 K. Oktay, L. Polat Kose, K. Şendil, M. S. Gültekin and İ. Gülçın, *Med. Chem. Res.*, 2017, **26**, 1619–1627.
145 B. Zengin Kurt, F. Sonmez, S. Durdagi, B. Aksoydan, R. Ekhteiari Salmas, A. Angeli, M. Kucukislamoglu and C. T. Supuran, *J. Enzyme Inhib. Med. Chem.*, 2017, **32**, 1042–1052.
146 İ. Gulçin, M. Abbasova, P. Taslimi, Z. Huyut, L. Safarova, A. Sujayev, V. Farzaliyev, Ş. Beydemir, S. H. Alwasel and C. T. Supuran, *J. Enzyme Inhib. Med. Chem.*, 2017, **32**, 1174–1182.
147 F. Erdemir, D. B. Celepci, A. Aktaş, P. Taslimi, Y. Gök, H. Karabıyık and İ. Gülçin, *J. Mol. Struct.*, 2018, **1155**, 797–806.
148 A. Behcet, T. Çağlılar, D. B. Celepci, A. Aktaş, P. Taslimi, Y. Gök, M. Aygün, R. Kaya and İ. Gülçin, *J. Mol. Struct.*, 2018, **1170**, 160–169.
149 M. Ahmed, M. A. Qadir, A. Hameed, M. N. Arshad, A. M. Asiri and M. Muddassar, *Bioorg. Chem.*, 2018, **76**, 218–227.
150 M. F. Ansari, D. Idrees, M. I. Hassan, K. Ahmad, F. Avecilla and A. Azam, *Eur. J. Med. Chem.*, 2018, **144**, 544–556.
151 L. Vats, V. Sharma, A. Angeli, R. Kumar, C. T. Supuran and P. K. Sharma, *Eur. J. Med. Chem.*, 2018, **150**, 678–686.
152 R. Kumar, L. Vats, S. Bua, C. T. Supuran and P. K. Sharma, *Eur. J. Med. Chem.*, 2018, **155**, 545–551.
153 M. G. El-Gazzar, N. H. Nafie, A. Nocentini, M. M. Ghorab, H. I. Heiba and C. T. Supuran, *J. Enzyme Inhib. Med. Chem.*, 2018, **33**, 1565–1574.
154 M. Ekiz, A. Tutar, S. Ökten, B. Bütün, Ü. M. Koçyiğit, P. Taslimi and G. Topçu, *Arch. Pharm.*, 2018, **351**, 1800167.
155 C. B. Mishra, S. Kumari, A. Angeli, S. Bua, M. Buonanno, S. M. Monti, M. Tiwari and C. T. Supuran, *Eur. J. Med. Chem.*, 2018, **156**, 430–443.
156 R. Qamar, A. Saeed, M. Saeed, Z. Ashraf, Q. Abbas, M. Hassan and F. Albericio, *Drug Dev. Res.*, 2018, **79**, 352–361.
157 B. N. Sağlık, U. A. Cevik, D. Osmaniye, S. Levent, B. K. Çavuşoğlu, Y. Demir, S. Ilgın, Y. Özkay, A. S. Koparal and Ş. Beydemir, *Bioorg. Chem.*, 2019, **91**, 103153.
158 A.-M. Alaa, A. S. El-Azab, S. Bua, A. Nocentini, M. A. A. El-Enin, M. M. Alanazi, N. A. AlSaif, M. M. Hefnawy and C. T. Supuran, *Bioorg. Chem.*, 2019, **87**, 425–431.
159 J. Mahar, A. Saeed, K. D. Belfield, F. A. Larik, P. A. Channar, M. A. Kazi, Q. Abbas, M. Hassan, H. Raza and S.-Y. Seo, *Bioorg. Chem.*, 2019, **84**, 170–176.
160 F. Turkan, A. Cetin, P. Taslimi, M. Karaman and İ. Gulçin, *Bioorg. Chem.*, 2019, **86**, 420–427.
161 P. S. Thacker, M. Alvala, M. Arifuddin, A. Angeli and C. T. Supuran, *Bioorg. Chem.*, 2019, **86**, 386–392.
162 B. Z. Kurt, A. Dag, B. Doğan, S. Durdagi, A. Angeli, A. Nocentini, C. T. Supuran and F. Sonmez, *Bioorg. Chem.*, 2019, **87**, 838–850.
163 B. Z. Kurt, F. Sonmez, D. Ozturk, A. Akdemir, A. Angeli and C. T. Supuran, *Eur. J. Med. Chem.*, 2019, **183**, 111702.
164 S. Bayindir, C. Caglayan, M. Karaman and İ. Gülcin, *Bioorg. Chem.*, 2019, **90**, 103096.
165 W. M. Eldehna, M. A. Abdelrahman, A. Nocentini, S. Bua, S. T. Al-Rashood, G. S. Hassan, A. Bonardi, A. A. Almehizia, H. M. Alkahtani, A. Alharbi and C. T. Supuran, *Bioorg. Chem.*, 2019, **90**, 103102.
166 M. Işık, S. Akocak, N. Lolak, P. Taslimi, C. Türkeş, İ. Gülçin, M. Durgun and Ş. Beydemir, *Arch. Pharm.*, 2020, **353**, 2000102.
167 A. A. Alkhaldi, M. M. Al-Sanea, A. Nocentini, W. M. Eldehna, Z. M. Elsayed, A. Bonardi, M. F. Abo-Ashour, A. K. El-Damasy, M. S. Abdel-Maksoud and T. Al-Warhi, *Eur. J. Med. Chem.*, 2020, **207**, 112745.
168 B. Sever, C. Türkeş, M. D. Altıntop, Y. Demir and Ş. Beydemir, *Int. J. Biol. Macromol.*, 2020, **163**, 1970–1988.
169 Q. Istrefi, C. Türkeş, M. Arslan, Y. Demir, A. R. Nixha, Ş. Beydemir and Ö. İ. Küfrevioğlu, *Arch. Pharm.*, 2020, **353**, 1900383.
170 M. A. Said, W. M. Eldehna, A. Nocentini, A. Bonardi, S. H. Fahim, S. Bua, D. H. Soliman, H. A. Abdel-Aziz, P. Gratteri, S. M. Abou-Seri and C. T. Supuran, *Eur. J. Med. Chem.*, 2020, **185**, 111843.
171 A. Khan, M. Khan, S. A. Halim, Z. A. Khan, Z. Shafiq and A. Al-Harrasi, *Front. Chem.*, 2020, **8**, 598095.
172 A. Saeed, P. A. Channar, M. Arshad, H. R. El-Seedi, Q. Abbas, M. Hassan, H. Raza and S. Y. Seo, *J. Heterocycl. Chem.*, 2020, **57**, 2831–2843.
173 R. F. George, S. Bua, C. T. Supuran and F. M. Awadallah, *Bioorg. Chem.*, 2020, **96**, 103635.
174 P. S. Thacker, A. Angeli, O. S. Argulwar, P. L. Tiwari, M. Arifuddin and C. T. Supuran, *Bioorg. Chem.*, 2020, **98**, 103739.
175 R. F. George, M. F. Said, S. Bua and C. T. Supuran, *Bioorg. Chem.*, 2020, **95**, 103514.
176 P. Singh, P. P. Yadav, B. Swain, P. S. Thacker, A. Angeli, C. T. Supuran and M. Arifuddin, *Bioorg. Chem.*, 2021, **108**, 104647.
177 S. Manzoor, A. Petreni, M. K. Raza, C. T. Supuran and N. Hoda, *Bioorg. Med. Chem. Lett.*, 2021, **48**, 128249.
178 B. Swain, P. Singh, A. Angeli, K. Aashritha, N. Nagesh, C. T. Supuran and M. Arifuddin, *Bioorg. Med. Chem. Lett.*, 2021, **37**, 127856.

179 F. Mancuso, A. Di Fiore, L. De Luca, A. Angeli, G. De Simone, C. T. Supuran and R. Gitto, *Bioorg. Med. Chem.*, 2021, **44**, 116279.
180 M. Abas, A. Bahadur, Z. Ashraf, S. Iqbal, M. S. R. Rajoka, S. Rashid, E. Jabeen, Z. Iqbal, Q. Abbas and A. Bais, *J. Mol. Struct.*, 2021, **1246**, 131145.
181 C. Yamali, H. Sakagami, Y. Uesawa, K. Kurosaki, K. Satoh, Y. Masuda, S. Yokose, A. Ece, S. Bua, A. Angeli and H. I. Gul, *Eur. J. Med. Chem.*, 2021, **217**, 113351.
182 A. H. Eldeeb, M. F. Abo-Ashour, A. Angeli, A. Bonardi, D. S. Lasheen, E. Z. Elrazaz, A. Nocentini, P. Gratteri, H. A. Abdel-Aziz and C. T. Supuran, *Eur. J. Med. Chem.*, 2021, **221**, 113486.
183 M. T. Nemr, A. M. AboulMagd, H. M. Hassan, A. A. Hamed, M. I. Hamed and M. T. Elsaadi, *RSC Adv.*, 2021, **11**, 26241–26257.
184 M. Saadiq, G. Uddin, A. Latif, M. Ali, N. Akbar, Ammara, S. Ali, M. Ahmad, M. Zahoor and A. Khan, *ACS Omega*, 2021, **7**, 705–715.
185 D. M. Elimam, A. A. Elgazar, A. Bonardi, M. Abdelfadil, A. Nocentini, R. A. El-Domany, H. A. Abdel-Aziz, F. A. Badria, C. T. Supuran and W. M. Eldehna, *Eur. J. Med. Chem.*, 2021, **225**, 113800.
186 S. Zaib, I. Khan, H. S. Anbar, S.-O. Zaraei, R. M. Sbenati, H. T. Maryam, H. S. Shah and M. I. El-Gamal, *J. Mol. Struct.*, 2022, **1262**, 133048.
187 P. Singh, N. S. Goud, B. Swain, S. K. Sahoo, A. Choli, A. Angeli, B. S. Kushwah, V. M. Yaddanapudi, C. T. Supuran and M. Arifuddin, *Bioorg. Med. Chem. Lett.*, 2022, **70**, 128809.
188 H. T. Abdel-Mohsen, A. M. El Kerdawy, M. A. Omar, A. Petreni, R. M. Allam, H. I. El Diwani and C. T. Supuran, *Eur. J. Med. Chem.*, 2022, **228**, 114004.
189 A. Kumar, K. Siwach, T. Rom, R. Kumar, A. Angeli, A. K. Paul, C. T. Supuran and P. K. Sharma, *Bioorg. Chem.*, 2022, **123**, 105764.
190 H. O. Tawfik, A. Petreni, C. T. Supuran and M. H. El-Hamamsy, *Eur. J. Med. Chem.*, 2022, **232**, 114190.
191 B. Swain, A. Khan, P. Singh, V. S. Marde, A. Angeli, K. K. Chinchilli, V. M. Yaddanapudi, S. Carradori, C. T. Supuran and M. Arifuddin, *Molecules*, 2022, **27**, 8028.
192 M. F. Said, R. F. George, A. Petreni, C. T. Supuran and N. M. Mohamed, *J. Enzyme Inhib. Med. Chem.*, 2022, **37**, 701–717.
193 P. S. Thacker, V. Newaskar, A. Angeli, D. K. Sigalapalli, N. S. Goud, H. Chirra, A. B. Shaik, M. Arifuddin and C. T. Supuran, *Arch. Pharm.*, 2022, **355**, 2200232.
194 H. T. Abdel-Mohsen, M. A. Omar, A. Petreni and C. T. Supuran, *Arch. Pharm.*, 2022, **355**, 2200180.
195 C. Ismail, A. Nocentini, C. T. Supuran, J. Y. Winum and R. Gharbi, *Arch. Pharm.*, 2022, **355**, 2100405.
196 A. Buza, C. Türkeş, M. Arslan, Y. Demir, B. Dincer, A. R. Nixha and Ş. Beydemir, *Int. J. Biol. Macromol.*, 2023, **239**, 124232.
197 M. A. Ragab, W. M. Eldehna, A. Nocentini, A. Bonardi, H. E. Okda, B. Elgendy, T. S. Ibrahim, M. M. Abd-Alhaseeb, P. Gratteri and C. T. Supuran, *Eur. J. Med. Chem.*, 2023, **250**, 115180.
198 C. Kakakhan, C. Türkeş, Ö. Güleç, Y. Demir, M. Arslan, G. Özkemahlı and Ş. Beydemir, *Bioorg. Med. Chem.*, 2023, **77**, 117111.
199 A. S. El-Azab, A.-M. Alaa, S. Bua, A. Nocentini, A. H. Bakheit, H. M. Alkahtani, M. M. Hefnawy and C. T. Supuran, *Saudi Pharm. J.*, 2023, **31**, 101866.
200 C. Öztürk, E. Kalay, S. Gerni, N. Balci, F. S. Tokali, O. N. Aslan and E. Polat, *Biotechnol. Appl. Biochem.*, 2024, **71**, 223–231.
201 H. Bostancı, U. Çevik, R. Kapavarapu, Y. Güldiken, Z. Ş. Inan, Ö. Güler, T. Uysal, A. Uytun, F. Çetin and Y. Özkay, *SAR QSAR Environ. Res.*, 2023, **34**, 543–567.
202 N. H. Metwally and E. A. El-Desoky, *ACS Omega*, 2023, **8**, 5571–5592.
203 R. Romagnoli, T. De Ventura, S. Manfredini, E. Baldini, C. T. Supuran, A. Nocentini, A. Brancale, C. Varricchio, R. Bortolozzi and L. Manfreda, *J. Enzyme Inhib. Med. Chem.*, 2023, **38**, 2270180.
204 H. Ünver, U. Acar Cevik, H. E. Bostancı, O. Kaya and Ü. M. Kocyigit, *ChemistrySelect*, 2023, **8**, e202301641.
205 İ. Çelik, U. Acar Çevik, K. Küçükoğlu, H. Nadaroglu, H. E. Bostancı, A. Işık, Y. Özkay and Z. A. Kaplancıklı, *Chem. Biol. Drug Des.*, 2024, **103**, e14351.
206 K. Kucukoglu, N. Faydali, D. Bul, H. Nadaroglu, B. Sever, M. D. Altıntop, B. Ozturk and I. Guzel, *J. Mol. Struct.*, 2023, **1276**, 134699.
207 P. Begines, A. Bonardi, A. Nocentini, P. Gratteri, S. Giovannuzzi, R. Ronca, C. Tavani, M. L. Massardi, Ó. López and C. T. Supuran, *Bioorg. Med. Chem.*, 2023, **94**, 117467.
208 N. A. Zahedi, M. Mohammadi-Khanaposhtani, P. Rezaei, M. Askarzadeh, M. Alikhani, M. Adib, M. Mahdavi, B. Larijani, S. Niakan, M. B. Tehrani and P. Taslimi, *J. Mol. Struct.*, 2023, **1276**, 134767.
209 A. Angeli, V. Kartsev, A. Petrou, B. Lichitsky, A. Komogortsev, A. Geronikaki and C. T. Supuran, *Bioorg. Chem.*, 2023, **138**, 106621.
210 B. I. Huwaimel, S. K. Jonnalagadda, S. Jonnalagadda, S. Kumari, A. Nocentini, C. T. Supuran and P. C. Trippier, *Drug Dev. Res.*, 2023, **84**, 681–702.
211 A. I. Alalawy, K. Alatawi, N. A. Alenazi, A. F. Qarah, O. M. Alatawi, R. B. Alnoman, A. Alharbi and N. M. El-Metwaly, *J. Mol. Struct.*, 2024, **1295**, 136609.
212 F. N. Takla, S. Zaib, W. A. Bayoumi, K. Shehzadi, S. M. El-Messery, S. Anjum, A. Faisal and M. N. Nasr, *J. Mol. Struct.*, 2024, **1300**, 137277.
213 U. A. Çevik, A. Işık, R. Kapavarapu, K. Küçükoğlu, H. Nadaroglu, H. E. Bostancı, Y. Özkay and Z. A. Kaplancıklı, *J. Mol. Struct.*, 2024, **1295**, 136770.
214 C. Efeoglu, O. Selcuk, B. Demir, E. Sahin, H. Sari, C. Türkeş, Y. Demir, Y. Nural and Ş. Beydemir, *J. Mol. Struct.*, 2024, **1301**, 137365.
215 S. Mert, Y. Demir, Y. Sert, R. Kasımoğulları and İ. Gülçin, *J. Mol. Struct.*, 2024, 139472.

216 P. Singh, S. G. Nerella, B. Swain, A. Angeli, Q. Ullah, C. T. Supuran and M. Arifuddin, *Int. J. Biol. Macromol.*, 2024, **268**, 131548.
217 M. M. Abdelhakeem, M. M. Morcoss, D. A. Hanna and P. F. Lamie, *Bioorg. Chem.*, 2024, **144**, 107154.
218 S. Higazy, N. Samir, A. El-Khouly, S. Giovannuzzi, P. Begines, H. M. Gaber, C. T. Supuran and K. A. Abouzid, *Bioorg. Chem.*, 2024, **144**, 107089.
219 C. M. Al-Matarneh, M. Pinteala, A. Nicolescu, M. Silion, F. Mocci, R. Puf, A. Angeli, M. Ferraroni, C. T. Supuran and S. Zara, *J. Med. Chem.*, 2024, **67**, 3018–3038.
220 S. Maddipatla, B. Bakchi, R. R. Gadhave, A. Ammara, S. Sau, B. Rani, S. Nanduri, N. P. Kalia, C. T. Supuran and V. M. Yaddanapudi, *Arch. Pharm.*, 2024, e2400064.
221 M. Sobati, M. Abdoli, A. Angeli, A. Bonardi, M. Ferraroni, C. T. Supuran and R. Žalubovskis, *Arch. Pharm.*, 2024, e2400038.
222 B. Swain, V. S. Marde, P. Singh, A. Angeli, A. Khan, V. M. Yaddanapudi, Q. Ullah, C. T. Supuran and M. Arifuddin, *Arch. Pharm.*, 2024, **357**, 2300718.
223 R. El Ati, N. Öztaşkın, A. Çağan, A. Akıncıoğlu, Y. Demir, S. Göksu, R. Touzani and İ. Gülçin, *Arch. Pharm.*, 2024, **357**, 2300545.
224 D. Moi, S. Vittorio, A. Angeli, C. T. Supuran and V. Onnis, *ACS Med. Chem. Lett.*, 2024, **15**, 470–477.
225 Ş. Özkul, E. Tunca, S. Mert, A. Bayrakdar and R. Kasımoğulları, *J. Biochem. Mol. Toxicol.*, 2024, **38**, e23704.
226 M. Palomba, A. Angeli, R. Galdini, A. Hughineata, G. Perin, E. J. Lenardao, F. Marini, C. Santi, C. Supuran and L. Bagnoli, *Org. Biomol. Chem.*, 2024, 6532–6542.
227 M. Durgun, S. Akocak, N. Lolak, F. Topal, Ü. M. Koçyiğit, C. Türkeş, M. Işık and Ş. Beydemir, *Chem. Biodiversity*, 2024, **21**, e202301824.
228 A. Angeli, A. Petrou, V. G. Kartsev, A. Zubenko, L. N. Divaeva, V. Chekrisheva, D. Iacopetta, M. S. Sinicropi, S. Sirakanyan and A. Geronikaki, *ChemMedChem*, 2024, e202400147.
229 H. Aslan, G. Renzi, A. Angeli, I. D'Agostino, R. Ronca, M. L. Massardi, C. Tavani, S. Carradori, M. Ferraroni and P. Governa, *RSC Med. Chem.*, 2024, 1929–1941.
230 F. F. Albelwi, M. S. Nafie, N. R. Albujuq, W. Hourani, A. Aljuhani, K. M. Darwish, M. M. Tawfik, N. Rezki and M. R. Aouad, *RSC Med. Chem.*, 2024, **15**, 2440–2461.
231 İ. Yetek, S. Mert, E. Tunca, A. Bayrakdar and R. Kasımoğulları, *Mol. Diversity*, 2024, 1–21.
232 C. T. Supuran, *Curr. Pharm. Des.*, 2008, **14**, 603–614.
233 V. Alterio, A. Di Fiore, K. D'Ambrosio, C. T. Supuran and G. De Simone, *Chem. Rev.*, 2012, **112**, 4421–4468.
234 A. Maresca, C. Temperini, L. Pochet, B. Masereel, A. Scozzafava and C. T. Supuran, *J. Med. Chem.*, 2010, **53**, 335–344.
235 D. Vullo, M. Franchi, E. Gallori, J. Pastorek, A. Scozzafava, S. Pastorekova and C. T. Supuran, *Bioorg. Med. Chem. Lett.*, 2003, **13**, 1005–1009.